DETERMINING THE ROLE OF THE CALCIUM-SENSING RECEPTOR (CaSR) IN PULMONARY FIBROSIS (PF) AND THE ABILITY OF A CaSR INHIBITOR TO REVERSE PROFIBROTIC CHANGES IN AN *IN VITRO* MODEL OF PF

Kasope Lucy Wolffs, BSc.

PhD Thesis 2022

SUMMARY

Idiopathic pulmonary fibrosis (IPF) is a disease with very poor prognosis and no curative therapies. Central to its progression is the activation of fibroblasts by TGFß, which initiates various fibrotic processes. The extracellular calcium-sensing receptor (CaSR) is a chemosensor which is activated by several agonists/modulators, including polyvalent cations, polyamines, and basic polypeptides. Previous studies have shown that CaSR activation drives pulmonary inflammation and remodelling in preclinical models of asthma, COPD and pulmonary hypertension. However, the role of the receptor in pulmonary fibrosis remains unknown.

During my PhD, I investigated CaSR expression in IPF lung tissue, expression of CaSR activators in PF patient saliva, and the role of the receptor in mediating TGFß-induced fibrotic response in primary human lung fibroblasts (NHLFs) using a negative allosteric modulator (NAM) of the CaSR, NPS2143. The *in vitro* studies were carried out using NHLFs treated with TGFß1 in the presence/absence of NAM or NAM alone for 72 hours. Data from these studies indicate five principal findings:

1. *In vivo* CaSR expression occurs in the bronchiolar epithelium, proliferated pulmonary neuroepithelial bodies (NEBs), and the interstitium of normal and IPF lungs.
2. Expression of certain CaSR activators, amino acids and polyamines are increased in the saliva of PF patients. Since these ligands can activate the CaSR expressed by epithelial cells or NEBs, our study identifies a potential role for the receptor in IPF pathogenesis.
3. The CaSR is functionally expressed by NHLFs *in vitro*, suggesting the receptor might contribute to fibrogenesis.

4. TGFß1 upregulates the expression of key profibrotic and metabolic reprogramming genes *in vitro,* and the NAM, NPS2143, prevents these changes.

5. NPS2143 prevents the cellular and molecular profibrotic responses (such as fibroblast activation, proliferation, collagen and IL-8 secretion) to TGFß1 *in vitro*. Together, these results strongly suggest a role for the CaSR in (I)PF aetiology.

DEDICATION

Dear dad,

I made it – Against All Odds!

ACKNOWLEDGEMENTS

I would like to thank the King's Commercialization Institute, Saunders Legacy Lung Research and Cardiff University School of Biosciences for funding my PhD.

I want to say a special thank you to Professor Daniela Riccardi and Professor Paul Kemp, who believed in me, fought for me and never gave up on me. Daniela, you are the best supervisor and mentor I could have ever hoped for, and I couldn't have done this without you. I also want to thank Professor Ben Hope-Gill for his unwavering support throughout my PhD. I'd like to thank my co-supervisor, Dr Ryan Moseley and Dr Jordanna Dally, for sharing their expertise, especially during the optimisation phase of my project. A huge thank you to the "lab fam", especially Beth, for keeping me sane towards the end.

My academic journey has been filled with people who saw my potential even before I did; Dr Sheila Amici-Dargan, Dr Sarah Hall and Dr Andrew Shore – thank you for making that 1st class degree possible. It set the foundation for the PhD I never thought I'd do. To Michael, Ruby, Nikki and Fliss, thank you for working tirelessly behind the scenes to make sure I had all the paperwork I needed, especially while navigating the crazy world of PhD motherhood. To Rhiannon, thank you for showing me that it is possible to be a PhD mum.

This journey began with a beautiful young man who encouraged me to pursue my dream of starting my Physiology degree – thank you, Alan, for being my rock for the past 10 years! A huge thank you to all my friends and family who have supported, encouraged, motivated, nagged and dragged me to the finish line. To all my mums, thank you for the prayers; I needed every single one. To my sisters, who took every opportunity to remind me that "you are doing this for all of us", we're nearly there, girls.

To my baby, my Ayo – I hope when you remember this period, your memories are of the great times we shared, not the moments I missed. I love you more than you'll ever know!

TABLE OF CONTENTS

LIST OF ABBREVIATIONS

Ab	Antibody
AMP	Adenosine monophosphate
AMPK	AMP-activated protein kinase
ANOVA	Analysis of variance
αSMA	Alpha smooth muscle actin
ATP	Adenosine triphosphate
BGN	Biglycan
BrdU	Bromodeoxyuridine
BSA	Bovine serum albumin
Ca^{2+}	Calcium ions
Ca^{2+}_o	Extracellular Ca^{2+}
Ca^{2+}_i	Intracellular Ca^{2+}
$CaCl_2$	Calcium chloride
cAMP	Cyclic adenosine monophosphate
CaSR	Extracellular calcium-sensing receptor
CDH	Cadherin
CDKN2A	Cyclin-dependent kinase inhibitor 2a
CDKN2B	Cyclin-dependent kinase inhibitor 2b
CEBPB	CCAAT enhancer binding protein beta
CO_2	Carbon dioxide
COL	Collagen
COMP	Cartilage oligomeric matrix protein
CTGF	Connective tissue growth factor
CXCL	C-X-C motif chemokine ligand
DAG	Diacylglycerol
DAPI	4', 6-diamidino-2-phenylindole
dd-H_2O	Double-distilled Water
DKK1	Dickkopf-related protein 1
DMSO	Dimethyl Sulphoxide
DNA	Deoxyribonucleic acid
DNase	Deoxyribonuclease

ECM	Extracellular matrix
EDTA	Ethylenediamine tetraacetic acid
EGF	Epidermal growth factor
EGFR	Epidermal growth factor receptor
ELISA	Enzyme-linked immunosorbent assay
ELN	Elastin
ERK	Extracellular signal-regulated kinase
FDA	U.S. Food and drug administration
FEV_1	Forced expiratory volume (in 1 second)
FGF	Fibroblast growth factor
FLN	Filamin
FN	Fibronectin
FVC	Forced vital capacity
GAPDH	Glyceraldehyde 3-phosphate dehydrogenase
GLS	Glutaminase
GPCR	G-protein coupled receptor
GRP	Gastrin-releasing peptide
GTPases	Guanosine triphosphate hydrolase enzymes
HCl	Hydrochloric acid
HEPES	4-(2-hydroxyethyl)-1-piperazineethanesulfonic acid
HRP	Horseradish peroxidase
ICC	Immunocytochemistry
IFN	Interferon
IGF	Insulin-like growth factor
IGFBP3	Insulin-like growth factor binding protein 3
IGFBP3	Insulin-like growth factor binding protein 7
IgG	Immunoglobulin G
IHC	Immunohistochemistry
IL	Interleukin
JNK	C-Jun N-terminal kinase
JUN	Jun proto-oncogene
KCl	Potassium chloride
LAMTOR	Late endosomal/Lysosomal adaptor, MAPK And MTOR activator

MAPK	Mitogen activated protein kinase
MEK	Mitogen-activated protein kinase kinase
$MgCl_2$	Magnesium chloride
MMP	Matrix metalloproteinase
mRNA	Messenger ribonucleic acid
mTOR	Mechanistic/mammalian target of rapamycin complex
NaCl	Sodium chloride
NaOH	Sodium hydoxide
NFKB	Nuclear factor kappa B
NHLF	Normal primary human lung fibroblast
O_2	Oxygen
P4HA2	Prolyl 4-Hydroxylase Subunit Alpha 2
PAI	Plasminogen activator inhibitor
PBS	Phosphate buffered saline
PDGF	Platelet-derived growth factor
PI3K	Phosphatidylinositide 3-kinase
PKC	Protein kinase C
RAC	Ras-related C3 botulinum toxin substrate
Rag	Ras-related GTPase
RAS	Rat sarcoma virus oncogene
Rheb	Ras homolog enriched in brain
RHO	Ras homolog gene family member
RNA	Ribonucleic acid
RNase	Ribonuclease
RNAseq	RNA sequencing
ROCK	Rho-associated coiled-coil containing protein kinase
ROI	Region of interest
ROS	Reactive oxygen species
rRNA	Ribosomal RNA
SEM	Standard error of the mean
SERPIN	Serpin peptidase inhibitor
SLC1A5	Solute carrier family 1 member 5
SLC3A2	Solute carrier family 3, member 2

SLC7A5	Solute carrier family 7, member 5
SLC16A1	Solute carrier family 16 member 1
SLC16A3	Solute carrier family 16 member 3
SM22α	Smooth muscle protein of 22 kDa isoform α
SMAD	Mothers against decapentaplegic
TGFβ	Transforming growth factor beta
TGFβR	TGFβ receptor
TIMP	Tissue inhibitor of metalloproteinase
TNC	Tenascin C
TNF	Tumour necrosis factor
VCAN	Versican
VEGF	Vascular endothelial growth factor
VIM	Vimentin
WNT	Wingless-related integration site

CHAPTER 1: INTRODUCTION

1.1. Pulmonary Fibrosis (PF)

Chronic respiratory diseases and infections are the third leading cause of death in Europe, with the majority of these deaths occurring in people over 65 (OECD/European Union 2020). This category includes chronic respiratory diseases (such as pulmonary fibrosis) whose mortality rate and prevalence also increase sharply with age (Thannickal *et al*. 2015; Bowdish 2019). The impact of these age-related diseases will be amplified in the coming years due to the ageing global population, which is projected to double by 2050 (WHO 2018).

In the young, fibrosis is a beneficial self-resolving wound-healing response to organ injury (Kurundkar and Thannickal 2016). However, as ageing occurs, this process is hijacked and underpins fibrotic diseases of the lungs, heart, kidney and liver (Rockey *et al*. 2015; Kurundkar and Thannickal 2016). Although the specific insults initiating the disease in different organs may vary, the path to organ fibrosis is similar, involving the activation of fibroblasts and excessive extracellular matrix (ECM) deposition (Murtha *et al*. 2017; Wicher *et al*. 2021).

Several respiratory diseases are characterised by fibrosis. For example, fibrosis can occur in the large airways in asthma, the small airways in chronic obstructive pulmonary disease (COPD), or the lung parenchyma in idiopathic pulmonary fibrosis (IPF) (Boorsma *et al*. 2014; Jones *et al*. 2016). Although fibrosis can affect both the parenchyma and the airways, the term pulmonary fibrosis (PF) is typically used to describe the pathological hallmark of interstitial lung diseases (ILDs) (Inui *et al*. 2021). This umbrella term encompasses over 200 diseases characterised by varying degrees of interstitial inflammation, aberrant cell proliferation, and fibrosis within the alveolar wall (Wuyts *et al*. 2013; Mikolasch *et al*. 2017; Lederer and Martinez

2018). If unresolved, the fibrotic process impedes gas exchange between the alveoli and pulmonary vasculature, leading to respiratory failure and ultimately death (Shenderov *et al*. 2021).

Clinical assessments aim to identify a possible cause of lung fibrosis; these include features of autoimmune/connective tissue diseases (such as rheumatoid arthritis or scleroderma), exposure to pneumotoxic drugs (such as the antiarrhythmic amiodarone or the chemotherapeutic bleomycin), radiation therapy, occupational exposures (such as coal, asbestos or silica), and implicated allergens (such as organic dust of animal or vegetable origin which cause hypersensitivity pneumonitis) (Ryu *et al*. 2007; Wallis and Spinks 2015; Riario Sforza and Marinou 2017). Determining the underlying cause is critical for correct diagnosis and disease management (Mikolasch *et al*. 2017). However, where no specific cause can be identified, these cases are referred to as idiopathic interstitial pneumonitis, the most studied being IPF with a worse 5-year survival rate (25%) than many cancers (Vancheri *et al*. 2010; Kolb and Vašáková 2019).

1.2. Idiopathic Pulmonary Fibrosis (IPF)

IPF is a progressive and fatal lung disease characterised by an unrelenting process that replaces normal lung parenchyma with excessive scar tissue. The respiratory decline which ensues is usually slowly progressive, with or without acute exacerbations, or accelerated, resulting in distinct survival patterns (King *et al*. 2011). The development of acute exacerbations is unpredictable and is associated with poorer outcomes with a median survival of approximately 3 months (Collard *et al*. 2016).

Pulmonary fibrosis (PF) currently accounts for 1 in 100 deaths in the UK (BLF 2016). A pan-European rise in IPF mortality rates has also been reported,

with the most significant increase observed in the UK and Finland (Marshall *et al*. 2018). In addition to the increased mortality rate, there is a rise in the incidence and prevalence of IPF (Navaratnam *et al*. 2011). Approximately 6,000 new IPF cases are diagnosed each year, with an estimated total of 32,500 patients in the UK (BLF 2016). These patients are primarily elderly and male, with a smoking history (Ley and Collard 2013). Clinically, patients present with exertional dyspnoea, dry cough and fatigue, which worsen with disease progression (King *et al*. 2011; Quinn *et al*. 2019). As symptoms worsen and lung function declines, patients experience psychological distress, anxiety and depression, which significantly diminishes their quality of life (Belkin and Swigris 2013; Janssen *et al*. 2020; Tzouvelekis *et al*. 2020).

There is currently no cure for this disease. Lung transplantation still represents the best therapeutic option; however, most patients are precluded from transplantation due to their advanced age/frailty and the presence of comorbidities such as pulmonary arterial hypertension (PAH), emphysema and lung cancer (Raghu *et al*. 2015a; Tarride *et al*. 2018). The two anti-fibrotics approved for IPF treatment, nintedanib and pirfenidone, have been shown to slow disease progression and lower the incidence of acute exacerbations (Richeldi *et al*. 2011; Ley *et al*. 2017b). However, these drugs do not significantly improve key patient-reported outcomes such as quality of life (Van Manen *et al*. 2017).

1.2.1. IPF Diagnosis

Confirmed IPF diagnosis requires a multidisciplinary team of ILD specialists (NICE 2013). It is centred around radiological/histological findings of usual interstitial pneumonia (UIP) and the absence of an identifiable aetiology (Raghu *et al*. 2011). This spatially heterogeneous UIP pattern is characterised by architectural distortion, interstitial thickening, fibroblastic foci, and honeycombing cystic remodelling (Selman and Pardo 2021). UIP is primarily

associated with IPF but can occur in other less common ILDs, collectively known as progressive pulmonary fibrosis, and are associated with increased mortality rates (Adegunsoye *et al*. 2019). These include connective tissue-disease ILDs and chronic hypersensitivity pneumonitis (caused by naturally occurring allergens). Furthermore, PF patients with coexisting emphysema also develop a UIP pattern which accelerates disease progression and worsens prognosis (Selman and Pardo 2021). On the molecular level, increased expression of the profibrotic factor, Wnt5a, was observed in IPF patients and rheumatoid arthritis-ILD (RA-ILD) patients with UIP histology (Martin-Medina *et al*. 2018; Yu *et al*. 2019). Cellularly, the UIP pattern is associated with markers of epithelial senescence, autophagy, and telomere dysfunction regardless of the underlying cause of the disease (Gallob *et al*. 2021; Lee *et al*. 2021).

1.2.2. Pathophysiology of IPF

The development of novel therapeutics for IPF has been hampered by the lack of in-depth understanding of the disease aetiology. However, giant strides have been made in delineating the central tenets of the disease over the last few years. This section will discuss critical mechanisms driving IPF progression and highlight the overlapping processes implicated in the development of the progressive fibrosing phenotype observed in other ILDs.

1.2.2.1. Genetic predisposition

Genetic transmission occurs in <4% of IPF patients (Marshall *et al*. 1997; Hodgson *et al*. 2002). Most familial IPF cases are autosomal dominant with incomplete penetrance, but some may arise sporadically *(King et al. 2011)*. Commonly affected genes include those involved in surfactant processing and telomere maintenance (Pardo and Selman 2021). Genetic association studies identified a gain-of-function *MUC5B* promoter polymorphism, rs35705950, as the most significant risk variant, accounting for 30% of the

total risk of developing IPF (Seibold *et al*. 2011; Fingerlin *et al*. 2013; Moore *et al*. 2019). This polymorphism has also been identified as a risk factor for RA-ILD, and is associated with increased mortality in patients with chronic hypersensitivity pneumonitis (Seibold *et al*. 2011; Ley *et al*. 2017a).

This rs35705950 variant is associated with increased mucin-5B expression in the epithelial cells lining distal airways and honeycomb cysts (Plantier *et al*. 2011; Seibold *et al*. 2013). Schwartz (2018) and Maher (2021) suggest a theory that links excessive mucin-5B secretion to IPF development. This theory suggests that mucin accumulation could lead to mucociliary impairment and the retention of inhaled harmful substances (such as pollutants, smoke, and microorganisms), thereby facilitating recurrent injury, repair, and aberrant regeneration at the bronchoalveolar junction.

1.2.2.2. IPF risk factors

Ageing

The natural ageing process is characterised by 10 hallmarks that underpin the structural and functional changes observed in the ageing lung: genomic instability, telomere attrition, epigenetic alterations, stem cell exhaustion, altered intercellular communication, cellular senescence, loss of proteostasis, mitochondrial dysfunction, dysregulated nutrient sensing and ECM dysregulation (Meiners *et al*. 2015). These altered processes are thought to occur in IPF at an accelerated or exaggerated rate (Pardo and Selman 2021). A complex interplay between these hallmarks contributes to the development and progression of IPF and other progressive ILDs (Selman and Pardo 2021).

Telomere attrition and genomic instability alter essential cell-cycle genes such as p53, p16 and p21, which promote senescence (Demopoulos *et al*.

2002; Muñoz-Espín and Serrano 2014). In IPF, senescent cells are characterised by a senescence-associated secretory phenotype (SASP), which results in the secretion of various pro-inflammatory, profibrotic and matrix-remodelling cytokines (Muñoz-Espín and Serrano 2014). This secretome impairs normal epithelial cell regeneration and facilitates fibroblast accumulation, driving progressive lung fibrosis (Muñoz-Espín and Serrano 2014). Furthermore, molecular markers of telomere dysfunction and senescence are pathologically expressed in both IPF and non-IPF UIP lungs, especially by the epithelial cells which line these cystic regions (Gallob *et al*. 2021; Lee *et al*. 2021). These honeycomb cysts also highly express Wnt signalling ligands which propagate critical signals from senescent epithelial cells leading to the activation and anti-apoptotic phenotype characteristic of fibroblasts within this region (Selman *et al*. 2016). The aberrant reactivation of the Wnt signalling pathway is one of many developmental pathways which enhance lung fibrosis (Baarsma and Königshoff 2017).

Other intracellular signalling pathways such as the mechanistic target of rapamycin (mTOR) pathway have also been implicated in IPF *via* nutrient-sensing dysregulation, loss of protein homeostasis (proteostasis), endoplasmic reticulum (ER) stress, and mitochondrial dysfunction (Lawrence and Nho 2018; Podolanczuk *et al*. 2021). Aberrant activation of mTOR signalling facilitates lung fibrosis by inducing fibroblast activation, ECM production, metabolic reprogramming, autophagy and senescence (Mercer *et al*. 2016; Woodcock *et al*. 2019; Platé *et al*. 2020).

Comorbidities

Given that IPF is commonly diagnosed in people over the age of 60, it is unsurprising that these patients also have or develop other chronic age-related conditions during the course of the disease. However, age alone does not fully account for this phenomenon since the prevalence of comorbidities

is higher in IPF patients compared to age-matched controls (Buendía-Roldán *et al*. 2017). It, therefore, follows that the higher frequency of comorbidities seen in IPF patients is in some part responsible for the high mortality rate associated with the disease (Kreuter *et al*. 2016). Several IPF comorbidities share common risk factors such as smoking (*e.g.*, lung cancer, COPD, and cardiovascular diseases) and genetic mutations (*e.g.*, emphysema), while others develop secondary to IPF (*e.g.*, PAH and ischemic heart disease) (Vancheri *et al*. 2010; Buendía-Roldán *et al*. 2017). Studies have also highlighted a cross-over in key oncogenic pathways that contribute to IPF aetiology, such as the RAS signalling pathway (Vancheri 2013).

A common IPF comorbidity is gastro-oesophageal reflux (GOR), with high variability in prevalence (0 – 94%) (Raghu *et al*. 2015b). Studies have suggested a potential role for GOR and chronic micro-aspiration in the initiation phase of IPF pathogenesis (Wuyts *et al*. 2013), with additional roles for GOR and pepsin in acute exacerbations (Tcherakian *et al*. 2011; Lee *et al*. 2012). However, the role of GOR in IPF remains highly controversial since the exact pathogenic constituent(s) of gastric fluid (*e.g.*, bile salts, pepsin, food particles or microbes) is yet to be identified (Johannson *et al*. 2017).

Viral infections

In addition to micro-aspiration, chronic viral infections may play a role in the initiation, progression, and exacerbation of IPF (Pardo and Selman 2021). Viruses implicated in the IPF pathogenesis include herpesviruses (Epstein-Barr virus (EBV), human herpesviruses 7 and 8, cytomegalovirus, herpes simplex virus), adenovirus, hepatitis C virus, parvovirus B19 and torque teno virus (Wuyts *et al*. 2013; Sack and Raghu 2019). A recent systematic review suggests that chronic viral infections (especially with herpesviruses) are associated with a greater risk of IPF (Sheng *et al*. 2020). EBV is the most-studied virus in relation to IPF. Although this virus usually infects the upper

respiratory tract, it is known to infect and replicate in the lower respiratory tract (Lung *et al*. 1985). EBV antigens specifically expressed during the replicative phase of an infection, are localised to bronchiolar and alveolar epithelial cells (AECs) in IPF tissue (Egan *et al*. 1995). Furthermore, latent EBV proteins in lung tissue from IPF patients have been associated with poorer outcomes (Tsukamoto *et al*. 2000). Studies have shown that EBV-induced epithelial injury increases transforming growth factor beta (TGFß) expression and potentiates its profibrotic activity *in vitro* (Malizia *et al*. 2008; Sides *et al*. 2012), providing a potential mechanism that links viral infections to the development of IPF.

Environmental stressors

Several occupational and environmental irritants that target the lung epithelium are associated with increased risk of developing IPF, including cigarette smoking, agriculture/farming, livestock, wood dust, metal dust, and stone/sand (Taskar and Coultas 2006). The most important environmental risk factors are smoking and exposure to metal dust (Taskar and Coultas 2008; Raghu *et al*. 2011). In IPF, exposure to ozone, nitrogen dioxide or particulate matter (less than 10 µm) is associated with a decline in lung function (Winterbottom *et al*. 2018), acute exacerbations (Johannson *et al*. 2014), and increased mortality (Sesé *et al*. 2018). Lung tissue from IPF patients also accumulates considerably higher levels of inorganic particles (such as aluminium, nickel and silica) when compared to tissue from non-IPF ILD patients (Tsuchiya *et al*. 2007; Sack and Raghu 2019). Although these toxic agents are not the main drivers of the disease, anecdotal evidence provides potential mechanisms through which these particles might accelerate fibrosis. For example, oxidative stress or direct damage from air pollution potentially enhances the susceptibility of the lung epithelium to injury from other exposures like cigarette smoke (Mookherjee *et al*. 2018).

Cigarette smoke components, nicotine and nickel, could directly damage epithelial cells inducing the production of reactive oxygen species (ROS), TGFß and connective-tissue growth factor (CTGF), which facilitate key profibrotic processes such as fibroblast activation, proliferation, and collagen deposition (Jensen *et al*. 2012; Wu *et al*. 2012). Additionally, cigarette smoke activates signalling pathways that induce cellular senescence, a key hallmark in the ageing process and IPF (Muñoz-Espín and Serrano 2014; Luppi *et al*. 2021).

1.2.2.3. The role of the epithelium in IPF

Although the initiating events leading to IPF are poorly understood, the consensus is that the disease occurs in (genetically) susceptible lungs constantly exposed to environmental stressors (Mikolasch *et al*. 2017). The lungs are constantly exposed to the external environment, which contains many harmful agents, including but not limited to microbes, toxic fumes, pollutants. This interaction is thought to establish a continuous cycle of epithelial injury, wound healing, and tissue repair (Sack and Raghu 2019; Wicher *et al*. 2021).

Over the past decade, novel pathogenic mechanisms of IPF have been elucidated that have shifted the concept of IPF from an inflammatory-driven to an epithelium-driven disease involving both alveolar and airway epithelial cells (Montesi *et al*. 2020). The current hypothesis suggests that unresolved epithelial injury stimulates a profibrotic milieu, at the centre of which is TGFß, which results in fibroblast expansion and excessive ECM deposition (Selman and Pardo 2021). Interestingly, all histological patterns of PF are characterised by a subset of collagen- and ECM-expressing epithelial cells, suggesting their role in ECM production and PF progression (Habermann *et al*. 2020).

Recent studies have discovered other atypical cells unique to the IPF lung (Podolanczuk *et al*. 2021). These include transitional AECs and aberrant basaloid epithelial cells. Transitional AECs bear markers of type II and type I AECs (Xu *et al*. 2016) and are associated with markers of DNA damage, senescence, and TGFβ enrichment (Kobayashi *et al*. 2020). The failure of these transitional cells to differentiate into type I AECs hinders re-epithelisation after tissue injury, which is crucial for the resolution of fibrosis (Auyeung and Sheppard 2021). In addition to the accumulation of transitional AECs, increased AEC apoptosis and senescence further contribute to aberrant re-epithelisation by inducing SASP-mediated fibroblast activation, which also attenuates AEC proliferation (Plataki et al. 2005; Blokland et al. 2020; Chen et al. 2020b).

Perhaps most notable is the recent identification and characterisation of the monolayer of epithelial cells located on the surface of IPF fibroblastic foci, sometimes referred to as hyperplastic alveolar cells. Adams *et al*. (2020) describe these cells as "aberrant basaloid cells", which co-express an array of IPF markers, including basal epithelial markers, mesenchymal markers, senescence markers and developmental factors. Given the recency of these findings, the origin and specific roles of these ectopic cells in progressive PF are yet to be fully elucidated.

1.2.2.4. The role of fibroblasts in IPF

Fibroblasts are mesenchymal cells typically found in small numbers within the quiescent lung interstitium (John *et al*. 2021). Mechanical and biochemical cues from the injury site activate and recruit fibroblasts to initiate repair (Shinde and Frangogiannis 2014). These fibroblasts are subdivided into matrix-, alveolar niche-, and αSMA (α smooth muscle actin)-expressing myofibroblasts, facilitating matrix production, alveolar regeneration and wound contraction, respectively (Ushakumary *et al*. 2021).

The resolution of the physiological fibrotic response is dependent on ECM reorganisation (Gonzalez *et al*. 2016) and myofibroblast clearance (Glasser *et al*. 2016). Failure to successfully terminates this stage results in myofibroblast accumulation and scar tissue formation (Horowitz and Thannickal 2006). The persistence of an abnormally stiff ECM exacerbates AEC dysfunction and fibroblast activation resulting in progressive fibrosis (White 2015; Wu et al. 2020a; Selman and Pardo 2021).

In IPF, the lung is characterised by the expansion of a diverse population of activated fibroblasts (Adams *et al*. 2020; Habermann *et al*. 2020). The highest collagen levels are expressed by a subpopulation of Cthrc1 (collagen triple helix repeat containing 1)-positive fibroblasts uniquely found within fibroblastic foci of IPF lungs (Tsukui *et al*. 2020). The fibroblastic foci are key diagnostic features of UIP (Renzoni *et al*. 2021), with increased (foci) number associated with poorer patient outcomes (Nicholson *et al*. 2002). As the name implies, these lesions are comprised of the key effectors of fibrogenesis, fibroblasts (Guillotin *et al*. 2020). They represent the leading edge of dysfunctional ECM deposition and parenchymal destruction (Yamaguchi *et al*. 2016). Essential transcriptional programmes involved in maintaining the fibroblastic foci and subsequent collagen expression include the TGFβ, mTOR and RhoA signalling pathways (Guillotin *et al*. 2020).

1.2.2.5. The role of TGFβ in pulmonary fibrosis

TGFβ is a ubiquitously expressed polypeptide with three mammalian isoforms, TGFβ1, TGFβ2 and TGFβ3, which signal through the same receptors (Prud'homme 2007). TGFβ is a pleiotropic cytokine that regulates cellular processes (such as apoptosis, proliferation and differentiation), embryonic development, immune regulation, and wound healing (reviewed by Inui *et al*. 2021). TGFβ1 is the archetypal member of the TGFβ superfamily and the most prevalent isoform (Chambers *et al*. 2003; Biernacka *et al*. 2011). Upon

injury, TGFβ1 is released by multiple cell types, including epithelial cells, (myo)fibroblasts, macrophages, and regulatory T cells, which promote wound healing and tissue repair via cytokine production, inflammatory cell recruitment, fibroblast activation, and ECM deposition (Hewlett *et al*. 2018).

Unlike other cytokines, TGFβ1 is synthesised in association with a latency-associated peptide (LAP) and latent TGFβ–binding protein (LTBP), which form a complex that tightly regulates TGFβ availability and prevents receptor activation (Biernacka *et al*. 2011). This latent TGFβ1 complex can be rapidly activated through various mechanisms involving proteases (such as matrix metalloproteases (MMPs), plasmin, and thrombin) that cleave the complex, or the matricellular protein, thrombospondin and integrins which bind to LAP and induce a conformational change consequently releasing active TGFβ1 (Prud'homme 2007). Other TGFβ1 activators include changes to extracellular stiffness, acidic pH and hydroxyl radicals from ROS, which cause structural modifications to the latent complex (Hinz 2010; Biernacka *et al*. 2011).

All three TGFβ isoforms elicit their biological effects by binding to cell-surface receptors and initiating the assembly of a receptor complex consisting of type I (RI), type II (RII), and type III (RIII) receptors (Vander Ark *et al*. 2018). RIII recruits one of the TGFβ ligands to RII, a constitutively active kinase that phosphorylates RI, which in turn activates canonical downstream mediators SMAD2 and 3 (mothers against decapentaplegic homolog 2 and 3) (Massagué 2003). Upon phosphorylation, SMAD2/3 form a heteromeric complex with SMAD4, which regulate gene transcription by recruiting transcriptional co-activators or co-repressors (Chambers *et al*. 2003; Massagué 2003). Inhibitory SMADs, SMAD6 and 7 block TGFβ signalling by competing with SMAD2/3 for RI binding (Smad7) or Smad4 recruitment (Smad6) (Biernacka *et al*. 2011).

TGFβ can also signal through non-SMAD pathways (also known as the non-canonical pathway). The mitogen-activated protein kinase (MAPK) family are serine/threonine-specific protein kinases that are activated in response to extracellular mitogenic and stress stimuli and regulate cell differentiation, proliferation, survival, and apoptosis (Soares-Silva *et al*. 2016). TGFβ activates all three known MAPK pathways: extracellular signal-regulated kinase (ERK), p38 MAPK, and c-Jun-N-terminal kinase (JNK), phosphoinositide 3-kinase (PI3K), AKT, mTOR, Ras homolog gene (Rho)-like GTPases, and Wnts (Mu *et al*. 2012; Guillotin *et al*. 2020). The induction of SMAD and non-SMAD pathways result in the transcription and release of several profibrotic mediators, including tumour necrosis factor alpha (TNFα), CTGF, platelet-derived growth factor (PDGF) and fibroblast growth factor (FGF), which drive (myo)fibroblast expansion, fibroblast activation, and ECM secretion (Lasky *et al*. 1998; Hewlett *et al*. 2018). The TGFβ signalling cascade is further complicated by interactions between the intracellular mediators of these pathways and SMADs (Vander Ark *et al*. 2018). For example, SMAD7, which inhibits the canonical pathway, facilitates the p38 MAPK and Wnt signalling pathways in some pathological settings (Edlund *et al*. 2005; Moustakas and Heldin 2005) (Figure 1.1).

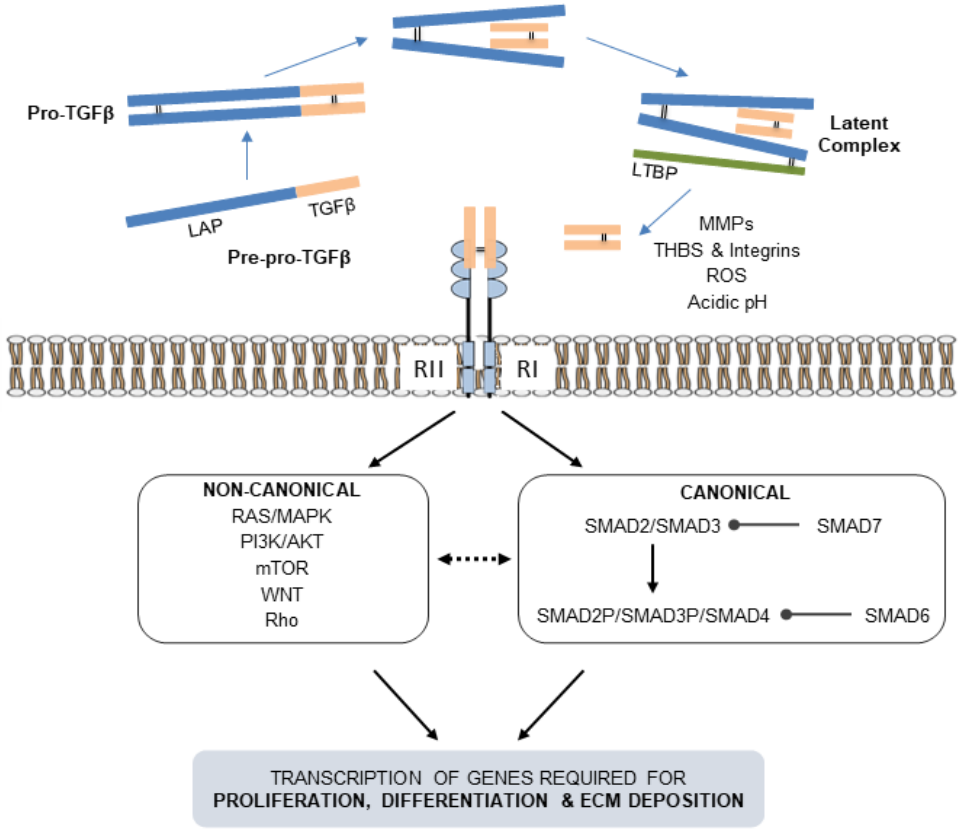

Figure 1.1 TGFß activation and signalling. TGFß must be released from its inactive latent complex to induce activation of the TGFß receptor (RI and RII). TGFß is produced as an inactive latent complex, consisting of a mature TGFß peptide and a latency-associated peptide (LAP). TGFß is cleaved from LAP but remains attached to LAP by noncovalent bonds. This intermediate complex is bound to the Latent TGFß-Binding Protein (LTBP) by disulfide bonds, forming a large latent complex. This modified complex is then bound to other extracellular matrix (ECM) proteins (such as elastin and fibronectin), thereby acting as a TGFß reservoir. The activation of latent TGFß involves proteases (such as matrix metalloproteases; MMPs), thrombospondin (THBS), and integrins which either cleave the complex or induce conformational changes in the LAP. A mildly acidic environment and hydroxyl radicals from ROS can also cause structural modifications to the latent complex which consequently release active TGFß. TGFß signals through SMAD-dependent (canonical) and SMAD-independent (non-canonical) pathways. Activation of these pathways regulate the transcription of fibrogenic genes. TGFß: transforming growth factor beta.

The concept that TGFβ is crucial for the development of PF is supported by *in vitro* studies, animal models of lung fibrosis, and clinical evidence (Yue *et al*. 2010). In IPF, its importance is underscored by increased levels in the bronchoalveolar lavage fluid of IPF patients compared to control (Salez *et al*. 1998). In addition, lung sections from IPF patients show increased expression of TGFβ or its receptor in bronchiolar epithelial cells, hyperplastic AECs, alveolar macrophages, and fibroblasts (Salez *et al*. 1998; Khalil *et al*. 2001).

The profibrotic role of TGFβ in lung fibrosis was first established in a study by Sime *et al*. (1997), which showed that transient overexpression of active TGFβ1 results in myofibroblast accumulation, extensive ECM deposition and persistent fibrosis in rat lungs. Building on these findings, other studies in mice showed that TGFβ1 overexpression suppresses airway regeneration (Warshamana *et al*. 2002) and induces honeycomb-like parenchymal remodelling (Lee *et al*. 2004). Furthermore, fibroblast-specific deletion of TGFβ receptors and SMAD3 deficiency markedly attenuate PF (Zhao *et al*. 2002; Wei *et al*. 2017).

The main cellular targets of TGFβ in PF are fibroblasts (Frangogiannis 2020). TGFβ induces mesenchymal expansion by activating epithelial cells (which is characterised by the expression of profibrotic markers such as αSMA), fibroblast proliferation and resistance to apoptosis, cytokine production, and myofibroblast accumulation (Murtha *et al*. 2017). Furthermore, TGFβ-responsive elements have been mapped to the promoter regions of genes encoding (myo)fibroblast contractile and ECM proteins (such as αSMA and collagen 1) (Inagakis *et al*. 1994; Hu *et al*. 2003). The presence of these responsive elements is supported by findings that suggest that an increase in TGFβ expression is required for collagen synthesis and ECM deposition in animal models of lung fibrosis (Hoyt and Lazo 1988; Yi *et al*. 1996).

Due to the reasons highlighted above, TGFß inhibition/modulation would be an attractive drug target for pulmonary fibrosis. However, directly targeting this cytokine is not feasible as an anti-fibrotic therapy due to the essential role TGFß plays in immunity and tissue homeostasis. In fact, complete knock-out of TGFß1 results in fatal cardiopulmonary inflammation (Kulkarni and Karlsson 1993) and increases susceptibility to lung malignancy (Tang *et al*. 1998). Therefore, it is imperative that the mechanisms that regulate and contribute to TGFß1-induced fibrosis are fully elucidated as this will impact the efficacy of novel therapeutics. Although this section focussed on TGFß1, it should be noted that TGFß2 and TGFß3 may also play a role in fibrosis (Coker *et al*. 1997).

The pathophysiological mechanisms discussed in this section are summarised in Figure 1.2.

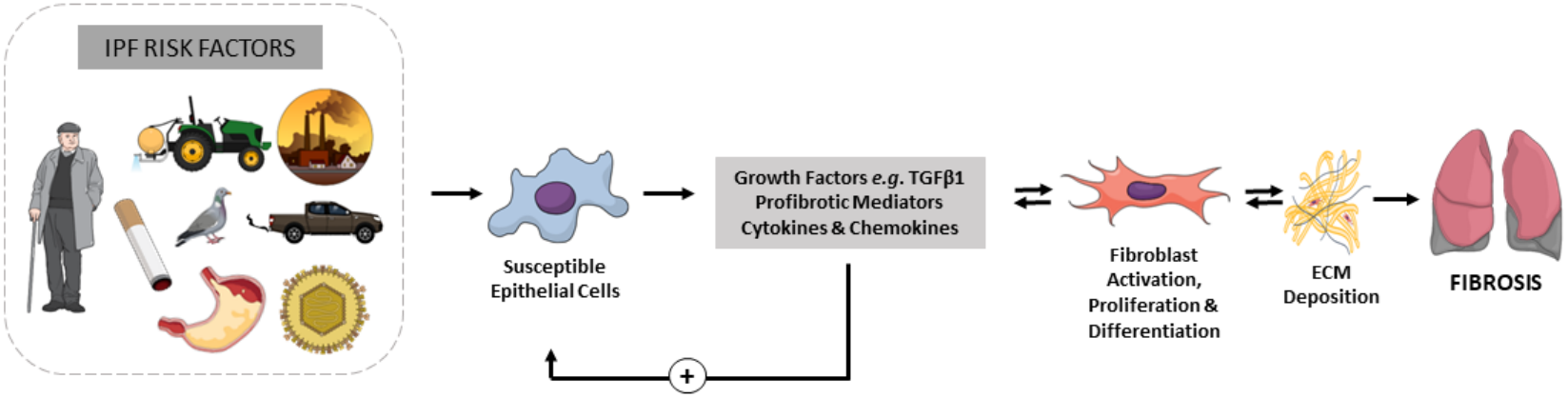

Figure 1.2 Summary of the mechanisms implicated in the initiation, development, and progression of IPF.
A complex interplay involving genetic predisposition, environmental triggers (*e.g.*, smoking, pollution and viruses), and host risk factors (*e.g.*, advanced age, male sex and comorbidities) results in the injury of susceptible distal airway and alveolar epithelium (initiation phase). The damaged/dysfunctional epithelium release a cocktail of profibrotic mediators (*e.g.*, TGFß and MMPs) which lead to fibroblasts activation and proliferation, fibroblast differentiation/myofibroblast expansion, and excessive extracellular matrix (ECM) deposition (development phase). The establishment of fibrosis (progressive phase) involves further activation of (myo)fibroblasts by the unrelenting increase in ECM stiffness thereby ensuring the destruction of functional lung tissue. IPF: idiopathic pulmonary fibrosis; MMPs: matrix metalloproteinases; TGF: transforming growth factor.

1.2.3. Current Therapies for IPF

Based on the premise that the disease was primarily driven by chronic inflammation, IPF patients were typically treated with corticosteroids (*e.g.*, prednisone) and immunosuppressants (*e.g.*, azathioprine) (Wilson and Wynn 2009). A two-drug combination of prednisone and azathioprine or a three-drug combination of prednisone, azathioprine, and the antioxidant, N-acetylcysteine were used to treat the disease (Raghu *et al*. 2012). However, neither class of drugs significantly improved clinical outcomes (Raghu *et al*. 1991; Selman *et al*. 2004). Furthermore, a Phase 3 trial of the three-drug combination regimen was terminated early due to increased mortality and hospitalisations compared to single-agent NAC or placebo (Raghu *et al*. 2012). In 2014, the US Food and Drug Administration (FDA) approved two anti-fibrotic drugs to treat IPF, pirfenidone and nintedanib, which slow decline in lung function (King *et al*. 2014; Richeldi *et al*. 2014). Although these therapeutic agents increase survival (Behr *et al*. 2020; Noor *et al*. 2021), they are associated with adverse events which limit drug tolerability (Galli *et al*. 2017). However, it is important to note that dose adjustment has been shown to improve the tolerability of both drugs without compromising therapeutic benefits (Maher and Strek 2019).

The underlying mechanisms of pirfenidone are yet to be fully elucidated. However, studies suggest that the therapeutic action of the drug is related to the suppression of TGFß gene expression (Iyer *et al*. 1998) and the translation of several pro-inflammatory cytokines (Nakazato *et al*. 2002). Nintedanib, a receptor tyrosine kinase inhibitor, inhibits FGF, PDGF and vascular endothelial growth factor (VEGF) signalling pathways which are essential for fibroblast proliferation, migration and activation (Fala 2015). The efficacy of both drugs might be due to their ability to target several profibrotic signalling cascades, which potentially slows down the replacement of parenchymal tissue with ECM, thereby reducing the decline in lung function (Conte *et al*. 2014; Wollin *et al*. 2015).

Since patients with significant comorbidities are typically excluded from clinical trials, it is currently unclear whether the anti-fibrotic agents improve symptoms associated with these comorbidities. This is especially important since the presence of comorbidities correlates with poor quality of life, contributes to disease progression, and increases mortality rate (Raghu *et al*. 2015). Therefore, there is an unmet clinical need in the treatment of IPF. New therapeutics should aim to target one or more of the following areas: slow, halt or reverse disease progression, improve symptom management and quality of life, and target comorbidities.

1.3. G Protein-coupled Receptors: Environmental Signal Integrators

G protein–coupled receptors (GPCRs) are a superfamily of signalling proteins, comprised of over 800 members, which transduce extracellular stimuli into intracellular signals (Fredriksson *et al*. 2003). The 5 main GPCR classes (glutamate, rhodopsin, adhesion, frizzled/taste2, and secretin) mediate responses to a diverse range of stimuli, including light, odorants, small molecules (such as amino acids and ions), and larger proteins (such as hormones and neurotransmitters) (Bockaert and Pin 1999). Once activated, the agonist-bound receptor interacts with heterotrimeric G proteins, resulting in the dissociation of the alpha (α) subunit from the beta-gamma (βγ) subunits which culminates in the regulation of processes such as gene expression and proliferation (Radeff-Huang *et al*. 2004). Due to their versatility, diversity and ubiquitous expression, GPCRs play essential roles in physiology. Thus, making this class of receptors an attractive target for drug development (Hauser *et al*. 2018). It is estimated that at least a third of all FDA approved drugs target GPCRs or their signalling machinery (Sriram and Insel 2018), and this number is set to increase as new functions for GPCRs are uncovered (Kroeze *et al*. 2003).

1.3.1. Role of G Protein-coupled Signalling in Pulmonary Fibrosis

Several GPCRs and their ligands (such as lysophosphatidic acid, endothelin, angiotensin and sphingosine-1-phosphate) have been implicated in the pathogenesis of PF, driving lung fibroblast recruitment and activation *in vitro* and organ fibrosis *in vivo* (Uguccioni *et al*. 1995; Tager *et al*. 2008; Huang and Natarajan 2015; Tan *et al*. 2018). Interaction of these ligands with their cognate receptors leads to the activation of key Gα proteins (G_i, $G_{q/11}$, and $G_{12/13}$), which induce a diverse range of downstream effectors, signalling cascades and transcriptional programs (Radeff-Huang *et al*. 2004; Flock *et al*. 2017). Activation of the G_i, $G_{q/11}$, $G_{12/13}$ and $G_{\beta\gamma}$ proteins contributes to cell proliferation, survival, and motility through the interaction of Rho and RAS/MAPK, PI3K/AKT, and Rho signalling pathways, respectively (Maekawa *et al*. 1999; Radeff-Huang *et al*. 2004) (Figure 1.3).

Activation of receptors coupled to the Gα protein, G_s (by ligands such as prostaglandin E2 and relaxin), activate adenylyl cyclase resulting in increased intracellular levels of cyclic adenosine monophosphate (cAMP), which inhibits profibrotic processes such as fibroblast activation, proliferation, contractility, and ECM protein expression (Bozyk and Moore 2011; Insel *et al*. 2012; Della Latta *et al*. 2013). However, loss of G_s-coupled GPCRs has been reported in IPF (Bozyk and Moore 2011; Tan *et al*. 2016).

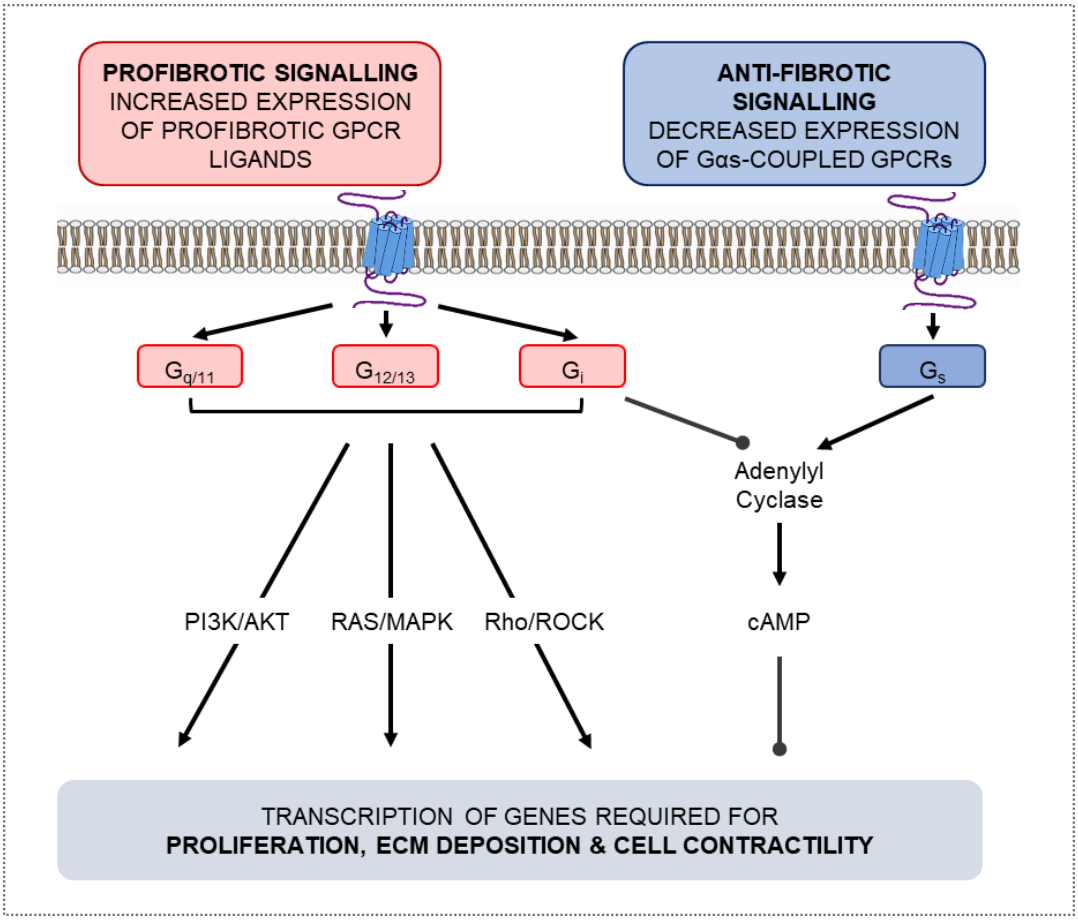

Figure 1.3 Role of G protein-coupled signalling in pulmonary fibrosis. Several profibrotic ligands implicated in IPF such as lysophosphatidic acid, endothelin, and serotonin activate G protein–coupled receptors (GPCRs) which signal via $G_{\alpha i/o}$, $G_{\alpha q/11}$, $G_{\alpha 12/13}$ activating multiple pathways including RAS/MAPK, Rho/ROCK, and PI3K/AKT. These pathways regulate profibrotic transcription factors required for fibroblast activation, proliferation, extracellular matrix (ECM) deposition, and cell contractility. Known transcript targets downstream of these pathways are the profibrotic genes: COL1A1, COL1A2, ACTA2, and CTGF. Gαs/cAMP signalling which protects against fibroblast activation and fibrosis is often repressed in IPF fibroblasts.

1.3.2 Targeting GPCR Signalling in IPF

Several drugs which target GPCRs are being developed for the treatment of IPF (Table 1.1).

Table 1.1 Clinical trials targeting GPCRs for IPF

Drug	Receptor activity	Outcomes	Status	Trial Number (Reference)
Bosentan	Endothelin receptor antagonist	No significant Improvements	Phase 3 (completed)	NCT00391443 (King *et al.* 2014)
PBI-4050	GPR40 agonist and GPR84 antagonist	Single/combination therapy was well tolerated	Phase 2 (completed)	NCT02538536 (Khalil *et al.* 2019)
BMS-986020	Lysophosphatidic acid receptor antagonist	Improved FVC (for the twice-daily group) compared to placebo	Phase 2 (completed)	NCT01766817 (Palmer *et al.* 2018)
Losartan	Angiotensin II receptor antagonist	Improved FVC	Pilot Study	NCT00879879 (Couluris *et al.* 2012)
Formoterol	ß2 Adrenergic agonist	Improved FEV_1 and forced expiratory flow	Pilot Study	EudraCT: 2013-004404-19 (Wright *et al.* 2017)
Ambrisentan	Endothelin receptor antagonist	The treatment group had more cases of disease	Phase 3 (terminated)	NCT00768300 (Raghu *et al.* 2013)

		progression and death compared to placebo		
Vismodegib	Smoothened antagonist	-	Phase 2 (terminated)	NCT02648048

However, the varied outcomes of these clinical trials highlight the difficulty in targeting this large and complex class of receptors. Since IPF is a multifaceted disease involving several cell types (Morse *et al*. 2019; Reyfman *et al*. 2019; Winters *et al*. 2019), completely inhibiting or amplifying all the signalling pathways downstream of a particular receptor could result in off-target effects with deleterious outcomes depending on where the GPCR is expressed (Luttrell 2014; Smith *et al*. 2018). Furthermore, the widespread expression of profibrotic GPCR ligands and the overlapping and convergent downstream signals would suggest a potential redundancy in the mechanisms which lead to fibroblast activation and pulmonary fibrosis (Haak *et al*. 2020).

Solutions to these challenges could utilise other well-known GPCR signalling mechanisms such as receptor modulation (Smith *et al*. 2018) and biased agonism (Kenakin and Christopoulos 2013). Some GPCRs can be allosterically modulated by ligands that bind to unique sites on the receptor, potentiating or dampening the effects of the main agonist; the key advantage of this mechanism is that the modulators only function when the main agonist is present (Christopoulos 2014). Biased agonism is a process through which structurally distinct agonists or modulators can stabilise specific GPCR signalling states, each activating or inhibiting a preferred subset of the intracellular signalling pathways coupled to a given receptor (Kenakin and Christopoulos 2013).

1.4. The Extracellular Calcium-sensing Receptor (CaSR)

In 1993, a novel GPCR responsible for the regulation of systemic calcium (Ca^{2+}) homeostasis was identified by Brown *et al*. (1993). Named after its primary physiological ligand, extracellular Ca^{2+} (Ca^{2+}_o), the calcium-sensing receptor (CaSR) is highly expressed in calcitropic organs (such as the parathyroid glands, kidneys and bone), which detect increases in free ionised extracellular Ca^{2+} concentration ($[Ca^{2+}]_o$) (Hannan *et al*. 2018a). The systemic response to CaSR activation is the suppression of calcium-retaining parathyroid hormone secretion and the inhibition of renal Ca^{2+} reabsorption, thereby maintaining $[Ca^{2+}]_o$ within the narrow physiological range of 1.1 – 1.3 mM (Riccardi and Brown 2010). The CaSR is also expressed by non-calcitropic organs, including by not limited to the skin (Komuves *et al*. 2002), vasculature (Schepelmann *et al*. 2016), heart (Sundararaman and van der Vorst 2021) and the lungs (Yarova *et al*. 2015), where it regulates differentiation, proliferation, inflammation, secretion and contractility. In the foetus, the CaSR is highly expressed in the respiratory system, nervous system and skeleton, where it plays a crucial role in lung growth, neurite outgrowth and growth plate development, respectively (Riccardi and Kemp 2012).

The CaSR receptor is a member of the family C GPCRs (Brown *et al*. 1993). This receptor family is comprised of 3 subclasses; group 1 consists of metabotropic glutamate receptors (mGluRs), group 2 consists of the CaSR and vomeronasal organ receptors and group 3 consists of γ-amino-butyric acid receptor family B (GABAB) receptors (Brown and MacLeod 2001). This family of receptors is characterised by an N-terminus that is folded into 2 domains which forms a ligand-binding cavity known as the Venus Flytrap (VFT) domain.

The CaSR is an obligate homodimer (Bai *et al*. 1998), with each protomer composed of 1078 amino acids with 4 structural domains (Hu and Spiegel 2007). These include a large extracellular N-terminal VFT domain, linked to a 7 transmembrane (7TM) domain via a cysteine-rich domain; the 7TM domain is followed by a long intracellular C-terminal domain (Figure 1.4) (Leach *et al*. 2020).

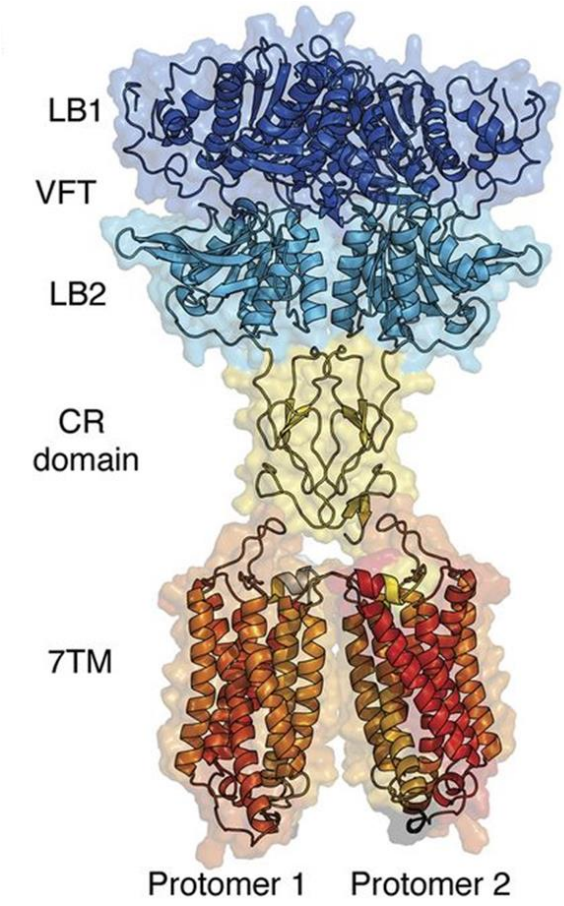

Figure 1.4 Current model of the calcium-sensing receptor (CaSR). The CaSR comprises an extracellular Venus Flytrap (VFT) domain composed of lobe 1 (LB1, dark blue) and lobe 2 (LB2, teal), and a cysteine-rich (CR) domain (yellow) anchored to the 7 transmembrane domain 7TM (orange) (Leach *et al*. 2020). Image used with permission.

1.4.1. Ligands of the CaSR

In addition to Ca^{2+}, the CaSR is activated by a wide range of orthosteric ligands such as polyvalent cations (Gd^{3+}, Al^{3+}, Mg^{2+}, Pb^{2+} and Cd^{2+}) (Handlogten *et al*. 2000; Brown and MacLeod 2001), polyamines (such as spermine and spermidine) which act as orthosteric and allosteric agonists (Quinn *et al*. 1997), and L-amino acids which act as endogenous positive allosteric modulators, increasing receptor affinity for Ca^{2+}_o (Conigrave and Hampson 2010). The receptor is also activated by polypeptides such as polyarginine and γ glutamyl peptides (*e.g*. glutathione) (Gerbino and Colella 2018).

The main binding sites for endogenous ligands are within the VFT motif; however, Ca^{2+} can also bind to sites within the 7TM and extracellular loop domain (Leach *et al*. 2014). Synthetic allosteric modulators typically bind to sites in the 7TM region and extracellular loops of the CaSR; examples include positive allosteric modulators (PAMs; such as cinacalcet) and negative allosteric modulators (NAMs; such as NPS2143), which increase and decrease receptor affinity for Ca^{2+}, respectively (Nemeth *et al*. 1998; Nemeth 2002). Aminoglycoside antibiotics (such as gentamycin and neomycin) also activate the receptor; however, their binding sites remain unknown (McLarnon *et al*. 2002; Ward *et al*. 2002).

1.4.2. Signal Transduction Pathways

The CaSR induces a wide array of intracellular signalling cascades by coupling to the $G_{q/11}$, G_i and $G_{12/13}$ protein subunits (Conigrave and Ward 2013). However, G_s signalling has also been reported in a pituitary tumour cell line and breast cancer cells (Mamillapalli *et al*. 2008; Mamillapalli and Wysolmerski 2010). CaSR-induced $G_{q/11}$ activity is considered the primary signal transduction pathway, involving the activation of phospholipase C (PLC), which hydrolyses phosphatidylinositol 4,5-bisphosphate (PIP) to 1,4,5-

tris-phosphate (IP_3) and diacylglycerol (DAG), leading to intracellular calcium (Ca^{2+}_i) mobilisation and protein kinase C (PKC) activation (Chang *et al*. 1998; Brennan and Conigrave 2009). For this reason, Ca^{2+}_i mobilisation is a common signalling read-out used to assess functional CaSR activation. Although the exact intracellular mechanisms and mediators activated by CaSR/$G_{12/13}$ signalling remain largely unknown (Leach *et al*. 2020), several studies have shown that CaSR ligands (such as amino acids) can activate the receptor inducing an increase in Ca^{2+}_i through a pathway dependent on $G_{12/13}$, Rho and the actin cytoskeleton (Rey *et al*. 2005). CaSR/$G_{12/13}$/RhoA signalling also plays a role in the Wnt/ß-catenin signalling cascade (Min *et al*. 2002).

CaSR coupling to G_i decreases intracellular cAMP levels by inhibiting the enzyme, adenylyl cyclase; upon dissociation from the G_i protein, the ßγ subunits mediate CaSR-induced RAS/MAPK activation and ERK1/2 phosphorylation (Chang *et al*. 1998; Kifor *et al*. 2001). The CaSR also activates other MAPK signalling cascades, including p38 MAPK and c-Jun N-terminal kinase (JNK), PI3K and mechanistic target of rapamycin (mTOR) pathways through pathways dependent on $G_{q/11}$ and G_i activation (Kifor *et al*. 2001; Tfelt-Hansen *et al*. 2003; Rybchyn *et al*. 2019). In addition to coupling to G-proteins, the CaSR intracellular domain also undergoes phosphorylation which facilitates receptor degradation and recycling (Breitwieser 2013).

Given that the CaSR is constantly exposed to activating concentrations of Ca^{2+}_o, the receptor has a unique regulatory feature known as agonist-driven insertional signalling (ADIS) to prevent desensitisation (Breitwieser 2013). Through ADIS, CaSR activation directly drives biosynthesis, maturation and shuttling of newly synthesised receptors from the endoplasmic reticulum to the cell membrane while endocytosis remains constitutively active (Grant *et al*. 2011). Therefore, unlike many other GPCRs, which undergo rapid

inactivation upon exposure to their agonists, signalling via the CaSR can be sustained, which is important for the receptor to perform its main function, *i.e.* “calcium-sensing”.

1.4.3. Biased Agonism and Biased Allosteric Modulation

As discussed in previous sections, the CaSR binds to a diverse range of endogenous ligands (including polyvalent cations, amino acids, and polyamines) and synthetic allosteric modulators (such as PAMs and NAMs). These ligands have been shown to induce biased signalling, resulting in the activation of distinct intracellular signalling pathways (Davey *et al*. 2012; Thomsen *et al*. 2012). For example, in immortalised human embryonic kidney cells overexpressing the CaSR (CaSR-HEKs), the preferred intracellular signals induced by Ca^{2+}_o and the polyamine, spermine is Ca^{2+}_i mobilisation and ERK1/2 phosphorylation, respectively, while L-amino acids activate both signals and inhibit cAMP synthesis (Lee *et al*. 2007; Thomsen *et al*. 2012). Synthetic compounds also exhibit biased modulation of the receptor; cinacalcet (PAM) and NPS2143 (NAM) preferentially potentiate or inhibit Ca^{2+}_o-induced Ca^{2+}_i mobilisation and membrane ruffling over ERK1/2 phosphorylation, respectively (Davey *et al*. 2012; Leach *et al*. 2016).

1.4.4. CaSR-related Disorders and CaSR-based Therapeutics

CaSR allosteric modulators have been developed as targeted therapies for parathyroid disorders and symptomatic hypercalcaemia and hypocalcaemia caused by loss- and gain-of-function CaSR mutations, respectively (Hannan *et al*. 2018b). *CASR* mutations and aberrant CaSR activity are responsible for several inherited disorders of mineral ion metabolism, for example, familial hypocalciuric hypercalcaemia (FHH) and neonatal severe hyperparathyroidism (NSHPT) (Brown 1997; Nemeth and Shoback 2013). NSHPT occurs due to homozygous inactivating mutations and is characterised by severe hypercalcaemia, under-mineralised bones and failure to thrive (Thakker 2004). FHH is an autosomal dominant disorder characterised by increased serum Ca^{2+}, normal PTH levels and decreased urinary Ca^{2+} excretion (Mrgan *et al*. 2014). FHH is caused by inactivating mutations in the *CASR* gene (FHH1), in one of the G proteins coupled to CaSR,

$G\alpha_{11}$ (*GNA11*, FHH2), or in adaptor-related protein complex 2, sigma 1 subunit (FHH3), which is involved in receptor endocytosis (Nesbit *et al*. 2013). On the hand, gain-of-function mutations in the *CASR* or *GNA11* genes lead to autosomal dominant hypocalcaemia (ADH) with hypercalciuria type 1, type 2 and type 5 Bartter syndrome (Nemeth and Shoback 2013; Nesbit *et al*. 2013; Letz *et al*. 2014).

Small molecule PAMs (also known as calcimimetics), which decrease PTH secretion and plasma calcium levels, are used for the treatment of hyperparathyroid disorders (Nemeth and Fox 1999; Nemeth and Shoback 2013). Cinacalcet, a phenylalkylamine compound, was the first FDA approved calcimimetic to be licensed for the treatment of hyperparathyroidism secondary to chronic kidney disease and inoperable forms primary hyperparathyroidism and parathyroid cancer (Nemeth and Goodman 2016). PAMs have also effectively treated patients with FHH1-3 and a subset of NSHPT patients (Hannan *et al*. 2018b).

Small molecule NAMs (also known as calcilytics) were initially investigated to treat osteoporosis, as they evoke a transient rise in PTH secretion, which had bone anabolic effects in preclinical models (Nemeth 2002). These compounds consist of two main classes: amino alcohols (such as ronacaleret, NPSP795 and JTT-305/MK-5442) and quinazolinones (such as AXT914 and ATF936) (Nemeth and Goodman 2016). NPS2143 was the first selective NAM to be developed (Gowen *et al*. 2000) and was subsequently modified to generate clinical-grade compounds such as ronacaleret and NPSP795 (Kumar *et al*. 2010). Although deemed safe and well-tolerated, the development of ronacaleret, NPSP795, JTT-305/MK-5442 and AXT914 was terminated after Phase II trials due to lack of efficacy for osteoporosis (Kumar *et al*. 2010; Fitzpatrick *et al*. 2011; Halse *et al*. 2014; John *et al*. 2014). These compounds have been investigated and are currently being considered for

repurposing as potential therapies for ADH (Hannan *et al*. 2018b) and asthma (Yarova *et al*. 2020).

1.4.5. Studies that have led to my PhD project

The CaSR is essential for embryological lung development, where it promotes lung expansion by regulating fluid secretion and branching morphogenesis (Finney *et al*. 2008; Riccardi *et al*. 2013; Brennan *et al*. 2016). Receptor expression peaks in late gestational stages (where the systemic prenatal environment is relatively hypercalcaemic (~1.6–1.7 mM in comparison to the adult) (Riccardi *et al*. 2013). There is a lack of data on the expression and physiological function of the CaSR in the adult lung. However, data from the protein atlas (Uhlén *et al*. 2015) and other studies have shown that the receptor is expressed in ciliated/alveolar epithelial cells (Uhlén *et al*. 2015), pulmonary neuroepithelial cells (Lembrechts *et al*. 2013), the large airways (Yarova *et al*. 2015), and the pulmonary vasculature (Tang *et al*. 2016).

1.4.5.1. Asthma and chronic obstructive pulmonary disease (COPD)

Over the last decade, several studies have demonstrated the role of the CaSR in chronic lung inflammation and remodelling. Airway remodelling is a prominent feature of inflammatory lung diseases (such as asthma and COPD) which involves structural changes in the small and large airways as a result of airway smooth muscle cell proliferation, fibroblast activation, excessive ECM deposition and subepithelial fibrosis (Jindal 2016; Jones *et al*. 2016; Hough *et al*. 2020). Studies from our laboratory showed that CaSR expression is increased in asthmatic patients and that endogenous polyamines acting at the receptor induce airway hyperresponsiveness and inflammation (Yarova *et al*. 2015). Furthermore, the CaSR also mediates inflammation and remodelling in experimental models of COPD (Yarova *et al*. 2016; Lee *et al*. 2017). Importantly, NAMs abrogate the pathological changes observed in these models of inflammatory lung disease (Yarova *et al*. 2015; Yarova *et al*. 2016; Lee *et al*. 2017; Yarova *et al*. 2020).

1.4.5.2. Pulmonary arterial hypertension (PAH)

Pulmonary hypertension frequently occurs in PF patients and is a major determinant of mortality in this patient group (Ruffenach *et al*. 2020). It is characterised by vascular remodelling, which stems from increased pulmonary arterial smooth muscle cell (PASMC) proliferation and decreased PASMC apoptosis (Smith *et al*. 2016). CaSR expression and $[Ca^{2+}]_i$ was increased in PASMC from patients with idiopathic PAH and animals with experimental pulmonary hypertension (Yamamura *et al*. 2012). Furthermore, genetic or pharmacological blockade of the CaSR attenuated Ca^{2+}-induced increase in $[Ca^{2+}]_i$, proliferation of IPAH PASMCs, vascular remodelling and inhibited the development/progression of experimental pulmonary hypertension (Yamamura *et al*. 2012; Guo *et al*. 2013; Tang *et al*. 2016; Tan *et al*. 2020).

1.4.5.3. Cardiac and lung fibrosis

Cardiac fibrosis develops due to sustained pressure from systemic or pulmonary hypertension, myocardial injury or heart failure (Andersen *et al*. 2019). The overarching changes observed are reminiscent of PF, namely, fibroblast activation and proliferation, excessive ECM and collagen deposition (Sundararaman and van der Vorst 2021). Furthermore, CaSR expression is upregulated by profibrotic factors (such as angiotensin and insulin) in cardiac fibroblasts, resulting in increased $[Ca^{2+}]_i$, TGFß1 expression, proliferation, ECM and collagen production (Rybczyńska *et al*. 2017; Chi *et al*. 2018; Yuan *et al*. 2019). Of note here is that NAMs of the CaSR exert anti-fibrotic effects *in vitro* and attenuate the development of myocardial fibrosis *in vivo* (Zhang *et al*. 2014; Lu *et al*. 2018; Yuan *et al*. 2019; Yuan *et al*. 2020). In support of these findings, studies from our laboratory showed that targeted deletion of the *Casr* gene from SM22α-expressing cells (*i.e*. smooth muscle cells and fibroblasts) protects 15-month-old mice against age-related cardiac fibrosis (Schepelmann *et al*. 2016). In this study, control (Cre-negative) and knock-out (KO;

$^{SM22\alpha}Casr^{\Delta flox/\Delta flox}$) animals were generated by breeding LoxP CaSR mice with SM22α-Cre recombinase mice as described previously (Schepelmann *et al*. 2016). Using the same mouse model, I conducted a preliminary study to determine whether the CaSR contributes to naturally occurring, age-related lung fibrosis. Masson's trichrome stained lung sections from 15-month-old control mice reveal significantly more extensive fibrosis, thicker interstitial walls and damage to the lung architecture compared with age-matched KO mouse lung sections (p = 0.01) (Figure 1.5, A-C). The absence of the CaSR from SM22α^{+} cells is also associated with a moderate reduction in collagen deposition around the small airways (p<0.02) (Figure 4.1D). Therefore, this preliminary study suggests that the CaSR mediates age-related remodelling of mouse lung parenchyma, and provides a rationale to study the role of the receptor in PF.

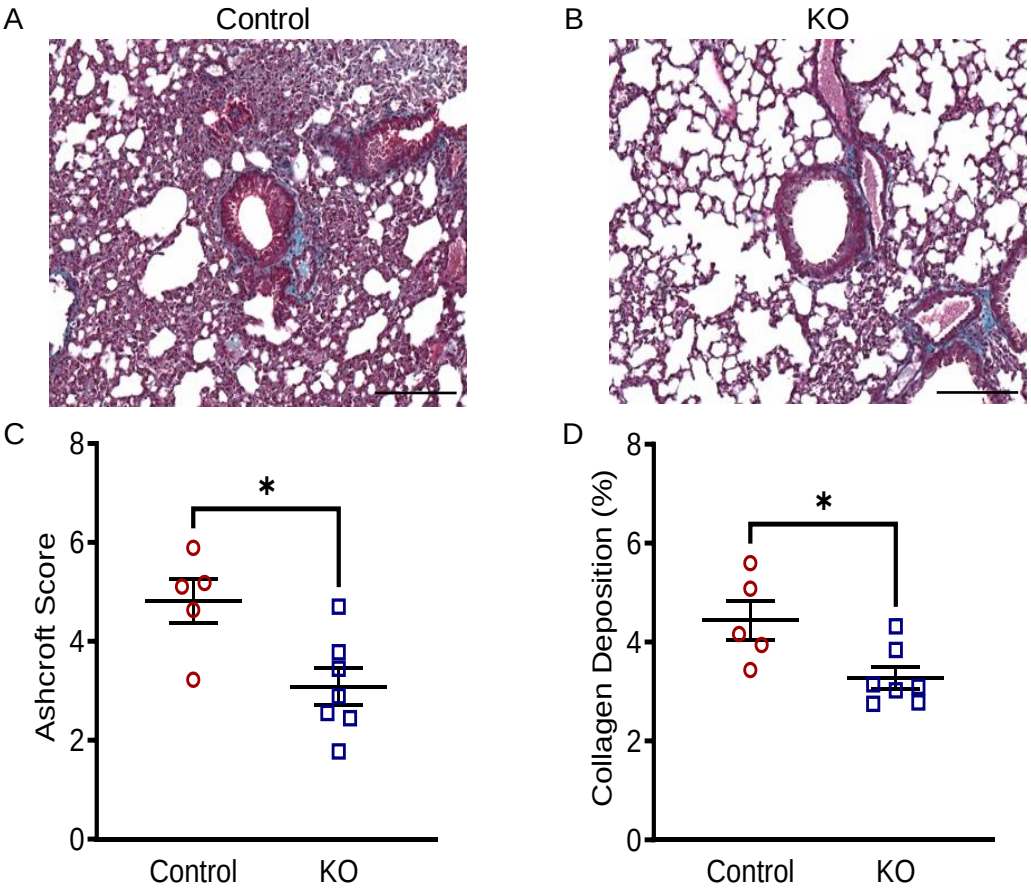

Figure 1.5 Targeted calcium-sensing receptor (CaSR) deletion from SM22α^{+} cells protects mice from age-related lung fibrosis. **A-B.** Histology of lungs from 15 month-old Control mice shows significant fibrotic remodeling compared to lungs from age-matched mice with targeted CaSR deletion (KO); **C.** quantified using the Ashcroft score. **D.** Collagen deposition is significantly decreased around the airway lumen of KO mice compared to control. CaSR gene was selectively deleted downstream of the SM22α promoter using the Cre-Lox system; Cre-negative (Control), $^{SM22\alpha}Casr^{\Delta flox/\Delta\alpha}$ (KO). Collagen deposition was quantified using StrataQuest - collagen expression (density of blue pixels) is presented as a percentage of the total lung surface area up to 10 μm away from airway lumen (%). Data are expressed as mean ± SEM. 2-tailed Student's t test, * $p<0.05$. $N = 5$ (Control); 7 (KO). Scale bar: 100 μm (**A-B**). *SM22α: smooth muscle-associated protein of 22kDa.*

1.5. Aims and Hypothesis

The novel and potentially beneficial effects of CaSR NAMs (which are referred to as NAMs from here on) in asthma, COPD, PAH, and cardiac fibrosis hold great promise for PF since these diseases are major comorbidities which share common pathological mechanisms (such as the activation of CaSR, the induction of TGF-β signalling and its downstream mediator, CTGF which result in excessive collagen production by fibroblasts and destructive tissue remodelling (Ahmed *et al*. 2004; Murtha *et al*. 2017; Luppi *et al*. 2021). However, the role of the CaSR in PF pathogenesis remains unknown. Therefore, during my PhD, I aimed to elucidate the role of the receptor and the effect of NAMs in PF, with a specific focus on lung fibroblasts, the principal cellular mediators of the disease.

Given the central role fibroblasts play in PF, they represent viable targets for the prevention, reduction, and reversal of scar tissue accumulation *in vivo*. The proof-of-concept studies presented in this thesis aim to examine whether the CaSR is involved in the profibrotic processes implicated in PF and whether the inhibition of the CaSR with the prototypical NAM, NPS2143, attenuates TGFβ-mediated profibrotic processes in activated lung fibroblasts, thus, providing a rationale for the pharmaceutical development of inhaled NAMs as novel therapeutic agents for the treatment of pulmonary fibrosis. Specifically, this project aims were to:

1. Establish CaSR expression in healthy and IPF lungs.
2. Investigate the expression of relevant CaSR activators in IPF patient saliva.
3. Determine the expression and function of the CaSR in primary normal human lung fibroblasts (NHLFs) *in vitro*.
4. Assess the effects of NPS2143 on cellular and molecular profibrotic responses to TGFβ1 *in vitro*.

This project will explore the hypothesis that the CaSR contributes to the pathogenesis of PF, and treatment with the NAM, NPS2143 will attenuate this process.

CHAPTER 2: METHODS

2.1. Human studies

2.1.1. CaSR expression in human lung tissue

2.1.1.1. Lung tissue collection

Human lung biopsy samples were taken from IPF patients for diagnostic purposes. IPF diagnosis was established in accordance with the diagnostic criteria (King *et al*. 2000). All data were link anonymised before the paraffin lung tissue blocks were obtained from consultant pathologist, Prof. Richard Attanoos (University Hospital of Wales, Cardiff). Regional ethical approval was obtained from Cardiff and Vale University Health Board. These samples were collected before 2006, for which consent is waived; however, the Human Tissue Act guidelines were followed. The control lung sections originate from regions adjacent to lung tumours, identified as histologically 'normal' by a thoracic pathologist. These paraffin lung tissue blocks belong to an archive for practical microscopic histology student courses and are not linked to patients or patient data. Prof. Dirk Adriaensen and Dr Line Verckist (University of Antwerp) provided control lung samples and assistance with immunohistochemistry.

2.1.1.2. Immunohistochemistry

Paraformaldehyde-fixed biopsies from human lungs were sliced into serial 5 µm-thick paraffin sections. Sections were mounted on poly-L-lysine-coated microscope slides, dried at 37°C (overnight), and processed for immunolabeling. Sections were deparaffinised in xylene and rehydrated in an ethanol series. For antigen retrieval, slides were boiled (95°C, 40 min) and cooled (room temperature, 20 min) in citrate buffer, pH 6.1. After retrieval, slides were rinsed in phosphate-buffered saline (PBS; pH 7.4; 2x5 min). All primary and secondary affinity-purified antibodies were diluted in PBS containing 10% non-immune serum of the host species of the secondary antibodies and 0.1% bovine serum albumin (BSA; blocking buffer). Prior to the immunohistochemical procedures, endogenous peroxidase activity in the

lung sections was blocked by H_2O_2 (3% in 50% methanol in PBS; 10 min). Afterwards, sections were preincubated (60 min) with blocking buffer containing 1% Triton-X-100, and incubated overnight with different primary antibodies (rabbit anti-human αSMA polyclonal antibody, 1:100, #ab5694; mouse anti-human CaSR mAb, 1:200, #ab19347; rabbit anti-human GRP polyclonal Ab, 1:1000, #ab22623; all Abcam, Cambridge, UK) on consecutive lung sections. Separated by rinsing steps in PBS (6 x 5 min), the sections were sequentially incubated with the secondary (DAM-BIOT, 1:500; DAR-BIOT, 1:500; Jackson ImmunoResearch, Cambridgeshire, UK) and ExtrAvidin-horseradish peroxidase (HRP, 1:1000 in PBS; Sigma-Aldrich, Gillingham, UK) for two hours. HRP enzyme activity was visualised using 3,3'-diaminobenzidine (DAB; Dako, Heverlee, Belgium) as a chromogen while monitoring formation of the brown precipitate under the light microscope, and the reaction was stopped by rinsing in distilled water. Finally, cell nuclei were counterstained with haematoxylin, and the lung sections were mounted in DPX standard aqueous mounting medium (Atom Scientific, Cheshire, UK). Negative control staining was performed by preabsorption and replacement of the CaSR antibody with custom-made CaSR-ADD antigenic peptide and IgG2a isotype control, respectively.

2.1.2. Metabolomics

2.1.2.1. Patient samples

The study "Novel Technologies for Diagnosing and Monitoring Respiratory Diseases" obtained regional ethical approval from Hywel Dda University Health Board (16/WA/0036). The study was conducted in accordance with the Helsinki principles (WMA 2013). Written informed consent was obtained from all participants at least 24 hours before sampling, at a previous clinical appointment, and all data was link anonymised by Prof. Luis Mur before analysis. Eligibility included a diagnosis of IPF/UIP at the time of sample collection, which was determined at regional respiratory multidisciplinary team meetings.

Control saliva samples were collected from spouses accompanying patients attending clinics. The study involved 6 patients with IPF (mean age 81 ± 5 yrs, 67% male) and 6 control participants (mean age 70 ± 14 yrs, 33% male) (Table 2.1). Data were analysed using Prism 9.0 software package (GraphPad Inc.). Quantitative data are shown as mean ± SEM.

Table 2.1 Demographic data in the study population: age, gender, and smoking status at the time of sample collection (data expressed as mean ± SEM)

	Controls (*N* = 6)	**IPF (*N* = 6)**	***p***
Age (years)	69.8 ± 5.7	81.2 ± 2.1	0.09
Sex (male:female)	2:4	4:2	0.29
Smoking Status	Never: 2 Ex-smoker: 4	Never: 2 Ex-smoker: 4	-

Statistical comparisons were performed on normally distributed data (determined by the Shapiro-Wilk's test) using an unpaired Student's t-test; *p*-values < 0.05 were considered significant. No statistical differences in patient demographics were observed. Spontaneous saliva samples were collected and stored at -80°C, then processed by Dr Rachel Paes de Araújo (Aberystwyth University) as described in Sections 2.1.2.2 and 2.1.2.3. The anonymised metabolomic patient data were provided and subsequently analysed as described in Sections 2.1.2.4.

2.1.2.2. Metabolite Extraction

Frozen saliva samples were thawed at 4°C. 50 µL of sample was transferred to a sterile 2 mL microcentrifuge tube, to which 7.5 mg of ≤ 106 µM acetone-washed glass beads (Sigma-Aldrich) were added. Samples were vortexed for 5 seconds, and 380 µL of High-performance liquid chromatograph (HPLC) grade-methanol and chloroform (4:1) was added. Samples were shaken on a microtube thermos shaker for (Favorgen Biotech Corp, Taiwan) for 20 minutes at 4°C then stored at -20°C for 20 minutes to allow protein precipitation. Afterwards, samples were centrifuged at 11000 x g for 6 minutes at 4°C and the supernatant added to a sterile 2 mL microcentrifuge tube. A 100 µl aliquot of the extraction (supernatant) was transferred to a 2 mL 11mm glass vial (Kinesis Scientific Experts, Cambridgeshire, UK) with 200 µL inserts (Thermo Fisher Scientific, Loughborough, UK) and sealed for flow infusion electrospray high-resolution mass spectrometry (FIE-HRMS). Samples were stored at -20°C until FIE-HRMS analysis.

2.1.2.3. Targeted metabolite fingerprinting by flow infusion electrospray high-resolution mass spectrometry (FIE-HRMS)

FIE-HRMS was used to evaluate the potential of saliva as a source of non-invasive polyamine biomarkers for IPF.

FIE-HRMS was performed using a Q exactive plus mass analyser instrument with UHPLC system (Thermo Fisher Scientific, Bremen, Germany), where mass/charge metabolites fingerprints were generated in positive and negative ionisation mode in a single run, as previously described by Baptista *et al*. (2018). All samples were run in duplicate.

2.1.2.4. Statistical analysis

Data were analysed with MetaboAnalyst 4.0 using R and Bioconductor packages (Xia *et al*. 2009). A data filtering parameter was applied to identify

and remove variables that were unlikely to be used when modelling the data based on the interquantile range (IQR) (Hackstadt and Hess 2009). The data were normalised by log transformation and pareto scaling (Dieterle *et al*. 2006). The univariate analyses used Student's 2-tailed t-test to identify significant m/z, p-value < 0.05. Principal component analysis (PCA) was used to distinguish the difference between the two sample groups. The matched compound and pathway identification were carried out using the *mummichog* algorithm within Metaboanalyst 4.0. Compounds were identified based on mass-to charge (*m/z*), the *p-value* and t-score, which were used to interrogate the KEGG library. This led to metabolite identification after considering all potential matched isotopes/adducts.

2.2. *In vitro* studies in primary human lung fibroblast

2.2.1. Preparation of Transforming Growth Factor Beta 1

Recombinant human transforming growth factor beta1 (TGFß1; R&D Systems, Inc., Oxford, UK; #240-B-002/CF) was reconstituted to 20 µg/mL in sterile 4 mM HCl containing 0.1% BSA. The solubilised stock was diluted to 500 ng/mL aliquots then stored at -20°C to minimise freeze-thaw effects. When required, diluted aliquots were thawed at room temperature, and a final experimental concentration of 5 ng/mL was used in the experimental medium (Section 2.2.5). Vehicle control solutions were also prepared using the same serial dilutions for HCl and BSA stock.

2.2.2. Preparation of CaSR Negative Allosteric Modulator, NPS2143

NPS2143 was purchased from Abcam (Cambridge, UK). The compound was solubilised in dimethyl sulfoxide (DMSO, >99.7 %; Sigma-Aldrich) under sterile laboratory conditions (Section 2.2.1). Powdered batches of NPS2143 were solubilised in 100% DMSO to produce 10 mM stock concentrations. The solubilised stock was diluted to 100 µM aliquots then stored at 4°C. The diluted aliquots (10 µL) were stored at -20°C to minimise freeze-thaw effects

and to ensure compound stability. When required, diluted aliquots were thawed at room temperature, and a final experimental concentration of 1 µM was used in the experimental medium (Section 2.2.5). Vehicle control solutions were also prepared in the experimental medium using the same serial dilution steps described in Sections 2.2.1 and 2.2.2, containing final concentrations of HCl (1 µM), BSA (0.000025%), DMSO (0.01%) to account for the presence of these diluents in compound-containing media.

2.2.3. Cell culture conditions

All consumables and equipment used for culturing cells were disinfected with 70% ethanol before commencing cell culture. The water bath and incubators were deep cleaned and sterilised weekly and monthly, respectively. Tissue culture consumables were purchased, sterilised and wiped with 70% ethanol before use.

Growth medium (Section 2.2.2), experimental medium (Section 2.2.3), foetal bovine serum (FBS), and 0.25% trypsin/0.53 mM ethylenediaminetetraacetic acid (trypsin-EDTA) were warmed to 37 °C in a water bath before use. Trypsin-EDTA and sterile distilled water (dH_2O) were purchased from Thermo Fisher Scientific (Loughborough, UK). Sterile OmniPur 10X phosphate buffered saline (PBS) was purchased from Merck Life Science (Gillingham, UK) and diluted with dH_2O to 1X working solution when required. Except otherwise stated culture vessels were purchased from Corning Costar (Buckinghamshire, UK).

2.2.3.1. NHLF growth medium

Lonza custom fibroblast growth medium (FGM-2) containing basal medium (FBM) (CC-3131) and FGM SingleQuots supplements (CC-4126): insulin, human fibroblast growth factor-B (hFGF-B), foetal bovine serum (FBS), gentamicin and amphotericin-B solution.

2.2.3.2. NHLF experimental medium

The experimental medium contained FBM, insulin, hFGF-B, and reduced serum (0.1% FBS).

The reduced serum conditions allowed cell-cycle synchronisation via growth arrest at the G_0 stage. Cell treatments and experiments were performed in the experimental medium to avoid potential effects from serum factors on profibrotic responses or gene expression.

Antibiotics were removed from the experimental medium as aminoglycoside antibiotics (such as gentamicin) are activators of the CaSR (McLarnon et al. 2002; Ward et al. 2002).

2.2.3.3. Cell culture

Human primary lung fibroblasts from normal patients (CC-2612) were purchased from Lonza (Slough, UK) in cryopreserved ampules. Donor ages range from 56 to 67 years (*N* = 4, 2 males and 2 females: Table 2.2).

Table 2.2: Primary Human Lung Fibroblast (NHLF) Donor Characteristics

	Age (years)	Sex	Ethnicity
Donor 1	57	Female	Caucasian
Donor 2	67	Male	Caucasian
Donor 3	56	Male	Black
Donor 4	66	Female	Black/Hispanic

NHLFs were cultured according to the protocol provided by Lonza. Briefly, a monolayer of fibroblasts was cultured by seeding cells at 5×10^3 cells/cm^3

in sterile 8-chamber Millicell EZ slides (Merck Life Science, UK), 6-well and 96-well plates. Cells were cultured in growth medium and changed to experimental medium when experiments commenced. Experiments were conducted between passages 2 and 4. NHLF seeding densities were optimised with the help of Dr Jordanna Dally (Cardiff University, School of Dentistry).

The cryopreserved NHLFs were immediately stored in liquid nitrogen until required. To set up cultures, culture flasks with 10 mL of growth medium were equilibrated in a 37°C, 5% CO_2 humidified incubator for 30 minutes, and the NHLF cryovials were wiped with 70% ethanol. NHLFs were quickly thawed (in <2 minutes) at 37°C in a sterile water bath (without completely submerging the vial). The cells were re-suspended into the prepared 75 cm^2 cell culture flasks and returned to the incubator with media changes every 48 -72 hours. Once the cells were 70 - 80% confluent, cells were either frozen (Section 2.2.8) or seeded into experimental vessels based on the experimental protocol (see Section 2.2.9).

2.2.3.4. Sub-Culture and Cell Counting

On reaching optimal confluence (Section 2.2.6), NHLFs were sub-cultured in 75 cm^2 flasks with the following reagents and were scaled down if 25 cm^2 culture flasks were used. For every 75 cm^2 of cells to be sub-cultured, growth medium was aspirated, and cells were rinsed with 1X Omnipur PBS to remove any residual traces of medium. NHLFs were evenly covered with 3 mL of 0.25 % trypsin-EDTA (Thermo Fisher Scientific) and incubated for 3-5 min at 37°C to ensure cells had detached from the flask. Following incubation and flask agitation, NHLFs were examined with a brightfield microscope to ensure detachment. Once cells were released, 6 mL of room temperature growth medium was added to the flask to neutralise protease activity, and the total volume was transferred into a 15 mL falcon tube and centrifuged for 5 min at 500 x g. After aspirating the supernatant, the cell pellet was re-suspended in 1 mL growth medium.

Luna™ automated fluorescence cell counter with Trypan Blue (0.4%) staining kit (Labtech, East Sussex, UK) was used to determine cell count and cell viability according to the manufacturer's instructions. Briefly, 10 µL aliquot of the cell suspension was mixed with 10 µL of Trypan Blue. 10 µL of this mixture was loaded into the chamber port on the Luna™ cell counting slide, and then the slide was inserted into the slide port of the counter. "With Trypan Blue (1:1)" staining option was selected, focus adjusted, and the cells were counted by choosing the "Count" button. The cell count and viability results appear on the screen of the counter. Live cells with intact cell membranes exclude Trypan Blue. The dye forms halos around live cells and stains the cytoplasm of dead cells or cells with compromised membranes. Counting was done in duplicate, and average cell number and viability was recorded. Once the cell number and viability were assessed, the cell suspension was further diluted with warmed growth medium to achieve the appropriate density then seeded into new cell culture flasks (10 mL growth medium/75 cm^2).

2.2.3.5. Cryopreservation, Storage and Revival

Excess cells obtained from various passages were routinely stored with passage number, date and sample ID noted. Cell pellets produced through the sub-culture process (Section 2.2.7) were re-suspended in freezing medium, consisting of 40% growth medium, 50% FBS, and 10% DMSO for cryopreservation. 1 mL cell suspensions were transferred into cryovials (Greiner Bio-One, Stonehouse, UK) and cooled slowly (1°C/minute) in isopropanol-containing freezing vessels (Sigma-Aldrich). After 24 hours at -80°C, the cryovials were transferred to liquid nitrogen (196°C) for long-term storage. When needed, cryopreserved NHLFs were retrieved and revived as previously described (Section 2.2.6).

2.2.4. Experimental protocol

NHLFs were seeded at 5 × 10^3 cells/cm^3. Once they reached 50 – 60% confluence, the growth medium was replaced with experimental medium, and NHLF were divided randomly into four groups: (1) vehicle control: treated with 0.01% DMSO; (2) NAM: treated with 1 µM NPS2143; (3) TGFβ: treated with 5 ng/mL TGFβ1; (4) TGFβ + NAM: pre-treated with 1 µM NPS2143 for 4 hours followed by 5 ng/mL TGFβ1. Treatment was carried out for 72 hours (Figure 2.1). Only cells in the vehicle control group were used for the experiments aimed at measuring intracellular free ionised calcium ($[Ca^{2+}]_i$). Cells were maintained at 37°C under humidified conditions in a 5% CO_2 incubator with media changes every 48 -72 hours.

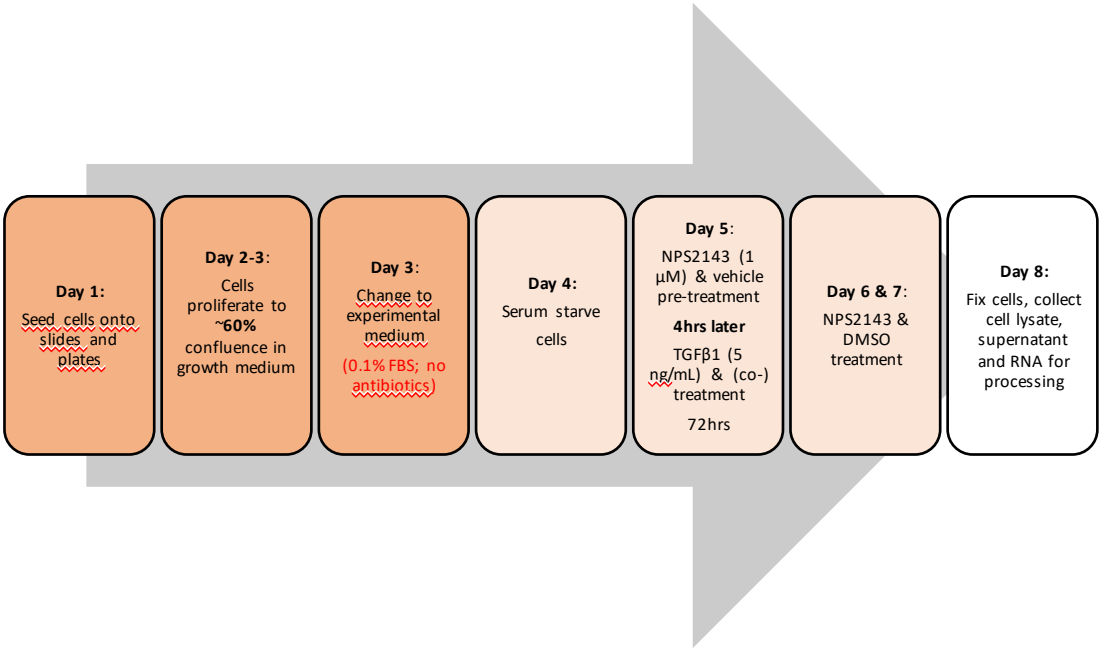

Figure 2.1 Experimental protocol for *in vitro* NHLF studies.

2.2.5. Measurements of intracellular free ionised calcium ($[Ca^{2+}]_i$)

Single-cell fluorescence Ca^{2+} imaging experiments were performed using a monochromator-based fluorimeter system (OptoFluor; Cairn Research, Kent, UK) and the ratiometric dye, Fura-2 Acetoxymethyl (Fura-2 AM) ester. Fura-2 AM is permeable to the cell membrane and cleaved into its active form, Fura-2, by cytosolic esterases (Farley 1994). Fura-2 is a double-wavelength indicator used to monitor cytoplasmic Ca^{2+} levels through a shift of fluorescence excitation spectrum toward shorter wavelength upon

Ca^{2+} binding (Grynkiewicz *et al*. 1985). Ca^{2+}-free Fura-2 molecules have maximum excitation wavelengths of ~380 nm, and Ca^{2+}-bound molecules have maximum excitation wavelengths of ~340 nm, while the maximum fluorescence emission wavelength detected for both forms is ~510 nm (Zanin *et al*. 2019). Therefore, cytoplasmic [Ca^{2+}] is proportional to the ratio of fluorescence intensity at the two different Fura2 excitation wavelengths (340/380) (Figure 2.2).

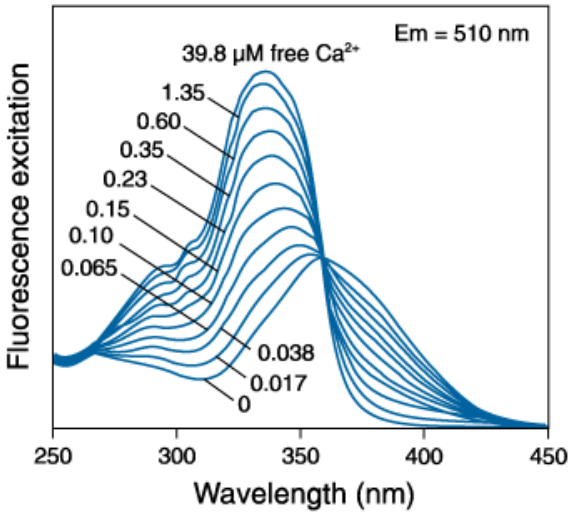

Figure 2.2 Fluorescence excitation spectra of Fura-2 in solutions containing 0 - 39.8 µM free Ca^{2+}. Fluorescence intensity at wavelengths of ~340 nm is directly proportional to free Ca^{2+} while at wavelengths of ~380 nm, fluorescence intensity is inversely proportional to free Ca^{2+} concentration. At low concentrations of the dye, the 340/380 nm excitation ratio allows accurate measurements of intracellular Ca^{2+} (Ca^{2+}_i) within the range of ~100 nM (under resting conditions) and ~1 µM (upon cell activation) (Bagur and Rgy Hajnó Czky 2017). Ratiometric measurements reduce the effects of uneven dye loading, dye leakage, photobleaching, and problems associated with measuring Ca^{2+}_i in cells of unequal thickness. Image taken from the Thermo Fisher Scientific website (Thermo Fisher Scientific).

NHLFs were sub-cultured as described in Section 2.2.9. Cells were seeded as 40 µL drops in the middle of PDL-coated 13mm glass coverslips in 24-well plates and returned to the incubator for 30 minutes. Coverslips were

examined with a brightfield microscope to ensure proper attachment. Once attached, 500 µL of growth medium was added to each well. At ~60% confluence, the growth medium was replaced with experimental medium for 48-72 hours before conducting Ca^{2+} imaging experiments.

Standard extracellular solution (ECS, Table 2.3) was made for each experiment. NaOH was added dropwise to ensure pH was between 7.38 – 7.42; pH was checked using a Mettler-Toledo pH meter (Leicester, UK). To conduct experiments, NHLF coverslips were transferred into the loading buffer (which comprised of standard ECS and 0.2% BSA) and 2 µM Fura-2 AM (Thermo Fisher) at 37°C for 1 hour. Fura-2 AM-containing solution was aspirated and replaced with loading buffer alone. The loaded NHLF coverslips were kept in the dark at room temperature.

Table 2.3 Standard Extracellular Solution

Component	Final Concentration (mM)
NaCl	135
KCl	5
$MgCl_2$	1.2
$CaCl_2$	1.25
Glucose	10
HEPES	5

Coverslips were placed in the perfusion chamber mounted on an inverted microscope (Olympus IX71, Olympus UK & Ireland, Essex, UK) and continuously perfused with a slow flow of standard ECS using a rapid perfusion system (RSC160, Intracel RSC160, Intracel, Royston, UK). Cells were manually selected from the mounted coverslip using the MetaMorph microscopy automation system (Cairn Research, Kent, UK). Loaded cells were alternately excited at 340 and 380 nm through a 40x quartz. The oil immersion objective and emission from each wavelength were measured at

505 nm using a charge-coupled device camera (Hamamatsu Orca, Tokyo, Japan) which coverts electrical signals into images; images were taken every 2 seconds. Figure 2.3 shows an image of the $Ca^{2+}{}_i$ imaging system.

Figure 2.3 Image of the $Ca^{2+}{}_i$ imaging system. Coverslips were placed in the perfusion chamber (inset) mounted on an inverted microscope (Olympus IX71) and continuously perfused with a slow flow of standard ECS using a rapid perfusion system (RSC160, Intracel RSC160, blue arrow). The RSC system allows constant flow of different experimental solutions at times programmed into the MetaMorph microscopy automation system (Caim Research). To the left of the perfusion chamber is a suction tube which slowly aspirates the solutions in chamber without disrupting the coverslip.

Individual $[Ca^{2+}]_i$ responses were obtained from single cells by defining regions of interest on the OptoFluor software. All intensities were background-subtracted before the 340:380 emission ratio was used to calculate maximal fold-change from baseline. Cells were initially perfused with standard ECS for 2 minutes at room temperature to establish a baseline $[Ca^{2+}]_i$ level. The RSC was used to apply the following compounds for 3 minutes in the presence and absence of NPS2143: 5 mM $[Ca^{2+}]_o$, 5 mM ornithine, and 1 mM spermine. 200 μM ATP was used as a positive control to

assess cell viability. When NAM was used, cells were incubated with the NAM, NPS2143 (1 μM) for 20 min before the experiment.

2.2.6. Immunocytochemistry

NHLFs were cultured using the experimental protocol (Section 2.2.9). At the end of the treatment, the cells were fixed with 2% paraformaldehyde for 30 mins. Non-specific Ab binding was prevented by using 3% goat serum and 1% BSA in PBS (blocking buffer), and as an antigen retrieval step, the cells were permeabilised for an hour with 0.1% Triton X-100 (in blocking buffer). Fibroblasts were incubated with primary antibodies (rabbit anti-human αSMA polyclonal Ab, 1:200, #ab5694; mouse anti-human CaSR (5C10-ADD) monoclonal Ab, 1:200, #ab19347; rabbit anti-human ROCK1 polyclonal Ab, 1:500, #21850-1-AP) at 4˚C overnight. After washing, secondary antibodies raised in goat (anti-rabbit AlexaFluor-488, 1:500, #ab150077; anti-mouse AlexaFluor-594, 1:1000, #ab150120) were applied for 1 hour and incubated in the dark. After washing, 6 µL of mounting medium was applied to the slide, and the cell nuclei were counterstained with DAPI using VECTASHIELD® Antifade Mounting Medium with DAPI (Vector Laboratories Ltd., Peterborough, UK). All antibodies were purchased from Abcam (Cambridge, UK) except the ROCK1 antibody, purchased from Proteintech (Manchester, UK). Negative control staining was performed by omitting primary antibodies and replacing the CaSR Ab with IgG2a isotype control (mouse, 1:100, #02-6200; Thermo Fisher).

Images were captured with constant exposure settings using a 20x objective on an Olympus BX61 upright epifluorescence microscope (Olympus UK & Ireland, Essex, UK). Quantitative immunofluorescence (see Section 2.2.6.1) was used to quantify protein expression with mean values representing data from 72-925 cells per experimental condition. Mr Richard Bruce (Cardiff University, School of Biosciences) provided the ROCK1 immunofluorescence images for analysis. Representative images presented in the relevant results chapters were enhanced to the same brightness and contrast, and the statement “images were contrast adjusted” has been added where appropriate.

2.2.6.1. Quantitative immunofluorescence microscopy

Fluorescence intensity was quantified according to protocols described previously (Schepelmann *et al*. 2016) and used to evaluate CaSR, αSMA, and ROCK1 expression by scanning slides with NHLFs stained for the relevant protein using StrataQuest (TissueGnostics GmbH, Vienna, Austria). 3-4 regions of interest (ROI) per well were randomly selected, and the images were acquired, keeping the settings of exposure and camera gain the same between the different slides, which contained batches of NHLFs from each experimental group. The acquired images from each slide were fused into a composite image using an automated image stitching algorithm available in the StrataQuest software. The composite image varied in size depending on the cell distribution in the individual wells but generally consisted of 12 – 20 ROIs. These regions were then analysed using StrataQuest, generating numerical values representing the expression levels of the different staining.

All the images from one batch of slides were loaded into the same StrataQuest project file. The software was programmed to identify nuclei contained within cells automatically. These nuclei are detected using background thresholding where positive objects (*i.e.*, nuclei) are discriminated from the background of the image using the image channel (colour) for the nuclear staining (DAPI). The identified cells were manually scrutinised, and the settings optimised to remove artefacts, debris or air bubbles (trapped in the mounting medium of the coverslip) to avoid false positives. After settings were optimised to allow the best possible nuclear detection results, these settings were used to analyse all images. Evaluation of expression levels (*i.e.*, staining intensities) in the channels other than the nuclear channel (*i.e.*, green fluorescence and red fluorescence) was performed using a growing algorithm from the nuclei to measure mean staining intensities in the cytosol and membrane of each identified cell (Figure 2.2).

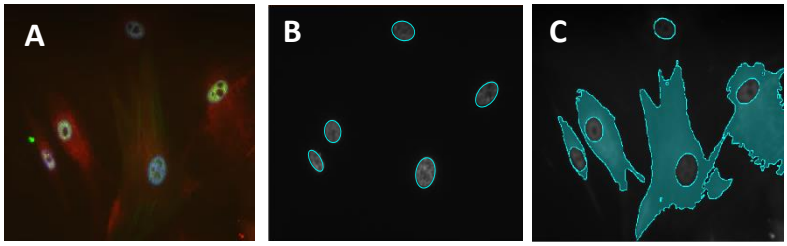

Figure 2.2 An example of StrataQuest profile nuclei identification and growing algorithm for the quantification of immunofluorescent staining intensities. Mean pixel intensities were measured within the areas highlighted in blue. (**A**) Representative image showing stacked image channels comprising of all three excitation wavelengths (DAPI - blue, 488 nm - green, 594 nm- red). Calcium-sensing receptor (CaSR) expression is shown in red and α smooth muscle actin (αSMA) expression is shown in green. (**B-C**) Representative images of the automatic identification of nuclei-containing cells (**B**) and the growing algorithm which indicates CaSR expression (**C**). Image contrast enhanced for better visualisation.

2.2.7. Fibroblast proliferation

NHLFs were cultured in 96-well plates as described in Sections 2.2.6 and 2.2.9. Cell proliferation was evaluated using a BrdU cell proliferation ELISA kit according to the manufacturer's instruction (Abcam). 20 µL 1X BrdU label was added to the relevant samples (48 hrs after experimental treatment) to be incorporated into the DNA of dividing cells. After 24 hours, the medium was aspirated from the cell wells. 200 µL of Fixing Solution was added to each well and incubated at room temperature for 30 minutes. The Fixing Solution was aspirated, and the plate was blotted dry. The plate was washed three times with 1X Wash Buffer before adding Detector Antibody. 100 µL/well of anti-BrdU monoclonal Detector Antibody was added, and the cells were incubated for 1 hour at room temperature. The plate was washed as previously described. 100 µL/well 1X Peroxidase Goat Anti-Mouse IgG Conjugate was added, and cells were incubated for 30 minutes at room temperature. The plate was washed as previously described. 100 µL/well

TMB Peroxidase substrate was added, and the cells were incubated for 30 minutes in the dark at room temperature. Positive wells showed a blue colour, the intensity of which is proportional to the amount of BrdU incorporation in the proliferating cells. The reaction was stopped by adding 100 µL of Stop Solution to each well. The colour of positive wells changed from blue to bright yellow. Absorbance at 450 nm was measured using CLARIOstar multi-well plate reader (BMG Labtech Ltd., Aylesbury, UK).

2.2.8. Collagen secretion

NHLFs were cultured in EZ slides (Merck Life Science) as described in Sections 2.2.6 and 2.2.9. Total collagen secretion in the cell culture supernatant was measured using Sircol™ soluble collagen assay (Biocolor, Belfast, UK) according to the manufacturer's instructions. Sircol is a dye that binds and quantifies acid-soluble and pepsin-soluble collagens. This assay assesses the production rate of newly synthesised collagen by binding to $[Gly\text{-}X\text{-}Y]_n$ helical structure found in collagen (types 1 -5).

Cell culture supernatant from each well was collected 72 hours after treatment. 110 µL of supernatant was mixed with 110 µL deionised H_2O to give a total test sample volume of 220 µL. Samples were added to 1 mL Sircol dye reagent (Sirius red in picric acid) to saturate collagen molecules thoroughly. A standard curve was generated using 5 µg, 10 µg and 15 µg of collagen reference standards. Each sample was assayed in duplicate. Samples were inverted gently and placed on a mechanical shaker for 30 minutes to form a collagen-dye complex. The samples were centrifuged for 10 minutes at 14600 x g, and the soluble unbound dye was aspirated. The complex was re-suspended in 750 µl of Acid Salt wash, centrifuged for 10 minutes at 14600 x g, and the unbound fraction carefully aspirated. The precipitate was dissolved in 250 µl of Alkali Reagent and transferred to a 96-well plate. Absorbance at 555 nm was measured with CLARIOstar multi-well

plate reader. Baseline collagen secretion (from vehicle and NAM groups) was too low to be quantified in 3 out of 5 experiments.

2.2.9. IL-8 secretion

NHLFs were cultured in EZ slides (Merck Life Science) as described in Sections 2.2.6 and 2.2.9. IL-8 SimpleStep ELISA kit (Abcam) was used to quantify concentrations of IL-8 in cell culture supernatant according to manufacturers' instructions. Cell culture supernatant from each well was collected 72 hours after treatment. 7.5 µL of supernatant was mixed with 150 µL Sample Diluent NS. A standard curve was generated in duplicate using 8 serial dilutions of IL-8 protein standard (400 pg/mL stock) (Figure 2.4).

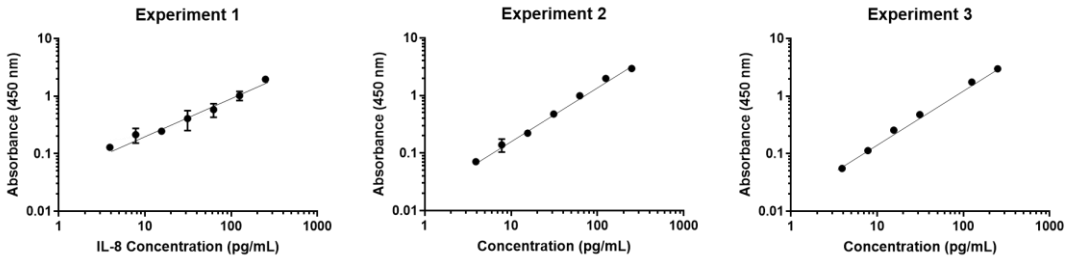

Figure 2.4 IL-8 standard curves. For each experiment, an IL-8 standard curve was generated in duplicate using 8 serial dilutions of IL-8 protein standard (400 pg/mL stock). Error bars indicate the range of raw data.

50 µL of samples or standards were added to the appropriate wells. Next, 50 µL of Antibody Cocktail was added, and cells were incubated for 1 hour at room temperature and gently rocked on a plate shaker. The plate was washed three times with 1X Wash Buffer PT before adding 100 µL TMB Peroxidase substrate to each well and incubating for 10 minutes in the dark on a plate shaker (as previously described). The reaction was stopped by adding 100 µL of Stop Solution to each well and mixing on a plate shaker for

1 minute. Absorbance at 450 nm was measured using CLARIOstar multi-well plate reader (BMG Labtech Ltd., Aylesbury, UK).

2.3. Statistical analysis

Data were analysed using Prism 9.0 software package (GraphPad Inc.). Quantitative data are shown as mean ± SEM. The effect of TGFß1 treatment was regarded as 100% for each experiment to reduce biological variability (except otherwise stated), and TGFß1+NAM data were presented as a percentage of these normalised data. Statistical comparisons were performed on normally distributed data (determined by the Shapiro-Wilk's test for normality) using Student's 2-tailed t-test or ANOVA (with Bonferroni post hoc analysis), *p*-values < 0.05 were considered significant. *N* denotes the number of patients, while *n* represents the number of independent experiments. Each independent experiment had 3-4 technical replicates.

2.4. RNA sequencing

Cardiff School of Biosciences Genome Hub performed RNA sequencing, and Dr Daniel Pass provided bioinformatics support.

2.4.1. RNA extraction

NHLFs were cultured in 6-well plates as described in Sections 2.2.6 and 2.2.9. Total RNA was extracted and purified using the RNeasy Mini Kit, including the optional on-column DNase digestion (Qiagen, Manchester, UK) according to the manufacturer's protocol for cell culture. All buffers and tubes used were provided in the kit. The experimental medium was aspirated, and cells were disrupted by adding 350 µL of Buffer RLT containing 0.1 % ß-mercaptoethanol. The cell lysate was collected into a microcentrifuge tube and homogenised to ensure there were no visible cell

clumps. The lysate was transferred directly into a QIAshredder spin column placed in a 2 mL collection tube, and centrifuged for 2 min at full speed. 350 µL of 70% ethanol was added to the homogenised lysate and mixed thoroughly. 700 µL of the sample was transferred to an RNeasy spin column placed in a 2 mL collection tube, centrifuged for 15 seconds at 10000 x g, and the flow-through discarded. To remove contaminating DNA, 350 µL of Buffer RW1 was added to the RNeasy spin column, centrifuged for 15 seconds at 10000 x g to wash the spin column membrane, and the flow-through was discarded. 10 µL of DNase I stock solution was added to 70 µL Buffer RDD and mixed gently by inverting the tube. The tube was centrifuged briefly to collect residual liquid. 80 µL of DNase I incubation mix was added directly to the RNeasy spin column membrane and placed on the benchtop at room temperature for 15 minutes. 350 µL of Buffer RW1 was added to the RNeasy spin column, centrifuged for 15 seconds at 10000 x g, and the flow-through discarded. 500 µL of Buffer RPE was added to the RNeasy spin column, centrifuged for 15 seconds at 10000 x g, and the flow-through discarded. This step was repeated with long centrifugation (2 minutes) to ensure no ethanol was carried over during RNA elution. The RNeasy spin column was transferred to a new 2 mL collection tube and centrifuged at full speed for 1 minute. The RNeasy spin column was transferred to a new 1.5 mL collection tube 50 µL of RNAse-free water was added directly to the spin column membrane, centrifuged for 1 minute at 10000 x g to elute the RNA.

RNA was quantitated for all samples using a Qubit RNA BR Assay Kit and Qubit® fluorometer (Fisher Scientific, Loughborough, UK), according to the manufacturer's instructions. All reagents used were provided in the kit. The Qubit® working solution was prepared by diluting the Qubit® RNA BR Reagent 1:200 in Qubit® RNA BR Buffer. 190 µL of Qubit® working solution was added to each tube used for the Qubit® standards. 10 µL of each Qubit® standard and sample was added to the appropriate tube and mixed by vortexing for 2–3 seconds. All tubes were incubated at room temperature for

2 minutes before reading on a Qubit® fluorometer. The fluorometer calculates the concentration of each sample in ng/µL.

The RNA integrity number (RIN) for each sample was measured using an Agilent 2200 TapeStation (Agilent Technologies, Stockport, UK), according to the manufacturer's instructions. The RIN is a widely recognised method for objective quality assessment of total RNA samples. The Agilent 2200 TapeStation software is equipped with an algorithm that uses the total RNA contained within a test sample to automatically generate a standardised number on a 10-point scale (1 represents most degraded/contaminated RNA while 10 represents the most intact RNA) that is indicative of RNA quality and purity (Connelly *et al*. 2016). All reagents and tubes used were provided in the kit. The reagents were equilibrated at room temperature and vortexed before use. The total purified RNA samples were kept on ice. 5 µL of RNA Sample Buffer was mixed with 1 µL of RNA Ladder or 1 µL of RNA sample to assess RNA integrity. The samples were vortexed using IKA vortex mixer and adaptor at 660 x g for 1 minute. The samples were denatured at 72°C for 3 minutes, placed on ice for 2 minutes and spun to position the samples at the bottom of the tube. Samples were placed into the sample block inside the TapeStation instrument and analysed with the TapeStation analysis software. RIN values for the samples were between 9.8 – 10 (Table 2.3).

Table 2.3 RNA integrity number (RIN) for the RNA sequencing samples. Replicate number indicates a different donor source

Sample	RNA integrity number (RIN)
Vehicle 1	10
Vehicle 2	9.8
Vehicle 3	10
NAM 1	10
NAM 2	10
NAM 3	10

TGFβ 1	9.9
TGFβ 2	10
TGFβ 3	10
TGFβ + NAM 1	10
TGFβ + NAM 2	9.8
TGFβ + NAM 3	10

2.4.2. Library preparation and sequencing

RNA library preparation, quantification and sequencing were performed by Ms Angela Marchbank (Cardiff School of Biosciences Genome Hub). Briefly, 500 ng of total RNA was used as input material for library preparation, performed with the Illumina TruSeq Stranded Total RNA Kit (Illumina, Cambridge, UK), according to the manufacturer's instructions. Dual Indexes were made using the Illumina Truseq RNA UD indexing plate to ensure accurate library sequencing. The resulting libraries were sequenced on the Illumina NextSeq 500 (Illumina) to generate 75 base-pair single-ended reads. A total of ~500 million reads were obtained across 12 samples. Each condition was sequenced in triplicate (the biological source of each replicate was a different donor, *i.e.* donors 2 – 4 in Table 2.2).

2.4.3. Bioinformatics analysis

Sequencing results were assessed for read length, base and sequence quality, GC content, and overall read composition with FastQC (Andrews 2010). Adaptors and low-quality bases were trimmed with Trimmomatic (Bolger *et al.* 2014). Genomic mapping to the Homo sapiens GRCh38.101 reference genome (Yates *et al.* 2020) was performed with Spliced Transcripts Alignment to a Reference (STAR) package (Dobin *et al.* 2013). RNAseq mapping was performed with STAR 2.7.3a, duplicates were marked/removed using Picard (Broad Institute), and the raw read counts were generated by featureCounts (Liao *et al.* 2014). An additional quality control step was carried out using SortMeRNA (Kopylova *et al.* 2012). An average of 6 million reads per sample were used for differential gene analysis following quality control steps. The SARTools (v1.7.3) pipeline (Varet *et al.* 2016) in DESeq2 (Love *et al.* 2014) was used to analyse differential gene expression (DEG). DEG was calculated by comparing two treatment groups, and the *p*-value was adjusted (p_{adj}) to account for false discovery rate using the Benjamini-Hochberg correction. Quantification, statistical analysis, ontological assignment, figure generation was performed using R (R Core Team 2018), GOnet (Pomaznoy *et al.* 2018) and Prism 9.0 (Graphpad).

CHAPTER 3: CASR IS EXPRESSED IN HUMAN LUNGS AND POLYAMINES WHICH ACTIVATE THE CaSR ARE UPREGULATED IN IPF

3.1. Overview

The experimental results of this thesis have been divided into three chapters. Chapter 3 investigates the expression of the CaSR in the lungs and analyses changes in the expression levels of known receptor activators, polyamines, in the saliva of IPF patients. Chapter 4 investigates the ability of the NAM, NPS2143, to suppress TGFβ1-induced profibrotic effects in primary human lung fibroblasts (NHLFs). Chapter 5 examines the effects of the NAM, NPS2143, on profibrotic gene expression and (poly)amine metabolism.

3.2. Introduction

IPF pathogenesis involves the activation of alveolar/bronchiolar epithelial cells (thought to be the site of the initial injury) (Maher 2021) and (myo)fibroblasts (the fibrogenic effectors) (Renzoni *et al*. 2021). These cells release several mitogenic factors that act as activating signals to the surrounding cells (Rockey *et al*. 2015; Haak *et al*. 2020). Of note here are pulmonary neuroepithelial cells (PNECs), which act as an interface between the external environment and the lungs sensing changes in chemical stimuli, and as a consequence, are implicated in smoking-associated lung diseases and progressive lung fibrosis (Tighe *et al*. 2019; Noguchi *et al*. 2021). Furthermore, it has been suggested that the CaSR is crucial for these cells to carry out their role in sensing, integrating and transducing signals that maintain the pulmonary microenvironment (Lembrechts *et al*. 2013).

In non-calcitropic organs, the CaSR acts as a multi-modal chemosensor for components of environmental pollutants (*e.g.*, urban particulate matter,

Ni^{2+} and Cd^{2+}) and endogenous polycations (*e.g.*, eosinophil cationic protein, major basic protein) (Handlogten *et al*. 2000; Brown and MacLeod 2001; Yarova *et al*. 2015; Mansfield *et al*. 2019). The CaSR is also activated by various polyamines (*e.g.* putrescine, spermine and spermidine), and basic amino acids (*e.g.* L-arginine and L-ornithine) which are particularly abundant in the lung (Hoet and Nemery 2000; Brown and MacLeod 2001). Pertinently, the expression of these CaSR activators is increased in lungs of IPF patients (Zhao *et al*. 2017). Taken together, these findings alongside the "sensing" function of the receptor and the role of the distal airway in IPF, provide a rationale to investigate the expression of the CaSR and its activators in patients with pulmonary fibrosis.

3.3. Results

3.3.1. The CaSR is expressed in the bronchiolar epithelium of the human lung

As a first step to explore the potential involvement of the CaSR in IPF, I investigated CaSR expression in areas of active fibrosis in lung biopsy samples from IPF patients compared to control lungs. Specific CaSR immunostaining is found in the respiratory epithelium of small peripheral bronchioles, particularly at the apical membranes of ciliated epithelial cells of both control (Figure 3.1A) and IPF lung tissue (Figure 3.1B). No immunoreactivity is observed when the CaSR antibody is pre-absorbed with specific antigenic peptide or when the primary antibody is replaced with an IgG isotype control (Figure S1).

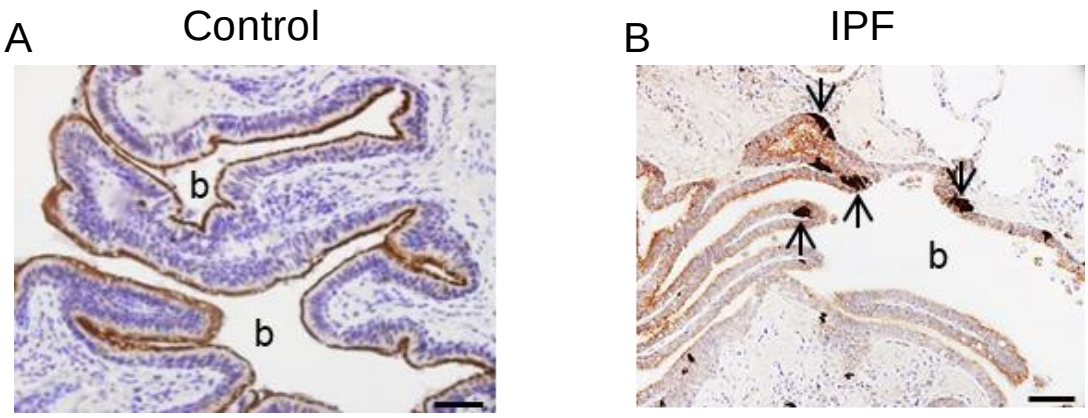

Figure 3.1 CaSR expression in control and IPF lungs. CaSR is expressed in the epithelium of peripheral bronchioles (shown in brown); especially on the apical membrane of ciliated cells in both control and IPF lungs **(A-B).** The peripheral bronchiole of an IPF patient also reveals interstitial CaSR expression and high numbers of grouped neuroendocrine-like cells with a strong CaSR immunostaining (arrows) (**B**). b: lumen of bronchiole. N = 5 control donors; 7 IPF donors. Scale bar: 100 µm.

CaSR immunostaining is also observed in the interstitium of IPF lung tissue; however, the strongest receptor expression is seen in grouped neuroendocrine-like cells, which occur in greater numbers in IPF tissue compared to control (Figure 3.1B).

3.3.2. Neuroepithelial bodies (NEBs), which highly express CaSR, are increased in the IPF lung

Since PNECs are found within the airway epithelium in clusters known as neuroendocrine bodies (NEBs) (Adriaensen *et al*. 2003) and their number isincreased in lung diseases (Noguchi *et al*. 2021), serial sections from IPF lung tissue were stained with the PNEC marker, gastrin-releasing peptide (GRP). These studies were done in collaboration with Prof. Dirk Adriaensen and Dr Line Verckist (University of Antwerp). The NEB-like cells were found to co-express CaSR and GRP (Figure 3.2). GRP immunostaining also revealed

some respiratory areas in IPF lungs which harbour NEBs that co-localise αSMA and CaSR expression (Figure 3.3).

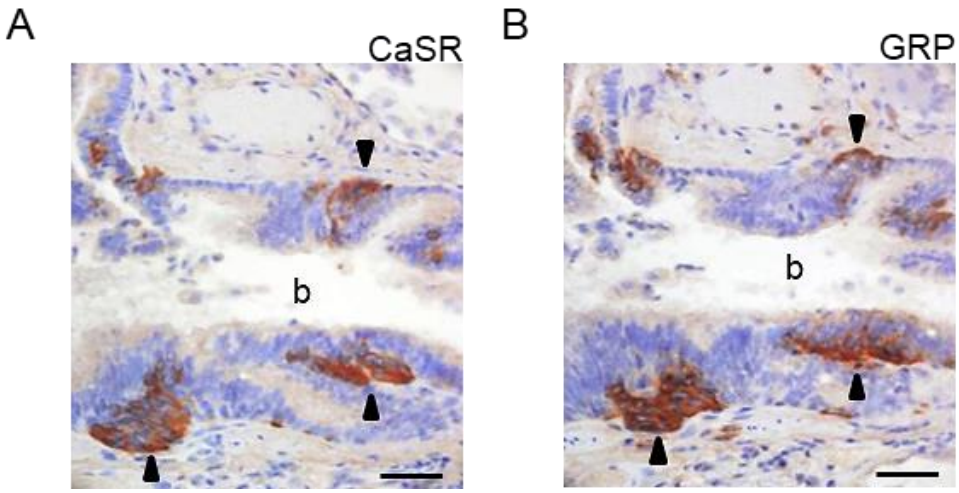

Figure 3.2 CaSR expression in the neuroepithelial bodies (NEBs) of IPF lungs. Representative images from serial sections of IPF lung tissue show grouped CaSR expressing NEB-like cells overlap with cells expressing the human NEB marker, gastrin-releasing peptide (GRP; arrowheads). b: lumen of bronchiole. N = 5 control donors; 7 IPF donors. Scale bar: 50 μm.

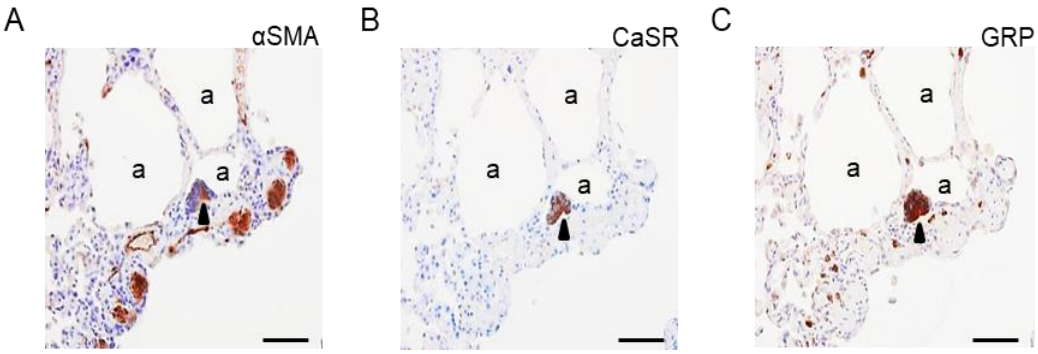

Figure 3.3 The alveolar region of IPF lungs co-express αSMA, CaSR and GRP. Consecutive paraffin sections reveals that the respiratory areas in some IPF patients also harbour NEB-like neuroendocrine cells (indicated by NEB marker, GRP) that co-localise αSMA (**A**) and CaSR (**B**) immunostaining (arrowheads). αSMA: α smooth muscle actin; a: lumen of alveoli; CaSR: calcium-sensing receptor; GRP: gastrin-releasing peptide. N = 5 control donors; 7 IPF donors. Scale bar: 50 μm.

3.3.3. CaSR and αSMA expression in the peripheral bronchioles and alveolar areas of IPF lungs

Given that the presence of αSMA is considered a marker of active fibrotic regions (Kuhn and McDonald 1991; Zhang *et al*. 1996), the next step was to investigate its expression in the bronchiolar and alveolar regions of IPF tissue. Immunohistochemistry of serial sections demonstrates almost complete absence of CaSR staining in alpha-smooth muscle actin (αSMA)-positive clusters in bronchiolar (Figure 3.4, A and B) and alveolar (Figure 3.4, C and D) regions of IPF lungs. αSMA immunoreactivity is observed in bronchiolar interstitial cells but not in the epithelium (Figure 3.4A). Epithelial cells in the bronchiolar region express CaSR with very low immunostaining in the interstitium; therefore, no strong relationship with αSMA expression can be demonstrated (Figure 3.3B). In IPF alveolar parenchyma, some interstitial cells show αSMA immunostaining (Figure

3.3C). However, CaSR expression is undetected in this region of the IPF lung (Figure 3.3D).

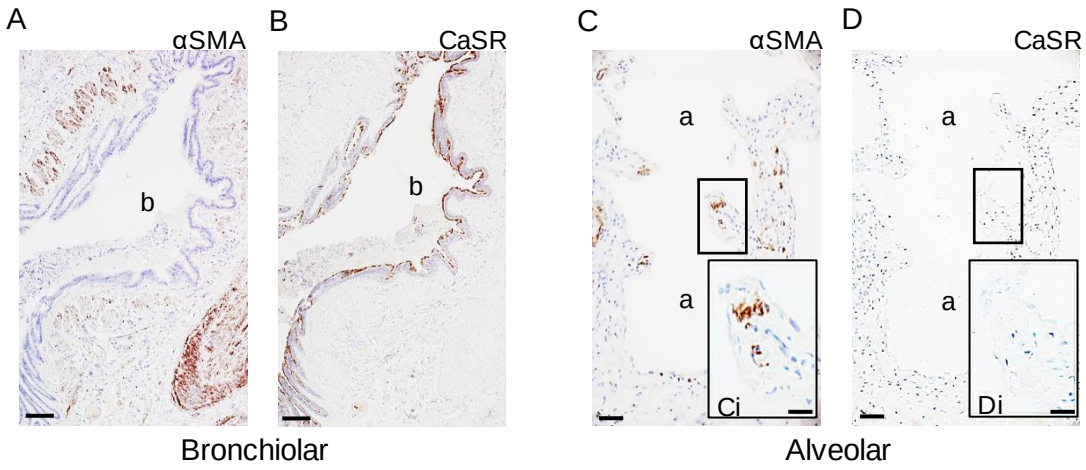

Figure 3.4 CaSR and αSMA expression in the peripheral bronchioles and alveolar areas of IPF lungs. Paraffin sections of IPF lungs. **A.** Peripheral bronchioles, and smooth muscle bundles surrounding airways and blood vessels show αSMA immunostaining. **B.** Bronchiolar epithelial cells appear to express CaSR with relatively low immunostaining in the interstitium; no strong relationship with αSMA can be demonstrated. **C.** In the alveolar area, some interstitial cells show αSMA immunostaining **(D)** No relationship with CaSR can be demonstrated in consecutive sections. a: lumen of alveoli; b: lumen of bronchiole. N = 5 control donors; 7 IPF donors. Scale bars: 25 μm **(Ci, Di)**; 50 μm **(C, D)**; 150 μm **(A, B)**.

In conclusion, CaSR is highly expressed in the epithelium of peripheral bronchioles and the NEBs of the respiratory epithelium of normal and IPF lungs, suggesting a role for the receptor as a chemosensor of endogenous and exogenous agents that damage the distal epithelium.

3.3.4. CaSR activators, polyamines, are increased in the saliva of PF patients

Specific metabolic pathways, such as the arginine pathway, are upregulated in the lung tissue of PF patients and have been shown to contribute to disease pathogenesis (Zhao *et al*. 2018). Therefore, metabolomic analysis was carried out to assess the metabolomic signature of PF patient saliva compared to controls. This analysis indicated the prominence of the arginine-polyamine pathway in IPF patient saliva samples (Figure 3.5 – 3.6).

The first step was to establish whether different polyamine signatures exist between patients diagnosed with progressive PF (PPF) compared with patients with confirmed IPF diagnosis. No difference in (poly)amine expression was observed between the fibrotic groups; however, disease-specific differences were observed between the fibrotic groups and control. Both IPF (p = 0.003) and PPF (p = 0.03) samples exhibit greater levels of arginine compared with controls (Figure 3.5A). IPF samples show greater ornithine intensity in comparison with controls (p = 0.009), while its expression in PPF patients is similar to control (Figure 3.5A). Putrescine is significantly elevated in PPF samples compared with controls (p = 0.02; Figure 3.5A). However, the difference in expression shows borderline significance when the IPF group is compared with control (p = 0.06; Figure 3.5A). Spermidine and spermine are not significantly altered in either IPF or PPF (Figure 3.6A). Since high polyamine levels have been reported in asthma, prostate cancer and colon cancer (Babbar and Gerner 2011; Yarova *et al*. 2015), control donors with these contraindications were excluded from further data analysis. Consequently, a clearer distinction between the fibrotic and control groups was observed for arginine, ornithine, and spermine (Figure 3.5B). Comparisons between IPF and control highlight the following differences in the order of magnitude (OOM) for each metabolite: arginine (OOM = 2.0; $p < 0.0001$), ornithine (OOM = 1.7; $p < 0.0001$), and spermine (OOM = 1.0; p = 0.01). Comparisons between PPF and control show

similar results albeit to a lesser extent: arginine (OOM = 1.6; p = 0.0001), ornithine (OOM = 1.2; p = 0.003), and spermine (OOM = 0.8; p = 0.03).

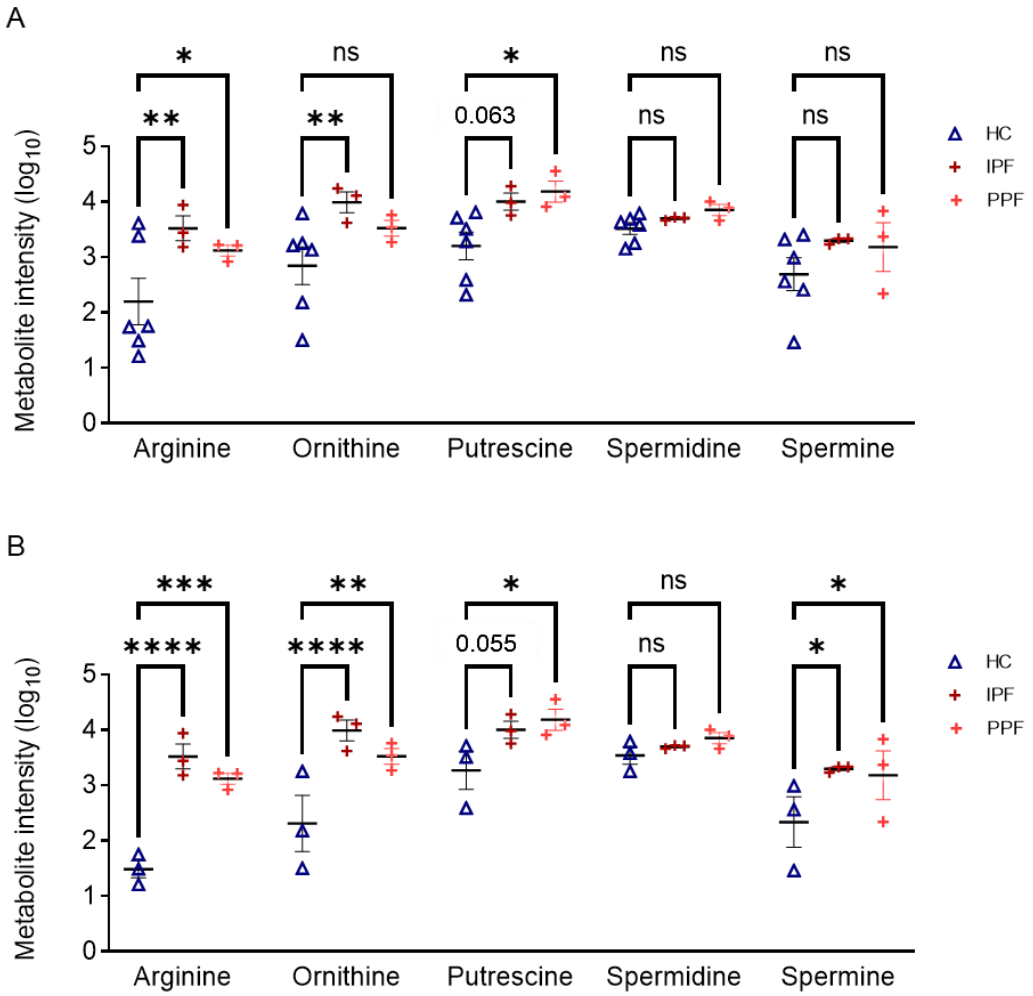

Figure 3.5 Expression of arginine pathway metabolites is similar in IPF and PF patient saliva samples. A. Patients were classified as progressive PF (PPF) where IPF diagnosis could not be confirmed due to missing clinical information. Saliva samples from IPF and progressive PF (pPF) patients highlights differences in metabolites of the arginine-polyamine pathway when compared to healthy controls, but no differences are observed between the two PF groups. **B.** Excluding control donors with conditions associated with increased polyamine concentrations (such as asthma and cancer) reduces HC metabolite intensity for arginine, ornithine, and spermine. Y-axis: Log_{10} normalization of metabolite intensity. 2-way ANOVA (Fisher's LSD post hoc test); *p<0.05, **p<0.01, ns: not significant. N = 6 controls; 3 IPF patients; 3 PF patients. *HC*: control; PF: pulmonary fibrosis.

Since there were no statistical differences between the PPF and IPF groups, both groups were combined for principal component analysis (PCA). PCA on the saliva samples demonstrates clear clustering of the combined PF group, distinct from a more diffuse control group (Figure 3.6A). Further analysis showed that PF patient saliva samples exhibit higher levels of arginine (p = 0.03, Figure 3.6B), ornithine (p= 0.04, Figure 3.6C), putrescine (p = 0.01, Figure 3.6D), spermidine (p = 0.06, Figure 3.6E), and spermine (p = 0.15, Figure 3.6F) when compared to control. In conclusion, the metabolomic profile of PF patient saliva indicates that metabolites from the arginine-polyamine pathway appear to be markers of progressive lung fibrosis.

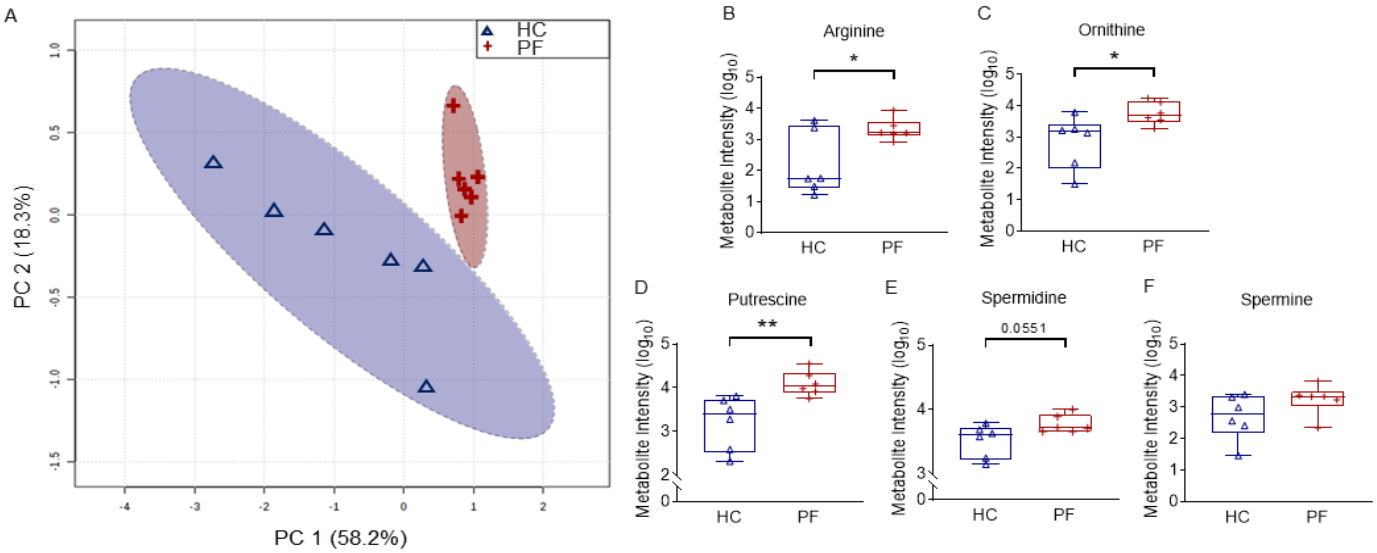

Figure 3.6 Expression of arginine pathway metabolites is increased in pulmonary fibrosis (PF) patient saliva samples. A. Principal component analysis (PCA) score plot between the main principal components (PC1 and PC2) shows a tight cluster of the PF samples based on their metabolic profile compared to controls with a 95% confidence ellipse drawn for each group (shown by the dotted lines). Assessment of PC1 and PC2, which account for 76.4% of the total variation between the control (HC) and PF clusters highlights the prominence of (poly)amines. **B-F.** Associated box and whisker plots of metabolites in the arginine-polyamine pathway highlights the differences between healthy and PF profiles: Arginine **(B)**, Ornithine **(C)**, Putrescine **(D)**, Spermidine **(E)**, and Spermine **(F)** are increased in PF patient saliva compared to control. Y-axis: Log_{10} normalization of metabolite intensity. 2-tailed Student's t-test; *p<0.05, **p<0.01. N = 6 controls; 6 PF patients.

3.4. Discussion

The key findings of this study highlight 1) CaSR expression in the epithelium of peripheral bronchioles and in proliferated pulmonary NEBs of IPF lungs; 2) naturally occurring polyamines are increased in PF patient saliva. Since CaSR ligands (such as polyamines) are increased in IPF saliva and can activate the CaSR expressed by epithelial cells or NEBs, our study identifies a potential role for the receptor in IPF pathogenesis or pathology.

The strong CaSR expression in the airway epithelium and NEBs shown in this chapter is supported by data from the human protein atlas database, which indicates that the CaSR is highly expressed by ciliated and alveolar epithelial cells, with relatively lower expression in lung fibroblasts (Uhlén *et al*. 2015). This pattern of expression could suggest that the CaSR could play a role in the initiation of the fibrotic cascade implicated in PF. Constant receptor activation by environmental pollutants (such as smoke, urban particulate matter) and microbes (such as bacteria and viruses) which contain a plethora of polycations/polyamines (Yarova *et al*. 2015; Mansfield *et al*. 2019), could induce downstream signalling pathways that result in the induction of profibrotic responses such as fibroblast proliferation and ECM secretion (Zhang *et al*. 2014). Furthermore, ciliated epithelial cells are key targets of viral infections, with chronic infections linked to mucociliary dysfunction and impaired mucus clearance (Davis and Wypych 2021). These processes have been shown to increase disease severity in human and murine models of the PF (Seibold *et al*. 2013; Hancock *et al*. 2018). Although further work is required to investigate the role of the receptor in the distal lung epithelium, these findings could suggest that the receptor might contribute to features of the disease, such as honeycombing and bronchiolisation of alveolar spaces (Prasse *et al*. 2019; Adams *et al*. 2020), through the involvement of CaSR-expressing ciliated airway epithelial cells.

Data presented in this chapter show an increase in the number of NEBs in the lungs of some IPF patients. NEBs occur in the human airway epithelium (Lauweryns *et al*. 1972; Adriaensen *et al*. 2003). They consist of complex innervated groups of pulmonary neuroepithelial endocrine cells (PNECs) that are typically crowned by Club-like cells (CLCs), leaving tiny apical processes of PNECs in direct contact with the airway lumen; the overall organoid structure is referred to as the NEB microenvironment (ME) (Brouns *et al*. 2021). NEBs have been suggested to serve diverse functions during foetal, perinatal, and postnatal life (Adriaensen *et al*. 2003; Linnoila 2006), including, but not limited to, development/growth of surrounding airway epithelium (Sorokin *et al*. 1997), and sensing/transducing hypoxic (Cutz and Jackson 1999), mechanical (Lembrechts *et al*. 2012), chemical (Lembrechts *et al*. 2013) stimuli from the environment. More recently, CLCs have been extensively characterised as a unique stem cell niche (Verckist *et al*. 2017; Verckist *et al*. 2018), involved in the homeostasis and repair of airway epithelium. Particularly relevant to our findings is the selective gene expression and strong surface membrane expression of fully functional CaSR reported in mouse NEBs (Lembrechts *et al*. 2013).

Among several other bioactive substances, human PNECs and NEBs synthesise, store and secrete GRP in health and disease (Sunday 2014), which was consequently used as a NEB marker in this study. Interestingly, NEB/PNEC hyperplasia and an increased release of PNEC-derived GRP have been implicated in (myo)fibroblast proliferation, collagen synthesis and alveolar wall thickening in various *in vivo* models of pulmonary fibrosis (Ashour *et al*. 2006; Sunday 2014; Tighe *et al*. 2019). Furthermore, GRP and other neuropeptides released by PNECs induce mucin expression and mast cell recruitment (Subramaniam *et al*. 2003; Atanasova and Reznikov 2018; Davis and Wypych 2021), processes that are implicated in IPF pathogenesis (Seibold *et al*. 2013; Overed-Sayer *et al*. 2014). The myofibroblast marker αSMA was present in some NEBs, which is reminiscent of a PF-related phenomenon known as epithelial-mesenchymal transition where epithelial

cells express proteins typically associated with mesenchymal cells (Gabasa *et al*. 2017). Therefore, I speculate that the sensory ability and neuropeptide release from these highly proliferating PNECs may be amplified in IPF due to significant changes in ECM stiffness and O_2 levels, the latter occurring due to the loss of functional tissue. These changes may further be potentiated by CaSR activation, $[Ca^{2+}]_i$ increase and subsequent GRP release, which could worsen the fibrotic process. Further work is required to elucidate the exact mechanisms induced by the CaSR in NEBs/PNECs and whether they are directly involved in PF pathogenesis or progression.

This study shows that PF patient saliva samples exhibit upregulation of metabolites associated with the arginine-polyamine pathway compared to controls. Notably, no significant difference was observed between the metabolic profiles of PPF and IPF patients. This conclusion is in line with previous findings, indicating increased arginine metabolism in IPF lungs (Zhao *et al*. 2017). Arginase is responsible for the enzymatic conversion of arginine into ornithine. Increased arginase I/II expression and activity have been reported in human and rodent models of PF (Maarsingh et al. 2008a; Luzina et al. 2015a). Ornithine and the enzyme responsible for its conversion into putrescine, ornithine decarboxylase (ODC), are considered the rate-limiting steps in polyamine synthesis (Wang *et al*. 1997; Morris 2007).

Interestingly, our split cohort indicates ornithine as a key metabolite in IPF samples. Since a dysfunctional wound-healing process characterises IPF, it is notable that ODC inhibition results in intracellular polyamine depletion and decreases TGFβ expression in epithelial cells after wounding (Wang *et al*. 1997). In addition to *de novo* synthesis, polyamines (putrescine, spermidine, and spermine) can be transported into CLCs, alveolar and bronchiolar epithelial cells from the extracellular environment and in high concentrations, lead to necrosis and altered epithelial barrier integrity (Hoet and Nemery 2000).

Polyamines also play a role in cell growth, survival, and proliferation thus are attractive therapeutic targets in highly proliferative diseases, *e.g.* cancer (Minois *et al*. 2011; López-Contreras *et al*. 2020). They are implicated in several lung diseases such as pneumonia (Lasbury *et al*. 2007), asthma (Yarova *et al*. 2015; Jain 2018), and pulmonary hypertension (Zhu *et al*. 2019). In asthma and pulmonary hypertension, direct activation of the CaSR with polyamines poly-L-arginine and spermine facilitates cytosolic calcium signalling, smooth muscle cell proliferation, pulmonary artery constriction, and airway hyperresponsiveness, which were all abolished by genetic or pharmacological inhibition of CaSR (Yarova *et al*. 2015; Yarova *et al*. 2016; Zhu *et al*. 2019). Although further work is needed to determine the role of polyamines in PF, these findings suggest a potential mechanism involving polyamines and the CaSR in the disease pathology.

3.5. Limitations and Future directions

The histopathology data in this chapter indicates protein localisation; therefore, the conclusions about the role of the potential role of the receptor in $CaSR^+$ cells are speculative and based on other published work. Future work could investigate the functional role of the CaSR in healthy and IPF small airway epithelial cells and NEBs through direct activation (with polyamines and cigarette-associated cations) and inhibition (with NAMs) of the receptor. Another limitation of this study was the use of historic IPF patient tissue. Although recent studies indicate that αSMA might not be a consistent marker of pathologic fibroblasts (Sun *et al*. 2016; Xie *et al*. 2018), the length of tissue storage and storage conditions could have affected the immunoreactivity observed in the tissue. Future work could reassess the expression of the CaSR, GRP and αSMA in tissue from recently diagnosed patients with idiopathic and non-idiopathic progressive PF.

A limitation of the metabolomic study is the sample size. The study could only recruit 6 patients diagnosed with UIP pattern of fibrosis (of which 3 were confirmed IPF patients), which is unsurprising due to the relatively low prevalence of IPF and the length of time available for patient recruitment. The results presented in this chapter act as a proof of concept, which shows that patient saliva could reveal biologically plausible biomarkers to aid progressive PF diagnosis and potentially aid disease stratification. Further work on a larger cohort is required to validate these findings and explore whether polyamine levels have the necessary sensitivity and specificity to differentiate PPF/UIP from other ILDs.

3.6. Conclusion

IPF diagnosis is hampered by the absence of reliable disease biomarkers (Jenkins *et al*. 2015). Our findings show that PF patient saliva samples exhibit upregulation of the arginine pathway metabolites compared to healthy controls. These results are consistent with previous studies showing increased arginase expression and activity in human and rodent models of PF (Maarsingh *et al*. 2008b) and increased ornithine-derived metabolites, putrescine and spermidine, in IPF lung tissue (Zhao *et al*. 2017). Moreover, in the arginine metabolic cycle, ornithine is the rate-limiting step in polyamine/polypeptide synthesis (Morris 2007). These findings suggest a potential role for ornithine and the ornithine-derived polyamines in progressive lung fibrosis through the activation of the CaSR. Since salivary biomarkers correlate with serum biomarkers in several systemic diseases (Malathi *et al*. 2014), the results presented provide a rationale to validate patient saliva as a non-invasive biofluid for disease detection, patient stratification and therapeutic response.

CHAPTER 4: EFFECTS OF NAM ON NORMAL HUMAN LUNG FIBROBLAST ACTIVATION BY TGFβ1: CELLULAR AND MOLECULAR RESPONSE

4.1. Overview

This results section investigates the ability of the NAM, NPS2143, to suppress TGFβ-induced profibrotic effects in primary human lung fibroblasts (NHLFs).

4.2. Introduction

It is widely recognised that TGFβ is the master mediator of fibrogenesis (Fernandez and Eickelberg 2012). TGFβ1 induces several signalling pathways implicated in the fibrotic process, including the mTOR pathway, PI3K/AKT pathway, MAPK pathway, and Rho kinase pathway (Mu *et al*. 2012; Guillotin *et al*. 2020) (Figure 4.1). mTOR is a serine/threonine protein kinase, which forms 2 complexes, *i.e*., mTORC1 and mTORC 2. mTORC1 is composed of mTOR/ mammalian lethal with sec-13 protein 8 (mLST8)/regulatory-associated protein of mTOR (Raptor)/proline-rich AKT substrate 40 kDa (PRAS40) complex and acts as a cellular sensor integrating extracellular signals from growth factors, amino acids, glucose, cellular energy levels and oxygen availability, which regulate various cellular processes, including growth, proliferation, differentiation, ECM production, autophagy, and senescence (Engelman 2009; Meng *et al*. 2018; Platé *et al*. 2020). The second complex, mTORC2, comprises mTOR, mLST8, Rictor (raptor independent companion of mTOR), mSIN1 (mammalian stress-activated protein kinase interacting protein 1) and Protor-1 (protein observed with rictor-1) (Platé *et al*. 2020). Activation of this complex by growth factors regulates cytoskeletal organisation (Dowling *et al*. 2009).

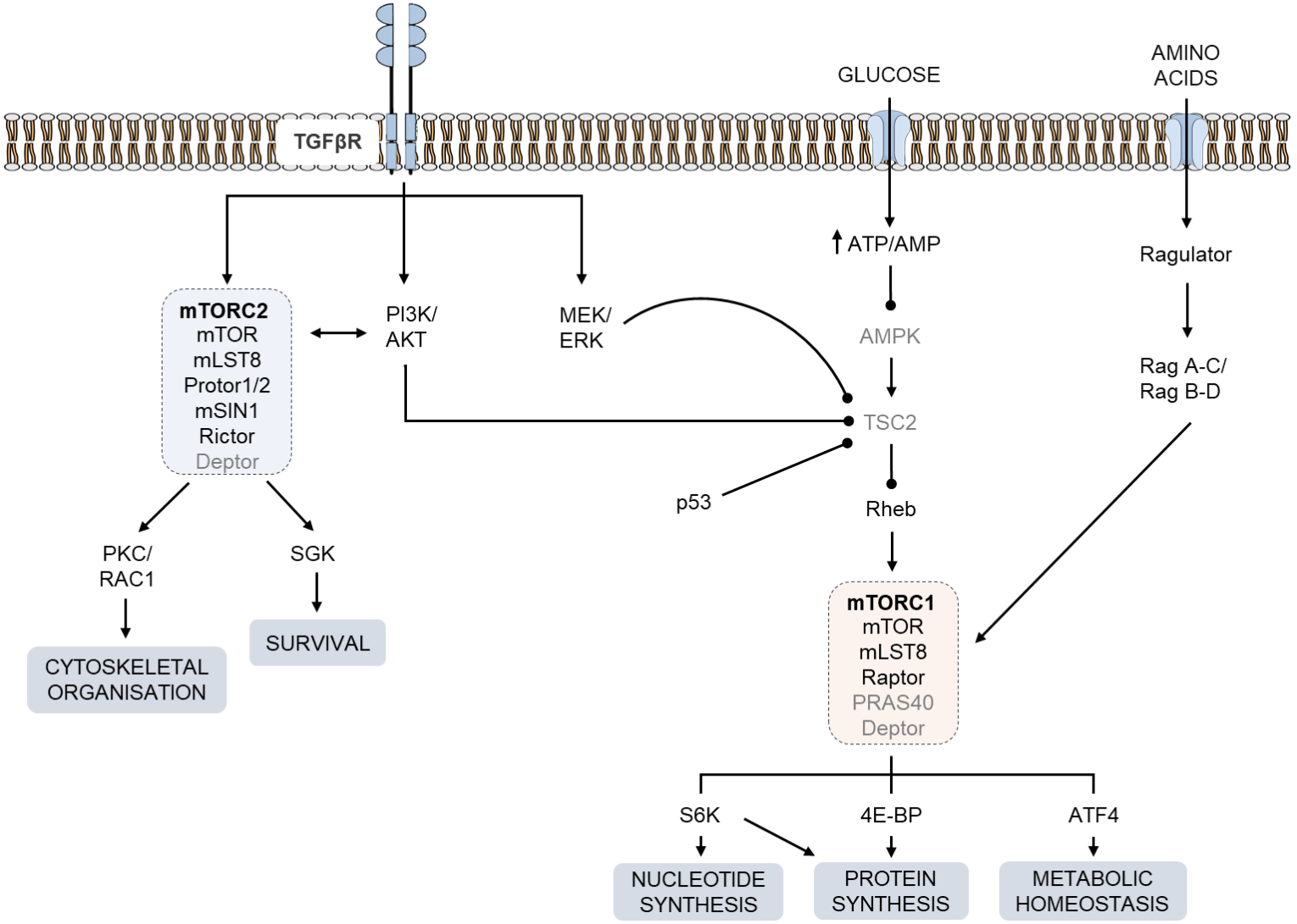
TGFβR
GLUCOSE
AMINO ACIDS
ATP/AMP
Ragulator
mTORC2
mTOR
mLST8
Protor1/2
mSIN1
Rictor
Deptor
PI3K/
AKT
MEK/
ERK
AMPK
Rag A-C/
Rag B-D
TSC2
p53
Rheb
PKC/
RAC1
SGK
SURVIVAL
CYTOSKELETAL ORGANISATION
mTORC1
mTOR
mLST8
Raptor
PRAS40
Deptor
S6K
4E-BP
ATF4
NUCLEOTIDE SYNTHESIS
PROTEIN SYNTHESIS
METABOLIC HOMEOSTASIS

Figure 4.1. The TGFß1/mTOR pathway. TGFß1 induces several signalling pathways implicated in the fibrotic process which sustain cell proliferation and differentiation (*via* MEK/ERK), and cell growth, motility and survival (*via* PI3K/AKT/mTOR). mTOR regulates cell growth by controlling nucleotide synthesis/mRNA translation, protein synthesis, and metabolism. The mTOR protein is part of two protein complexes: mTORC1 and mTORC2. mTORC1 is activated by growth factor signalling and amino acids resulting in S6K, 4E-BP and ATF4 activation. Cellular energy status negatively regulates mTORC1 through AMPK-mediated TSC phosphorylation. The TSC complex is an important checkpoint as it is inactivated by other intracellular signals (*e.g.*, AKT, MAPK and the senescence marker, p53). mTORC2 is also activated by mitogenic signals *via* the PI3K/AKT axis and phosphorylates AKT, PKC and SGK. Activating proteins are shown in black, inhibiting proteins in grey. AMPK: AMP-activated protein kinase; Deptor: DEP-domain containing mTOR-interacting protein; 4E-BP: eukaryotic translation-initiation factor 4E-binding protein; ERK1/2: extracellular signal-regulated kinase 1/2; MEK: mitogen-activated protein kinase kinase; mLST8: mammalian lethal with Sec13 protein 8; mSIN1: mammalian stress-activated protein kinase-interacting protein; mTORC: mammalian target of rapamycin complex; PI3K: phosphoinositide-3 kinase; PKC: protein kinase C; PRAS40: praline-rich Akt substrate of 40 kDa; RAG: Ras-related GTP-binding protein; Raptor: regulatory-associated protein of TOR; Rheb: Ras homolog enriched in the brain; Rictor: rapamycin-insensitive companion of mTOR; S6K: p 70 ribosomal S6 kinase; SGK: serum/glucocorticoid-regulated kinase; TGFßR: TGFß receptor; TSC: tuberous sclerosis complex.

Another way that TGFß could exert its profibrotic effects is *via* signal convergence downstream of CaSR activation (Figure 4.2). CaSR activation drives the pro-proliferative response in many cell types, including fibroblasts, resulting in the release of intracellular Ca^{2+} and activation of MAPKs (McNeil *et al*. 1998). Cell proliferation in response to increases in extracellular calcium is mediated via cross-talk between CaSR signalling and tyrosine receptor kinase-dependent RAS/Raf/MEK/ERK signalling pathway (Hobson *et al*. 2000).

Data from the previous chapter showed that the CaSR is expressed in bronchiolar interstitial cells, and ligands that activate the receptor, such as polyamines and basic amino acids, are increased in IPF. Ligand-specific CaSR activation can induce unique conformations of the receptor, which may lead to preferential coupling of different G proteins (reviewed in Leach *et al*. 2020). For example, an increase in intracellular Ca^{2+} is mediated via $G_{q/11}$ coupling (Brown and MacLeod 2001), increase in MAPK-mediated growth and differentiation is mediated via $G_{\beta\gamma}$ coupling (Kifor *et al*. 2001), and increase in Rho kinase-mediated actin stress fibre assembly (via $G_{q/11}$ and possibly $G_{12/13}$ coupling (Davies *et al*. 2006). Previously, CaSR signalling has been implicated in the remodelling and proliferative process of several diseases, including asthma (Yarova *et al*. 2015), cardiac fibrosis (Schepelmann *et al*. 2016), pulmonary arterial hypertension (Yamamura *et al*. 2012), and COPD (Yarova *et al*. 2016). Pertinently, the last two diseases are common IPF comorbidities. Whether polyamines, acting at the CaSR, also play a role in the pathogenesis of IPF has never been studied. The aim of this chapter is to determine whether the CaSR is functionally expressed in NHLFs and to investigate the role of the receptor in key profibrotic processes mediated by TGFß1 *in vitro*.

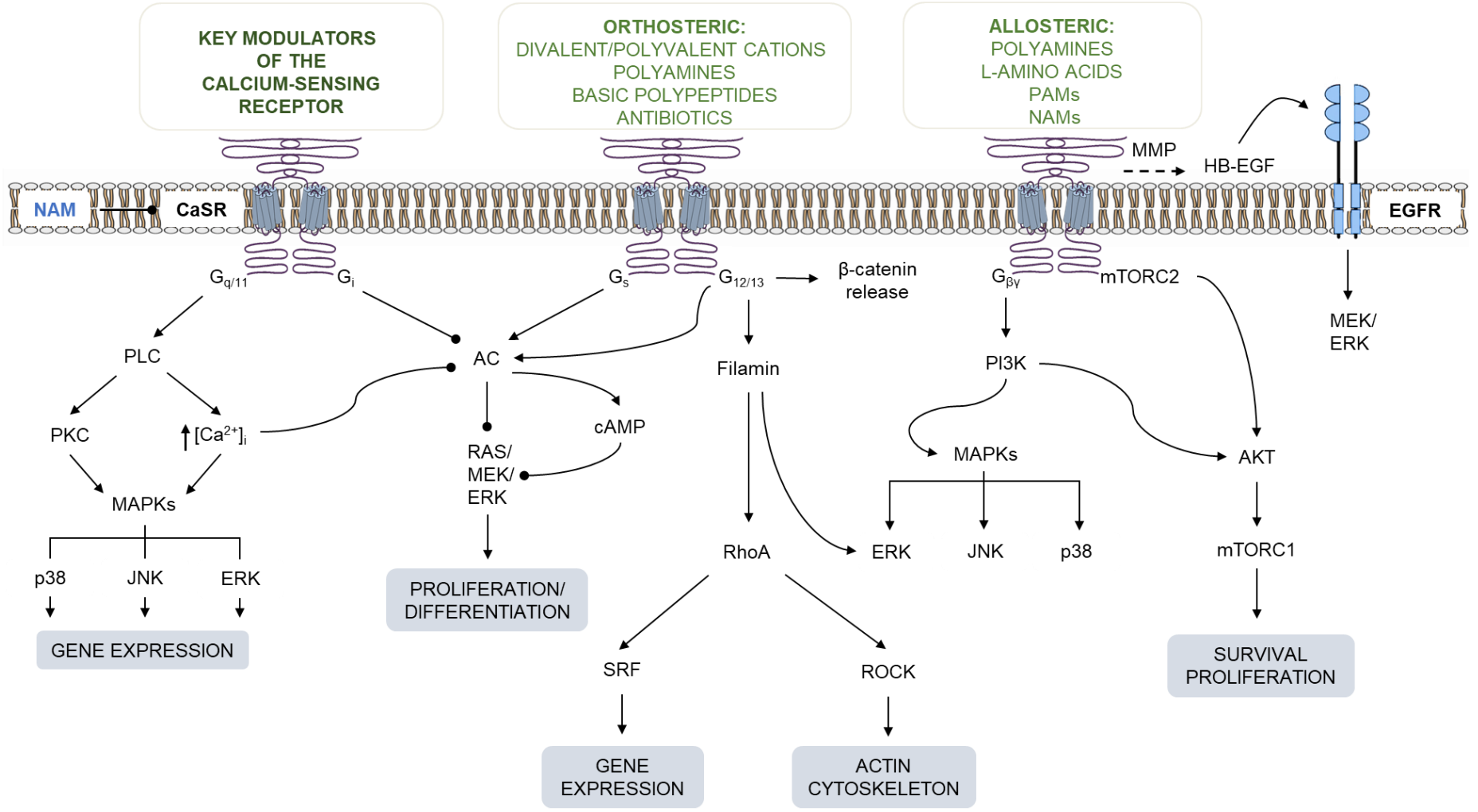
KEY MODULATORS OF THE CALCIUM-SENSING RECEPTOR
ORTHOSTERIC:
DIVALENT/POLYVALENT CATIONS
POLYAMINES
BASIC POLYPEPTIDES
ANTIBIOTICS
ALLOSTERIC:
POLYAMINES
L-AMINO ACIDS
PAMs
NAMs
NAM
CaSR
MMP
HB-EGF
EGFR
$G_{q/11}$
G_i
G_s
$G_{12/13}$
β-catenin release
$G_{\beta\gamma}$
mTORC2
MEK/ ERK
PLC
AC
Filamin
PI3K
PKC
$\uparrow[Ca^{2+}]_i$
cAMP
RAS/ MEK/ ERK
MAPKs
AKT
MAPKs
p38
JNK
ERK
PROLIFERATION/ DIFFERENTIATION
RhoA
ERK
JNK
p38
mTORC1
GENE EXPRESSION
SRF
ROCK
SURVIVAL PROLIFERATION
GENE EXPRESSION
ACTIN CYTOSKELETON

Figure 4.2. CaSR-mediated signalling pathways. The CaSR is activated by a plethora of endogenous and exogenous ligands which directly activate (orthosteric) or modulate (allosteric) receptor signalling. CaSR signals through three main groups of heterotrimeric G-proteins, $G_{q/11}$, G_i, and $G_{12/13}$ which regulate gene expression, cell proliferation, differentiation, motility and survival. $G_{q/11}$ activation phosphorylates PKC and PLC, with the latter inducing cytosolic Ca^{2+} mobilisation from intracellular stores; both pathways activate MAPK signalling. The activation of G_i inhibits adenylyl cyclase, which reduces levels of cyclic AMP and indirectly activates the MEK/ERK signalling pathway. Activation of $G_{12/13}$ mainly induces the RhoA signalling pathway. The βγ subunits activate PI3K which is induces several MAPK pathways and AKT. AKT is also required for CaSR-dependent activation of mTORC2 which initiates mTORC1 signalling. The CaSR can also induce growth factor signalling (specifically EGFR) through the cleavage of membrane-bound ligands. Gs signalling has been implicated in some pathological contexts, such as human breast cancer. CaSR: calcium-sensing receptor; EGFR: epidermal growth factor receptor ERK: extracellular signal-regulated kinase 1/2; HB-EGF: heparin-bound EGF; MAPK: mitogen activated protein kinase; MEK: mitogen-activated protein kinase kinase; MMP: matrix metalloproteinase; mTORC: mammalian target of rapamycin complex; PI3K: phosphoinositide-3 kinase; PLC: Phospholipase C.

4.3. Results

4.3.1. The CaSR is functionally expressed in human lung fibroblasts

Expression of CaSR protein in NHLF was confirmed by immunofluorescence microscopy (Figure 4.3A) showing both plasma and intracellular CaSR protein expression. Natural polyamines and basic amino acids are positively charged at physiological pH and activate the CaSR, evoking an increase in intracellular free ionised calcium concentration ($[Ca^{2+}]_i$) (Quinn *et al*. 1997). In many cell types, CaSR activation leads to $Ca^{2+}{}_i$ release and consequent increased cytosolic Ca^{2+} concentration.

Fibroblasts are thought to be the key mediators of the profibrotic response in IPF, and crucial to this process are increases in $[Ca^{2+}]_i$, which underpins key cellular functions such as gene expression, cell proliferation and differentiation (Janssen *et al*. 2015). Therefore, I hypothesised that CaSR activators, Ca^{2+} and polyamines could mediate CaSR-induced Ca^{2+} signalling in fibroblasts. To test this hypothesis, I measured the changes in $[Ca^{2+}]_i$ induced by these CaSR agonists. CaSR is half-maximally active at the physiological $[Ca^{2+}]_o$ concentration (~1.2 mM) which was used as the baseline response (Brown *et al*. 1993). Fibroblasts were maintained at this resting $[Ca^{2+}]_i$, after which treatment with various CaSR ligands: 5 mM $[Ca^{2+}]_o$ (divalent cation), 5 mM ornithine (basic amino acid), or 1mM spermine (polyamine) evoked a significant rise in $[Ca^{2+}]_i$ from baseline (Figure 4.3, B, Ci, Di and Ei). This rise in $[Ca^{2+}]_i$ induced by 5 mM $[Ca^{2+}]_o$, ornithine and spermine is completely abolished in the presence of NAM (1 μM) ($p < 0.0001$, $p = 0.0003$ and $p = 0.001$, respectively) (Figure 4.3, B, Cii, Dii and Eii), indicating an involvement of the receptor in $[Ca^{2+}]_i$ mobilisation.

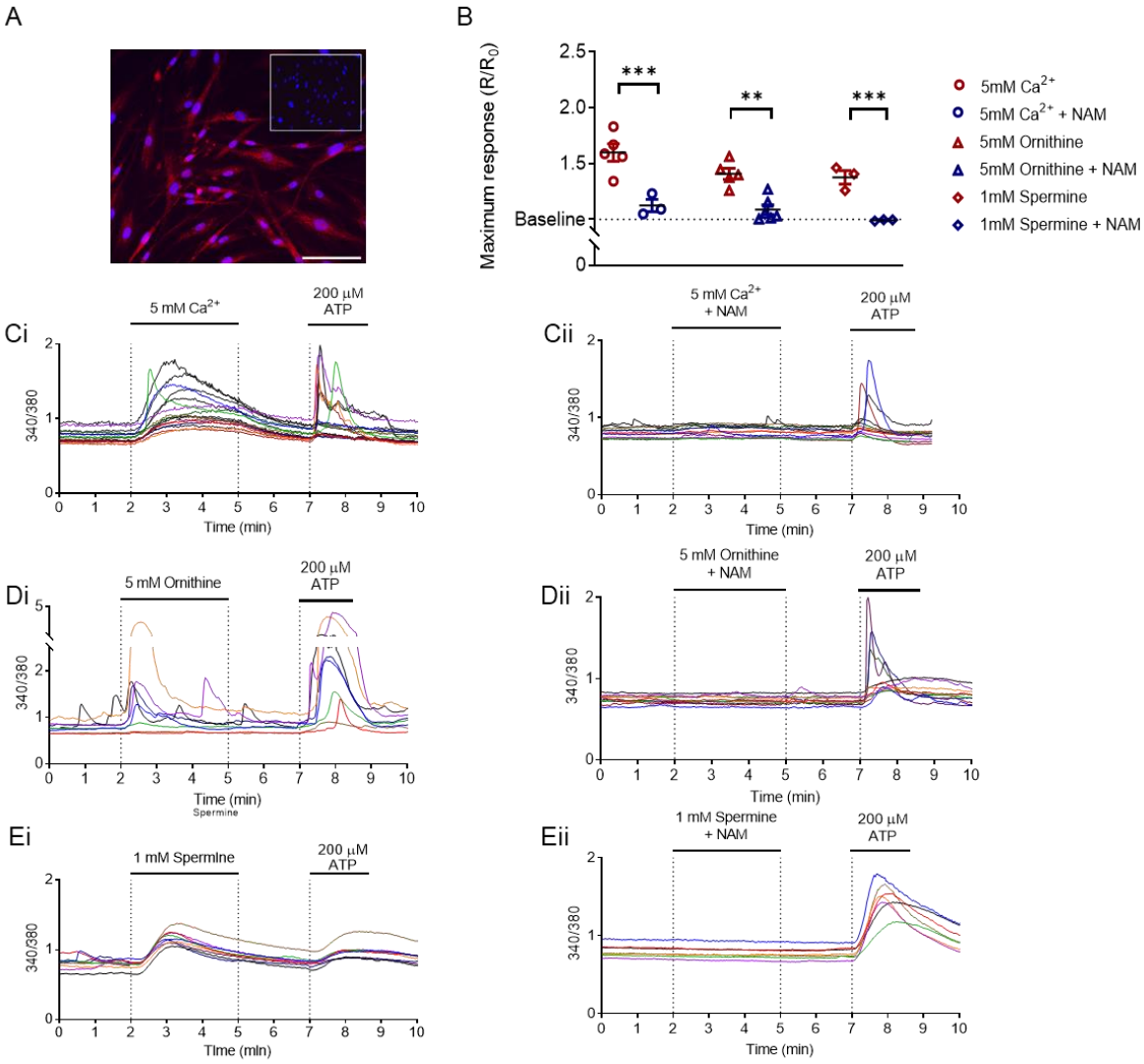

Figure 4.3. Calcium-sensing receptor (CaSR) is expressed in normal human lung fibroblasts (NHLFs) and is activated by polyamines upregulated in PF. **A.** Representative image of CaSR expression in NHLFs (red), nuclei (blue), negative control (insert). **B.** Summary data of intracellular calcium levels ($[Ca^{2+}]_i$) in NHLF in response to: **Ci.** 5 mM $Ca^{2+}{}_o$ (divalent cation); **Di.** 5 mM L-ornithine (basic amino acid); and **Ei.** 1 mM spermine (polyamine). **B, Cii-Eii.** Treatment with NAM prevents these increases in $[Ca^{2+}]_i$. **C-E.** Representative traces of NHLF $[Ca^{2+}]_i$ response to CaSR activators. Data are shown as mean ± SEM. ANOVA (Bonferroni post hoc test); $^{**}p<0.01$, $^{***}p<0.001$. 5 mM Ca^{2+} (*n* = 3-6; 108 cells), L-ornithine (*orn; n* = 5-6; 109 cells) and spermine (*spm; n* = 3; 39 cells). *N* = 6 donors. Scale bar: 100 µm. CaSR negative allosteric modulator; NAM, NPS2143 (1 µM). Pulmonary fibrosis; PF.

4.3.2. TGFβ1 increases CaSR expression in primary human lung fibroblasts

Studies have shown that TGFβ and CaSR mediate similar cellular processes such as proliferation, cytoskeletal changes, remodelling, and cytokines secretion. This led to the hypothesis that CaSR signalling potentiates the profibrotic effects of TGFβ in NHLFs. Once I established the presence of the receptor in NHLFs, I explored the effect of TGFβ1 on CaSR expression. The results show that CaSR expression in NHLF was doubled by TGFβ1 (5 ng/mL) treatment for 72 hours (p = 0.02), compared to vehicle-treated cells (Figure 4.4, A-C, red). However, NAM treatment did not significantly alter CaSR expression in the presence and absence of TGFβ1 (Figure 4.4C).

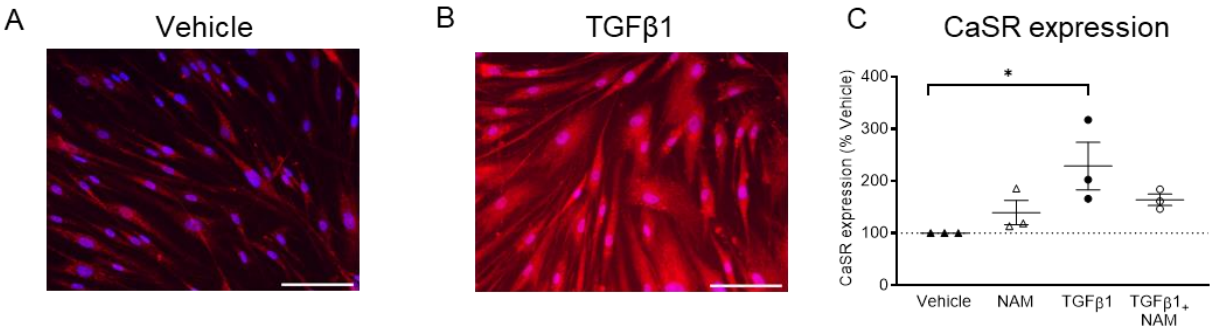

Figure 4.4. TGFβ1 treatment upregulates expression of the calcium-sensing receptor (CaSR) in normal human lung fibroblasts (NHLFs). A. Representative image showing baseline CaSR expression (red) in NHLFs. **B-C.** NHLFs treated with TGFβ1 show significantly greater CaSR expression compared to control (vehicle). Semi-quantitative data are normalized to the vehicle control (which was set at 100%, dashed line) and expressed as mean ± SEM. Statistical comparisons: ANOVA with Bonferroni post hoc test; *p<0.05. (**C**). *N* = 3 donors; n = 3 independent experiments. Scale bars: 100 µm. CaSR negative allosteric modulator; NAM, NPS2143 (1 µM).

4.3.3. Anti-fibrotic effects of NAM mediated via key signalling pathways

Multiple signalling molecules are associated with the pathogenesis of IPF through the interaction of common signalling pathways. The PI3K/AKT/mTOR pathway and RAS/RAF/MEK/MAPK pathway are well characterised and known to mediate cellular proliferation, survival, migration, and protein synthesis. Using RNA sequencing, I was able to delineate the signalling molecules induced by TGFβ1 treatment, determine the effect of NAM on the gene expression of these molecules, and suggest a hypothesis that links these signalling molecules and IPF-related profibrotic processes (Figure 4.5 – 4.7).

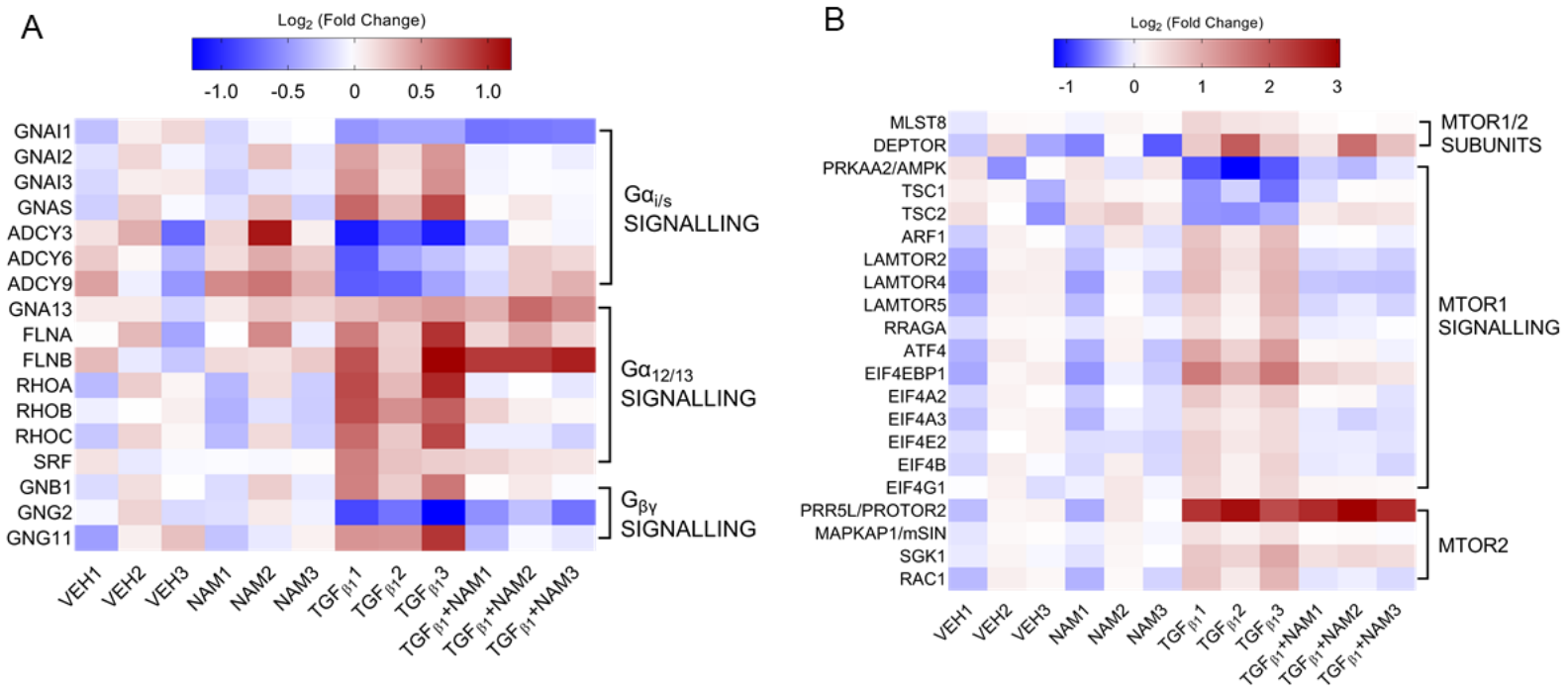

Figure 4.5 TGFß1 alters genes associated with CaSR and mTOR signalling while NAM restores baseline response. The heatmaps show the log2 ratio of differentially expressed genes (versus vehicle) implicated in CaSR signalling **(A)** and mTOR signalling **(B).** Exogenous TGFß treatment results in the upregulation of most genes while co-treatment with the NAM, NPS2143 (1 μM) reduces gene expression. Notably, the opposite effect was seen for genes encoding adenylyl cyclase, AMPK and TSC. Bioinformatics analysis was done on normalised data using R-package DESeq2. A Benjamini-Hochberg p-value adjustment was performed in all statistical tests; level of controlled false positive rate was set to 0.05. N = 3 donors. NAM: Calcium-sensing receptor (CaSR) Negative Allosteric Modulator treatment; TGFß: Transforming growth factor ß (TGFß) treatment; TGFß+NAM: TGFß and CaSR Negative Allosteric Modulator co-treatment.

The finding that TGFß1 upregulates genes associated with CaSR and mTOR signalling (Figure 4.5) led to the investigation of the expression of RAS genes since this pathway is associated with TGFß1, CaSR and mTOR signalling cascades. Figure 4.6A shows *CALM2* (gene encoding calmodulin 2, p_{adj} *value* = $6x10^{-4}$), *GRB2* (p_{adj} *value* = $1x10^{-2}$) and several members of the RAS oncogene family - *HRAS* (p_{adj} *value* = $5x10^{-3}$), *NRAS* (p_{adj} *value* = $7x10^{-5}$), *RRAS* (p_{adj} *value* = $2x10^{-2}$), and *MRAS* (p_{adj} *value* = $9x10^{-9}$) were upregulated by TGFß1 treatment. Co-treatment with NAM repressed the expression of all genes, although this decrease was not significant for *NRAS* and *MRAS* (Figure 4.6A).

One of the pathways activated by RAS is the MEK/ERK pathway. Here, I show that MEK2 (encoded by *MAP2K2*) was increased by exogenous TGFß1 application (fold change *MAP2K2* = 1.4), and baseline MAP2K2 expression was restored by NAM treatment (p_{adj} *value* = $1x10^{-3}$; Figure 4.6B). MAPKs also activate JUNB and JUND signalling, which mediate proliferation, collagen synthesis and cytokine synthesis (Florin *et al*. 2006; Wygrecka *et al*. 2012). TGFß1 treatment doubled *JUNB* expression while *JUND* expression increased by 40%, baseline expression of both genes was restored in the presence of NAM (p_{adj} *value JUNB* = $3x10^{-4}$, *JUND* = $2x10^{-4}$; Figure 4.6B). TGFß1 treatment had opposite effects on the expression of *CEBPB* and *NFKB*. *CEBPB* expression was upregulated while NFKB was downregulated by TGFß1; NAM co-treatment abolished these changes (p_{adj} *value: CEBPB* = $7x10^{-4}$, *NFKB* = $9x10^{-4}$; Figure 4.6B).

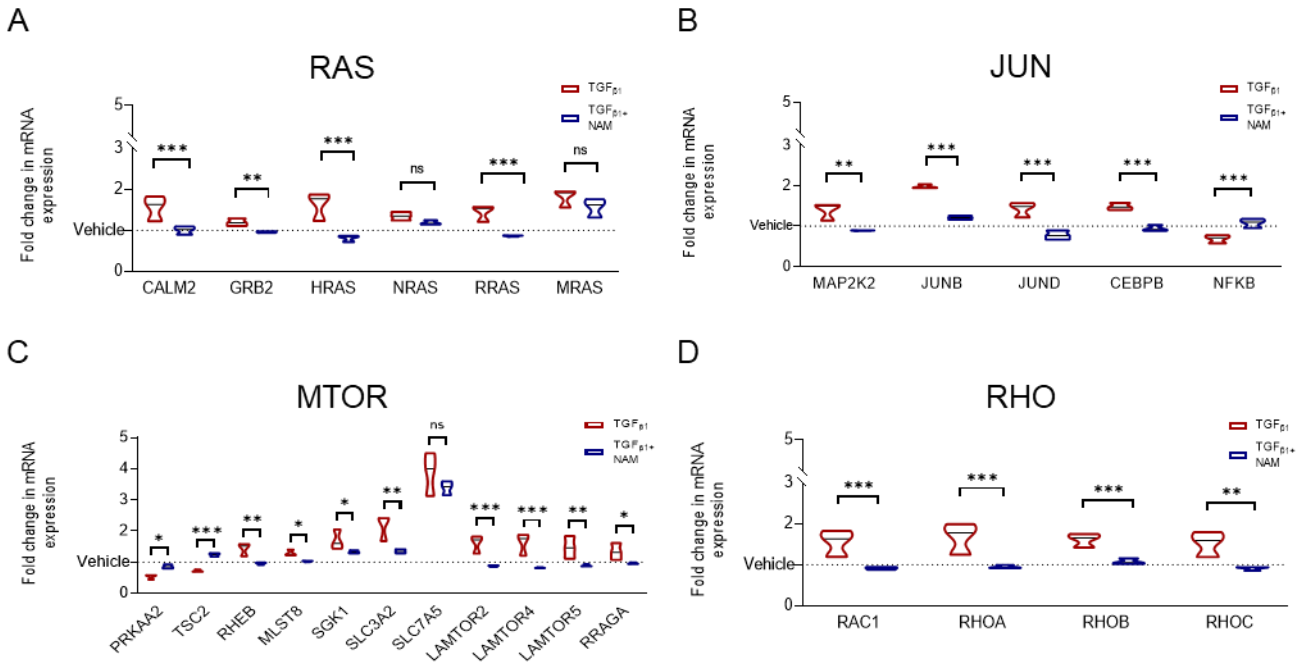

Figure 4.6 RNAseq analysis: CaSR negative allosteric modulator, NPS2143 attenuates TGFß1-induced upregulation of key profibrotic signalling genes in normal human lung fibroblasts. Differential gene expression between treatment groups using DESeq2. NAM restores baseline expression of: **A.** Positive regulators of the *RAS* oncogene pathway, and RAS proteins. **B.** MAPKs (*MAP2K2* (encodes MEK2), *JUNB*, and *JUND*), and the transcription factors, *CEBPB* and *NFKB*. **C.** Positive and negative regulators of *MTOR* signalling. Expression of amino acid transporters, *SLC3A2* and *SLC7A5*, are downregulated by the presence of NAM. **D.** The increased expression of genes associated with *RHO* signalling is also abolished with NAM co-treatment. Benjamini-Hochberg *p*-value adjustment was performed in all statistical tests; level of controlled false positive rate was set to 0.05. * $p<0.05$, ** $p<0.01$, *** $p<0.001$, ns – not significant. *N* = 3 donors. CaSR negative allosteric modulator: NAM, NPS2143 (1 μM).

The mTORC pathway, which is indirectly linked to RAS signalling via MAPKs, has been linked with proliferation, cell survival, cytoskeletal organisation, and cell migration (Engelman 2009; Platé *et al*. 2020). Adenosine 5′ monophosphate-activated protein kinase (AMPK, encoded *PRKAA2*), a negative regulator of *MTOR*, was downregulated two-fold by TGFβ1 treatment while this change was abolished in the presence of NAM (Figure 4.6C). Tuberous sclerosis complex-2 (TSC2), a negative regulator of *MTOR* which is activated by AMPK, was also downregulated by TGFβ1 treatment albeit to a lesser extent (p_{adj} *value* = $5x10^{-2}$); the TGFβ1-mediated effects on expression was also abolished in the presence of NAM (p_{adj} *value* = $8x10^{-4}$; Figure 4.6C). *RHEB*, which activates MTOR, is upregulated in the presence of TGFβ1, and baseline expression levels are restored with NAM co-treatment (p_{adj} *value* = $1x10^{-3}$; Figure 4.6C). *MLST8*, a component of mTORC1 and 2, was moderately increased in the presence of TGFβ1 while baseline expression was restored with NAM co-treatment (p_{adj} *value* = $2x10^{-2}$; Figure 4.6C).

Serum- and glucocorticoid-regulated kinases (SGK1), and *RHO* are downstream of mTOR activation. *SGK1* expression was increased by 69% from baseline, while NAM treatment halved the TGFβ1-induced response (p_{adj} *value* = $4x10^{-2}$). Amino acids can regulate the *MTOR* pathway *via* ragulator (encoded by *LAMTOR*) and RAG (encoded by *RRAG*) (Gatica and Klionsky 2017). Amino acid entry into the cell is mediated *via* solute-carrier type transporters, SLC3A2 and SLC7A5. The baseline expression of *SLC3A2* was doubled while *SLC7A5* was quadrupled with TGFβ1 treatment. NAM treatment resulted in decreased expression of both genes although levels remained above baseline (p_{adj} *value*: *SLC3A2* = $2x10^{-3}$, and *SLC7A5* = not significant; Figure 4.6C). *LAMTOR2*, *LAMTOR4*, *LAMTOR5*, and *RRAGA* expression were increased in the presence of exogenous TGFβ1 (fold change *LAMTOR2* = 1.6, *LAMTOR4* = 1.6, *LAMTOR5* = 1.5 and *RRAGA* = 1.3; Figure 4.6C) while baseline expression levels were restored in the presence of NAM

(p_{adj} *value LAMTOR2* = $3x10^{-4}$, *LAMTOR4* = $4x10^{-4}$, *LAMTOR5* = $4x10^{-3}$ and *RRAGA* = $1x10^{-2}$).

The gene expression of the 3 *RHO* isoforms, *RHOA*, *RHOB* and *RHOC*, were increased in response to exogenous TGFβ1 treatment (fold change *RHOA* = 1.7, *RHOB* = 1.6 and *RHOC* = 1.5; Figure 4.6D) while NAM co-treatment completely abrogated these changes in expression (p_{adj} *value* = $7x10^{-4}$, p_{adj} *value* = $8x10^{-5}$ and p_{adj} *value* = $1x10^{-3}$, respectively). *RHO* can also be activated via the RAS/RAC1 pathway; TGFβ1 treatment increased *RAC1* expression by 55%, while baseline expression was observed in the presence of NAM (p_{adj} *value* = $6x10^{-4}$; Figure 4.6D). Figure 4.7 suggests a hypothesis that links these signalling genes to the profibrotic processes highlighted in this chapter.

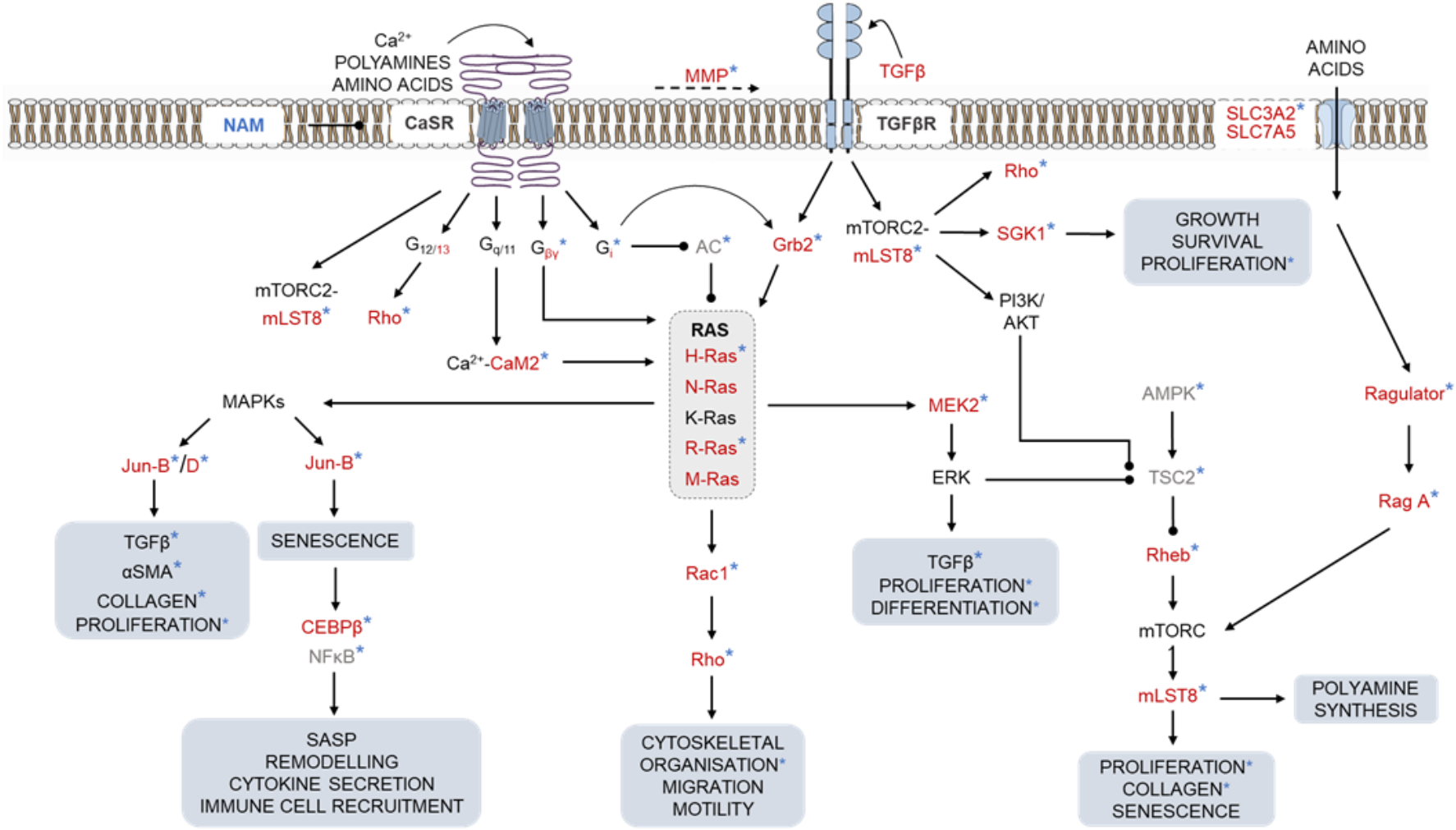
Ca2+
POLYAMINES
AMINO ACIDS
MMP*
TGFβ
AMINO ACIDS
NAM
CaSR
TGFβR
SLC3A2*
SLC7A5
Rho*
G12/13
Gq/11
Gβγ*
Gi*
AC*
Grb2*
mTORC2-
mLST8*
SGK1*
GROWTH
SURVIVAL
PROLIFERATION*
mTORC2-
mLST8*
Rho*
PI3K/
AKT
Ca2+-CaM2*
RAS
H-Ras*
N-Ras
K-Ras
R-Ras*
M-Ras
MAPKs
MEK2*
AMPK*
Ragulator*
Jun-B*/D*
Jun-B*
ERK
TSC2*
Rag A*
TGFβ*
αSMA*
COLLAGEN*
PROLIFERATION*
SENESCENCE
TGFβ*
PROLIFERATION*
DIFFERENTIATION*
Rheb*
CEBPβ*
NFκB*
Rac1*
mTORC
Rho*
mLST8*
POLYAMINE
SYNTHESIS
SASP
REMODELLING
CYTOKINE SECRETION
IMMUNE CELL RECRUITMENT
CYTOSKELETAL
ORGANISATION*
MIGRATION
MOTILITY
PROLIFERATION*
COLLAGEN*
SENESCENCE

Figure 4.7 CaSR and TGFβR drive pulmonary fibrosis via signalling crosstalk mechanisms. A schematic diagram of a cell showing CaSR and TGFβ receptors at the plasma membrane, and components of the mTOR, Ras, and MAPK signalling pathways. TGFβ activates its cognate receptors (TGFβRI/II) which can induce downstream signalling cascades which regulate mTOR activity. mTOR complexes 1 and 2 share a common positive regulator, mLST8. mTORC1 is controlled by mTORC2 and Ras-MAPK pathways. mTORC2 phosphorylates AKT directly or indirectly (via PI3K). Activated AKT then promotes mTORC1 activity by inhibiting TSC2, thereby activating Rheb. mTORC2 phosphorylates SGK1 which also inhibits TSC2. The Ras-MAPK pathway regulates mTORC1 via ERK which also inhibits TSC2. DNA damage and energy deprivation also regulate mTORC1, acting via AMPK. Amino acids enter the cell through solute transporters, SLC3A2 and 7A5, and regulate mTOR signalling via direct and indirect mechanisms. Indirect activation of mTORC1 involves the Ragulator-Rag complex. Ragulator, composed of 5 LAMTOR subunits, activates Rag A/B. mTORC2 signalling also directly activates Rho signalling. mTOR signalling regulates proliferation, collagen synthesis, cytoskeletal changes, cell survival, senescence, and autophagy.

The Ras family can be subdivided into 3 categories: p21 Ras (H-, N-, K-Ras), R-Ras, and M-Ras. Ras signalling can be independently activated via the CaSR and TGFβR. CaSR (via $G_{q/11}$) and TGFβR signalling result in the increase of intracellular Ca^{2+}. Ca^{2+}-calmodulin complex, G_i, and the $G_{\beta\gamma}$ subunit activate all 5 Ras isoforms. TGFβRs activate Grb2 resulting in the activation of p21 Ras and M-Ras. Ras activation induces (i) MEK-ERK which regulates TGFβ synthesis, proliferation, and differentiation; (ii) Rac1/Rho which regulates cytoskeletal organisation, motility, and migration; (iii) MAPKs which activate Jun-B and Jun-D thereby mediating a plethora of cellular processes including inflammation, proliferation, protein synthesis, and senescence. Senescence involves several mediators including transcription factors, CEBPβ and NFκB, which control the senescence-associated secretory phenotype (SASP). SASP act in a feedforward fashion facilitating remodelling, cytokine secretion and immune cell recruitment. Lastly, CaSR can potentially transactivate TGFβR via membrane-bound MMPs (a mechanism established for EGFR) thus potentially providing a direct link between the CaSR and TGFβ signalling.

Red represents genes upregulated by exogenous TGFβ treatment (5 ng/mL; 72 hrs). Grey represents genes downregulated by TGFβ treatment. Blue asterisks show the antagonistic action of NAM on various signalling targets. Arrows represent activation while circles represent inhibition.

4.3.4. NAM diminishes TGFß1-induced human lung fibroblast proliferation

To assess the effect of NAM on TGFß1-induced fibroblast proliferation, NHLF were loaded with BrdU for incorporation into newly synthesised DNA 24 hours before the experiments were terminated. Figure 4.8 shows exogenous TGFß1 supplementation resulted in increased proliferation (mean BrdU incorporation relative to vehicle (%) = 142.1 ± 13.6; p = 0.04). Co-treatment with NAM induced a 50% decrease in the TGFß1-induced response (p = 0.01), restoring baseline levels of proliferation.

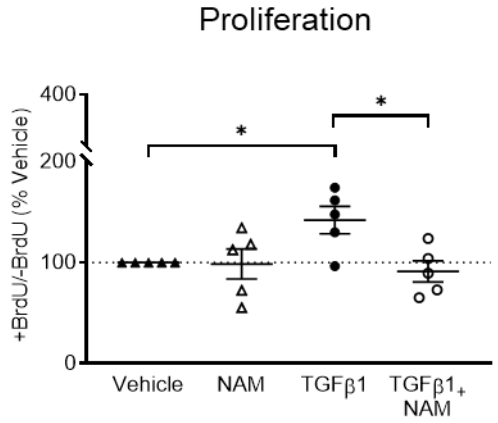

Figure 4.8 The negative allosteric modulator of the calcium-sensing receptor (NAM), NPS2143 abolishes TGFß1-induced proliferation in normal human lung fibroblasts (NHLFs). NPS2143 is ineffective in the absence of fibrotic stimulus. Data are normalized to the vehicle control (which was set at 100%, dashed line) and expressed as mean ± SEM. Statistical comparisons: ANOVA with Bonferroni post hoc test; *p<0.05. *N* = 4 donors; n = 5 independent experiments. CaSR negative allosteric modulator; NAM, NPS2143 (1 µM).

4.3.5. NAM reduces TGFβ1-induced human lung fibroblast activation

Fibrotic fibroblasts are characterised by increased αSMA expression (Conte *et al*. 2014). *In vitro,* TGFβ1-stimulated αSMA expression and stress fibre formation is used as an indicator of pathological fibroblast activation, also known as myofibroblasts. CaSR and TGFβ1 induce cytoskeletal changes through the induction of the Rho-ROCK pathway (Davies *et al*. 2006; Costanza *et al*. 2017). Here, I investigated the effect of NAM co-treatment on NHLF activation. In these experiments, TGFβ1-induced response was set as the baseline, *i.e.*, 100% and the NAM effect was assessed relative to TGFβ1 response. NHLFs treated with TGFβ1 (5 ng/mL) for 72 hours showed αSMA expression and stress fibre formation (Figure 4.9, A-B, green). Co-treatment with NAM significantly reduced αSMA protein levels and stress fibre formation (mean expression relative to TGFβ1 (%) = 75.8 $\pm$ 7.2; p = 0.04) (Figure 4.9, B-C). Mean quantified αSMA expression in unstimulated cells was detectable in 3 of 5 experiments (indicated in Figure 4.9C as baseline). Furthermore, ROCK1 is expressed in the presence of exogenous TGFβ1, and NAM treatment reduced ROCK1 protein expression (mean expression relative to TGFβ1 (%) = 81.4 $\pm$ 6.2; p = 0.06) (Figure 4.9, D-F).

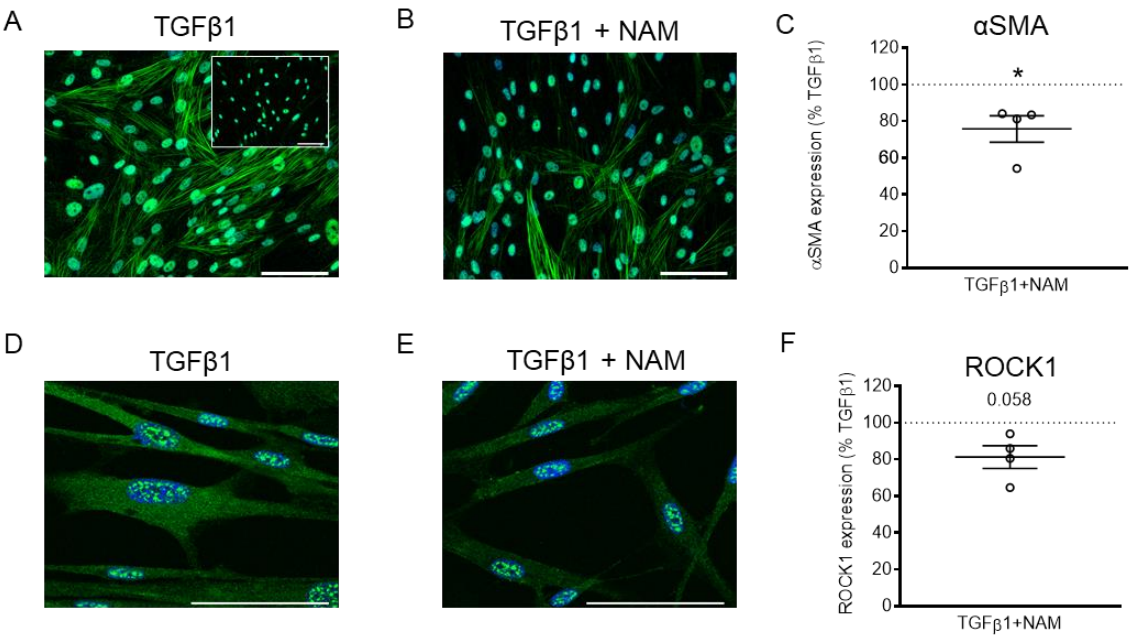

Figure 4.9 The CaSR negative allosteric modulator, NPS2143 attenuates TGFβ1-induced normal human lung fibroblast (NHLF) activation. A. TGFβ1 treatment increases alpha smooth muscle actin (αSMA) expression (green) and stress-fiber formation. Inset panel shows baseline expression. **B.** NAM decreases αSMA protein and stress-fiber expression. **C.** Semi-quantified data showing that TGFβ1-induced αSMA expression (set to 100%) reduces with NAM co-treatment. As a reference, baseline expression in unstimulated NHLFs is shown relative to TGFβ1 (*n* = 3 independent experiments). **D-F**. NAM inhibits TGFβ1-induced ROCK1 expression (a surrogate for Rho-kinase activation; green). For each experiment, data were generated from 58-1767 cells per condition, normalized to TGFβ1 (which was set at 100%, dotted line), and expressed as mean ± SEM. 2-tailed t-test; **p*<0.05. *N* = 2-4 donors; *n* = 3-5 independent experiments. Scale bars: 100 μm. Calcium-sensing receptor: CaSR; CaSR negative allosteric modulator: NAM, NPS2143 (1 μM).

4.3.6. NAM reduces TGFß1-induced soluble collagen secretion in human lung fibroblasts

Fibrotic remodelling involves the perturbation of the balance between ECM deposition and degradation with the scales tipped in favour of deposition. TGFß1 acts as a 'master switch' for the secretion of collagen and other ECM proteins from myofibroblasts (Upagupta *et al*. 2018). I explored the effect of NPS2143 on soluble collagen (I-V) secretion. Figure 4.10 shows co-treatment with NAM reduced collagen secreted by activated NHLF by 35% ($p = 0.02$).

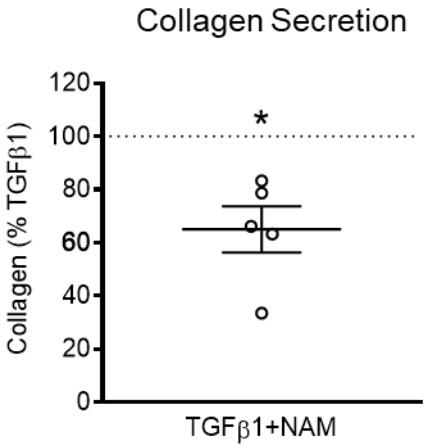

Figure 4.10 The NAM, NPS2143 attenuates TGFß1-induced collagen secretion in normal human lung fibroblasts (NHLFs). Data are normalized to TGFß1 (which was set at 100%, dotted line) and expressed as mean ± SEM. 2-tailed t-test; *p<0.05, **p<0.01. N = 3 donors; n = 3-5 independent experiments. Scale bars: 100 µm. Calcium-sensing receptor: CaSR; CaSR negative allosteric modulator: NAM, NPS2143 (1 µM).

4.3.7. NAM reduces TGFβ1-induced IL-8 secretion in human lung fibroblasts

Although the role of inflammation is somewhat controversial in IPF, several studies have proposed IL-8 as a potential IPF biomarker with higher serum concentration correlating with a worse prognosis (Guiot *et al*. 2017). Exogenous application of TGFβ1 to NHLFs induced IL-8 secretion while NAM treatment reduced the cytokine secretion by 10% (p = 0.01) (Figure 4.11; Figure S3).

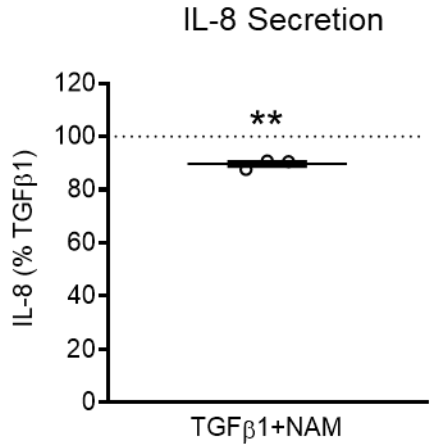

Figure 4.11 The NAM, NPS2143 attenuates TGFβ1-induced IL-8 secretion in normal human lung fibroblasts (NHLFs). Data are normalized to TGFβ1 (which was set at 100%, dotted line) and expressed as mean ± SEM. 2-tailed t-test; *p<0.05, **p<0.01. N = 3 donors; n = 3-5 independent experiments. Scale bars: 100 µm. Calcium-sensing receptor: CaSR; CaSR negative allosteric modulator: NAM, NPS2143 (1 µM).

4.4. Discussion

Recent evidence demonstrates the importance of GPCR signalling in PF (Uguccioni *et al*. 1995; Tager *et al*. 2008; Huang and Natarajan 2015; Tan *et al*. 2018). The results show 1) CaSR is expressed in NHLFs and receptor expression is increased by TGFβ1 treatment; 2) CaSR is physiologically functional in NHLF; 3) treatment with NAM, NPS2143, attenuated *in vitro* hallmarks of PF: proliferation, αSMA expression, collagen and IL-8 secretion; 4) NAM treatment restores baseline expression of signalling genes implicated in IPF. Therefore, these findings highlight a role for the GPCR, CaSR in IPF aetiology.

During lung development, the TGFβ and CaSR pathways play overlapping roles in regulating branching morphogenesis and vasculogenesis (Riccardi *et al*. 2013; Chanda *et al*. 2019). The re-initiation of several developmental pathways, albeit aberrantly, has been implicated in IPF and other age-related lung diseases (Chanda *et al*. 2019). In IPF, the aberrant activation of TGFβ signalling facilitates proliferation, remodelling and inflammation (Baarsma and Königshoff 2017). Incidentally, these processes have also been associated with increased CaSR activation in PAH and COPD (Tang *et al*. 2016; Yarova *et al*. 2016), providing a rationale to investigate the role of the CaSR in IPF.

The most studied CaSR-associated signalling pathways involve intracellular $Ca^{2+}{}_i$ mobilisation and ERK1/2 phosphorylation (Leach *et al*. 2020). CaSR couples with $G\alpha_q$ signalling protein to activate phospholipase C, resulting in Ca^{2+} mobilisation from intracellular stores and ERK1/2 activation, leading to proliferation, apoptosis, differentiation, and secretion in health and disease (Brennan *et al*. 2013; Schreckenberg and Schlüter 2018). Normal fibroblast function is regulated by intracellular calcium oscillations evoked by many growth factors, including TGFβ1 (Janssen *et al*. 2015). Janssen *et al*. (2015)

discuss several mechanisms for calcium homeostasis in pulmonary fibroblasts with a focus on calcium/cationic channels. Interestingly, their results showed the elimination of Ca^{2+} oscillations in the absence of extracellular Ca^{2+}. In HEK-293 cells stably transfected with CaSR, $Ca^{2+}{}_i$ oscillations were induced by small perturbations in extracellular Ca^{2+} while positive allosteric modulators of the receptor resulted in CaSR-induced Ca^{2+} release from intracellular stores (Breitwieser 2006). In addition to calcium influx via calcium/cationic channels, the data presented make a case for alternative mechanisms involving extracellular calcium signalling via the CaSR since receptor activators, Ca^{2+}, ornithine and spermine, all induce Ca^{2+} mobilisation. Since injured or dying cells secrete polyamines (Zhang *et al*. 2000), these findings provide a potential mechanism where activation of the CaSR mediates epithelial cell injury, thereby contributing to (myo)fibroblast activation and fibrosis.

The CaSR might contribute to αSMA expression and stress fibre formation by interacting with the $G\alpha_{12/13}$ or mTORC2 pathway. CaSR has been shown to activate Rho-kinases, essential for actin remodelling, cytoskeletal changes and motility (Schreckenberg and Schlüter 2018). Employing the same signalling mechanism, CaSR induces actin formation in breast cancer cells which the authors suggest could contribute to cell motility and metastases (Brennan *et al*. 2013). In IPF, a recent study identified the RhoA/ROCK pathway as the most enriched pathway in the cells found within the fibrotic foci (Guillotin *et al*. 2020). Since TGFβ1-induced ROCK1 and αSMA expression were reduced to similar levels by NAM, my data suggests that the CaSR mediates αSMA expression through the RhoA/ROCK pathway.

Another G protein-coupled pathway altered by exogenous TGFβ1 application is the $G\alpha_i$ signalling pathway. Although this pathway was only investigated at the gene level, it is worth noting that the data presented in this chapter shows that NPS2143 restores baseline expression of $G\alpha_i$ and adenylyl cyclase isoforms which were upregulated and downregulated in the presence of

TGFβ1, respectively. This is of relevance here because increases in cyclic AMP, which occurs in response to $G\alpha_i$ inhibition, $G\alpha_s$ activation, or adenylyl cyclase activation, prevent fibroblast proliferation, αSMA expression and collagen synthesis in lung fibroblasts and *in vivo* models of PF (Lindenschmidt and Witschi 1985; Huang *et al*. 2008).

The RAS/MEK/ERK signalling cascade can be activated by several G protein subunits, including $G\alpha_q$, $G\alpha_i$, and Gβγ (Luttrell 2003). The data presented in this chapter shows that several genes from the RAS and MAPK pathways that regulate ERK signalling were increased by TGFβ treatment and NAM treatment effectively abolished the upregulation of these genes. The RAS/MEK/ERK signalling pathway, which is the primary component of the MAPK pathway, plays a key role in regulating cell proliferation, survival, senescence, and differentiation (Braicu *et al*. 2019). This is the case in NHLFs where MEK inhibition was shown to suppress ERK phosphorylation, fibroblast activation and αSMA expression (Kohan *et al*. 2010). *In vivo*, MEK inhibition reduces bleomycin-induced lung fibrosis in mice (Galuppo *et al*. 2011). Recent studies have shown that this signalling pathway contributes to cardiac fibroblast proliferation, activation and collagen synthesis (Wu *et al*. 2016; Chi *et al*. 2018).

Furthermore, the promotion of these profibrotic processes is associated with a CaSR-induced increase in Ca^{2+}_i and MEK activation (Chi *et al*. 2018). Similarly, CaSR activation in vascular smooth muscle cells activates the MEK/ERK pathways and the PLC-IP_3 pathway (which induces Ca^{2+}_i mobilisation), thus increasing cell proliferation and survival while inhibiting the CaSR, MEK or PLC attenuated these responses (Molostvov *et al*. 2008). Although the latter studies were not performed using lung fibroblast and further experiments are required to validate the effect of NAMs on MEK and ERK activation with phosphorylation studies in TGFβ1-treated NHLFs, these findings suggest a potential mechanistic link between the CaSR, fibroblast activation and the accumulation of collagen observed in PF.

Another signalling pathway activated by RAS is the mTOR cascade which is implicated in metabolic homeostasis, protein synthesis and cell growth (Braicu *et al*. 2019). Previous studies have shown that mTORC1 signalling is crucial for collagen expression in HLFs, and pharmacological or genetic inhibition of this pathway abolishes this profibrotic response in NHLFs, IPF-HLFs and *ex vivo* slices from IPF lungs (Mercer *et al*. 2016; Woodcock *et al*. 2019; Guillotin *et al*. 2020). In addition, the enzymatic activity of AMPK, an inhibitor of the mTORC1 pathway, is reduced in IPF fibroblasts while activation of this protein significantly attenuates bleomycin-induced PF in mice (Rangarajan *et al*. 2018).

Although inflammation is thought to play a limited role in established IPF, it may be crucial in the early stages of the disease (Wynn 2011). The inflammatory cytokine, IL-8, is an important mediator of IPF-related processes such as fibroblast proliferation and migration (Yang *et al*. 2018). These processes are most pronounced in mesenchymal progenitor cells and macrophages located at the leading edge of active fibrotic lesions where high levels of IL-8 and its receptor, CXCR1, ensure the maintenance and expansion of fibrotic foci (Yang *et al*. 2018). Furthermore, activation of the transcription factors CEBPβ and NF-κB induces chronic IL-8 expression, thereby reinforcing the profibrotic microenvironment through the induction of senescent pathways and SASP (Kuilman *et al*. 2008; Acosta *et al*. 2013; Hansel *et al*. 2020). Taken together, these findings suggest that in a profibrotic environment, the CaSR could contribute to fibroblast activation by inducing IL-8 mediated senescence, proliferation and migration.

4.5. Limitations and Future directions

Although the signalling pathways discussed in this chapter have been previously demonstrated in other cells, a limitation of this study is the lack of experimental evidence functionally validating some of these intracellular signalling pathways in NHLFs. Future studies could address this limitation by investigating the effect of NAMs on TGFβ1-induced MEK, ERK, PI3K, AKT and mTOR phosphorylation in NHLFs. These events could be assessed using Western blots.

4.6. Conclusion

Since the CaSR ligands (*i.e.*, polyamines), which are increased in the saliva of IPF patients, can activate the CaSR *in vitro*, my study provides a potential mechanistic link between receptor activation and intracellular signalling pathways which facilitate profibrotic processes underpinning PF pathogenesis. Furthermore, TGFβ1 increases CaSR expression, potentially augmenting the CaSR-mediated pathway, leading to a vicious cycle. Therefore, NAMs could interrupt this cycle by attenuating pathological hallmarks of IPF: fibroblast proliferation, myofibroblast accumulation, and collagen deposition. These findings suggest that the CaSR contributes to mechanisms involved in fibroblast activation and that NAMs may be beneficial in inhibiting TGFβ1-induced PF.

CHAPTER 5: NAM MODULATES THE TRANSCRIPTOME OF TGFβ1-TREATED NORMAL HUMAN LUNG FIBROBLASTS

5.1. Overview

This section assesses the suitability of TGFβ1 treatment of NHLFs as an *in vitro* model of PF, and examines the effects of the NAM, NPS2143, on profibrotic gene expression and amino acid metabolism.

5.2. Introduction

Metabolic reprogramming is increasingly being recognised as a player in the pathogenesis of lung fibrosis, facilitating fibroblast activation, growth, contractility and proliferation (Bernard *et al*. 2015; Bernard *et al*. 2018; Selvarajah *et al*. 2019). Cellular metabolism refers to a broad range of biochemical reactions which provide the large energy requirements needed to sustain these processes, thereby determining cell fate and function (Deberardinis and Thompson 2012; Amelio *et al*. 2014). The major metabolic pathways in fibroblasts rely on glucose and glutamine to provide intermediates for the tricarboxylic acid (TCA) cycle, thereby generating energy (Para *et al*. 2019) (Figure 5.1).

Glucose uptake and its subsequent breakdown into pyruvate occur through a series of steps known as glycolysis which yields adenosine triphosphate (ATP) and nicotinamide adenine dinucleotide (NADH). In the cytosol, the glycolytic process is terminated with the conversion of pyruvate to lactate, typically under hypoxic conditions (Xie *et al*. 2015). Interestingly, this process is augmented in bleomycin-treated mouse lungs, human IPF lung tissue and TGFβ-treated lung fibroblasts from normal and IPF patients even under aerobic conditions (Bernard *et al*. 2015; Xie *et al*. 2015). TGFβ treatment also enhances aerobic mitochondrial ATP production and oxygen consumption in fibroblasts (Bernard *et al*. 2015). In the presence of sufficient

oxygen, pyruvate is oxidised to acetyl coenzyme A (acetyl-CoA), which is incorporated into the TCA cycle in the mitochondria, generating NADH and flavin adenine dinucleotide, which are utilised in the production of ATP through a process known as oxidative phosphorylation (Zhao *et al*. 2018).

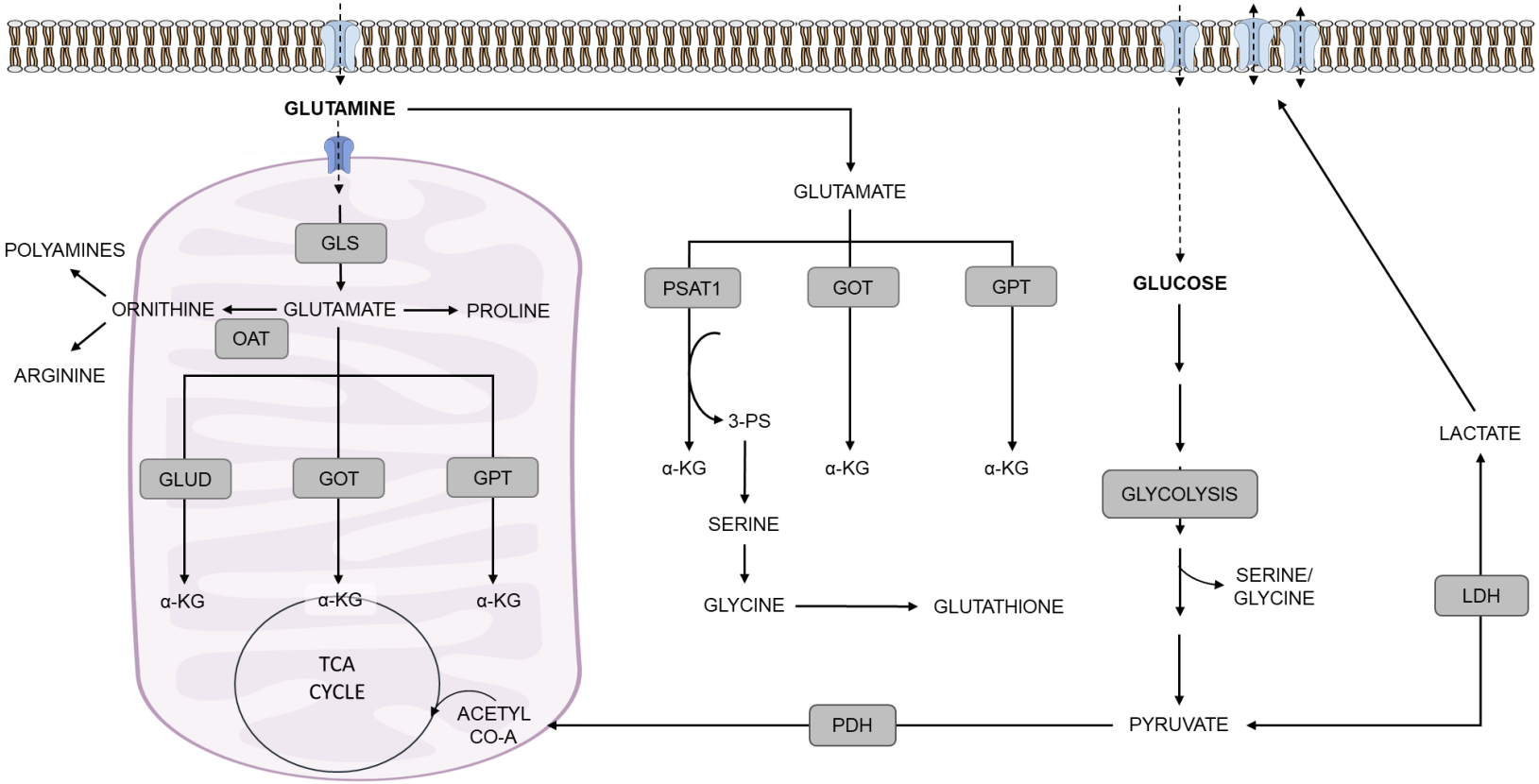

Figure 5.1 Metabolic reprogramming implicated in IPF pathogenesis. Major metabolic pathways in fibroblasts rely on glucose and glutamine to provide intermediates for the tricarboxylic acid (TCA) cycle for energy production in the presence of fibrotic stimuli. The glycolytic pathway also provides substrates for serine and glycine synthesis which are important for collagen deposition. Collagen can also be produced from glutamine through the polyamine pathway. Glutamine metabolism provides non-essential amino acids required to sustain fibroblast growth and proliferation. A-KG: α-ketoglutarate; GLS: glutaminase; GLUD: glutamate dehydrogenase; Gly: glycine; GOT: glutamate-oxaloacetate transaminase; GPT: glutamate-pyruvate transaminase; OAT: ornithine aminotransferase; PDH: pyruvate dehydrogenase; PS: phosphoserine; PSAT: phosphoserine aminotransferase.

In addition to its anaplerotic role in oxidative phosphorylation, the glycolytic pathway provides an essential substrate, 3-phosphoglycerate, for *de novo* serine/glycine metabolism, which is essential for the production of collagen by activated fibroblasts (Nigdelioglu *et al*. 2016; Hamanaka *et al*. 2018). Serine is synthesised from 3-phosphoglycerate through a series of steps involving 3 different enzymes, phosphoglycerate dehydrogenase (PHGDH), phosphoserine aminotransferase 1 (PSAT1), and phosphoserine phosphatase (PSPH); this pathway is terminated by the conversion of serine to glycine, which is catalysed by serine hydroxymethyltransferase (SHMT) (Amelio *et al*. 2014). Glycine serves as a precursor for various biosynthetic pathways, including protein, purine, and glutathione synthesis, which facilitate proliferation (Schulze and Harris 2012). Furthermore, PSAT1 indirectly fuels proliferation by using a metabolite of the serine pathway, 3-phosphohydroxypyruvate, to convert glutamate to α-ketoglutarate and other TCA intermediates (Possemato *et al*. 2011).

Proliferating cells metabolise available nutrients to produce ATP and cellular components vital for replication and division (Zhao *et al*. 2018). One such nutrient required by growth factor-stimulated cells is glutamine (Deberardinis and Thompson 2012). Glutamine is the most abundant free amino acid in the blood, and its anaplerotic role replenishes the TCA cycle with α-ketoglutarate and acetyl-CoA *via* glutaminolysis and reductive carboxylation, respectively (Yang *et al*. 2014; Zhao *et al*. 2018). Glutaminolysis provides essential carbon and nitrogen atoms, which are incorporated into nucleotides, glutathione, and other amino acids. The first step in this process involves the conversion of glutamine to glutamate through the enzymatic action of glutaminase (GLS), glutamate is then converted to α-ketoglutarate by glutamate dehydrogenase (GLUD) or aminotransferases (Hamanaka *et al*. 2019). Overexpression of aminotransferases have been implicated in liver fibrosis and cancer; these enzymes catalyse the transfer of nitrogen from glutamate to an α-ketoacid, forming another amino acid and α-ketoglutarate (Altman *et al*. 2016). For

example, PSAT1 in the serine/glycine biosynthetic pathway transfers nitrogen from glutamate to 3-phosphohydroxypyruvate to produce phosphoserine and α-ketoglutarate. The primary role of glutamine/glutamate metabolism in activated fibroblasts is to provide a source of the non-essential amino acids, glycine and proline, required for collagen synthesis (Bernard *et al*. 2018; Hamanaka *et al*. 2019). Another route for proline synthesis is through the reversible conversion of ornithine to P5C by the aminotransferase (OAT), producing arginase, an enzyme that is upregulated in PF (Kitowska *et al*. 2008). The three polyamines synthesised by humans are produced through a series of steps from arginase (Maarsingh et al. 2008a). These polyamines (putrescine, spermidine and spermine) are known to activate the CaSR, regulating transcription and translation and promoting cell survival and growth (Quinn *et al*. 1997; Landau *et al*. 2010).

The aim of this chapter was to determine whether differences exist between the genetic profiles of unstimulated NHLFs compared with TGFβ1-stimulated samples and to assess the effects of NAM on unstimulated and TGFβ1-induced differential gene expression. To this end, RNA sequencing was performed to assess the transcriptomic signatures of the different treatment groups.

5.3. Results

5.3.1. NHLFs treated with TGFβ1 display a profibrotic genetic profile

TGFβ is the most employed *in vitro* model of inducing a fibrotic phenotype in fibroblasts (Kolb *et al*. 2002; Hu *et al*. 2003; Wei *et al*. 2017; Vander Ark *et al*. 2018; Woodcock *et al*. 2019; Frangogiannis 2020). Therefore, I used this model to carry out an in-depth analysis of the effect of NAM on the transcriptome of these fibrotic NHLFs. Firstly, I assessed the suitability of TGFβ1 as a profibrotic mediator by exploring the experimental variability between samples. Principal component (PC) analysis shows that the main sources of variance in the dataset are TGFβ1 treatment, patient sex and ethnicity. PC1, which accounts for 61% variance, separates samples based on TGFβ1 treatment (Figure 5.2, A). PC2 clusters the samples based on sex (Figure 5.2, Ai), while PC3 groups the samples based on ethnicity (Figure 5.2, Aii). Collectively, PC2 and PC3 represent 31% of the total variance in the dataset.

Another method of assessing sample variability is to perform hierarchical clustering of the whole sample set (Koch *et al*. 2018). The dendrogram shows how the 12 samples cluster based on dissimilarity, which is determined as a function of height (Figure 5.2, B). The most similar samples, *i.e.*, the shortest distance from the origin, are the untreated donor 1 vehicle (Veh1) and NAM (NAM1), next is donor 2 (Veh2 and NAM2), then donor 3 (Veh3 and NAM3). The samples appear to differ from each other (signified by the length of linking arms) based on their biological origin. However, no differences are observed based on the experimental condition, *i.e.*, vehicle and NAM treatment. Furthermore, the untreated arm shows the greatest similarity between donor 1 and 2 while donor 3 is on a different branch, supporting the PCA analysis (Figure 5.2, Ai). TGFβ1 treatment has the most significant effect inducing the highest dissimilarity between the groups, thereby culminating in a treatment arm which consists of the TGFβ1-treated (TGFb) and TGFβ1 and NAM (TGFb.NAM) co-treated samples (Figure 5.2, B). Less

variability is observed in the TGFβ1-treated group compared with the untreated arm. However, the samples cluster in a manner reminiscent of the untreated arm, with donors 1 and 2 showing the highest level of similarity within this treatment group. Samples co-treated with NAM show the least variability within the group (Figure 5.2, B). However, donor 2 is on a separate branch indicating a slight difference in NAM response compared to the other 2 samples.

TGFβ1 treatment significantly altered 4756 genes compared to vehicle control (Figure 5.3, A). Given the role of TGFβ in gene expression, it is unsurprising that 58% of the differentially expressed genes were upregulated. Co-treating NHLFs with NAM significantly upregulated 2150 genes whilst downregulating 2608 genes when compared to TGFβ1 treated fibroblasts (Figure 5.3, B). However, a comparison of the co-treatment cohort to vehicle showed 1033 genes were upregulated while 871 were downregulated (Figure 5.3, C), suggesting NAM induces a genetic profile considerably closer to baseline than TGFβ1 treatment. Treating the fibroblasts with NAM on its own did not induce any significant changes in gene expression (Figure 5.3, D). These findings are consistent with the fact that NAMs are allosteric modulators as such, are inactive in the absence of ligands (Christopoulos 2014).

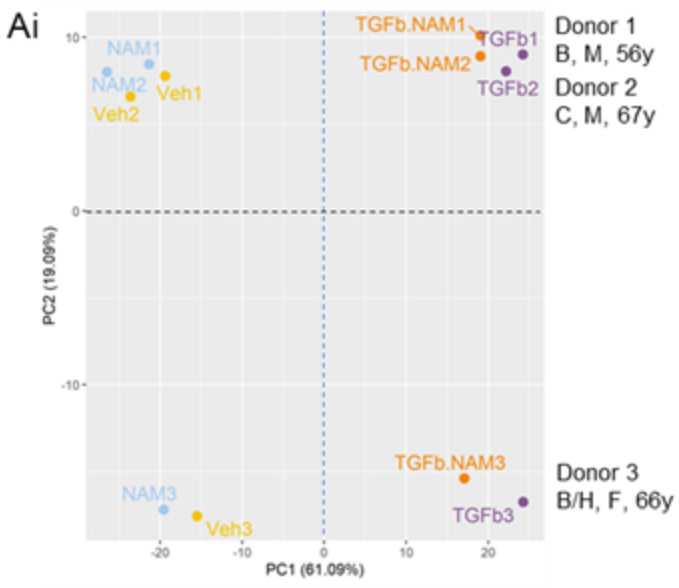
Ai
TGFb.NAM1
TGFb1
TGFb.NAM2
TGFb2
NAM1
NAM2
Veh1
Veh2
Donor 1
B, M, 56y
Donor 2
C, M, 67y
TGFb.NAM3
NAM3
Veh3
TGFb3
Donor 3
B/H, F, 66y
PC2 (19.09%)
PC1 (61.09%)

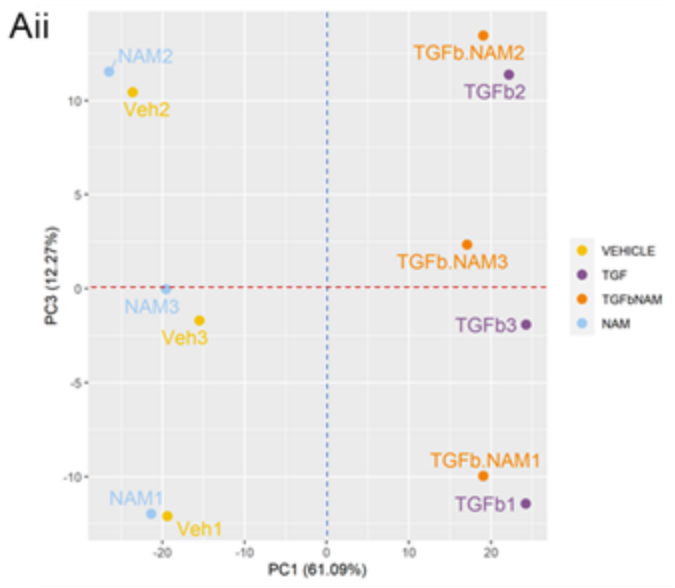
Aii
NAM2
TGFb.NAM2
TGFb2
Veh2
TGFb.NAM3
NAM3
Veh3
TGFb3
TGFb.NAM1
NAM1
Veh1
TGFb1
VEHICLE
TGF
TGFbNAM
NAM
PC3 (12.27%)
PC1 (61.09%)

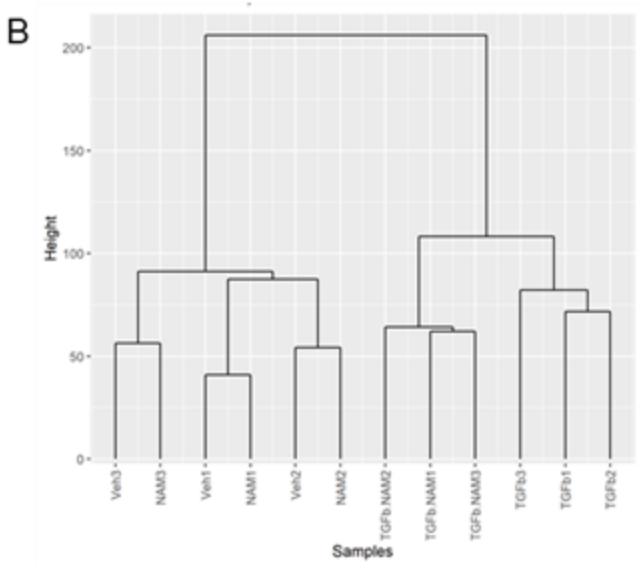
B
Height
Samples
Veh3
NAM3
Veh1
NAM1
Veh2
NAM2
TGFb.NAM2
TGFb.NAM1
TGFb.NAM3
TGFb3
TGFb1
TGFb2

Figure 5.2 TGFβ1 treatment induces distinct experimental sample clusters in RNA sequencing experiment. Gene expression changes in primary human lung fibroblasts were investigated after 72-hour treatment with vehicle (0.01% DMSO), NAM (1 μM NPS2143), TGFβ1 (5ng/mL), and TGFβ1+NAM. **A.** Principal component analysis shows principal component (PC) 1, 2, and 3 account for 92.5% of the total variance between the treatment groups. PC1 separates samples based on TGFβ1 treatment, suggesting this variable is the main source of variance (accounting for 61.1%, blue line) in the dataset. PC2 accounts for 19.1% variance, further clusters the samples (black line) probably based on sex while PC3 which accounts for 12.3% variance separates the groups into 3 distinct clusters (red line) probably based on ethnicity. **B.** Dendrogram cluster analysis (based on Ward's criterion and Euclidean distance) shows samples are grouped based on biological replicates and treatment conditions. The height of the vertical lines indicates the degree of difference between branches; the longer the line, the greater the difference. The unstimulated group (Veh and NAM) cluster based on biological source while the stimulated group (TGFb and TGFb.NAM) cluster based on the type of treatment. Bioinformatics analysis done on variance stabilising transformed data using R-package DESeq2. N = 3 donors. B: Black; B/H: Black/Hispanic; C: Caucasian; F: Female; M: Male; NAM: Calcium-sensing receptor (CaSR) Negative Allosteric Modulator treatment; TGFb: Transforming growth factor β1 (TGFβ1) treatment; TGFb.NAM: TGFβ1 and CaSR Negative Allosteric Modulator co-treatment; Veh: vehicle treatment; y: Years old.

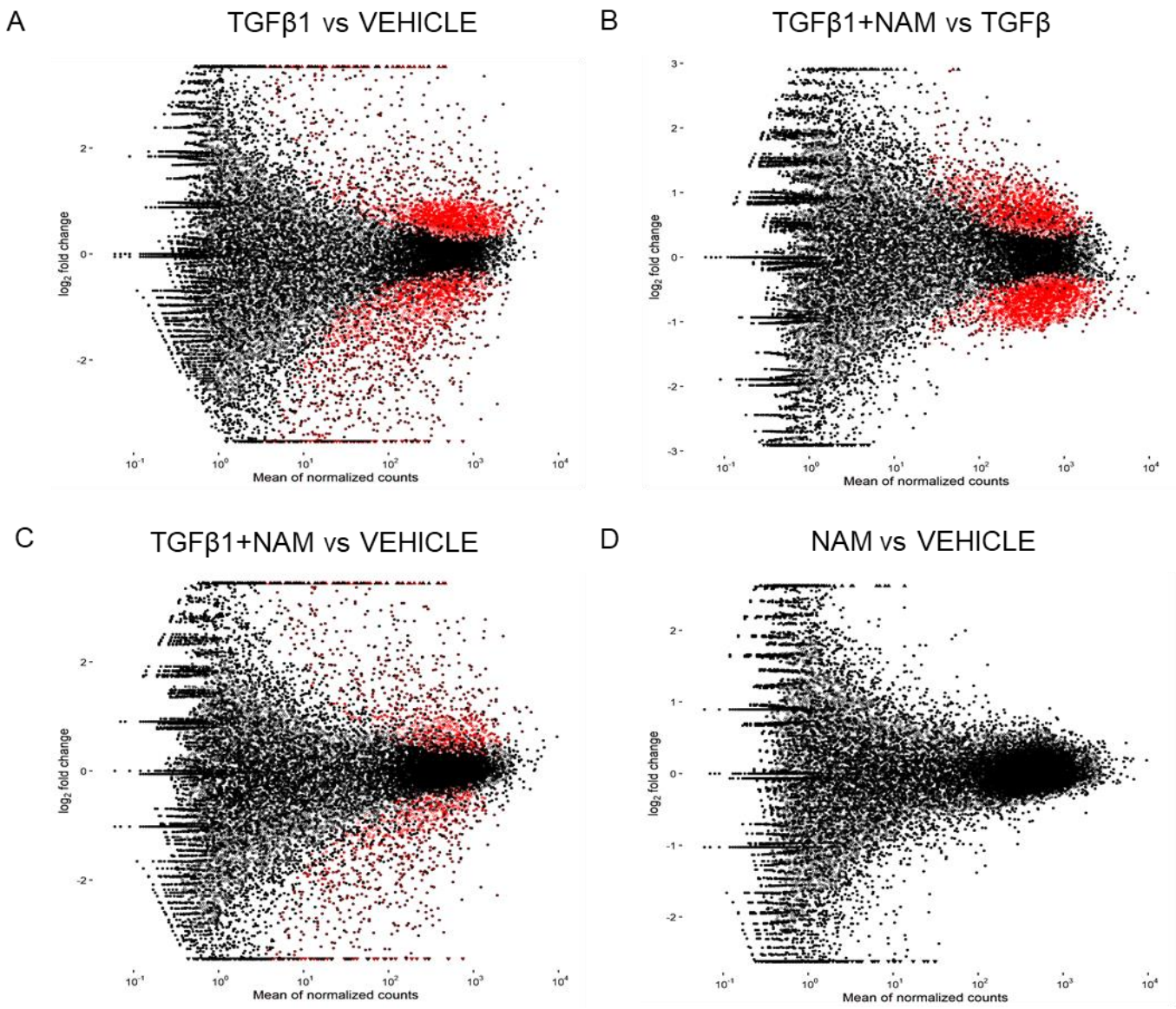
A
TGFβ1 vs VEHICLE
B
TGFβ1+NAM vs TGFβ
C
TGFβ1+NAM vs VEHICLE
D
NAM vs VEHICLE
log2 fold change
Mean of normalized counts

Figure 5.3 Summary of the RNA sequencing results. Volcano plot representation of differential expressed genes in primary human lung fibroblasts treated with vehicle (0.01% DMSO), NAM (1 μM NPS2143), TGFß1 (5ng/mL), and TGFß+NAM for 72-hours. Statistically significant differentially expressed genes for each comparison shown in red. The x-axis shows mean of normalized gene counts; y-axis shows $\log_2$ fold-changes in expression (positive values represent upregulated genes while negative values denote downregulation). **A.** TGFß1 treatment resulted in 1999 downregulated genes and 2757 upregulated genes compared to vehicle. **B.** Co-treatment of TGFß1+NAM induced downregulation of 2608 genes and upregulation of 2150 genes compared to TGFß1. **C.** TGFß1+NAM dowregulated 871 genes whilst upregulating 1033 genes when compared to vehicle. **D.** No significant difference in expression was observed when the NAM-treated cohort was compared with vehicle. Bioinformatics analysis done on normalised data using R-package DESeq2. Benjamini-Hochberg *p*-value adjustment was performed in all statistical tests; level of controlled false positive rate was set to 0.05. N = 3 donors. NAM: Calcium-sensing receptor (CaSR) Negative Allosteric Modulator treatment; TGFß1: Transforming growth factor ß1 (TGFß1) treatment; TGFß1+NAM: TGFß1 and CaSR Negative Allosteric Modulator co-treatment.

5.3.2. TGFβ1 regulates gene expression, and NAM alters TGFβ1-mediated biological processes – Gene ontology network (GOnet) analysis

Microarray and single-cell RNA sequencing approaches have been applied in the study of transcriptional changes in IPF patient-derived lung fibroblasts (Emblom-Callahan *et al*. 2010; Rodriguez *et al*. 2018; Reyfman *et al*. 2019; Adams *et al*. 2020; Habermann *et al*. 2020; Tsukui *et al*. 2020). Table 5.1 compares the most enriched genes in these studies to the gene expression pattern observed in my RNA sequencing dataset. The most enriched genes in my dataset are associated with the regulation and organisation of the ECM (O'Dwyer *et al*. 2017; Posey *et al*. 2018). These include *COMP* (cartilage oligomeric matrix protein), which was upregulated ~1000-fold and is essential for collagen assembly, *POSTN* (periostin), *COL5A1*, and *COL1A1*. CTHRC1, which was shown by a previous study as a marker of invasive matrix-depositing fibroblasts (Tsukui *et al*. 2020), was also significantly upregulated in my data set. However, some genes which are normally elevated in IPF-HLFs such as *WNT2* (Reyfman *et al*. 2019), C-X-C motif chemokine ligand 14 (*CXCL14*) (Rodriguez *et al*. 2018; McDonough *et al*. 2019a; Adams *et al*. 2020), and the IL-1β receptor, IL1R2 (Emblom-Callahan *et al*. 2010), were downregulated or unaltered in my dataset. In addition, *HBEGF* (Heparin Binding EGF Like Growth Factor) gene count, which has been shown to reduce in IPF lung fibroblasts (Reyfman *et al*. 2019), doubled in my experiment.

Table 5.1 Normal human lung fibroblasts (HLFs) treated with TGFß1 (5 ng/mL) for 72 hours show comparable gene expression to HLFs from IPF patients. Genes following the expected direction of regulation are highlighted in blue.

Gene/Protein	Log_2 (fold change)	*P*-value (adjusted)	Differential expression in IPF-HLFs	References
ACTA2/α-smooth muscle actin	1.118	9.38E-08	UP	(Rodriguez *et al*. 2018; Reyfman *et al*. 2019; Adams *et al*. 2020; Habermann *et al*. 2020)
CCN2/Connective tissue growth factor	1.159	8.60E-09	UP	(Peyser *et al*. 2019)
COL1A1/Collagen 1	1.292	1.19E-07	UP	(McDonough *et al*. 2019a; Reyfman *et al*. 2019; Adams *et al*. 2020; Tsukui *et al*. 2020)
COL3A1/Collagen 3	0.871	0.003145	UP	(McDonough *et al*. 2019a; Reyfman *et al*. 2019; Adams *et al*. 2020; Tsukui *et al*. 2020)
COL5A1/Collagen 5	1.603	1.20E-13	UP	(McDonough *et al*. 2019a; Adams *et al*. 2020)
COMP/Cartilage oligomeric matrix protein	10.182	2.51E-21	UP	(McDonough *et al*. 2019a)
CTHRC1/Collagen Triple Helix Repeat Containing 1	1.063	9.77E-07	UP	(McDonough *et al*. 2019a; Tsukui *et al*. 2020)

***CXCL14*/C-X-C motif chemokine ligand 14**	-0.744	-	UP	(Rodriguez *et al*. 2018; McDonough *et al*. 2019a; Adams *et al*. 2020)
***FN1*/Fibronectin**	1.18	3.46E-05	UP	(Emblom-Callahan *et al*. 2010; Tsukui *et al*. 2020)
***HBEGF*/Heparin binding EGF-like growth factor**	0.93	0.020293	DOWN	(Reyfman *et al*. 2019)
***IL1R2*/Interleukin 1 Receptor Type 2**	-1.599	-	UP	(Emblom-Callahan *et al*. 2010)
***ITGB5*/Integrin Subunit ß5**	0.675	2.49E-06	UP	(Emblom-Callahan *et al*. 2010)
***LTBP1*/Latent TGFß Binding Protein 1**	0.535	0.006943	UP	(Peyser *et al*. 2019)
***LTBP2*/Latent TGFß Binding Protein 2**	0.672	0.008195	UP	(Peyser *et al*. 2019)
***MMP1*/Matrix metalloproteinase 1**	0.527	0.061387	UP	(Emblom-Callahan *et al*. 2010; Peyser *et al*. 2019)
***MMP2*/Matrix metalloproteinase 2**	0.82	0.000649	UP	(Emblom-Callahan *et al*. 2010; Peyser *et al*. 2019)
***PDGFRA*/Platelet-derived growth factor receptor α**	-0.298	0.179007	UP	(Reyfman *et al*. 2019; Habermann *et al*. 2020)

POSTN/Periostin	1.781	7.30E-11	UP	(Reyfman *et al*. 2019; Tsukui *et al*. 2020)
SERPINE1/Plasminogen activator inhibitor1	1.19	2.26E-08	UP	(Peyser *et al*. 2019)
TAGLN/Smooth muscle protein 22α	0.924	1.06E-05	UP	(Peyser *et al*. 2019; Reyfman *et al*. 2019)
TIMP1/MMP inhibitor 1	1.175	1.54E-05	UP	(Reyfman *et al*. 2019)
TIMP3/MMP inhibitor 3	0.949	5.84E-06	UP	(Peyser *et al*. 2019)
***WNT2*/Wingless-related integration site 2**	-1.874	0.022654	UP	(Reyfman *et al*. 2019)
WNT5A/Wingless-related integration site 5A	0.63	0.00245	UP	(Reyfman *et al*. 2019)

Gene ontological network (GOnet) enrichment analysis of the top 1500 differentially expressed genes indicated that TGFß1 stimulation upregulated genes belonging to signalling pathways (namely TGFß, non-canonical Wnt, NFκB, TNF, MAPK, IL-1, and IL-12), metabolic pathways (including oxidative phosphorylation, ROS, serine, proline and polyamine biosynthesis), profibrotic processes (*e.g.*, ECM, collagen and cytoskeletal organisation, fibroblast proliferation, and cell ageing) (Figure 5.4, A). GOnet analysis of the top 1500 downregulated genes showed that most of the aforementioned pathways were inhibited in the presence of TGFß1 and NAM (Figure 5.4, B).

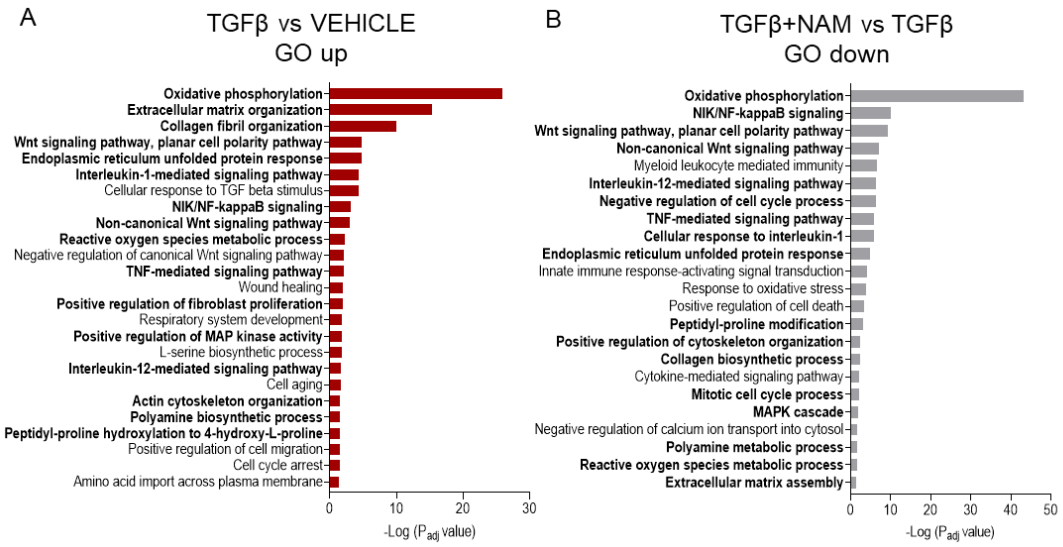

Figure 5.4 Negative allosteric modulator of the CaSR downregulates gene ontology pathways induced by TGFß1 in human primary lung fibroblasts. Gene ontological (GO) network enrichment pathway analysis of the top 1500 significantly upregulated (red) and downregulated (grey) genes in **A.** TGFß1-treated *versus* vehicle-treated cells; **B.** TGFß1+NAM *versus* TGFß1 group. The pathways common to both panels are highlighted in bold. The enriched pathways are plotted against their -log(adjusted *p* value), with the most significant *p* values indicated by the longest bars. *p*-value adjustment was performed for all statistical tests; level of controlled false positive rate was set to 0.05. *N* = 3 donors. NAM: CaSR negative allosteric modulator, NPS2143 (1 μM).

Co-treatment with NAM also prevented pathways associated with response to innate immunity, oxidative stress, and cell death. Conversely, TGFß1 downregulated genes related to the regulation of $[Ca^{2+}]_i$, and several signalling pathways (including cytokine-mediated, adenylate cyclase/cAMP-mediated GPCR, TGFß, protein kinase B, Notch and STAT) (Figure 5.5, A). Co-treatment with NAM upregulated protein ubiquitination, DNA repair and cAMP metabolism while inhibiting mTOR signalling and cytoskeletal organisation (Figure 5.5, B).

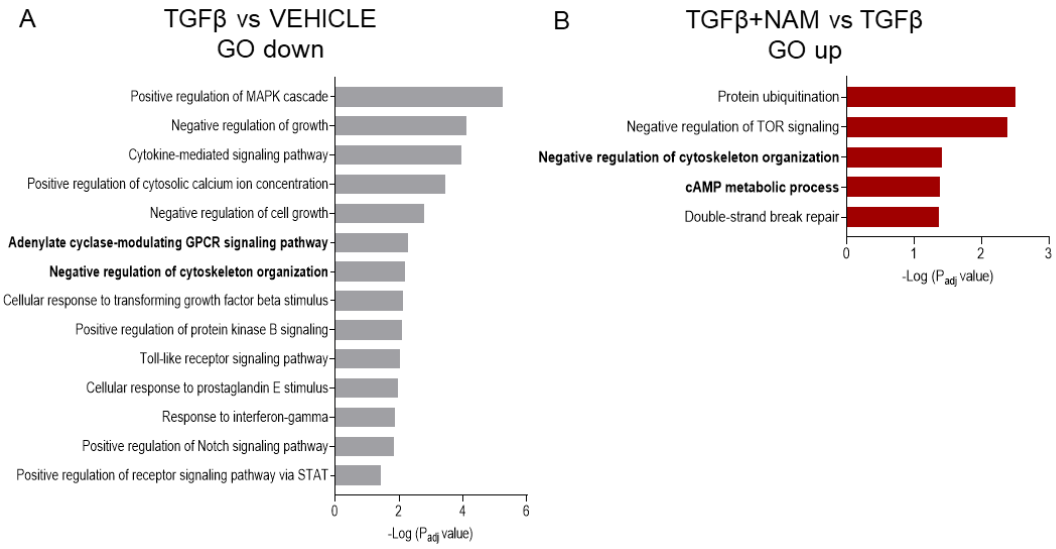

Figure 5.5 TGFß1 downregulates genes associated with signalling pathways implicated in IPF in human primary lung fibroblasts. Gene ontological (GO) network enrichment pathway analysis of the top 1500 significantly upregulated (red) and downregulated (grey) genes in **A.** TGFß1-treated *versus* vehicle-treated cells; **B.** TGFß1+NAM *versus* TGFß1 group. The pathways common to both panels are highlighted in bold. The enriched pathways are plotted against their -log(adjusted *p* value), with the most significant *p* values indicated by the longest bars. *p*-value adjustment was performed for all statistical tests; level of controlled false positive rate was set to 0.05. *N* = 3 donors. NAM: CaSR negative allosteric modulator, NPS2143 (1 µM).

5.3.3. NAM downregulates profibrotic gene expression induced by TGFβ1

Several signalling pathways implicated in lung development are chronically (re)activated in IPF such as TGFβ, CaSR, Wnt, and FGF (Brennan *et al*. 2016; Chanda *et al*. 2019). GOnet analysis indicated "respiratory system development" as one of the pathways enriched by exogenous TGFβ1 application (Figure 5.4, A). Further analysis my RNA sequencing data shows increased expression of *TGFB1*, *TGFB2*, *THBS1*, *LTBP1*, *LTBP2* and *SMAD7* while *TGFB3* and *SMAD3* were downregulated (fold change TGFB1 = 2.6, TGFB2 = 2.1, TGFBI = 2.4, THBS1 = 1.8, LTBP1 = 1.5, SMAD7 = 2.1, TGFB3 = 0.3, SMAD3 = 0.3; p_{adj} *value* < 0.05) (Figure 5.6, A). *SMAD2* expression was not altered in the presence of exogenous TGFβ1 (fold change SMAD2 = 1.02; p_{adj} *value* = 0.89), while *SMAD4* was increased (fold change SMAD4 = 1.2; p_{adj} *value* = 0.06) (Figure 5.6, A). The efficacy of the NAM, NPS2143 in modulating TGFβ signalling was assessed; *THBS1* expression was restored to baseline, and endogenous *TGFB1* expression declined by 32% (p_{adj} *value* < 0.05; Figure 5.6, A). Co-treatment with NAM resulted in a marginal increase in *SMAD3* expression although levels remain below baseline (p_{adj} *value* < 0.05). No significant change in *TGFB2*, *TGFB3*, *LTBP1*, *SMAD6* and *SMAD7* expression was observed (Figure 5.6, A).

TGFβ1 treatment had dual effects on growth factor expression whereby *CCN2* (CTGF*), FGF2, FGF14, HBEGF* and *PDGFC* were upregulated and *FGF5* was downregulated (fold change CTGF = 2.2, FGF2 = 1.9, FGF14 = 3.0, HBEGF = 1.9, PDGFC = 1.6, FGF5 = 0.5; p_{adj} *value* < 0.05) (Figure 5.6, B). Co-treatment with NAM restored baseline expression of *CCN2*, *FGF5* and *PDGFC* (p_{adj} *value* < 0.05; Figure 5.6, B). However, no significant NAM effect was observed in the expression of the other growth factors.

Key mediators of canonical and non-canonical Wnt signalling are altered in the presence of exogeneous TGFβ1. The expression of *WNT2, WNT2B* and

DVL2 were downregulated in the presence of TGFβ1, with the opposite effect observed in *CTNNB1* (β-catenin), *TCF7L2* (TCF4), *WNT5A*, *WNT5B* and *DKK1* expression (fold change WNT2 = 0.3, WNT2B = 0.3, DVL2 = 0.7, CTNNB1 =1.4, TCF7L2 =1.4, WNT5A = 1.6, WNT5B = 1.5, FZD8 = 18.1; p_{adj} *value* < 0.05) (Figure 5.6, C). Co-treatment with NAM re-established baseline levels of *CTNNB1*, *DVL2* and *WNT5B* (p_{adj} *value* < 0.05; Figure 5.6, C). The expression of *WNT2*, *WNT2B*, *TCF7L2* (TCF4), frizzled receptor 8 (FZD8), and *WNT5A* were not significantly altered by NAM treatment.

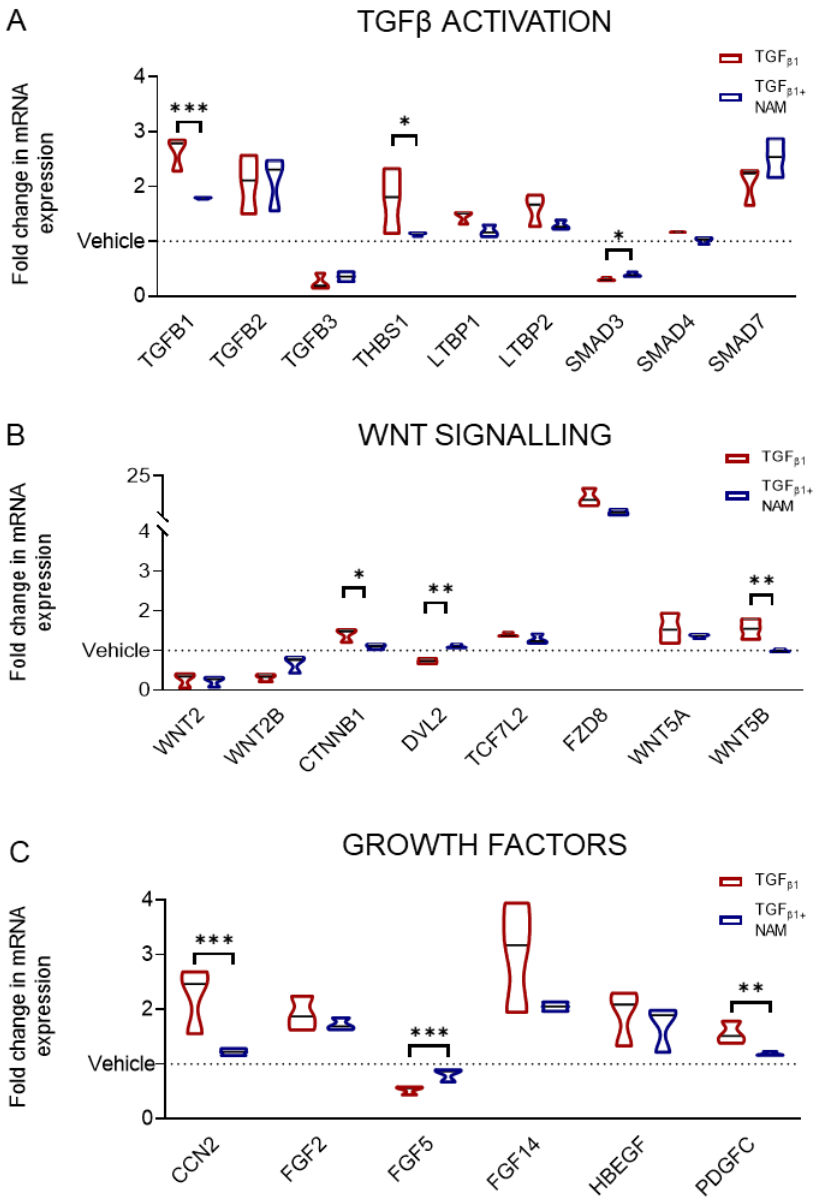

Figure 5.6 CaSR negative allosteric modulator, NPS2143 attenuates TGFß1-induced upregulation of developmental genes implicated in fibrosis. Differential gene expression between treatment groups using DESeq2. **A-C.** Exogenous TGFß1 application alters the expression of genes implicated in growth factor and Wnt signalling (padj <0.05). **A.** NAM decreases expression of TGFß1 and THBS1, whilst upregulating SMAD3. **B.** NAM restores baseline expression of canonical and non-canonical Wnt signalling mediators: *CTNNB1* (encoding ß-catenin), *DVL2* (encoding dishevelled protein 2) and *WNT5B*. **C.** NAM restores baseline expression of CTGF (encoded by *CCN2*), FGF5, and PDGFC. Benjamini-Hochberg p-value adjustment was performed in all statistical tests; level of controlled false positive rate was set to 0.05. * padj <0.05, ** padj <0.01, *** padj <0.001. N = 3 donors. CaSR negative allosteric modulator: NAM, NPS2143 (1 µM); connective tissue growth factor: CTGF; fibroblast growth factor: FGF; frizzled receptor: FZD; heparin-bound epidermal growth factor: HBEGF; latent TGFß binding protein: LTBP1; platelet-derived growth factor C: PDGFC; thrombospondin 1: THBS1; transcription factor 7 like 2: TCF7L2/TCF4

Cytoskeletal changes, excessive collagen and ECM deposition, are central to IPF pathophysiology. Unsurprisingly, GOnet analysis of my data showed that genes implicated in these pathways were enriched by TGFβ1 treatment (Figure 5.4, A). In support of my findings at the protein level, *ACTA2* (αSMA) expression doubled in the presence of TGFβ1 (p_{adj}<0.001; Figure 5.7, A). The baseline expression of the actin cross-linking gene, *TAGLN* (SM22α), also doubled in TGFβ1-treated fibroblasts (p_{adj} <0.001; Figure 5.7, A). Co-treatment with NAM completely abolished the profibrotic effect (p_{adj}<0.001; Figure 5.6, A). Several collagen subtypes were upregulated by TGFβ1 application, *e.g.* fibrillar collagens (*COL1A1, COL3A1* and *COL5A1*), *COL6A2*, and *COL7A1* (p_{adj} *value* < 0.05; Figure 5.7, A). Genes that maintain collagen fibre integrity were also upregulated by TGFβ1, such as *P4HA2* (prolyl 4-hydroxylase, alpha polypeptide II) (p_{adj} *value* < 0.0001; Figure 5.7, A). Co-treatment with NAM restored baseline expression of all genes except COL5A1 and COL7A1, which were reduced by 30% and 22%, respectively (p_{adj} *value* < 0.05; Figure 5.7, A).

A panel of IPF-related ECM genes were selected to assess the effect of TGFβ1 and NAM treatment. The ECM genes were upregulated by TGFβ1, with the most enriched genes identified as *CDH2* (N-cadherin; fold change: 7.1) and *IGFBP3* (insulin-like growth factor-binding protein 3; fold change: 10.2) (p_{adj} < 0.05; Figure 5.7, B). *FN1* (fibronectin), *ELN* (elastin), *VCAN* (versican), *BGN* (biglycan), *VIM* (vimentin), and *IGFBP7* were among the ECM genes explored. Several ECM regulators were also upregulated by profibrotic stimuli, including matrix-metallopeptidases (MMPs): MMP1, MMP2, MMP14, tissue inhibitors of metalloproteinases (TIMPs): TIMP1, TIMP3, serine protease inhibitors (SERPINs): SERPINE1 and SERPINE2 (p_{adj} < 0.05; Figure 5.7, C). Although expression levels of *TIMP2* increased, this change resulted in borderline statistical significance (p_{adj} < 0.06; Figure 5.7, C). NAM treatment diminished the expression of FN1 (p_{adj} < 0.06), *ELN*, *BGN, VIM, IGFBP3, IGFBP7,* and all the above-mentioned ECM regulators (p_{adj} < 0.05; Figure 5.7, B-C).

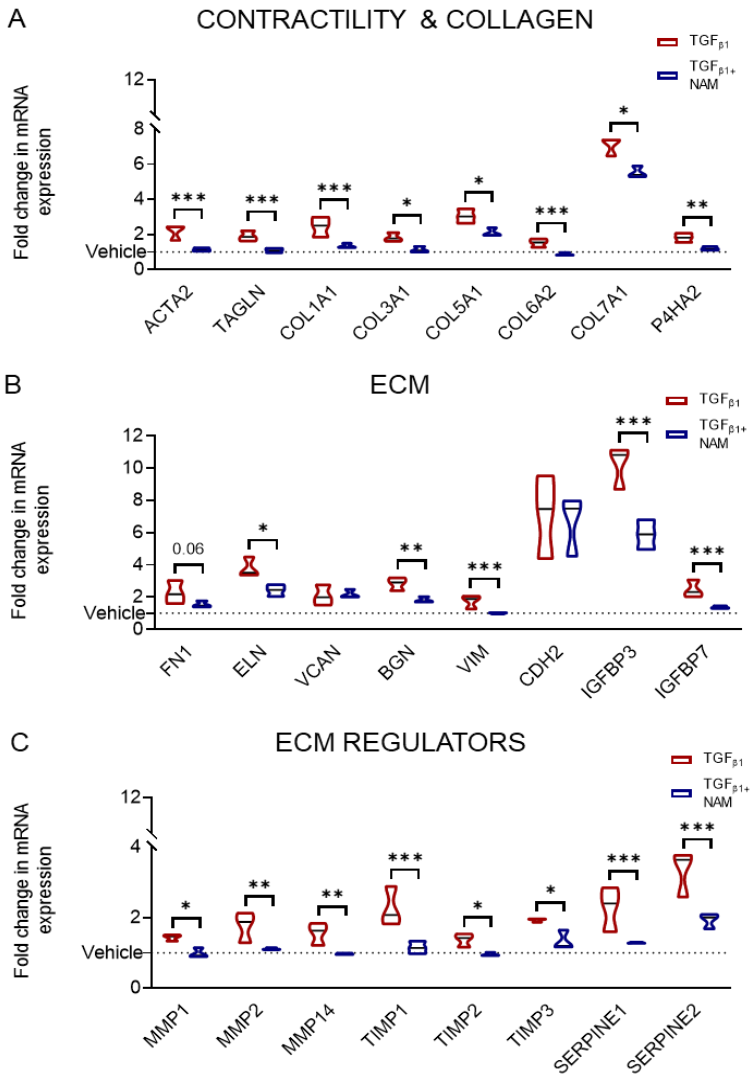

Figure 5.7 CaSR negative allosteric modulator, NPS2143 attenuates TGFβ1-induced upregulation of ECM remodelling genes in normal human lung fibroblasts. Differential gene expression between treatment groups using DESeq2. **A-C**. Exogenous TGFβ1 application upregulates genes related to cellular contractility and ECM remodelling (p_{adj} <*0.05*). NAM reduces the expression of genes associated with: **A.** Fibroblast contractility and collagen deposition; **B.** Extracellular matrix (ECM) deposition; **C.** ECM maintenance. Benjamini-Hochberg p-value adjustment was performed in all statistical tests; level of controlled false positive rate was set to 0.05. * p_{adj} <0.05, ** p_{adj} <0.01, *** p_{adj} <0.001. *N* = 3 donors. CaSR negative allosteric modulator: NAM, NPS2143 (1 μM).

Exogenous TGFß1 application increased expression of genes related to proliferation, cell cycle, and senescence; all processes known to play a role in IPF. The proliferation gene, *PCNA* (proliferating cell nuclear antigen), was upregulated by TGFß1. The following cell cycle regulators were also upregulated by TGFß1 treatment: *CCNA2* (cyclin A2), and cyclin-dependent kinases, *CDK4, CDK5, CDK6,* and *CDK7,* while *CCNE2* (cyclin E2) expression decreased (p_{adj} < 0.05; Figure 5.8, A). The expression of key senescence mediators was also amplified by TGFß1 treatment: *CDKN1A* ($p21^{CIP1}$), *CDKN2A* ($p16^{INK4A}$), *CDKN2B* ($p15^{INK4B}$), *IL11,* and *GLB1* (ß-galactosidase), with the greatest impact on *IL11* expression resulting in a 5-fold increase (p_{adj} < 0.05; Figure 5.8, B). NAM restored baseline expression of *PCNA, CCNE2, CDK4, CDK5, CDK7*, *CDKN1A*, and *CDKN2A* (p_{adj} < 0.05; Figure 5.8, A-B). Although a 2-fold decrease in *IL11* expression was observed in the presence of NAM, this effect was not statistically significant because the baseline expression observed in NHLF2 was 3 times lower than NHLF1 and NHLF3 (p_{adj} > 0.05; Figure 5.8, A-B).

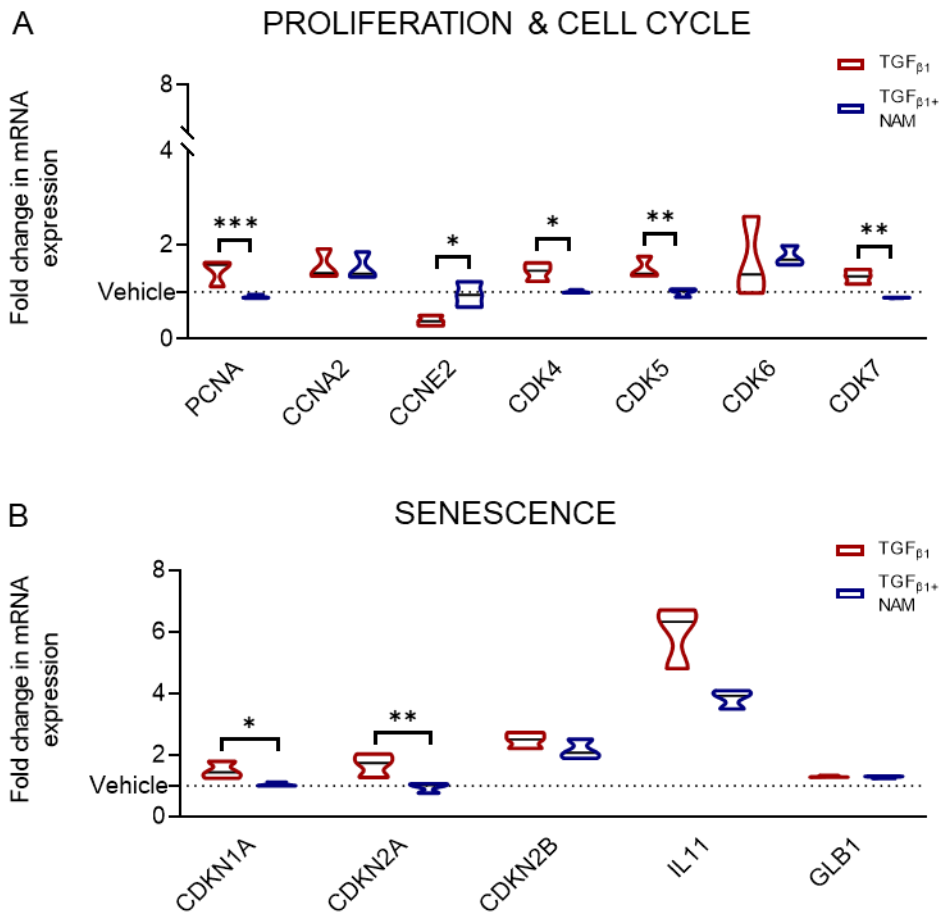

Figure 5.8 CaSR negative allosteric modulator, NPS2143 attenuates TGFβ1-induced upregulation of profibrotic genes in normal human lung fibroblasts. Differential gene expression between treatment groups using DESeq2. **A-C**. Exogenous TGFβ1 application alters the expression of genes implicated in proliferation, cycle cycle, and senescence (p_{adj} <*0.05*). NAM restores baseline expression of the genes implicated in: **A.** Proliferation and cell cycle: *PCNA, CCNE2, CDK4, CDK5, and CDK7*; **B.** Cellular senescence: *CDKN1A* (p21) and *CDKN2A* (p16). Benjamini-Hochberg p-value adjustment was performed in all statistical tests; level of controlled false positive rate was set to 0.05. * p_{adj} <0.05, ** p_{adj} <0.01, *** p_{adj} <0.001. *N* = 3 donors. CaSR negative allosteric modulator: NAM, NPS2143 (1 μM).

5.3.4. NAM restores baseline expression of glycolytic genes induced by TGFβ1

GOnet analysis indicated oxidative phosphorylation as the most enriched pathway induced by TGFβ1 treatment (Figure 5.4, A). Since the glycolytic pathway fuels aerobic ATP synthesis, I found genes related to 4 out of the 5 steps in the energy investment part of the pathway were upregulated, the outliers being hexokinase 2 and fructose-bisphosphate aldolase (Figure 5.9). Genes related to the 5 energy payoff steps displayed greater enrichment compared to the first half of the process (Figure 5.9). However, *ENO2* (encoding enolase 2) was downregulated in the presence of TGFβ1 (Figure 5.9). TGFβ1 also increased the expression of *SLC2A1,* which encodes the glucose transporter, GLUT1.

NAM restored baseline expression of *TPI1* (triosephosphate isomerase), *GAPDH* (glyceraldehyde 3-phosphate dehydrogenase), *PGK1* (phosphoglycerate kinase 1), PGAM1 (phosphoglucomutase-1), *ENO1/2*, *PKM* (pyruvate kinase), *LDH* (lactate dehydrogenase) A/B, and *PDH* (pyruvate dehydrogenase) A1/B, while *BPGM* (bisphosphoglycerate/phosphoglycerate mutase) expression was reduced by 58% (Figure 5.10). The lactate transporters, monocarboxylate transporter (MCT) 1 and 4 (encoded by SLC16A1 and SLC16A3, respectively), were also downregulated by NAM (Figure 5.9).

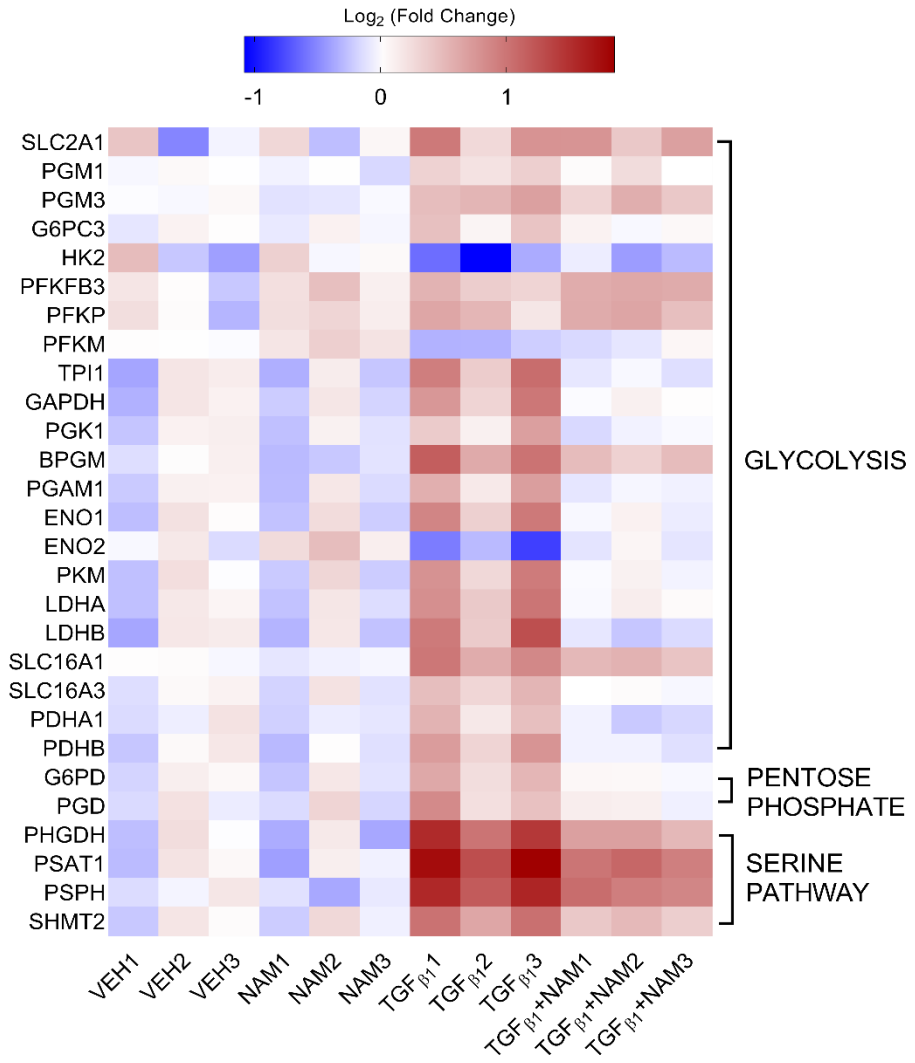

Figure 5.9 TGFß1 upregulates genes associated with metabolic reprogramming while NAM abrogates this response. Heatmap shows the log2 ratio of differentially expressed genes (versus vehicle) implicated in glycolysis, pentose phosphate, serine metabolic pathways. Exogenous TGFß treatment results in significant upregulation of genes, while co-treatment with the NAM, NPS2143 (1 µM) reduces gene expression except *HK2* and *ENO2* which were upregulated. Bioinformatics analysis was done on normalised data using R-package DESeq2. A Benjamini-Hochberg p-value adjustment was performed in all statistical tests; level of controlled false positive rate was set to 0.05. N = 3 donors. NAM: Calcium-sensing receptor (CaSR) Negative Allosteric Modulator treatment; SLC2A1: GLUT1 transporter; SLC16A1/A3: Lactate transporter 1/4. TGFß: Transforming growth factor ß (TGFß) treatment; TGFß+NAM: TGFß and CaSR Negative Allosteric Modulator co-treatment.

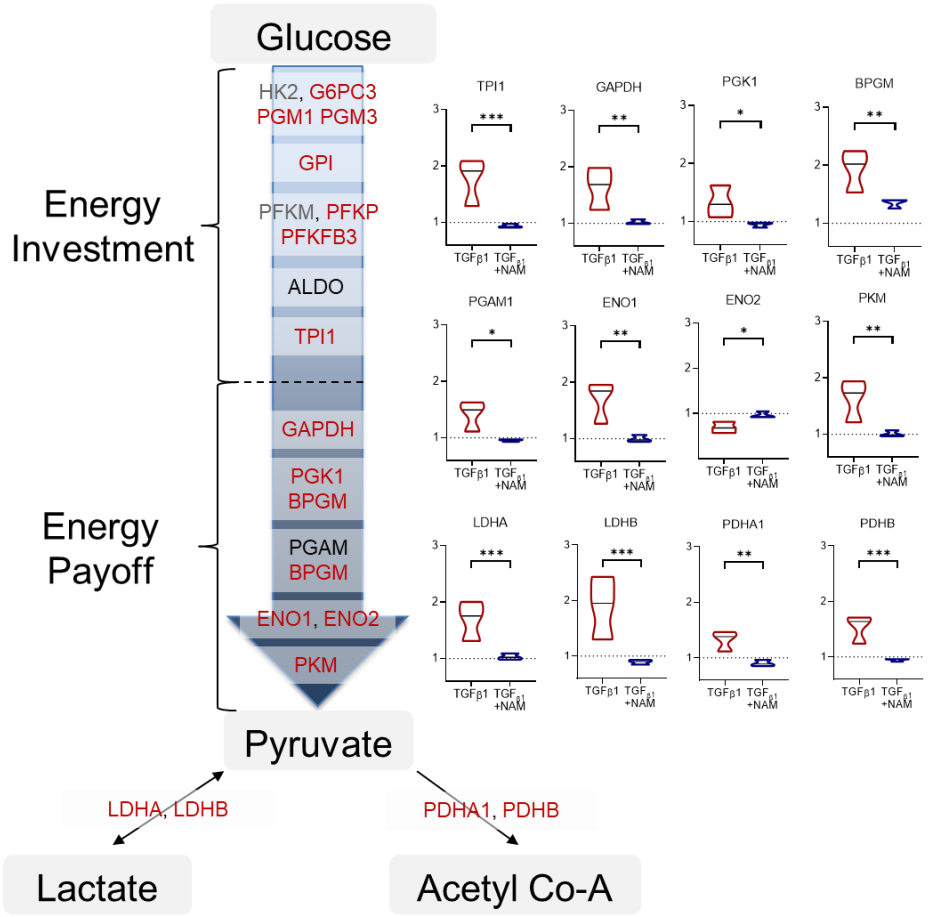

Figure 5.10 CaSR-NAM diminishes TGFβ1-induced expression of genes involved in glycolysis. TGFβ1 treatment upregulates genes involved in glycolysis (significantly upregulated genes – red; downregulated genes – grey; unaltered - black). Associated graphs show CaSR treatment restores baseline expression of 'energy payoff' genes (y-axis represents fold change relative to mRNA expression in vehicle control which is represented by the dashed line). Data in the violin plots represent median fold change compared to vehicle (black line), truncated at minimum and maximum values. Benjamini-Hochberg p-value adjustment was performed for all statistical tests; level of controlled false positive rate was set to 0.05. *p<0.05, **p<0.01, ***p<0.001. N = 3 donors. ALDO: Fructose-bisphosphate aldolases; BPGM: Bisphosphoglycerate/phosphoglycerate mutase; GAPDH: Glyceraldehyde 3-phosphate dehydrogenase; GPI: Glucose-6-phosphate isomerase; HK2: Hexokinase 2; LDHA, LDHB: Lactate dehydrogenase; NAM: CaSR negative allosteric modulator, NPS2143; PDHA1, PDHB: Pyruvate dehydrogenase; PFKM, PFKP: 6-phosphofructokinases 1; 6-phosphofructo-2-kinase/fructose-2,6-biphosphatase 3; PGK1: Phosphoglycerate kinase; PGAM1: Phosphoglucomutase-1; PKM: Pyruvate kinase; TPI1: Triosephosphate isomerase.

5.3.5. NAM downregulates genes associated with amino-acid metabolism

The glycolytic enzymes PGK1 and BPGM facilitate the formation of 3-phosphoglycerate, which is required for serine/glycine synthesis (Hashimoto *et al*. 2019). Since studies in fibroblasts have shown that enzymes required for *de novo* glycine synthesis are essential for collagen production (Nigdelioglu *et al*. 2016), I assessed the effect of TGFβ1 on this pathway. The expression of the rate-limiting enzyme in this pathway, 3-phospho glycerate dehydrogenase (PHGDH), was upregulated by TGFβ1 treatment (fold change = 2.5; Figure 5.11). Baseline expression of the 3 enzymes downstream of PHGDH, PSAT1, phosphoserine phosphatase (PSPH) and serine hydroxymethyltransferase (SHMT2) were also increased in the presence of exogenous TGFβ1, with PSAT1 showing the greatest change (fold change *PSAT1* = 3.2; *PSPH* = 2.7; *SHMT2* = 1.9; Figure 5.11). Co-treatment with NAM resulted in significant downregulation of all 4 enzymes compared with TGFβ1 (percent decrease in fold change: *PHGDH* = 40%; *PSAT1* = 38%; *PSPH* = 30%; *SHMT2* = 26%; Figure 5.10).

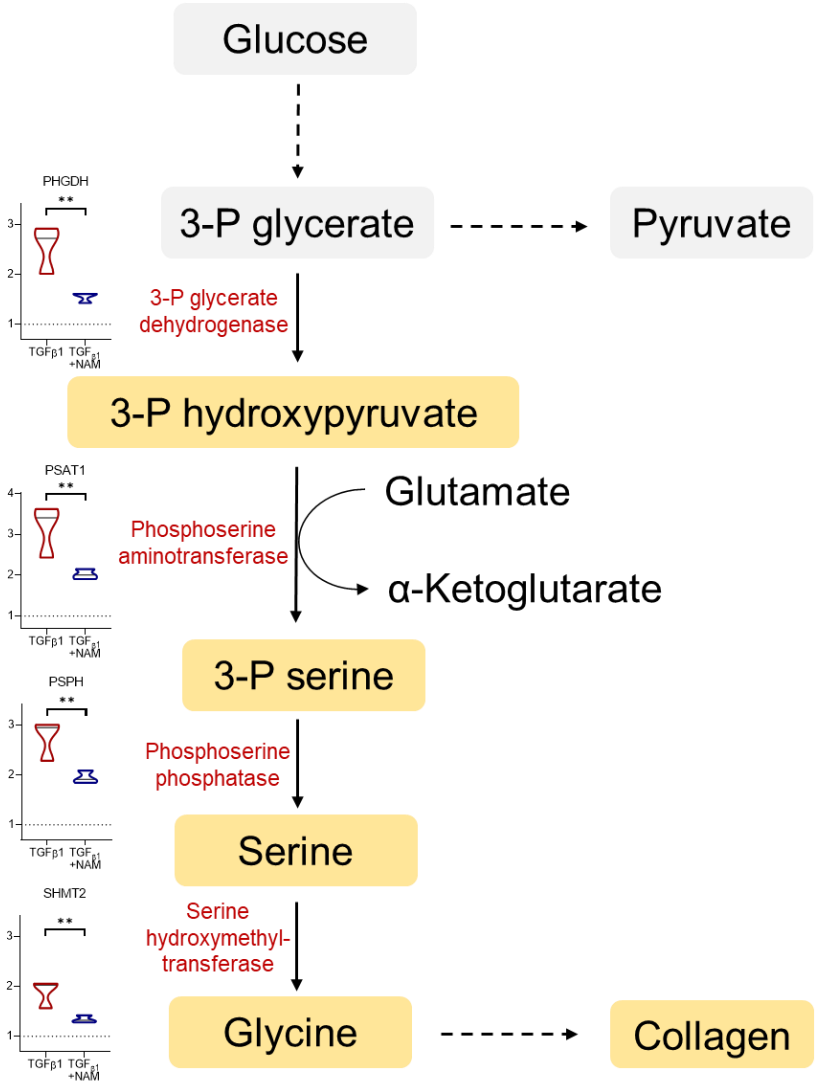

Figure 5.11 CaSR-NAM reduces TGFß-induced upregulation of genes involved in glycine synthesis. TGFß treatment upregulates genes involved in de novo production of glycine, a key component of collagen (significantly upregulated genes – red). The yellow boxes indicate the formation of glycine from glucose through a series of steps beginning with glycolysis and the glycolytic intermediate, 3-P glycerate (indicated by the grey boxes). Conversion of 3-P glycerate to glycine involves the following enzymes: PHGDH (3-P glycerate dehydrogenase), PSAT1 (phosphoserine aminotransferase), PSPH (phosphoserine phosphatase) and SHMT2 (serine hydroxymethyl-transferase). Associated graphs show that NAM decrease enzyme gene expression (y-axis represents fold change relative to mRNA expression in vehicle control which is represented by the dashed line). Data in the violin plots represent median fold change compared to vehicle (black line), truncated at minimum and maximum values. Benjamini-Hochberg p-value adjustment was performed for all statistical tests; level of controlled false positive rate was set to 0.05. **p<0.01. N = 3 donors. 3-P: 3-phospho; NAM: CaSR negative allosteric modulator, NPS2143 (1 μM).

Amino acid import across the plasma membrane was upregulated by TGFβ1 as indicated by GOnet analysis (Figure 5.4, A). Since glutamine is transported in and out of the cell via multiple SLC transporters (Bhutia and Ganapathy 2016), I assessed the gene expression of these transporters. Exogenous TGFβ1 application resulted in the upregulation of the following SLC transporter genes: *SLC1A4/1A5* (encodes ASCT1/2), *SLC7A5* (encodes LAT1) and *SLC38A5*, while co-treatment with NAM restored baseline levels of *SLC1A5* (Figure 5.12). Several mediators of glutamine metabolism are upregulated by TGFβ1 treatment. The aminotransferases, *GOT1* and *GPT2*, which mediate the generation of α-ketoglutarate, are upregulated by TGFβ1 treatment (Figure 5.12). The expression of the transcription factor, ATF4, which is a key downstream effector of glutamine signalling, doubled in the presence of TGFβ1 (Figure 5.12). Of these mediators, NAM decreased the expression of GOT1 whilst completely abolishing the TGFβ1-induced increase in ATF4 expression (Figure 5.12).

As previously discussed, the first step of glutaminolysis is the conversion of glutamine to glutamate, which is catalysed by GLS and essential for a myriad of biosynthetic processes, including *de novo* proline synthesis (Phang *et al*. 2015). TGFβ1 significantly increased the expression of genes involved in this process, *i.e.*, *GLS*, *ALDH18A1*, *PYCR1/2*, and *OAT*, whilst downregulating the expression of *GLUL* (glutamine synthetase) and *ALDH4A1* (P5C dehydrogenase), which favour the conversion of P5C back into glutamine (Figure 5.12). In the presence of TGFβ1, CaSR-NAM decreased *GLS* expression and restored baseline levels of *PYCR2* and *OAT* (Figure 5.11; Figure 5.13).

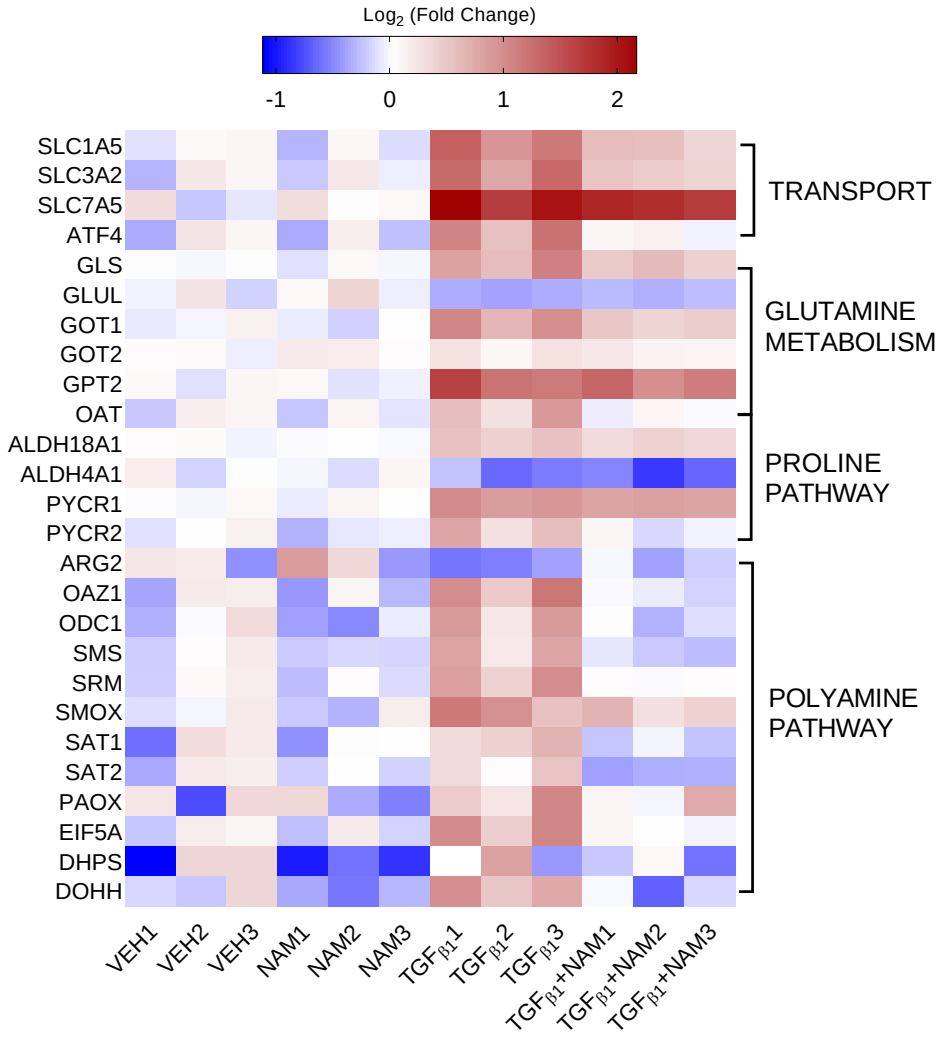

Figure 5.12 TGFß upregulates genes involved in glutamine, proline, and polyamine metabolism while NAM abrogates this response. Heatmap shows the log2 ratio of differentially expressed genes (versus vehicle) implicated in these metabolic pathways. Exogenous TGFß treatment results in upregulation of genes while co-treatment with the NAM, NPS2143 (1 µM) reduces gene expression except *GLUL* and *ALDH4A1*. Bioinformatics analysis done on normalised data using R-package DESeq2. A Benjamini-Hochberg p-value adjustment was performed in all statistical tests; level of controlled false positive rate was set to 0.05. N = 3 donors. NAM: Calcium-sensing receptor (CaSR) Negative Allosteric Modulator treatment; TGFß: Transforming growth factor ß (TGFß) treatment; TGFß+NAM: TGFß and CaSR Negative Allosteric Modulator co-treatment.

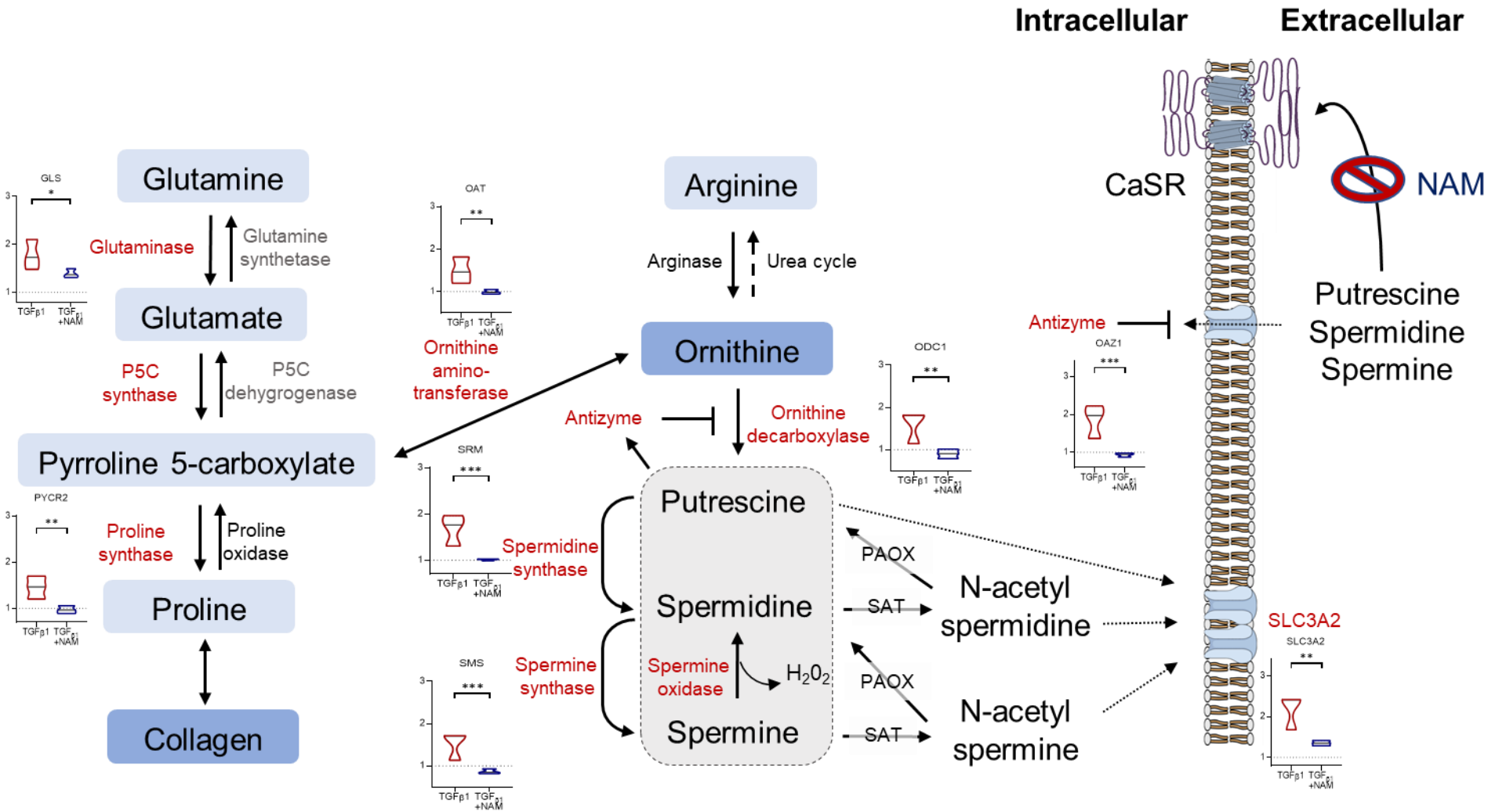
Intracellular
Extracellular
Glutamine
Glutaminase
Glutamine synthetase
Glutamate
P5C synthase
P5C dehygrogenase
Pyrroline 5-carboxylate
Proline synthase
Proline oxidase
Proline
Collagen
Arginine
Arginase
Urea cycle
Ornithine
Ornithine amino-transferase
Antizyme
Ornithine decarboxylase
Putrescine
Spermidine synthase
Spermidine
Spermine synthase
Spermine oxidase
H_2O_2
Spermine
PAOX
SAT
N-acetyl spermidine
PAOX
SAT
N-acetyl spermine
CaSR
NAM
Antizyme
Putrescine
Spermidine
Spermine
SLC3A2
GLS
OAT
PYCR2
SRM
SMS
ODC1
OAZ1
TGFβ1
TGFβ1 +NAM

Figure 5.13 CaSR-NAM restores TGFβ1-induced increase in polyamine metabolism to baseline. TGFβ1 treatment upregulates genes involved in amino-acid metabolism which result in polyamine (putrescine, spermidine and spermine) synthesis and proline-induced collagen synthesis (significantly upregulated genes – red; downregulated genes - grey; unaltered genes - black). Associated graphs show that NAM restores enzyme gene expression to baseline levels (y-axis represents fold change relative to mRNA expression in vehicle control which is represented by the dashed line). This highlights a role for CaSR-NAM in reduction of proline and polyamine synthesis, and extracellular polyamine transport. High intracellular polyamine concentrations increases the expression of OAZ which acts a regulator blocking the synthetic pathway downstream of ODC, and import mechanisms. Furthermore, extracellular polyamines can also activate the CaSR which is known to drive fibrosis. Negative allosteric modulation of the receptor dampens this signalling pathway limiting pro-fibrotic responses e.g. collagen deposition and proliferation. Genes encoding antizyme (OAZ1), arginase (ARG), glutaminase (GLS), glutamine synthetase (GLUL), ornithine aminotransferase (OAT), ornithine decarboxylase (ODC1), polyamine oxidase (PAOX), proline oxidase (PRODH), pyrroline 5-carboxylate dehygrogenase (ALDH4A1), pyrroline 5-carboxylate reductase (PYCR2), pyrroline 5-carboxylate synthase (ALDH18A1), solute transporter 3A2 (SLC3A2), spermidine synthase (SRM), spermidine/spermine acetyltransferase (SAT), spermine oxidase (SMOX), spermine synthase (SMS) are involved in these pathways. Data in the violin plots represent median fold change compared to vehicle (black line), truncated at minimum and maximum values. Benjamini-Hochberg p-value adjustment was performed for all statistical tests; level of controlled false positive rate was set to 0.05. * $p<0.05$, ** $p<0.01$, *** $p<0.001$. N = 3. NAM: CaSR negative allosteric modulator, NPS2143 (1 μM).

Polyamines and their associated metabolites are important for the induction of growth in response to mitogenic stimuli (Arruabarrena-Aristorena *et al*. 2018). Furthermore, polyamine concentration is tightly regulated through a series of enzymes since they activate cellular processes implicated in fibrosis, such as cell cycle progression, RhoA synthesis and β-catenin activation (Guo *et al*. 2002; Arruabarrena-Aristorena *et al*. 2018). Ornithine, a key metabolite in the polyamine biosynthetic pathway, can be synthesised from 2 basic amino acids, arginine and glutamine. As previously discussed, glutamine can be converted into ornithine *via* the aminotransferase, OAT. Conversely, arginine catabolism occurs through the action of arginase (Maarsingh et al. 2008a).

In my model, TGFβ1 treatment appeared to reduce *ARG2* expression although not significantly (p_{adj} *value* > 0.05; Figure 5.12). However, the gene transcripts of all other enzymes involved in the polyamine synthesis from arginine were significantly increased; fold change relative to vehicle expression were as follows: ornithine decarboxylase 1 (*ODC1*) = 1.6, ornithine decarboxylase antizyme 1 (*OAZ1*) = 1.9, spermidine synthase (*SRM*) = 1.7, and spermine synthase (*SMS*) = 1.5 (Figure 5.13). Baseline expression of the aforementioned genes was restored in the presence of NAM (Figure 5.12). The expression of *SMOX* (spermine oxidase), which converts spermine back into spermidine, was also increased with TGFβ1 treatment (fold change = 1.9). *SAT1/2* (spermidine/spermine acetyltransferase 1/2) and *PAOX* (polyamine oxidase) expression, which facilitate the conversion of acetylated-spermidine/spermine into putrescine, also increased although not significantly (p_{adj} *value* > 0.05; Figure 5.12). Co-treatment with NAM restored baseline expression of SAT1 (p_{adj} *value* = 0.02), SAT2 (p_{adj} *value* = 0.002), and SMOX (p_{adj} *value* = 0.06) but no discernible effect on PAOX was observed.

Polyamine transport is crucial for the maintenance of intracellular polyamine homeostasis (Gamble *et al*. 2019). Gene expression of candidate polyamine

transporters was determined after TGFβ1 treatment. TGFβ1 increased the expression of *SLC3A2* and *SLC7A1 (Figures 5.12)*. *SLC3A2* expression is restored to baseline in the presence of NAM (Figure 5.13). Figure 5.14 summarises the metabolic programmes discussed in this chapter and the potential NAM targets.

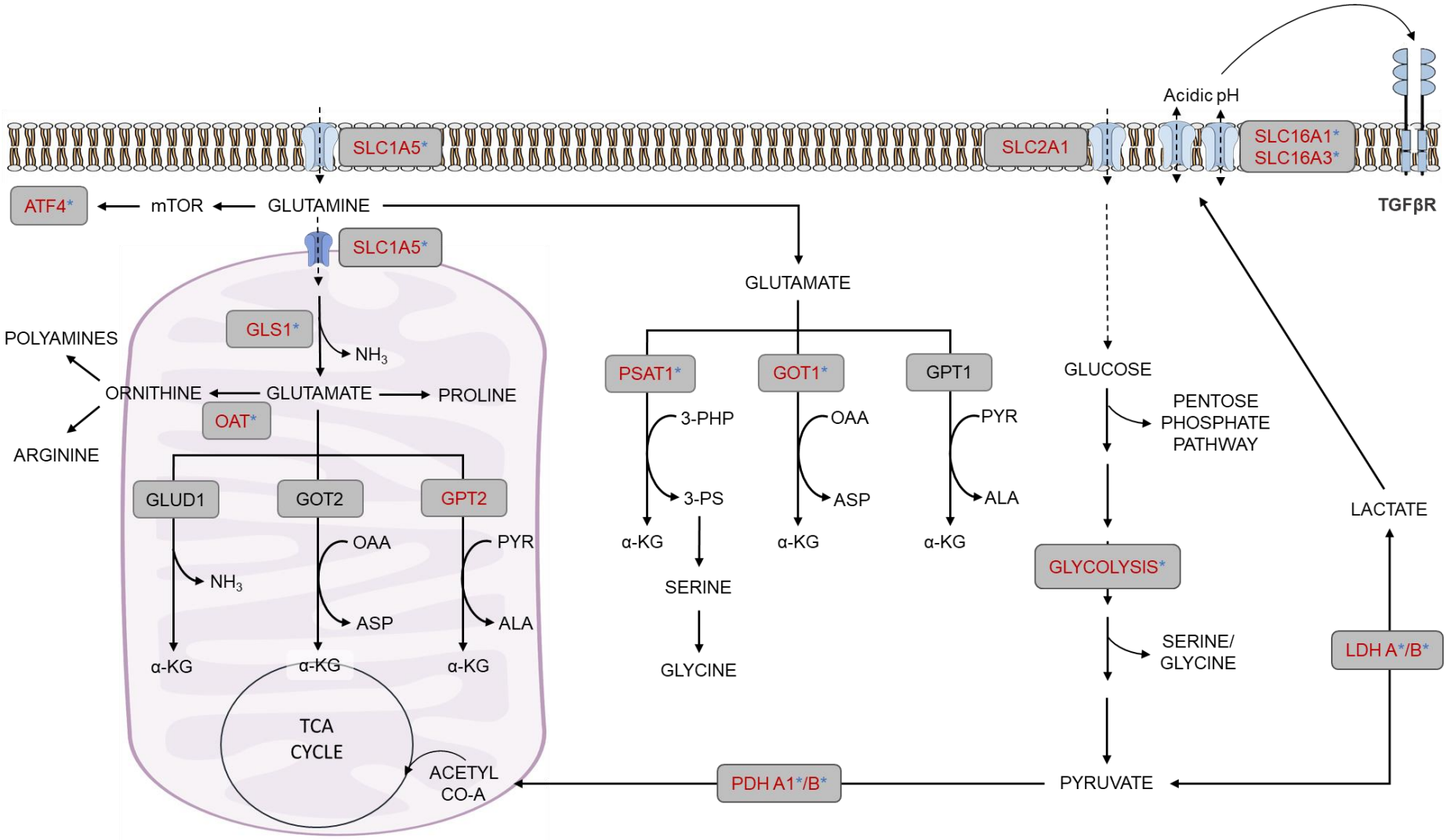
Acidic pH
SLC1A5*
SLC2A1
SLC16A1*
SLC16A3*
TGFβR
ATF4*
mTOR
GLUTAMINE
SLC1A5*
GLUTAMATE
POLYAMINES
GLS1*
NH3
ORNITHINE
GLUTAMATE
PROLINE
OAT*
ARGININE
GLUD1
GOT2
GPT2
NH3
OAA
ASP
PYR
ALA
α-KG
α-KG
α-KG
TCA
CYCLE
ACETYL
CO-A
PSAT1*
GOT1*
GPT1
3-PHP
3-PS
OAA
ASP
PYR
ALA
α-KG
α-KG
α-KG
SERINE
GLYCINE
GLUCOSE
PENTOSE
PHOSPHATE
PATHWAY
GLYCOLYSIS*
SERINE/
GLYCINE
LACTATE
LDH A*/B*
PDH A1*/B*
PYRUVATE

Figure 5.14 Pulmonary fibrosis is characterised by increased TGFβ1 signalling. TGFβ1 enhances glucose uptake via SLC2A1 (GLUT1) and the expression of glycolytic enzymes. Under fibrotic conditions, glucose-derived pyruvate is predominantly converted into lactate via LDH (lactate dehydrogenase) and exported to the extracellular space through the lactate transporters, SLC16A1 (MCT1) and SLC16A3 (MCT4). The accumulation of lactate in the extracellular environment can activate latent TGFβ1 molecules resulting in a positive feedback loop. Concurrently, fibroblasts become reliant on glutaminolysis as a source of energy, non-essential amino acids (NEAAs) and polyamines which sustain the fibrotic phenotype via DNA activation, protein translation and intracellular signalling. Glutamine-derived glutamate is a substrate for several aminotransferases responsible for the direct and indirect production of ornithine, aspartate, alanine, serine, proline, arginine, polyamines, cysteine, and glycine. Glutamine activates ATF4, a master transcriptional regulator stimulated under stress conditions while glutamine-derived NEAAs block this response. Grey boxes indicate genes assessed with RNA sequencing (red – upregulated; black – unaltered; * inhibited by NAM). aKG: α-ketoglutarate; Ala: alanine; Asp: aspartate; ATF: activating transcription factor; Gln: glutamine; GLS: glutaminase; Glu: glutamate; GLUD: glutamate dehydrogenase; Gly: glycine; GOT: glutamate-oxaloacetate transaminase; GPT: glutamate-pyruvate transaminase; NAM: CaSR negative allosteric modulator; NPS2143; OAA: oxaloacetate; OAT: ornithine aminotransferase; PDH: pyruvate dehydrogenase; PHP: phosphohydroxypyruvate; Pro: proline; PS: phosphoserine; PSAT: phosphoserine aminotransferase; Pyr: pyruvate; Ser: serine.

5.4. Discussion

The main findings of this thesis chapter are that prolonged TGFß treatment induces a fibrotic response characterised by reactivation of embryological genes, upregulation of ECM proteins, metabolic reprogramming, and the induction of polyamine metabolic pathways. These responses are significantly reduced and, in some cases, completely abolished by the NAM, NPS2143. My results also show that, under unstimulated experimental conditions, there is no difference between vehicle control and NAM-treated NHLFs. Together, these observations suggest that the CaSR might contribute to key pathological mechanisms implicated in PF pathogenesis/progression.

5.4.1. NHLFs treated with TGFß1 display a profibrotic profile

Based on extensive experimental data, TGFß1 is recognised as an effective method of inducing fibrosis *in vitro* (Ask *et al*. 2008; Gharaee-Kermani *et al*. 2009; Kim *et al*. 2018; Schwörer *et al*. 2020). It is clear from my data that TGFß1-treated NHLFs form a distinct cluster due to their transcriptomic profile, which differs from the unstimulated groups (vehicle and NAM). This profile is characterised by the upregulation of key IPF-related genes including but not limited to αSMA, Collagens (1, 3 and 5), CTGF, COMP, IL-11, MMP (1, 2, 14), SERPINE1, and NOX4 (NADPH oxidase isoform 4) (Emblom-Callahan *et al*. 2010; Lindahl *et al*. 2013; Rodriguez *et al*. 2018; McDonough *et al*. 2019b; Peyser *et al*. 2019).

It is, however, important to note that this experimental model did not induce some molecular pathways implicated in PF. For example, sustained treatment of NHLFs with TGFß1 (for 72 hours) downregulated genes associated with $[Ca^{2+}]_i$ mobilisation, AKT and Notch signalling, which previous studies have shown to be upregulated and activated in TGFß1-treated (Wygrecka *et al*. 2012; Janssen *et al*. 2015; Mukherjee *et al*. 2015) and IPF fibroblasts (Boon *et al*. 2009; Aoyagi-Ikeda *et al*. 2012; Chanda *et al*.

2019; Scruggs *et al*. 2020). Although TGFß-dependent STAT signalling is increased cultured IPF fibroblasts (Guillotin *et al*. 2020), GOnet analysis indicated downregulation of genes related to this pathway. The finding presented in this chapter is in line with the study by Emblom-Callahan *et al*. (2010), which reported decreased expression of key STAT signalling genes, STAT3 and STAT5A, in non-cultured IPF fibroblasts. This disparity might be due to the effect culturing IPF fibroblasts has on gene expression if the cultured cells are not exposed to exogenous fibrotic stimuli (Rodriguez *et al*. 2018). It is also possible that STAT signalling and the other downregulated pathways previously discussed (AKT and Notch) were switched on at an earlier timepoint.

The role of inflammation is controversial in the development of IPF (Bringardner *et al*. 2008; Wynn 2011). Inflammation and immune-related responses are crucial to a broad range of PF pathologies (including IPF) where cytokines such as IL-1ß, IL-6, IL-8 and TNFα facilitate collagen expression and proliferation in lung fibroblasts (Plantier *et al*. 2016; Papiris *et al*. 2018). On the other hand, cytokines such as interferon-γ suppress collagen and αSMA expression, growth and migration of human lung fibroblasts (Elias *et al*. 1987; Vu *et al*. 2019). In addition, the toll-like receptor (TLR3), which plays a role in initiating an antiviral immune response, is defective in some IPF patients, and an inactivating polymorphism of this gene is associated with accelerated decline in lung function (O'Dwyer *et al*. 2013). Genetic deletion of this receptor in mice results in increased lung fibrosis and reduced survival after bleomycin treatment (O'Dwyer *et al*. 2013). These findings are in line with the pathways indicated by GOnet analysis where TGFß1 treatment induced the upregulation of IL-1-mediated and TNF-mediated signalling pathways while downregulating TLR and interferon-γ signalling pathways. Interestingly, IL-1ß, IL-6 and IL-8, which are known mediators of fibrosis, were unaltered at the point of analysis, suggesting these mediators might play an earlier role in fibrogenesis where inflammation-driven signals may be more apparent.

In addition to fibroblasts, an aberrant inflammatory and immune response is mediated by leucocytes in IPF (Luzina et al. 2015b). In rapidly progressing IPF or during acute exacerbations, the number of innate leucocytes (neutrophils and macrophages) are in increased in the lungs (Balestro *et al*. 2016) and correlates with increased mortality (Parra *et al*. 2007). Neutrophils are recruited to the site of lung injury through the release of cytokines and further propagate the fibroproliferative process via TGFß1, IL-1ß and IL-8 expression/release (O'Dwyer *et al*. 2018; Warheit-Niemi *et al*. 2019). GOnet analysis of NHLFs co-treated with TGFß1 and NAM shows not only a downregulation of the genes associated with cytokine-mediated signalling but also innate immune response and myeloid leucocyte mediated signalling. Although further work is required to directly explore the efficacy of NAMs in the innate immune cells implicated in IPF, this finding potentially indicates an anti-inflammatory role of the drug in IPF, targeting one of the underlying mechanisms of acute exacerbations and rapidly progressing IPF.

5.4.2. NAM attenuates TGFß1-induced upregulation of developmental genes implicated in fibrosis.

My study indicates that chronic activation of NHLFs with TGFß1 upregulates key developmental pathways implicated in the pathogenesis of IPF. Approximately 20% of the dysregulated genes associated with IPF belong to molecular signalling pathways responsible for regulating embryological lung development (Selman *et al*. 2016). These pathways include several members of growth factor families such as TGFß, FGF, CTGF, VEGF and PDGF, and transcription factor families such as WNT signalling pathways.

TGFß signalling

The TGFß isoforms (ß1, ß2 and ß3) are well-known mediators of the aberrant wound-healing process which underlies fibrotic conditions, with TGFß1 showing the most prominent association with the development of IPF (Akhurst and Hata 2012; Fernandez and Eickelberg 2012). Accordingly, the RNA sequencing data presented here show that *de novo TGFB1* expression is increased 2.6-fold compared to baseline; *TGFB2* expression doubled while *TGFB3* expression decreased. Furthermore, the specificity of the NAM, NPS2143 to the *TGFB1* transcript is evident since the drug had no effect on the expression of the other isoforms.

Since TGFß1 is the focal point of this thesis, this section briefly explores the roles of TGFß2 and TGFß3 in fibrosis. Both isoforms have been reported to have profibrotic effects *in vitro* (Shah *et al*. 1995; Lee *et al*. 1999). However, their role in PF remained unclear until recently (Sun *et al*. 2021). Sun *et al*. (2021) show increased *TGFB2* and *TGFB3* expression in IPF lungs compared to control, and selective inhibition of TGFß2 or TGFß3 decreases bleomycin-induced lung fibrosis and prevents the increased inflammation associated with pan-TGFß isoform inhibition. This suggests that drugs which target a specific TGFß isoform might be more beneficial in the treatment of PF.

Other studies have also indicated a role for TGFß3 in wound-healing and fibrosis that diverges from the typical progressive fibrotic response, which could be a reason for its decreased expression in my study. For example, in cutaneous wounds, exogeneous application of TGFß3 reduced deposition of ECM proteins (collagen 1, collagen 3, and fibronectin), resulting in reduced scarring, while a similar response was achieved with topical application of neutralising antibodies to TGFß1 and TGFß2 (Shah *et al*. 1995). In an *in vivo* model of PF, intratracheal administration of TGFß3 inhibited TGFß1-induced expression of TGFß1 and TIMP1, resulting in the resolution of established fibrosis (Ask *et al*. 2008). These findings support the data presented in this

chapter and suggests that TGFβ1 and TGFβ3 might play antagonistic or redundant roles. However further research using IPF tissue is required since *TGFB3* expression is shown to be upregulated in IPF fibroblasts (Emblom-Callahan *et al*. 2010) and lung tissue (Sun *et al*. 2021).

The TGFβ isoforms are synthesised in their latent form and can be activated through various mechanisms involving thrombospondin (*THBS1*), extracellular acidification, proteolytic cleavage, and reactive oxygen species (*e.g.*, *NOX4*) (Prud'homme 2007). Latent TGFβ is covalently bound to latent TGFβ binding proteins (LTBPs), which act as structural components of the ECM and modulate TGFβ availability. All 3 isoforms are inactivated by their interaction with LTBPs (Yue *et al*. 2010). Since NAM downregulates the genes implicated in the regulation of TGFβ activation and inactivation (with the exception of *NOX4*), these findings suggest that CaSR regulates TGFβ1 expression and availability through ROS-independent mechanisms.

Canonical TGFβ signalling occurs through the same receptor, TGFβR, which phosphorylates SMAD-2 and SMAD-3; the SMADs recruit SMAD-4, forming a complex which binds to DNA resulting in the activation or repression of hundreds of genes (Rubtsov and Rudensky 2007). Conversely, SMAD-7 acts as a negative regulatory mechanism that inhibits TGFβ signalling by blocking the activation of SMAD-2, -3, and -4 (Hayashi *et al*. 1997). The data presented in this chapter shows a sustained increase in *SMAD7* expression after TGFβ1 treatment, which suggests that canonical signalling might have occurred at an earlier timepoint in the experiment and that inhibiting these SMADs might result in reduced gene expression. Furthermore, TGFβ also induces several non-canonical pathways such as RAS, JNK, AKT/mTOR and Rho-GTPases (Li *et al*. 2006) (discussed in greater detail in chapter 4).

Development signalling

Key developmental signalling pathways including Wnt, Sonic hedgehog (SHH), TGFß, PDGF and FGF are reactivated in IPF (Klinkhammer *et al*. 2018; Chanda *et al*. 2019). These pathways interact with TGFß signalling to regulate epithelial dedifferentiation, fibroblast activation and proliferation (Chanda *et al*. 2019). This section will mainly focus on the Wnt signalling pathway.

Canonical Wnt signalling is initiated when Wnt binds to its receptor on the plasma membrane resulting in the translocation of ß-catenin into the nucleus, where it activates transcription factors belonging to the T Cell factor (TCF) family of genes, e.g., TCF4, regulating genes implicated in lung fibrosis such as MMPs (Wu *et al*. 2007), cell-cycle regulators (Davidson and Niehrs 2010), oncogenes (Zhan *et al*. 2017). Although two non-canonical Wnt pathways exist, this section will focus on the Wnt/planar cell polarity (PCP) pathway. The Wnt/PCP pathway typically activates JNK and Rho-signalling (Kühl *et al*. 2000; Pandur *et al*. 2002), regulating genes involved in cell migration, cell polarity, and stem cell maintenance (Chanda *et al*. 2019). Of note here are (canonical) *WNT*2/2b and (non-canonical) *WNT5a/5b* (Torres *et al*. 1996; Pongracz and Stockley 2006; Ackers and Malgor 2017), which downregulated and upregulated by TGFß1 treatment, respectively. Despite the decrease in gene expression of *WNT2/2b*, the opposite effect is observed for *CTNNB1* (ß-catenin), which could suggest the canonical pathway was activated at an earlier timepoint in the experiment.

In healthy adult lungs, ß-catenin is localised to endothelial and epithelial cells; however, in IPF lungs, ß-catenin accumulates in the nucleus of highly proliferative epithelial and fibroblastic lesions (Chilosi *et al*. 2003). The Wnt/ß-catenin signalling pathway profibrotic phenotypes in activated lung fibroblasts, promoting fibroblast proliferation and differentiation, cellular senescence and survival (Lam and Gottardi 2011; DY *et al*. 2013; Hamburg *et*

al. 2015). In bleomycin-induced murine models of PF, inhibition of this signalling pathway resulted in attenuation of lung fibrosis (Henderson *et al*. 2010; Kim *et al*. 2011). In the Kim *et al*. (2011) study, genetic silencing of ß-catenin resulted in decreased ß-catenin expression, collagen deposition, MMP2 and TGF-ß1 expression in the lungs; while Henderson *et al*. (2010) demonstrated that pharmacologically inhibiting Wnt/ß-catenin prevented and partially reversed bleomycin-induced fibrosis. In another study, Wnt inhibition with the drug, XAV939 alleviated lung fibrosis in bleomycin mice through TGFß1 and FGF-2 inhibition (Chen *et al*. 2016). These studies suggest therapeutic agent which targets this signalling pathway might be beneficial in the treatment of PF.

In normal lung fibroblasts, Wnt5A promotes proliferation, prevents apoptosis, and increases the expression of the ECM protein, fibronectin (Vuga *et al*. 2009). An increase in non-canonical Wnt signalling (with a concomitant decrease in canonical Wnt signalling) has been reported in ageing human lungs (Kovacs *et al*. 2014) and ageing mouse lungs (Paxson *et al*. 2013). Therefore, the Wnt signalling results presented in this chapter appears to model an ageing-related phenotype which might be more relevant to IPF given its strong association with ageing. Notably, *WNT5A* overexpression has been reported in IPF lung fibroblasts (Vuga *et al*. 2009; Newman *et al*. 2016). Although *WNT5B* shares 84% homology with *WNT5A* and is functionally similar (Rydell-Törmänen *et al*. 2016), little is known about *WNT5B* expression in IPF. Its cognate receptor, *FZD8,* is however, highly expressed in IPF lungs and correlates with rapid disease progression (Lam 2014). Accordingly, *WNT5B* and FZD8 are highly expressed in response to TGFß treatment in human lung fibroblasts (Baarsma *et al*. 2011; Spanjer *et al*. 2016). Furthermore, recombinant Wnt5B signalling via FZD8 mimicked the TGFß-induced gene expression of profibrotic markers (such as collagen, fibronectin, αSMA and CTGF) in lung fibroblasts, while FZD8 knockdown downregulated these genes in vitro and attenuated bleomycin-induced lung fibrosis in vivo (Spanjer *et*

al. 2016). These findings suggest that non-canonical Wnt signalling also contributes to IPF pathogenesis.

Since NAM reduces and, in some cases, restored baseline expression of canonical and non-canonical Wnt signalling molecules, these findings suggest it could be effective in targeting these pathways and potentially beneficial in the treatment of (I)PF. However, further work is required to validate these pathways in vivo.

Growth factor signalling

In normal fibroblasts, TGFß facilitates the wound healing process in collaboration with many other growth factors, of which CTGF is a major contributor (Prud'homme 2007). The RNA sequencing data presented in this chapter shows that the CTGF is one of the highly upregulated growth factors at the mRNA level in response to TGFß1 stimulation. CTGF, a potent ECM-associated mitogen, promotes fibroblast proliferation, migration, and production of extracellular matrix proteins, and it is highly expressed in fibrotic lesions of the skin, kidney, liver, and lungs (Moussad and Brigstock 2000; Plantier *et al*. 2016). In the developing lung, CTGF overexpression disrupts alveologenesis and induces fibrosis (Wu *et al*. 2010). Similarly, CTGF (its gene transcript, *CCN2*) is overexpressed in IPF, specifically within highly proliferating alveolar epithelial cells and fibroblasts (Allen *et al*. 1999; Pan *et al*. 2001). In IPF fibroblasts, CTGF expression and fibroblast activation are dependent on the non-canonical TGFß1 signalling pathways, MAPK and RhoA (Watts *et al*. 2006; Plantier *et al*. 2016). Interestingly, *CCN2* expression was three-fold higher than *TGFB1* expression in IPF fibroblasts compared to control (Murray *et al*. 2008). This could be because CTGF potentiates TGFß1 signalling by enhancing receptor binding (Abreu *et al*. 2002), thereby activating a positive feedback loop, further augmenting its expression. TGFß has also been shown to upregulate *CCN2*/CTGF expression in cultured normal human fibroblasts, IPF fibroblasts, and fibroblasts from mice with bleomycin-induced lung fibrosis (Lasky *et al*. 1998; Murray *et al*. 2008). Further implicating CTGF in the pathogenesis of pulmonary fibrosis, intratracheal

administration of bleomycin increased CTGF mRNA expression and collagen deposition in bleomycin-sensitive mouse lungs, but neither response was observed in a bleomycin-resistant mouse strain that does not develop lung fibrosis (Lasky *et al*. 1998). In support of these findings, a recent phase 2 clinical trial highlights the therapeutic potential of a recombinant monoclonal antibody targeting CTGF, pamrevlumab, which slowed the decline in lung function and disease progression (Richeldi *et al*. 2020).

5.4.3. NAM attenuates TGFβ1-induced upregulation of profibrotic genes implicated in fibrosis.

Results presented in this chapter show that NAM attenuates the expression of several profibrotic genes involved in cytoskeletal changes, ECM deposition, proliferation, and senescence. The diversity of these genes highlights the complex regulation of matrix production/turnover and cell cycle involved in the early stages of lung fibrosis (Emblom-Callahan *et al*. 2010; Cabrera *et al*. 2013).

Cytoskeletal changes

Consistent with the increased expression of myofibroblast markers identified by single-cell sequencing of bleomycin-treated mouse lungs (Xie *et al*. 2018; Peyser *et al*. 2019), the RNA sequencing results presented in this chapter show that both *TAGLN* and *ACTA2* were enriched in the TGFβ1-activated NHLFs. For decades, αSMA/*Acta2* has been purported to be the key marker of myofibroblasts, a distinct population of fibroblasts thought to be central to the development and progression of organ fibrosis (Wynn 2007; Hinz *et al*. 2012; Phan 2012). Accordingly, a study using bleomycin-treated αSMA-GFP-reporting mice showed that αSMA$^+$ cells are dramatically expanded during lung fibrogenesis (Xie *et al*. 2016). However, evidence from recent studies questions the validity of the use of αSMA as a lone marker of matrix-depositing (myo)fibroblasts since the *ACTA2* gene was only

expressed by 60% of activated fibroblasts and present in 11% of the non-activated fibroblast population (Xie *et al*. 2018). Furthermore, studies have found that only a subgroup of αSMA$^+$ cells produces collagen, a key marker of fibrogenicity (Sun *et al*. 2016; Xie *et al*. 2018).

In fibrotic mouse lungs, fibroblasts that express *Col1a1* also typically expressed *Acta2* or *Ltbp2* (Peyser *et al*. 2019). *Ltbp2* was also found to be expressed in 78% of activated fibroblasts compared to 8% of non-activated fibroblasts (Xie *et al*. 2018), suggesting that *Col1a1* expression or a panel of all 3 genes might be a better indication of activated fibroblasts. Given the heterogeneity of fibrotic fibroblasts and the current lack of well-characterised markers for these cells, the experimental model presented in this chapter can be considered robust since TGFß-activated NHLFs show an overlap in gene expression with pathologic fibroblasts.

ECM production

In addition to contractile genes (*ACTA2* and *TAGLN*), the data presented here show that activated NHLFs also express genes associated with the pathogenesis of lung fibrosis, *e.g.*, ECM production, ECM turnover, cell-matrix interaction, and cell signalling (Selman *et al*. 2000; Pardo *et al*. 2005; Emblom-Callahan *et al*. 2010; Cabrera *et al*. 2013). Since collagen-rich ECM deposition is central to IPF pathogenesis (Pardo 2008), the upregulation of several fibrillar collagen genes (*COL1A1, COL3A1, COL5A1, COL6A2*) along with fibril-associated collagen (*COL7A1*) might be beneficial in maintaining the integrity of newly deposited ECM and influencing cellular processes such as migration and adhesion (Ricard-Blum 2011; Kular *et al*. 2014). Of relevance here is the role of *COL7A1* in dermal fibroblast migration and wound healing (Nyström *et al*. 2013). Furthermore, upregulation of this collagen isoform might also facilitate increased interactions with fibronectin (*FN1*) (Lapiere *et al*. 1994), resulting in a greater fibrogenic response. Upregulation of collagen genes was also identified in studies using human and animal models of IPF (Emblom-Callahan *et al*. 2010; Akamatsu *et al*. 2013; McDonough *et al*. 2019a).

Procollagen is produced by fibroblasts through the catalytic activity of enzymes, including prolyl 4-hydroxylase (P4H), procollagen lysyl hydroxylase, and heat shock protein 47 (Akamatsu *et al*. 2013). P4H is an αKG-dependent hydroxylase that catalyses the 4-hydroxylation of proline required to form and stabilise collagen fibrils (Gorres and Raines 2010). The α-subunit, P4HA is responsible for substrate binding and catalytic activity (Annunen *et al*. 1998). P4HA1 is expressed by most cell types, while P4HA2, which is the main isoform in cartilaginous tissue, accounts for less than 30% of the total P4H activity in lung fibroblasts (Myllyharju 2008). Nonetheless, Emblom-Callahan *et al*. (2010) report increased expression of *P4HA2* in non-cultured IPF fibroblasts, suggesting a degree of translation between TGFß1-treated NHLFs and diseased fibroblasts. Therefore, NAM induced the downregulation of genes that encode, modify and stabilise collagen.

ECM turnover

Approximately three times the amount of ECM is deposited in the fibrotic lung compared to normal (Pardo *et al*. 2008). In IPF, signals are highly skewed towards ECM deposition compared to degradation (Emblom-Callahan *et al*. 2010). Maintaining the structural integrity of the ECM involves MMPs, which primarily breakdown collagen and their inhibitor proteins, TIMPs. The MMPs upregulated in IPF that are also upregulated in this study include MMP1, which is responsible for fibrillar collagen degradation and MMP2, responsible for basement membrane degradation (Pardo *et al*. 2008). These MMPs have also been shown to have intracellular activity associated with cell dysfunction and resistance to apoptosis (Wang *et al*. 2002; Kwan *et al*. 2004; Limb *et al*. 2005). The upregulation of MMPs (especially MMP1) might seem paradoxical in IPF given its role as interstitial collagenase, but it is important to note that both proteases also cleave and activate a plethora of cytokines, including pro-TNFα, pro-1L-1ß and IGFBP3 (Pardo and Selman 2006; Manicone and McGuire 2008), which play key roles in the disease. Interestingly, extracellularly MMP1 and 2 also activate their pro-peptides

resulting in a positive feedback loop. Intracellular MMP1 accumulates during mitosis and inhibiting this enzyme resulted in a faster induction of apoptosis compared to untreated cells, suggesting that it might be important in maintaining the balance between cell division and cell death (Limb *et al*. 2005). Pro-MMP2 is cleaved into its active form by a trimolecular complex consisting of membrane-bound MMP14 and TIMP2; TIMP3 but not TIMP1 can replace TIMP2 in this activation complex (Zhao *et al*. 2004; Manicone and McGuire 2008). Extracellularly MMP2 colocalises and effectively degrades components of the basement membrane, indicating a role in the disruption of the epithelium (Hayashi *et al*. 1996; Pardo and Selman 2006). Furthermore, like MMP1, it can also degrade fibrillar collagens, fibronectin, and elastin (Pardo and Selman 2006). In a model of myocardial fibrosis, CaSR-activated neutrophils released 1L-1ß, which upregulated the expression of MMP2, collagen 1 and collagen 3 in cardiac fibroblasts (Ren *et al*. 2020); this suggests that the CaSR can stimulate and maintain an environment favourable for the pathological activation of fibroblasts through the transcriptional regulation of interstitial collagens and MMP2. In addition, other positive feedback mechanisms involving the CaSR, growth factor receptors, and MMPs could also exist. Studies have shown that MMP activity is required for the transactivation of the epithelial growth factor receptor (EGFR) by CaSR (John MacLeod *et al*. 2004; Yano *et al*. 2004; Tomlins *et al*. 2005) , while EGFR transactivation by TGFß induces renal fibrosis through ROS-dependent (Samarakoon *et al*. 2013) or metalloprotease-dependent mechanisms (Rayego-Mateos *et al*. 2018b). EGFR activation can also be amplified by TGFß through the upregulation of one of its ligands, CTGF/CNN2 (Rayego-Mateos *et al*. 2013), with EGFR activation further augmenting TGFß intracellular activity by facilitating TGFßR2 translocation to the cell membrane (Shu *et al*. 2019). Among all EGFR ligands, CTGF is of special relevance here because it mediates ECM production (Rayego-Mateos *et al*. 2018a). Although these signalling pathways and activation mechanisms are yet to be explored in this context, these findings suggest that fibroblast activation could involve dynamic interactions between MMPs, CaSR, EGFR and TGFßR signalling.

Lastly, the concomitant increase in protease inhibitors: TIMP1, the main inhibitor of MMP1 (and MMP2), TIMP2, TIMP3, SERPINE1 and SERPINE2 suggest that CaSR may facilitate a profibrotic environment weighted significantly towards a non-degrading collagen-rich ECM, which is a defining feature of human and animal models of lung fibrosis (Selman *et al*. 2000; Bergeron *et al*. 2010).

Cell cycle

The cell cycle plays an important role in cell proliferation (Zhang *et al*. 2018). It is subdivided into four phases: G1 (first growth phase), S (DNA replication/synthesis phase), G2 (second growth phase) and M (mitosis). PCNA, a member of the cyclin family, acts as an interaction site for proteins that regulate cell cycle progression and is highly expressed during the transition from G1 to S phase (Stewart and Dell'orco 1992; Pablos *et al*. 1997; Lv *et al*. 2015); as a result, it is considered a surrogate for cell proliferation. It also plays an essential role in DNA synthesis, replication and repair (Chiang *et al*. 2000; Wang *et al*. 2018). Increased PCNA expression has been observed in highly proliferative conditions such as cancer (Stoimenov and Helleday 2009), oral submucous fibrosis (Chiang *et al*. 2000; Keshav and Narayanappa 2015), liver fibrosis (Kim *et al*. 2009), cystic fibrosis (Leigh *et al*. 1995), and bleomycin-induced PF (Zhao *et al*. 2020).

In addition to PCNA, transition through cell cycle checkpoints is triggered by complex interactions between other members of the cyclin family and cyclin-dependent kinases (CDKs) (Bartkova *et al*. 1996). Cyclin D/CDK4/CDK6 promote progression into the G1 phase, cyclin E/CDK2 are required for G1/S transition, cyclin A/CDK2 facilitate S/G2 progression, and cyclin B/CDK1 promote progression into the M phase (Yoshihara *et al*. 2020). Of note in this study, TGFβ induced gene expression of CDK4, CDK5 and CDK7. CDK4 is considered a proto-oncogene and is essential for tumorigenesis (Bartkova *et*

al. 1996; Bai *et al*. 2017), while CDK7 is indispensable for proliferation and silencing this gene leads to cell-cycle arrest culminating premature ageing-related phenotypes (Ganuza *et al*. 2012). However, CDK5 is unique in that it has no direct role in cell cycle progression (Zhang *et al*. 2008). It, however, facilitates proliferation and migration in breast cancer cells (Xu *et al*. 2014) and elicits profibrotic responses in fibroblasts (Wei *et al*. 2018).

The effect of NAM treatment on gene expression of PCNA, cyclin E2 and CDK4 suggests that CaSR might drive proliferation by regulating transition into the G1/S phase of the cell cycle while its effect on CDK5 and CDK7 indicates how this drug could be beneficial in maintaining the balance between proliferative and senescent cell signals.

Cell senescence

Cell senescence is a state of the irreversible arrest of cell proliferation with the acquisition of a specific secretory phenotype (Campisi and D'Adda Di Fagagna 2007). In IPF, this senescence-associated secretory phenotype (SASP) is characterised by the production of growth factors (TGFß, CTGF, FGF, PDGF), cytokines (TNFα, IL-1ß, IL-8), MMPs (MMP2, MMP3, MMP9) and other profibrotic molecules, which contribute to inflammation, wound-healing and ECM remodelling through autocrine and paracrine signalling (Campisi 2016; Lin and Xu 2020).

RAS-induced senescence was first observed in human fibroblasts when the oncogenic RAS (H-ras-V12) was expressed in these cells leading to permanent cell cycle arrest (Serrano *et al*. 1997). RAS signalling causes aberrant DNA replication and activation of the DNA damage response pathway, which drives senescence through the upregulation of cyclin-dependent kinase inhibitor CDKN1A/p21CIP1 (Lujambio 2016), whilst indirectly activating replicative senescence through the CDKN2A locus (p14ARF, p15INK4B and p16INK4A) which represses cyclin-dependent kinases (Gil and Peters 2006).

CDKN2A/p14ARF activation further reinforces the CDKN1A/p21CIP1 pathway (Kamijo *et al*. 1998; Zhang *et al*. 1998), while the loss of CDKN2B/p15INK4B has been shown to promote fibrosis (Scruggs *et al*. 2018). Since NAM treatment abolished the TGFβ1-induced upregulation of CDKN1A and CDKN2A but not CDKN2B, this suggests a potential role of the CaSR in preventing cell cycle arrest and SASP, thereby abrogating the profibrotic cycle. However, the moderate effect of TGFβ1 on the gene expression of a key senescence marker in IPF, GLB1 (β-galactosidase) (Lin and Xu 2020), suggests that further work is required to validate the senescence genes discussed at a post-translational level.

Another key mediator of senescence is the cytokine IL-11. Senescent lung fibroblasts and epithelial cells highly secrete TGFβ and IL-11, which promote MEK/ERK signalling, resulting in αSMA expression and collagen deposition *in vitro* and facilitating lung fibrosis in mice (Chen et al. 2020a). TGFβ1 predominantly induces IL-11 expression in primary human fibroblasts, and the IL-11/ERK intracellular signal is required to mediate the fibrogenic effect (Schafer *et al*. 2017). Fibroblast-specific IL-11 overexpression induced cardiac and renal fibrosis while genetic ablation of the IL-11 receptor abrogated this response (Schafer *et al*. 2017). In the lungs, human stromal cells and epithelial cell lines infected with viruses associated with IPF pathogenesis (such as respiratory syncytial virus, rhinovirus, and parainfluenza virus type 3) also express and secrete high levels of IL-11 (Ng *et al*. 2020; Mostafaei *et al*. 2021), which could heighten the profibrotic response by stimulating surrounding cells, e.g. fibroblasts. This is of relevance since IL11 expression is highly upregulated in invasive IPF fibroblasts (Geng *et al*. 2019), and anti-IL-11 therapy inhibits fibroblast activation, migration, and ECM production in vitro and reverses bleomycin-induced pulmonary fibrosis in vivo (Ng *et al*. 2020).

Although these cell cycle mediators have only been investigated at the transcriptional level, this section highlights the potential role of the CaSR in

the complex interplay between ECM deposition, proliferation, and senescence.

5.4.4. NAM targets cellular metabolism in activated NHLFs.

The key pathological phenotype of activated fibroblasts, *i.e.* excessive ECM secretion and αSMA expression, relies on metabolic reprogramming of the cells (Bernard *et al.* 2018). These pathological fibroblasts have been implicated in tissue fibrosis and cancer pathobiology (Radisky *et al.* 2007; Duffield *et al.* 2013). Aerobic glycolysis, glutamine metabolism, macromolecule synthesis, and redox homeostasis are some of the metabolic pathways currently being considered as therapeutic targets in a variety of pathological conditions, including cancer (Luengo *et al.* 2017), severe acute respiratory syndrome coronavirus 2 (SARS-CoV-2) (Bharadwaj *et al.* 2021), neurological disorders (Thomas and Beal 2010), and heart diseases (Ardehali *et al.* 2012). Although these pathways have only been explored preclinically for pulmonary fibrosis, these findings appear promising and suggest that metabolic pathways could be viable therapeutic targets for this disease (Table 5.2).

Table 5.2: Summary of metabolic pathways/genes that could be potential targets for future anti-fibrotic development. Potential pathways/genes downstream of CaSR signalling indicated by the results in this chapter are highlighted in blue.

Pathway	Target Genes	Proposed Outcome: ↓	References
Glycolysis	*PKM2*	Proliferation	(Nie *et al*. 2017)
Pentose Phosphate	*G6PD, PGD*	NADPH/Nucleotide synthesis	(Liu and Summer 2019)
Serine/Glycine	*PHGDH, PSAT1, PSPH, SHMT*	Collagen synthesis	(Nigdelioglu *et al*. 2016; Hamanaka *et al*. 2018)
Lactate Production	*LDHA/B*	TGFβ activation αSMA expression Collagen synthesis	(Kottmann *et al*. 2012)
Nutrient Sensing	*AMPK* mTOR	Collagen synthesis Proliferation	(Rangarajan *et al*. 2018) (Ge *et al*. 2018)
Glutaminolysis	*GLS*	αSMA, fibronectin & COL1A1 expression Collagen synthesis	(Bernard *et al*. 2018) (Ge *et al*. 2018)
Proline/ Polyamine	*ALDH18A1, PYCR, OAT, P4HA, ODC, DOHH* Transporters: *SLC1A5, SLC3A2*	Collagen synthesis Proliferation	(Auvinen *et al*. 1992; Sievert *et al*. 2014)

Glycolysis

The GOnet analysis reported in this chapter indicates that fibroblast activation requires oxidative phosphorylation since it was the pathway most enriched by TGFß1 treatment. Furthermore, it has been suggested that myofibroblast differentiation requires metabolic reprogramming, a process characterised by an increase in oxidative phosphorylation and glycolysis (Bernard *et al*. 2015). Since the end-glycolytic product, pyruvate provides lactate and acetyl-CoA, the expression of genes implicated in glycolysis were explored to determine their role in fibroblast activation.

The results presented in this chapter suggest that glycolysis plays a key role in the TGFß1-induced activation of lung fibroblasts. Although glycolysis is regarded as a less efficient method of generating ATP compared to oxidative phosphorylation, aerobic glycolysis seen in diseases such as IPF could be more beneficial to the pathological process since it is occurring at a faster rate (Para *et al*. 2019), potentially providing an alternative source of energy to IPF fibroblasts which have poor mitochondrial function and limited aerobic respiration capacity (Zank *et al*. 2018). Suppressing glycolysis by blocking the enzyme, 6-phosphofructo-2-kinase/fructose-2,6-biphosphatase 3 (PFKFB3) in TGFß-treated normal and IPF HLFs attenuated αSMA expression and cell contractility, as well as protecting against bleomycin- and TGFß-induced pulmonary fibrosis (Xie *et al*. 2015). Although *PFKFB3* expression was not reduced by NAM treatment, baseline expression of the enzymes which catalyse 6 out of the 10 glycolytic steps was restored. Among these enzymes is pyruvate kinase M2 (PKM2), a rate-limiting glycolytic enzyme, which facilitates the final step of glycolysis, i.e. pyruvate production (Wu et al. 2020b). Pharmacological inhibition of PKM2 inactivates AKT/mTOR signalling, which decreases glucose consumption and lactate production in acute myeloid leukaemia cells (Wu et al. 2020b), abrogates proliferation and invasiveness of A549 lung cancer cells (Wang *et al*. 2013), and suppresses pulmonary fibroblast proliferation (Nie *et al*. 2017). Since co-treatment with NAM restored baseline gene expression of several glycolytic enzymes, this

suggests a mechanism through which NAM might prevent fibroblast migration and proliferation.

PKM2 upregulation can also be directly linked to the excessive production of lactate which is typical of activated fibroblasts (Para *et al*. 2019) since pyruvate is converted into lactate by the enzyme lactate dehydrogenase (LDH). LDH is a promising target in several diseases because it replenishes NAD^+ levels required for redox balance, glycolysis, TCA cycle and oxidative phosphorylation (Xie *et al*. 2020). A large study involving 172,933 patients, which examined 48 diseases, showed that serum LDH activity is a highly specific biomarker candidate for lung fibrosis (Wu *et al*. 2021). Interestingly, serum LDH also correlates with worse outcomes in critically ill SARS-CoV-2 patients, where the greatest LDH values reported were in non-survivors during the fibrotic phase of the disease (Lv *et al*. 2020). Although the Wu *et al*. (2021) study did not define which conditions were classified as lung fibrosis, this finding is in line with the elevated LDH expression reported in lung tissue and fibroblasts from PF and IPF patients, respectively (Kottmann *et al*. 2012). Furthermore, a synergistic effect was also observed between lactic acid and TGFß whereby activation of extracellular TGFß by lactic acid resulted in a profibrotic feedback loop and greater extracellular acidification rates in IPF fibroblasts compared to control (Kottmann *et al*. 2012). In normal and IPF HLFs, LDH inhibition suppressed TGFß activity, extracellular acidification, αSMA and collagen expression (Kottmann *et al*. 2015), which could have an implication on the cells within and adjacent to the fibrotic foci. In addition, blocking LDH activity induces anti-tumour effects, such as cytostasis and apoptosis (Sun *et al*. 2009; Lin *et al*. 2013), and abrogates viral replication and cytokine expression in SARS-CoV-2 infected cells (Codo *et al*. 2020). Given that these pathological processes are also implicated in IPF and that NAM treatment restored baseline expression levels of *LDHA* and *LDHB,* NAM could potentially halt virus-initiated fibrosis. Since both LDH subunits are affected, there could be a post-translational effect on all 5 LDH isozymes encoded by *LDHA* and *LDHB* (LDH1: B4, LDH2: B3A1, LDH3: B2A2,

LDH4: B1A3, and LDH5: A4), which could be associated with a reduction in αSMA expression, collagen secretion and fibroblast proliferation.

Glycolysis also supplies metabolites that are used to upregulate other metabolic pathways in highly proliferating cells, such as the pentose phosphate pathway and *de novo* serine/glycine synthesis (Para *et al*. 2019). For example, glucose-6-phosphate (G6P), the first metabolite of the glycolysis, is diverted into the pentose phosphate pathway where G6P dehydrogenase (*G6PD*) and 6-Phosphogluconate dehydrogenase (*PGD*) facilitate the production of nucleotides and fatty acids (Liu and Summer 2019). Specific to lung fibroblasts is the finding that the enzymes (PHGDH, PSAT1, PSPH and SHMT2) in the serine/glycine synthetic pathway are known transcriptional targets of TGFβ (Nigdelioglu *et al*. 2016; Hamanaka *et al*. 2018). Furthermore, silencing PHGDH and SHMT2, which are upregulated in IPF lungs, attenuates collagen synthesis (Nigdelioglu *et al*. 2016), suggesting that this pathway might play a key role in IPF pathophysiology. Using carbon-labelling studies, Nigdelioglu *et al*. (2016) showed that activated lung fibroblasts redirect glycolytic intermediates to produce collagen in response to TGFβ stimulation. Since glycine accounts for approximately one-third of the amino acids found in collagen (Ricard-Blum 2011), fibroblasts must depend on *de novo* serine/glycine metabolism for collagen production. The therapeutic potential of this pathway was demonstrated by the attenuation of bleomycin-induced lung fibrosis in mice treated with a PHGDH inhibitor (Hamanaka *et al*. 2018).

Glutamine metabolism

Metabolomic analysis of IPF lung tissue show increased glutamine and glutamate levels compared to normal lungs (Kang *et al*. 2016; Zhao *et al*. 2017). Furthermore, activated lung (myo)fibroblasts also exhibit increased glutaminolytic flux (Bernard *et al*. 2018; Ge *et al*. 2018). In this pathological state, the glucose-derived carbon diverted from the TCA cycle is in most cases replenished by glutaminolysis which provides a constant supply of

αKG through the enzymatic activity of GLS (DeBerardinis *et al*. 2007; DeBerardinis *et al*. 2008; Para *et al*. 2019). GLS, specifically GLS1, positively correlates with increased cell proliferation (Pérez-Gómez *et al*. 2005)and is highly expressed within the regions of active fibrosis in human and murine models of lung fibrosis (Ge *et al*. 2018). Several studies have shown that TGFβ treatment augments glutaminolysis by upregulating GLS1 expression in lung fibroblast (Bernard *et al*. 2018; Ge *et al*. 2018; Hamanaka *et al*. 2019). This was further confirmed by the increase in intracellular glutamate concentration and concurrent decrease in glutamine concentration observed in TGFβ-treated fibroblasts (Bernard *et al*. 2018). Withdrawing extracellular glutamine or silencing GLS1 pharmacologically or genetically inhibits TGFβ-induced expression of αSMA, fibronectin and collagen (Bernard *et al*. 2018; Ge *et al*. 2018; Hamanaka *et al*. 2019).

The glutaminolytic end-product, αKG, promotes mTORC1-mediated collagen translation and inhibits collagen degradation (Ge *et al*. 2018). In the presence of TGFβ, this is achieved through the upregulation of activating transcription factor 4 (ATF4), the transcriptional master regulator of amino acid metabolism, which increases the expression of the glucose transporter 1 (GLUT1/*SLC2A1*) and the enzymes in the serine/glycine pathway (*e.g.* PSAT1) to ensure enhanced collagen production is maintained in activated fibroblasts (Selvarajah *et al*. 2019). Nonetheless, the role of αKG as an energetic substrate is still somewhat controversial. Although a recent study by Schwörer *et al*. (2020) showed that TGFβ facilitates the use of glutamine as an alternative source of carbon for the TCA cycle, glutamine-derived αKG does not appear essential for TGFβ-induced increase in oxygen consumption as this process is independent of glutamine or GLS (Hamanaka *et al*. 2019). As previously discussed, αKG can be synthesised from glutamate through the catalytic activities of GLUD and transaminases (PSAT1, GOT1/2, OR GPT1/2). Hamanaka *et al*. (2019) present similar results where TGFβ treatment of NHLFs induced mRNA and protein expression of PSAT1, GOT1, GOT2, and GPT2. In this study, silencing *GLUD, GPT2* and *GOT1/2* had no effect on

collagen and αSMA expression, further supporting the theory that mitochondrial αKG plays a limited role in the activation of lung fibroblasts. Notably, silencing cytoplasmic PSAT1 significantly decreased collagen synthesis in these cells. Given the efficacy of NAM in downregulating PSAT1 expression, the findings from the Hamanaka *et al*. (2019) study suggest a potential mechanism for the inhibition of collagen expression observed in my project, thereby suggesting a crucial role for PSAT1 in TGFß-treated fibroblasts, linking enhanced glycolysis and glutamate metabolism to the production of collagen.

Another way glutamine contributes to collagen synthesis is *via* proline (Hamanaka *et al*. 2019). TGFß enhances the incorporation of glutamine-derived carbon into proline, with this newly synthesised proline being used to stabilise collagen through the catalytic activity of prolyl 4-hydroxylase (P4H) (Fandiño *et al*. 2020; Schwörer *et al*. 2020). The results in this chapter show that TGFß increases the gene expression of the enzymes in the *de novo* proline synthesis pathway, *i.e*. GLS, *ALDH18A1*/P5C synthase, OAT and P5C reductases/proline synthases (PYCR1/2), which is supported by previous findings (Hamanaka *et al*. 2019; Schwörer *et al*. 2020). Lung homogenates from IPF patients and bleomycin-treated mice express greater levels of *ALDH18A1*/P5C synthase, with *ALDH18A1* knockdown abrogating *TGFß-induced* collagen expression in NHLFs and IPF-HLFs, which could not be rescued by proline supplementation (Hamanaka *et al*. 2019). In vascular smooth muscle cells, inhibiting OAT blocks TGFß–mediated collagen production, suggesting that endogenous proline synthesis is required for TGFß–induced collagen synthesis (Durante *et al*. 2001). Moreover, metabolomic and genomic analysis indicates increased OAT expression and proline production in IPF lungs, with greater OAT gene expression correlating with poor IPF prognosis *(*Kang *et al*. 2016*)*.

The final step in proline biosynthesis, which converts P5C into proline, is catalysed by one of the three PYCR isozymes, PYCR1, PYCR2 or PYCR3.

PYCR1 and 2 share a high degree (84%) of amino acid sequence homology, both localise to the mitochondria and generate proline from glutamate, while PYCR3 has 46% sequence homology, localises to the cytosol and is suggested to preferentially generate proline from the precursor, ornithine through the catalytic activity of *OAT (de Ingeniis et al. 2012; Guo et al. 2019a)*. In mice, PYCR1 and 2 are functionally redundant, with *PYCR2*$^{-/-}$ mice displaying a more severe phenotype (Stum *et al*. 2021). Genetic silencing of PYCR1 and/or PYCR2 in human fibroblasts impedes proliferation while silencing both genes increase sensitivity to oxidative stress and reduces the expression of 4-hydroxyproline, an essential ECM component whose level is increased in IPF (Zhao *et al*. 2017). The lack of NAM effect on PYCR1, which also facilitates the proline synthesis from ornithine, suggests enzymatic interchangeability with *PYCR2*, specificity of the NAM to the glutamate-proline pathway, or *PYCR2*-induced proliferation.

Lastly, glutamine metabolism is also essential for the progression of viral infections. The link between viral infections and IPF has been long established (Egan *et al*. 1997), and meta-analysis of data from several studies comparing IPF patients to control over a period of 35 years reports that the risk of developing IPF is three times greater in patients with chronic viral infections of the lung compared to patients with acute infections (Sheng *et al*. 2020). Cells infected by viruses associated with IPF (*e.g*. adenovirus, Epstein-Barr virus, hepatitis C virus, human herpesviruses) show increased glucose and glutamine utilisation (Egan *et al*. 1997; Pulkkinen *et al*. 2012; Sheng *et al*. 2020; Bharadwaj *et al*. 2021) which are the same metabolic processes altered in activated NHLFs upon TGFβ treatment. Furthermore, inducing virus replication in primary human alveolar epithelial cells increased TGFβ expression and apoptosis (Malizia *et al*. 2008) while inhibiting metabolic enzymes such as GLS reduced virus replication in primary human bronchial epithelial cells (Thai *et al*. 2015), indicating a potential mechanistic link between epithelial injury, glutaminolysis and lung fibrosis. Although work directly exploring the link between metabolic reprogramming and PF is still required, pharmacological agents such as NAM,

which target these pathways and their genes, might limit the fibrotic process by limiting virus-induced epithelial cell dysfunction and fibroblast activation.

Polyamine metabolism

Natural polyamines are small, positively charged biogenic molecules that consist of diamines (putrescine and cadaverine) and oligoamines (spermidine and spermine) (Hoet and Nemery 2000). These polycations mediate their physiological functions by interacting with a plethora of negatively-charged macro-molecules, which results in cell growth, proliferation, differentiation, survival, nucleic acid and protein synthesis, protection from oxidative damage, chromatin stabilisation, and regulation of ion channels and receptors (Quinn *et al*. 1997; Ahern *et al*. 2006; Pegg and Casero 2011; Minois 2014). Polyamines are also implicated in several lung-related pathologies such as cancer (Liu *et al*. 2017), asthma (Yarova *et al*. 2015), cystic fibrosis (Grasemann *et al*. 2012), PAH (Grasemann *et al*. 2015; He *et al*. 2020) and viral infections (Firpo and Mounce 2020). Thus, provide the rationale to explore the potential impact of this pathway in fibrosis.

Polyamines are ubiquitous, with intracellular concentrations tightly regulated within the millimolar range via synthetic and catabolic pathways, import and efflux (Michael 2016; Casero *et al*. 2018). *De novo* polyamine synthesis begins with either arginine or methionine. Of relevance here is the arginine-polyamine pathway, which will be the focus of this section. The conversion of arginine to ornithine is catalysed by arginase (encoded by *ARG*) as part of the urea cycle. Although TGFβ treatment increases ARG1/2 expression (Kitowska *et al*. 2008), extremely low gene expression levels were observed across all treatment groups in this study, while ARG2 expression remained unchanged. Once ornithine is synthesised, it is decarboxylated via ornithine decarboxylase (ODC) to putrescine. ODC expression is the rate-limiting step and is upregulated by the presence of growth factors, oncogenes, and unbound polyamines which promote proliferation (Pegg

2006). Specifically, ODC activity is crucial for maintaining normal fibroblast morphology and proliferative capacity (Auvinen *et al*. 1992; Moshier *et al*. 1993), and this enzymatic activity is regulated by RAS (Shantz 2004) and $G\alpha_{i/o}$ signalling (Hurta *et al*. 2001), which are signalling pathways induced by the CaSR. ODC activity is negatively regulated by an increase in intracellular polyamine concentration through antizyme (OAZ), which tags ODC for rapid degradation and prevents the further import of polyamines (Casero *et al*. 2018). In this study, TGFβ treatment upregulated OAZ expression while NAM restored baseline expression of both *ODC1* and *OAZ1*, which suggests that in normal fibroblasts TGFβ induces the OAZ feedback mechanism to potentially limit the impact of *de novo* polyamine synthesis by preventing intracellular polyamine accumulation.

In addition to ODC, the next enzyme in the polyamine synthetic pathway, SRM, which converts putrescine to spermidine, is increased in the presence of TGFβ (Chambers *et al*. 2003). At a molecular level, spermidine can facilitate cell growth through the hypusination and activation of the eukaryotic initiation factor (eIF) 5A (Casero *et al*. 2018). Several oncogenes, such as the RAS family, simultaneously increase spermidine synthesis (*via* ODC) and eIF5A expression (Nakanishi and Cleveland 2016). this increase results in an abundance of substrates for deoxyhypusine synthase (DHPS) and deoxyhypusine hydroxylase (DOHH), which form the active hypusinated form of eIF5A, a process completely reliant on the intracellular availability of spermidine (Abbruzzese *et al*. 1986; Wolff *et al*. 1995; Puleston *et al*. 2019). Hypusinated eIF5A interacts with and stabilises the ribosome, preventing translation stalling and facilitating translation elongation and termination required for protein synthesis (Saini *et al*. 2009; Huter *et al*. 2017; Schuller *et al*. 2017; Puleston *et al*. 2019). Furthermore, deletion of DOHH reduced proliferation and a complete loss of hypusine modification in 3T3 fibroblasts (Sievert *et al*. 2014). Since TGFβ induces RAS signalling, the upregulation of spermidine and eIF5A could potentiate hypusine-dependent translation driving protein synthesis required for excessive proliferation or growth (Flynn and Hogarty 2018). The polyamine-eIF5A pathway could also enhance

the energy production, which is essential for highly metabolically active cells since inhibition of DHPS and DOHH reduces the expression of select TCA cycle enzymes and mitochondrial respiration (Puleston *et al*. 2019). In addition to the aforementioned roles, *eIF5A* is a known regulator of the *RhoA* signalling pathway, the amplification of *eIF5A* hypusination facilitated the translation and activation of RhoA, increasing cancer cell motility and invasion *in vitro*, and tumour growth *in vivo* (Muramatsu *et al*. 2016). Taken together, these findings suggest a potential role for the spermidine-eIF5A axis in metabolic activity, proliferation, and migration.

Both spermidine and spermine have been implicated in rodent models of pulmonary hypertension (Olson *et al*. 1985; Atkinson *et al*. 1987). Recently, work by He *et al*. (2020) builds on these findings by showing increased plasma spermine levels in patients with idiopathic PAH compared to controls and that the inhibition of its synthetic enzyme (SMS) attenuates growth factor-mediated PASMC proliferation *in vitro* and remodelling of the pulmonary vasculature and pulmonary hypertension *in vivo*. However, in relation to IPF, two contradictory findings have been published. Metabolomic analysis carried out by Zhao *et al*. (2017) showed increased putrescine and spermidine levels in IPF lung tissue compared to controls, while Baek *et al*. (2020) report opposite findings and show that exogenous spermidine attenuates bleomycin-induced pulmonary fibrosis in mice. This paper also reports cytotoxicity with higher concentrations of spermidine which could be as a result of the ability of spermidine to bind and condense chromatin preventing transcription and translation (Hoet and Nemery 2000), or SMOX-mediated conversion of spermidine to spermine which generates hydrogen peroxide and acrolein, with both processes culminating in cell death (Pegg 2013). Although the metabolomic and transcriptomic data presented in this thesis support the findings by Zhao *et al*. (2017), a study with a larger cohort of IPF patients stratified into disease severity stages using the GAP model could be invaluable in explaining these disparities. In an attempt to explain the findings by Baek *et al*. (2020), it is plausible that exogenous spermidine

prevents intracellular accumulation of bleomycin since both polyamines could be in direct competition for the same transport system (Aouida *et al*. 2010); since exogenous spermidine also prevents the recruitment of inflammatory cells and attenuates inflammation (Minois 2014), its anti-fibrotic role might be more relevant to inflammation-driven PF which is not the underlying mechanism for human IPF. Notably, extracellular spermidine regulates and sensitises ion channels such as the transient receptor potential vanilloid subtype 1 (TRPV1) (Ahern *et al*. 2006), a cough receptor implicated in human IPF whose expression and function are also upregulated in bleomycin-treated guinea pigs (Hope-Gill *et al*. 2003; Guo *et al*. 2019b). The role polyamines play in disease is not fully understood especially within the context of lung fibrosis therefore further work elucidating whether this pathway is protective, deleterious or both is required to establish the therapeutic potential of this pathway.

The polyamine metabolic pathway and polyamine transport system (PTS) have been targeted as potential areas of therapeutic intervention for the treatment of cancer and pathogen-mediated diseases (Abdulhussein and Wallace 2014). Although the exact process of polyamine transport is not fully understood, the general consensus is that this process involves multiple mechanisms, including caveolin- and glypican-mediated endocytosis, vesicular sequestration, and membrane transporters (Belting *et al*. 2003; Soulet *et al*. 2004; Palmer and Wallace 2010; Uemura *et al*. 2010). Of importance here are membrane transporters thought to play a key role in compensating for the changes in intracellular polyamine concentration. Known polyamine transporters include SLC3A2 (Uemura *et al*. 2008) and SLC22A16 (Aouida *et al*. 2010), which mediate export and import, respectively. Although SLC22A16 has been identified as both a high-affinity polyamine and bleomycin-A5 importer (Aouida *et al*. 2010), expression of the SLC22A16 gene was largely undetectable in all the treatment groups. SLC3A2 is a bi-directional polyamine/arginine exchanger mainly responsible for the extrusion of putrescine and acetylated polyamines (Uemura *et al*. 2008; Uemura *et al*. 2010). This transporter also dimerises with SLC7A5, which

extrudes glutamine in exchange for essential amino acids leading to the activation of the mTOR signalling pathway (Nachef *et al*. 2021). Thereby resulting in a feedforward mechanism where mTORC1 upregulates the transcription factor, ATF4, which in turn increases the transcription of SLC3A2, SLC7A5, and glutamine importer, SLC1A5 (Park *et al*. 2017). Interestingly, NAM reduces the expression of the genes implicated in this transport system which indicates a method by which metabolic reprogramming could be attenuated in activated fibroblasts. It is worth noting that of the genes discussed, *SLC7A5* expression remained unaltered in the presence of TGFß. A reason for this might be that high levels of this transporter are still required to restore physiological levels of intracellular glutamine.

Since these transporters are important for metabolic activity and proliferation, previously, it has been shown that their pharmacological inhibition prevents cancer cell growth and survival (Hassanein *et al*. 2015; Hayes *et al*. 2015; Napolitano *et al*. 2017). These findings could have potential implications for other diseases such as SARS-CoV-2. The SARS-CoV-2 virus invades host cells through its spike protein which binds to receptors located on the plasma membrane, such as CD147 (Wang *et al*. 2020). CD147 is a receptor highly expressed by metabolically active cells, which forms a super-complex with SLC3A2. Knockdown experiments show an association between CD147/SLC3A2 ablation and decreased cell proliferation (Xu and Hemler 2005), suggesting a mechanism through which viruses, specifically SARS-CoV-2, could mediate lung fibrosis.

5.5. Limitations and Future directions

The main limitation of this study is that differential gene expression was assessed at the 72-hour timepoint in keeping with the experimental conditions used for the profibrotic studies presented in this thesis. An earlier time point (such as 24 hours used in the Peyser *et al*. study) could have been

used to assess changes in the expression of intracellular signalling genes, which might have occurred earlier, such as those associated with canonical TGFβ1-, AKT-, and cytokine-mediated signalling. That said, it is clear that sustained activation of NHLFs with TGFβ1 for 72 hours alters the expression of several genes which drive fibrosis.

Other future investigations are required to assess the post-translational impact of metabolic reprogramming in TGFβ1-treated NHLFs and the effect NAMs may have on this response. To this end, experimental assays that directly assess cellular glucose and glutamine uptake, glycolytic flux, LDH activity and cellular oxygen consumption could be used to validate the transcriptomic data presented in this chapter. In addition, the efficacy of NAMs in blocking polyamine synthesis, catabolism and transport could also be investigated at the protein level using commercially available polyamine assay kits.

5.6. Conclusion

Amino acids and polyamines are essential for fibroblast growth, proliferation, and survival. They can also activate the metabolic regulator, mTOR, which further enhances oncogenic (RAS) signalling and cell metabolic activity, thus providing activated fibroblasts with a metabolic adaptation that enhances the uptake and the use of nutrients. Manipulating therapies to decrease excessive nutrient uptake, metabolic reprogramming, polyamine biosynthesis and (poly)amine transport in NHLFs could enhance anti-fibrotic effects and lead to new developments in the field.

CHAPTER 6: THESIS CONCLUSIONS AND FUTURE DIRECTIONS

The key findings of the studies presented in this thesis are 1. *in vivo* CaSR expression occurs in the bronchiolar epithelium, proliferated pulmonary NEBs, and interstitium of normal and IPF lungs; 2. increased expression of certain CaSR activators, (poly)amines is seen in the saliva of IPF patients; 3. CaSR is functionally expressed by NHLFs *in vitro*; 4. TGFß1 upregulates the expression of key metabolic reprogramming genes *in vitro,* and the NAM, NPS2143, which blocks CaSR, prevents these changes; 5. NPS2143 prevents the cellular and molecular profibrotic responses to TGFß1 *in vitro*. Together, these results strongly suggest a role for the CaSR in IPF aetiology.

6.1. CaSR is expressed in human lungs, and polyamines that activate the CaSR are upregulated in (I)PF

The strong CaSR expression in the airway epithelium and NEBs might suggest a role of the receptor in continuously monitoring the external microenvironment of the lungs. Continuous stimulation from environmental pollutants and biological agents such as cigarette smoke, urban particulate matter, and viruses, all of which contain a plethora of polycations/polyamines, known to activate the receptor (Yarova *et al*. 2015), could be the initiation point of the fibrotic cascade implicated in IPF. The increased number of NEBs in the lung of IPF patients further supports the potential of this group of cells as a unique stem cell reservoir (Verckist *et al*. 2017; Verckist *et al*. 2018), which could be involved in the repair of damaged airway epithelium. Further work is required to investigate the potential role of CaSR in epithelial cell/NEB proliferation, metaplasia and dysplasia. To investigate this hypothesis, normal and IPF small airway epithelial cells (SAECs) could be treated with CaSR activators such as polyamines (which are produced endogenously and found in viral capsids) (Firpo and Mounce 2020) and positive allosteric modulators of the CaSR (positive control) in the presence and absence of NAMs. I anticipate that if CaSR contributes to epithelial cell hyperplasia, an increase in cellular

proliferation would be observed in the presence of receptor activators and that NAMs would attenuate this response.

Interestingly, NEB hyperplasia or an increased release of NEB-derived GRP have been implicated in (myo)fibroblast proliferation, collagen synthesis and alveolar wall thickening in *in vivo* models of PF (Ashour *et al*. 2006; Sunday 2014; Tighe *et al*. 2019). The working hypothesis is that the sensory ability and neuropeptide release from these highly proliferating NEBs may be amplified in IPF due to significant changes in ECM stiffness and O_2 levels. These changes may further be potentiated by CaSR activation, $[Ca^{2+}]_i$ increase and consequent GRP release, which could worsen the fibrotic process. Further work is required to elucidate the exact mechanisms induced by the CaSR in NEBs and whether they are directly involved in the pathogenesis of IPF.

I also demonstrated that in NHLFs, ornithine and the ornithine-derived polyamine, spermine activate CaSR resulting in $[Ca^{2+}]_i$ mobilisation, the latter shown by previous studies to underpin profibrotic processes in lung fibroblasts and murine models of fibrosis (Mukherjee *et al*. 2015). Interestingly, the same (poly)amines were enriched in the saliva of (I)PF patients compared to controls. Given the need for early diagnosis in IPF, these findings, together with patient preference for non-invasive methods of disease monitoring, provide a rationale to investigate further the potential for these metabolites to act as biomarkers from biofluids (such as saliva) in a larger cohort of IPF patients.

6.2. Effects of NAM on normal human lung fibroblast activation by TGFβ1: Cellular response

In this study, I demonstrated that NHLF exposure to TGFβ1 upregulates CaSR expression and that receptor blockade with NAM attenuates TGFβ1-driven profibrotic responses *in vitro*. These responses (proliferation, collagen secretion, and αSMA expression) occur as a result of TGFβ1-induced intracellular signalling pathways such as Ras/MEK/ERK (Leask 2012), mTOR (Platé *et al*. 2020), and Rho-kinase (Ji *et al*. 2014). Since these pathways are also downstream of CaSR activation (MacLeod *et al*. 2004; Yano *et al*. 2004; Davies *et al*. 2006; Rybchyn *et al*. 2019), NAMs might mediate their anti-fibrotic effects by modulating these molecular signals. However, further work is required to explore the mechanistic link between the CaSR and TGFβ1 and test the involvement of these signalling molecules in HLFs.

Since TGFβ1 increases CaSR expression, this growth factor likely induces a positive feedback response which could potentially exacerbate the disease process. These findings suggest that the CaSR could control mechanisms involved in fibroblast activation, which is central to IPF pathology and that NAMs might interrupt this cycle by limiting TGFβ1-mediated responses. That said, it is important to note that although TGFβ1 is crucial to IPF pathogenesis, other growth factors such as VEGF and PDGF also play a role in this disease (Wollin *et al*. 2015). Therefore, essential work investigating the therapeutic potential of NAMs should be carried out using animal models of the disease or precision-cut human lung slices in which the effects of the NAMs are tested against the current standard of care, *i.e*. pirfenidone and nintedanib.

The role of the CaSR in remodelling is well established in various pulmonary diseases (Maarsingh *et al*. 2011; Grasemann *et al*. 2015; Tang *et al*. 2016; Yarova *et al*. 2016). In a preclinical model of cardiac fibrosis, CaSR-mediated increase in $[Ca^{2+}]_i$ resulted in proliferation, migration and collagen secretion

while pharmacological inhibition of CaSR prevented cellular profibrotic changes and cardiac fibrosis (Zhang *et al*. 2014). Furthermore, deletion of CaSR from SM22α^{+} cells (which includes fibroblasts) also leads to reduced collagen deposition and cardiac remodelling in mice (Schepelmann *et al*. 2016). Since excessive proliferation and ECM deposition are crucial in the establishment of fibrosis, the ability of NAMs to completely abolish the proliferative effects of TGFβ1 and TGFβ1-induced collagen secretion provides another rationale for exploring the potential efficacy of NAMs as anti-fibrotic agents.

6.3. NAM modulates the transcriptome of TGFβ1-treated normal human lung fibroblasts

I have shown that at the transcriptional level, NAM effectively targets at least 5 biosynthetic pathways (glycolysis, serine/glycine synthesis, glutamine metabolism, proline synthesis, and polyamine metabolism), which provide a constant source of macromolecules that replenish the TCA cycle, provide the amino acids (glycine and proline) required for collagen synthesis, and polyamines (spermidine), which play a key role in proliferation. The biological relevance of these findings *in vivo* will have to be identified in future studies; for example, by using radiographically visible glucose or glutamine molecules in mice treated with bleomycin in the presence and absence of NAMs. Another line of inquiry that could be explored in future studies is whether CaSR activation by secreted polyamines could contribute to TGFβ1-induced fibrogenesis, thereby IPF pathogenesis.

Although the focus of this thesis and majority of the studies exploring the alterations in cellular metabolism that occur in (I)PF have been done using fibroblasts, it should be noted that the pathogenesis of lung fibrosis involves other cell types, such as alveolar epithelial cells and macrophages (Wolters et al. 2014; Selman and Pardo 2021). TGFβ1 produced by activated fibroblasts could activate adjacent cells resulting in altered cellular

metabolism, as is the case with TGFβ1-induced αSMA expression in epithelial cells (referred to as epithelial-mesenchymal transition, EMT) (Willis and Borok 2007). Although the role of EMT in IPF is controversial, this process is associated with increased glycolysis, NOX4 production, and fatty acid synthesis (Rock *et al*. 2011; Hua *et al*. 2020). Furthermore, cells infected by viruses associated with IPF show increased glucose and glutamine metabolism (Egan *et al*. 1997; Pulkkinen *et al*. 2012; Sheng *et al*. 2020; Bharadwaj *et al*. 2021), and inhibiting these pathways reduces viral replication and TGFβ expression (Thai *et al*. 2015). More work is required to explore the potential link between virus-mediated epithelial cell injury, metabolic reprogramming, and lung fibrosis and determine whether altered metabolism in the abnormal epithelium overlying the myofibroblasts contributes to fibrosis.

Studies have shown that IPF lungs have increased ^{18}FDG uptake, which correlates with the extent of honeycombing and poorer lung function (Groves *et al*. 2009), disease severity (Justet *et al*. 2017), and increased risk of mortality (Win *et al*. 2018). Future research should focus on validating techniques and approaches that monitor alterations in cellular metabolites and their metabolic pathways, which might aid early diagnosis and provide ways to monitor disease progression and treatment efficacy.

The mechanisms and consequences of metabolic reprogramming are yet to be fully elucidated. Still, it is clear that these metabolic processes underpin several pathological conditions and are currently being explored as therapeutic targets (Bharadwaj *et al*. 2021). Metabolic compensation also needs to be considered when targeting amino acid-associated metabolism and non-metabolic signalling pathways (Muhammad *et al*. 2020). Since cells possess alternative biosynthetic pathways to ensure enhanced demand for macromolecules is met, an effective therapeutic agent should target multiple metabolic pathways simultaneously (e.g. glycolysis and

glutaminolysis which can both act as sources of energy and amino acids in metabolically active cells).

6.4. Future directions

6.4.1. Future ex vivo experiments to explore non-invasive biomarkers in IPF

Building on the preliminary data presented in my thesis, metabolites from non-invasive biofluids (saliva/urine) in a larger cohort of IPF patients could be analysed using FIE-HRMS. Metabolite concentration, demographic and clinical data could be used to identify biomarkers and develop optimal regression models for the diagnosis and prognosis of IPF. This methodology is currently being used for diseases with poor prognoses, such as lung cancer (Ruiying *et al*. 2020), oral squamous cell cancer (Yang *et al*. 2020) and COVID-19 (López-Hernández *et al*. 2021). The study would aim to use untargeted and targeted metabolomics to 1. distinguish age-matched IPF patients from healthy controls; 2. determine whether patients can be stratified based on disease severity; 3. identify a panel of metabolites with IPF-specific sensitivity and specificity that can be developed into an immuno-based assay to aid early disease detection.

6.4.2. Future *in vitro* experiments to elucidate the role of the CaSR in small airway epithelial cells and IPF fibroblasts

Aim 1: To determine the role of the CaSR and its therapeutic potential in IPF, commercially sourced IPF HLFs patients will be cultured and analysed for profibrotic processes such as proliferation, SASP expression and ECM protein expression in the presence/absence of TGFβ1, spermine and NAM. The efficacy of NAM in altering these readouts will be compared to one of the currently approved drugs, pirfenidone. The signalling pathways (mTOR and Ras/MEK/ERK) indicated in my thesis will be validated with phosphorylation studies and Western blotting in healthy and IPF fibroblasts.

Aim 2: To determine whether exposure of SAECs to viral particles and/or particulate matter induces the release of profibrotic cytokines and polyamines and the ability of NAM to reverse the effects of these stimuli *in vitro*.

Studies have shown that urban particulate matter (UPM) activates the CaSR (Mansfield *et al*. 2019) and that exposure of AECs to PM2.5 resulted in TGFβ1 activation and cell contractility (Dysart *et al*. 2014). These findings, coupled with the data presented in my thesis, provide a rationale to determine the role of the CaSR in epithelial cell injury. Commercially sourced SAECs will be stimulated with PM2.5 or herpes simplex virus 1 as previously described (Dysart *et al*. 2014; Shivkumar *et al*. 2016). The effects of these stimuli on profibrotic cytokine expression (TGFβ1, IL-1β and IL-8) will be determined in the presence/absence of NAM.

6.4.3. Future *in vivo* experiments to elucidate the role of the CaSR in bleomycin-induced PF

Although no animal model fully recapitulates the hallmarks of IPF, they provide tools to investigate the complex interplay between various cells involved in IPF pathophysiology (Moore *et al*. 2013). The bleomycin model is the most widely used model of experimental (I)PF, although it is an imperfect model of progressive pulmonary fibrosis since it does not result in UIP histology (Carrington *et al*. 2018). This proposed study would aim to deliver an intratracheal dose of bleomycin to assess whether treatment with NAMs would attenuate murine lung fibrosis. NAM dosage would be optimised, and its therapeutic effects would be compared to the current standard of care, pirfenidone and nintedanib. The effects of exposure to inhaled NAM in control and bleomycin-exposed animals would be determined by assessing levels of inflammatory and profibrotic cytokines in bronchoalveolar fluid (BALF), inflammatory cell infiltration in BALF and lung tissue, lung function

and parenchymal remodelling, as previously described (Oku *et al*. 2008; Schaefer *et al*. 2011; Yarova *et al*. 2015; Yarova *et al*. 2016).

6.5. Closing remarks

Some pathological aspects of IPF pathology, such as epigenetics and autophagy, were not investigated in this project due to time constraints. However, the work presented in this thesis provides a strong rationale to further investigate the role of the CaSR in IPF. Figure 6.1 builds on my findings, suggesting avenues for further research and potential mechanisms through which NAMs could attenuate lung fibrosis by targeting several cellular mediators upstream of the fibrotic process. Thus, NAMs could potentially confer a unique mechanistic advantage over existing approved medications improving patient outcomes and quality of life.

6.6. Graphical summary

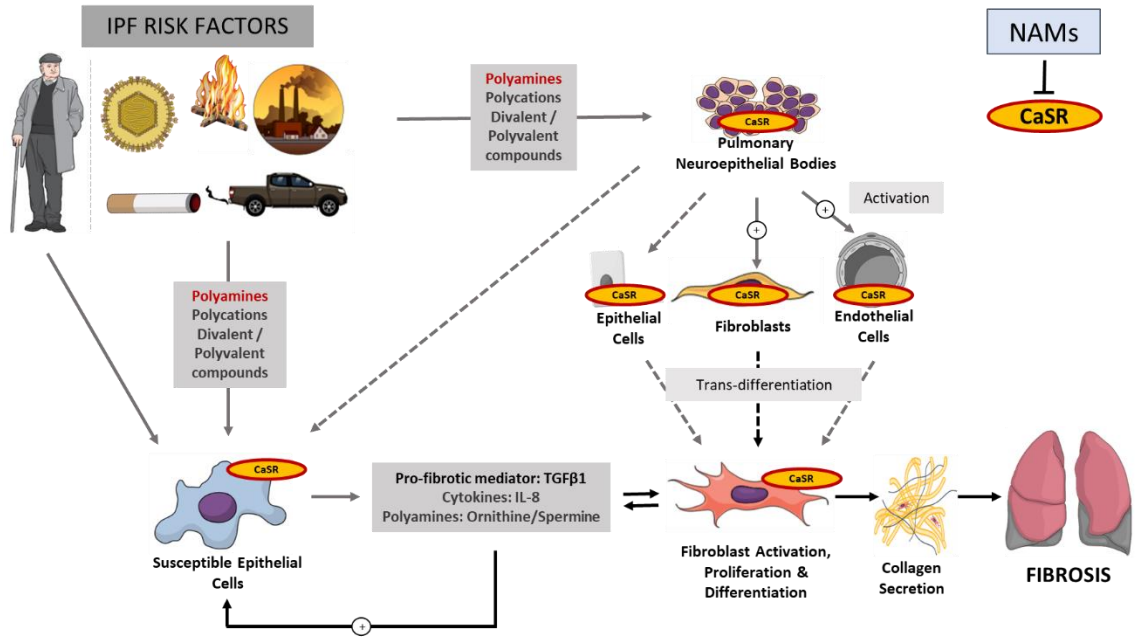

Figure 6.1 Schematic diagram illustrating the potential role of the calcium-sensing receptor (CaSR) in the IPF pathogenesis. Environmental triggers (*e.g.*, urban particulate matter, cigarette smoke, viral particles) contain polycations which are known CaSR activators, as are the polyamines associated with the arginase pathway. These polycations and polyamines can activate the CaSR in the bronchiolar/alveolar epithelium and neuroepithelial bodies (NEBs), leading to release of profibrotic factors. The most researched (I)PF-related cytokine, TGFß1, drives fibroblast activation, proliferation, and differentiation into (myo)fibroblasts resulting in excessive ECM deposition. Furthermore, fibroblasts also secrete cytokines which can facilitate a positive feedback loop resulting in epithelial cell activation thereby exacerbating the fibrotic process. NEBs act as a potential stem-cell niche for epithelial cells and release profibrotic neuropeptides *e.g.*, gastrin-releasing peptide (GRP) which activate fibroblasts and endothelial cells. These CaSR-expressing cells are also cellular mediators of common IPF comorbidities, pulmonary arterial hypertension, and emphysema. Senescent cell accumulation and increased TGFß1 expression are key hallmarks of ageing that increase susceptibility of epithelial cells to injury thereby reinforcing the fibrotic pathway.

REFERENCES

Abbruzzese, A., Park, M.H. and Folk, J.E. 1986. Deoxyhypusine hydroxylase from rat testis. Partial purification and characterization. *Journal of Biological Chemistry* 261(7), pp. 3085–3089. doi: 10.1016/s0021-9258(17)35750-2.

Abdulhussein, A.A. and Wallace, H.M. 2014. Polyamines and membrane transporters. *Amino Acids* 46(3), pp. 655–660. doi: 10.1007/s00726-013-1553-6.

Abreu, J.G., Ketpura, N.I., Reversade, B. and De Robertis, E.M. 2002. Connective-tissue growth factor (ctgf) modulates cell signalling by bmp and TGF-ß. *Nature Cell Biology* 4(8), pp. 599–604. doi: 10.1038/ncb826.

Ackers, I. and Malgor, R. 2017. Interrelationship of canonical and non-canonical Wnt signalling pathways in chronic metabolic diseases: *https://doi.org/10.1177/1479164117738442* 15(1), pp. 3–13. doi: 10.1177/1479164117738442.

Acosta, J.C. et al. 2013. A complex secretory program orchestrated by the inflammasome controls paracrine senescence. *Nature Cell Biology* 15(8), pp. 978–990. doi: 10.1038/ncb2784.

Adams, T.S. et al. 2020. Single-cell RNA-seq reveals ectopic and aberrant lung-resident cell populations in idiopathic pulmonary fibrosis. *Science Advances* 6(28), p. eaba1983. doi: 10.1126/sciadv.aba1983.

Adegunsoye, A. et al. 2019. Computed tomography honeycombing identifies a progressive fibrotic phenotype with increased mortality across diverse interstitial lung diseases. *Annals of the American Thoracic Society* 16(5), pp. 580–588. doi: 10.1513/AnnalsATS.201807-443OC.

Adriaensen, D., Brouns, I., Van Genechten, J. and Timmermans, J.-P. 2003. Functional morphology of pulmonary neuroepithelial bodies: Extremely complex airway receptors. *The Anatomical Record* 270A(1), pp. 25–40. doi: 10.1002/ar.a.10007.

Ahern, G.P., Wang, X. and Miyares, R.L. 2006. Polyamines are potent ligands for the capsaicin receptor TRPV1. *Journal of Biological Chemistry* 281(13), pp. 8991–8995. doi: 10.1074/jbc.M513429200.

Ahmed, M.S. et al. 2004. Connective tissue growth factor--a novel mediator of angiotensin II-stimulated cardiac fibroblast activation in heart failure in rats. *Journal of molecular and cellular cardiology* 36(3), pp. 393–404. doi: 10.1016/J.YJMCC.2003.12.004.

Akamatsu, T. et al. 2013. Direct isolation of myofibroblasts and fibroblasts from bleomycin-injured lungs reveals their functional similarities and differences. *Fibrogenesis and Tissue Repair* 6(1), p. 15. doi: 10.1186/1755-1536-6-15.

Akhurst, R.J. and Hata, A. 2012. Targeting the TGFß signalling pathway in disease. *Nature Reviews Drug Discovery* 11(10), pp. 790–811. doi: 10.1038/nrd3810.

Allen, J.T., Knight, R.A., Bloor, C.A. and Spiteri, M.A. 1999. Enhanced insulin-like growth factor binding protein-related protein 2 (connective tissue growth

factor) expression in patients with idiopathic pulmonary fibrosis and pulmonary sarcoidosis. *American Journal of Respiratory Cell and Molecular Biology* 21(6), pp. 693–700. doi: 10.1165/ajrcmb.21.6.3719.

Altman, B.J., Stine, Z.E. and Dang, C. V. 2016. From Krebs to clinic: Glutamine metabolism to cancer therapy. *Nature Reviews Cancer* 16(10), pp. 619–634. doi: 10.1038/nrc.2016.71.

Amelio, I., Cutruzzolá, F., Antonov, A., Agostini, M. and Melino, G. 2014. Serine and glycine metabolism in cancer. *Trends in Biochemical Sciences* 39(4), pp. 191–198. doi: 10.1016/j.tibs.2014.02.004.

Andersen, S., Nielsen-Kudsk, J.E., Vonk Noordegraaf, A. and De Man, F.S. 2019. Right Ventricular Fibrosis. *Circulation* 139(2), pp. 269–285. doi: 10.1161/CIRCULATIONAHA.118.035326.

Andrews, S. 2010. Babraham Bioinformatics - FastQC A Quality Control tool for High Throughput Sequence Data. Available at: https://www.bioinformatics.babraham.ac.uk/projects/fastqc/ [Accessed: 2 November 2021].

Annunen, P., Autio-Harmainen, H. and Kivirikko, K.I. 1998. The novel type II prolyl 4-hydroxylase is the main enzyme form in chondrocytes and capillary endothelial cells, whereas the type I enzyme predominates in most cells. *Journal of Biological Chemistry* 273(11), pp. 5989–5992. doi: 10.1074/jbc.273.11.5989.

Aouida, M., Poulin, R. and Ramotar, D. 2010. The Human Carnitine Transporter SLC22A16 Mediates High Affinity Uptake of the Anticancer Polyamine Analogue Bleomycin-A5 * □ S. doi: 10.1074/jbc.M109.046151.

Aoyagi-Ikeda, K. et al. 2012. Notch Induces Myofibroblast Differentiation of Alveolar Epithelial Cells via Transforming Growth Factor-β-Smad3 Pathway. *https://doi.org/10.1165/rcmb.2009-0140OC* 45(1), pp. 136–144. doi: 10.1165/RCMB.2009-0140OC.

Ardehali, H. et al. 2012. Targeting myocardial substrate metabolism in heart failure: Potential for new therapies. *European Journal of Heart Failure* 14(2), pp. 120–129. doi: 10.1093/eurjhf/hfr173.

Vander Ark, A., Cao, J. and Li, X. 2018. TGF-β receptors: In and beyond TGF-β signaling. *Cellular Signalling* 52, pp. 112–120. doi: 10.1016/j.cellsig.2018.09.002.

Arruabarrena-Aristorena, A., Zabala-Letona, A. and Carracedo, A. 2018. Oil for the cancer engine: The cross-talk between oncogenic signaling and polyamine metabolism. *Science Advances* 4(1), p. eaar2606. doi: 10.1126/sciadv.aar2606.

Ashour, K., Shan, L., Lee, J.H., Schlicher, W., Wada, K., Wada, E. and Sunday, M.E. 2006. Bombesin Inhibits Alveolarization and Promotes Pulmonary Fibrosis in Newborn Mice. *American Journal of Respiratory and Critical Care Medicine* 173(12), pp. 1377–1385. doi: 10.1164/rccm.200507-1014OC.

Ask, K. et al. 2008. Progressive pulmonary fibrosis is mediated by TGF-β isoform 1 but not TGF-β3. *International Journal of Biochemistry and Cell Biology* 40(3),

pp. 484–495. doi: 10.1016/j.biocel.2007.08.016.

Atanasova, K.R. and Reznikov, L.R. 2018. Neuropeptides in asthma, chronic obstructive pulmonary disease and cystic fibrosis. *Respiratory research* 19(1). doi: 10.1186/S12931-018-0846-4.

Atkinson, J.E., Olson, J.W., Altiere, R.J. and Gillespie, M.N. 1987. Evidence that hypoxic pulmonary vascular remodeling in rats is polyamine dependent. *Journal of Applied Physiology* 62(4), pp. 1562–1568. doi: 10.1152/jappl.1987.62.4.1562.

Auvinen, M., Paasinen, A., Andersson, L.C. and Hölttä, E. 1992. Ornithine decarboxylase activity is critical for cell transformation. *Nature* 360(6402), pp. 355–358. doi: 10.1038/360355a0.

Auyeung, V.C. and Sheppard, D. 2021. Stuck in a Moment: Does Abnormal Persistence of Epithelial Progenitors Drive Pulmonary Fibrosis? *American journal of respiratory and critical care medicine* 203(6), pp. 667–669. doi: 10.1164/RCCM.202010-3898ED.

Baarsma, H.A. et al. 2011. Activation of WNT/ β-catenin signaling in pulmonary fibroblasts by TGF-β 1 is increased in chronic obstructive pulmonary disease. *PLoS ONE* 6(9). doi: 10.1371/journal.pone.0025450.

Baarsma, H.A. and Königshoff, M. 2017. 'WNT-er is coming': WNT signalling in chronic lung diseases State of the art review. *Thorax* 72, pp. 746–759. doi: 10.1136/thoraxjnl-2016-209753.

Babbar, N. and Gerner, E.W. 2011. Targeting polyamines and inflammation for cancer prevention. *Recent Results in Cancer Research* 188, pp. 49–64. doi: 10.1007/978-3-642-10858-7_4.

Baek, A.R., Hong, J., Song, K.S., Jang, A.S., Kim, D.J., Chin, S.S. and Park, S.W. 2020. Spermidine attenuates bleomycin-induced lung fibrosis by inducing autophagy and inhibiting endoplasmic reticulum stress (ERS)-induced cell death in mice. *Experimental and Molecular Medicine* 52(12), pp. 2034–2045. doi: 10.1038/s12276-020-00545-z.

Bagur, R. and Rgy Hajnó Czky, G. 2017. Molecular Cell Review Intracellular Ca 2+ Sensing: Its Role in Calcium Homeostasis and Signaling. *Molecular Cell* 66, pp. 780–788. doi: 10.1016/j.molcel.2017.05.028.

Bai, M., Trivedi, S. and Brown, E.M. 1998. Dimerization of the extracellular calcium-sensing receptor (CaR) on the cell surface of CaR-transfected HEK293 cells. *The Journal of biological chemistry* 273(36), pp. 23605–23610. doi: 10.1074/JBC.273.36.23605.

Bai, Y., Xiao, Y., Dai, Y., Chen, X., Li, D., Tan, X. and Zhang, X. 2017. Stanniocalcin 1 promotes cell proliferation via cyclin E1/cyclin-dependent kinase 2 in human prostate carcinoma. *Oncology Reports* 37(4), pp. 2465–2471. doi: 10.3892/or.2017.5501.

Balestro, E. et al. 2016. Immune Inflammation and Disease Progression in Idiopathic Pulmonary Fibrosis. *PloS one* 11(5), p. e0154516. doi: 10.1371/journal.pone.0154516.

Baptista, R., Fazakerley, D.M., Beckmann, M., Baillie, L. and Mur, L.A.J. 2018. Untargeted metabolomics reveals a new mode of action of pretomanid (PA-824). *Scientific reports* 8(1), p. 5084. doi: 10.1038/s41598-018-23110-1.

Bartkova, J., Zemanova, M. and Bartek, J. 1996. Expression of CDK7/CAK in normal and tumour cells of diverse histogenesis, cell-cycle position and differentiation. *International Journal of Cancer* 66(6), pp. 732–737. doi: 10.1002/(SICI)1097-0215(19960611)66:6<732::AID-IJC4>3.0.CO;2-0.

Behr, J. et al. 2020. Survival and course of lung function in the presence or absence of antifibrotic treatment in patients with idiopathic pulmonary fibrosis: long-term results of the INSIGHTS-IPF registry. *The European respiratory journal* 56(2). doi: 10.1183/13993003.02279-2019.

Belkin, A. and Swigris, J.J. 2013. Health-related quality of life in idiopathic pulmonary fibrosis: where are we now? *Current opinion in pulmonary medicine* 19(5), pp. 474–479. doi: 10.1097/MCP.0B013E328363F479.

Belting, M. et al. 2003. Glypican-1 is a vehicle for polyamine uptake in mammalian cells: A pivotal role for nitrosothiol-derived nitric oxide. *Journal of Biological Chemistry* 278(47), pp. 47181–47189. doi: 10.1074/jbc.M308325200.

Bergeron, S. et al. 2010. The serine protease inhibitor serpinE2 is a novel target of ERK signaling involved in human colorectal tumorigenesis. *Molecular Cancer* 9(1), pp. 1–15. doi: 10.1186/1476-4598-9-271.

Bernard, K. et al. 2015. Metabolic Reprogramming Is Required for Myofibroblast Contractility and Differentiation. *The Journal of Biological Chemistry* 290(42), p. 25427. doi: 10.1074/JBC.M115.646984.

Bernard, K., Logsdon, N.J., Benavides, G.A., Sanders, Y., Zhang, J., Darley-Usmar, V.M. and Thannickal, V.J. 2018. Glutaminolysis is required for transforming growth factor-β1–induced myofibroblast differentiation and activation. *Journal of Biological Chemistry* 293(4), pp. 1218–1228. doi: 10.1074/jbc.ra117.000444.

Bharadwaj, S., Singh, M., Kirtipal, N. and Kang, S.G. 2021. SARS-CoV-2 and Glutamine: SARS-CoV-2 Triggered Pathogenesis via Metabolic Reprograming of Glutamine in Host Cells. *Frontiers in Molecular Biosciences* 7. doi: 10.3389/fmolb.2020.627842.

Bhutia, Y.D. and Ganapathy, V. 2016. Glutamine transporters in mammalian cells and their functions in physiology and cancer. *Biochimica et Biophysica Acta - Molecular Cell Research* 1863(10), pp. 2531–2539. doi: 10.1016/j.bbamcr.2015.12.017.

Biernacka, A., Dobaczewski, M. and Frangogiannis, N.G. 2011. TGF-β signaling in fibrosis. *Growth factors (Chur, Switzerland)* 29(5), pp. 196–202. doi: 10.3109/08977194.2011.595714.

BLF 2016. Idiopathic pulmonary fibrosis statistics | British Lung Foundation. Available at: https://www.blf.org.uk/support-for-you/idiopathic-pulmonary-fibrosis-ipf/statistics [Accessed: 6 March 2018].

Blokland, K.E.C. et al. 2020. Senescence of IPF Lung Fibroblasts Disrupt Alveolar

Epithelial Cell Proliferation and Promote Migration in Wound Healing. *Pharmaceutics* 12(4), p. 389. doi: 10.3390/PHARMACEUTICS12040389.

Bockaert, J. and Pin, J.P. 1999. Molecular tinkering of G protein-coupled receptors: an evolutionary success. *The EMBO Journal* 18(7), p. 1723. doi: 10.1093/EMBOJ/18.7.1723.

Bolger, A.M., Lohse, M. and Usadel, B. 2014. Trimmomatic: a flexible trimmer for Illumina sequence data. *Bioinformatics (Oxford, England)* 30(15), pp. 2114–2120. doi: 10.1093/BIOINFORMATICS/BTU170.

Boon, K. et al. 2009. Molecular Phenotypes Distinguish Patients with Relatively Stable from Progressive Idiopathic Pulmonary Fibrosis (IPF). Eickelberg, O. ed. *PLoS ONE* 4(4), p. e5134. doi: 10.1371/journal.pone.0005134.

Boorsma, C.E., Dekkers, B.G.J., van Dijk, E.M., Kumawat, K., Richardson, J., Burgess, J.K. and John, A.E. 2014. Beyond TGFß – Novel ways to target airway and parenchymal fibrosis. *Pulmonary Pharmacology & Therapeutics* 29(2), pp. 166–180. doi: 10.1016/J.PUPT.2014.08.009.

Bowdish, D.M.E. 2019. The Aging Lung: Is Lung Health Good Health for Older Adults? *CHEST* 155(2), pp. 391–400. doi: 10.1016/J.CHEST.2018.09.003.

Bozyk, P.D. and Moore, B.B. 2011. Prostaglandin E2 and the pathogenesis of pulmonary fibrosis. *American journal of respiratory cell and molecular biology* 45(3), pp. 445–452. doi: 10.1165/RCMB.2011-0025RT.

Braicu, C. et al. 2019. A Comprehensive Review on MAPK: A Promising Therapeutic Target in Cancer. *Cancers* 11(10), p. 1618. doi: 10.3390/CANCERS11101618.

Breitwieser, G.E. 2006. Calcium Sensing Receptors and Calcium Oscillations: Calcium as a First Messenger. *Current Topics in Developmental Biology* 73, pp. 85–114. doi: 10.1016/S0070-2153(05)73003-9.

Breitwieser, G.E. 2013. The calcium sensing receptor life cycle: trafficking, cell surface expression, and degradation. *Best practice & research. Clinical endocrinology & metabolism* 27(3), pp. 303–313. doi: 10.1016/J.BEEM.2013.03.003.

Brennan, S. and Conigrave, A. 2009. Regulation of Cellular Signal Transduction Pathways by the Extracellular Calcium-Sensing Receptor. *Current Pharmaceutical Biotechnology* 10(3), pp. 270–281. doi: 10.2174/138920109787847484.

Brennan, S.C. et al. 2013. Calcium sensing receptor signalling in physiology and cancer. *Biochimica et Biophysica Acta (BBA) - Molecular Cell Research* 1833(7), pp. 1732–1744. doi: 10.1016/j.bbamcr.2012.12.011.

Brennan, S.C. et al. 2016. The extracellular calcium-sensing receptor regulates human fetal lung development via CFTR. *Scientific Reports* 6(1), p. 21975. doi: 10.1038/srep21975.

Bringardner, B.D., Baran, C.P., Eubank, T.D. and Marsh, C.B. 2008. The role of inflammation in the pathogenesis of idiopathic pulmonary fibrosis. *Antioxidants*

and Redox Signaling 10(2), pp. 287–301. doi: 10.1089/ars.2007.1897.

Brouns, I., Verckist, L., Pintelon, I., Timmermans, J.P. and Adriaensen, D. 2021. The Pulmonary NEB ME Is a Complex Intraepithelial Unit. In: *Advances in Anatomy Embryology and Cell Biology*. Springer Science and Business Media Deutschland GmbH, pp. 7–18. doi: 10.1007/978-3-030-65817-5_2.

Brown, E.M. et al. 1993. Cloning and characterization of an extracellular Ca2+-sensing receptor from bovine parathyroid. *Nature* 366(6455), pp. 575–580. doi: 10.1038/366575a0.

Brown, E.M. 1997. Mutations in the Calcium-Sensing Receptor and Their Clinical Implications. *Hormone Research in Paediatrics* 48(5), pp. 199–208. doi: 10.1159/000185516.

Brown, E.M. and MacLeod, R.J. 2001. Extracellular Calcium Sensing and Extracellular Calcium Signaling. *Physiological Reviews* 81(1), pp. 239–297. doi: 10.1152/physrev.2001.81.1.239.

Buendía-Roldán, I., Mejía, M., Navarro, C. and Selman, M. 2017. Idiopathic pulmonary fibrosis: Clinical behavior and aging associated comorbidities. *Respiratory medicine* 129, pp. 46–52. doi: 10.1016/J.RMED.2017.06.001.

Cabrera, S., Selman, M., Lonzano-Bolaños, A., Konishi, K., Richards, T.J., Kaminski, N. and Pardo, A. 2013. Gene expression profiles reveal molecular mechanisms involved in the progression and resolution of bleomycin-induced lung fibrosis. *American Journal of Physiology - Lung Cellular and Molecular Physiology* 304(9), p. L593. doi: 10.1152/ajplung.00320.2012.

Campisi, J. 2016. Cellular senescence and lung function during aging: Yin and Yang. In: *Annals of the American Thoracic Society*. American Thoracic Society, pp. S402–S406. doi: 10.1513/AnnalsATS.201609-703AW.

Campisi, J. and D'Adda Di Fagagna, F. 2007. Cellular senescence: When bad things happen to good cells. *Nature Reviews Molecular Cell Biology* 8(9), pp. 729–740. doi: 10.1038/nrm2233.

Carrington, R., Jordan, S., Pitchford, S.C. and Page, C.P. 2018. Use of animal models in IPF research. *Pulmonary Pharmacology & Therapeutics* 51, pp. 73–78. doi: 10.1016/J.PUPT.2018.07.002.

Casero, R.A., Murray Stewart, T. and Pegg, A.E. 2018. Polyamine metabolism and cancer: treatments, challenges and opportunities. *Nature Reviews Cancer* 18(11), pp. 681–695. doi: 10.1038/s41568-018-0050-3.

Chambers, R.C., Leoni, P., Kaminski, N., Laurent, G.J. and Heller, R.A. 2003. Global Expression Profiling of Fibroblast Responses to Transforming Growth Factor-β1 Reveals the Induction of Inhibitor of Differentiation-1 and Provides Evidence of Smooth Muscle Cell Phenotypic Switching. *The American Journal of Pathology* 162(2), p. 533. doi: 10.1016/S0002-9440(10)63847-3.

Chanda, D., Otoupalova, E., Smith, S.R., Volckaert, T., De Langhe, S.P. and Thannickal, V.J. 2019. Developmental pathways in the pathogenesis of lung fibrosis. *Molecular Aspects of Medicine* 65, pp. 56–69. doi: 10.1016/J.MAM.2018.08.004.

Chang, W., Pratt, S., Chen, T.H., Nemeth, E., Huang, Z. and Shoback, D. 1998. Coupling of calcium receptors to inositol phosphate and cyclic AMP generation in mammalian cells and Xenopus laevis oocytes and immunodetection of receptor protein by region-specific antipeptide antisera. *Journal of bone and mineral research : the official journal of the American Society for Bone and Mineral Research* 13(4), pp. 570–580. doi: 10.1359/JBMR.1998.13.4.570.

Chen, H. et al. 2020a. TGF-β1/IL-11/MEK/ERK signaling mediates senescence-associated pulmonary fibrosis in a stress-induced premature senescence model of Bmi-1 deficiency. *Experimental and Molecular Medicine* 52(1), pp. 130–151. doi: 10.1038/s12276-019-0371-7.

Chen, X. et al. 2016. Inhibition of Wnt/β-catenin signaling suppresses bleomycin-induced pulmonary fibrosis by attenuating the expression of TGF-β1 and FGF-2. *Experimental and Molecular Pathology* 101(1), pp. 22–30. doi: 10.1016/j.yexmp.2016.04.003.

Chen, X. et al. 2020b. Epithelial cell senescence induces pulmonary fibrosis through Nanog-mediated fibroblast activation. *Aging (Albany NY)* 12(1), p. 242. doi: 10.18632/AGING.102613.

Chi, J. et al. 2018. Activation of calcium-sensing receptor-mediated autophagy in angiotensinII-induced cardiac fibrosis in vitro. *Biochemical and biophysical research communications* 497(2), pp. 571–576. doi: 10.1016/J.BBRC.2018.02.098.

Chiang, C.P., Lang, M.J., Liu, B.Y., Wang, J.T., Leu, J.S., Hahn, L.J. and Kuo, M.Y.P. 2000. Expression of proliferating cell nuclear antigen (PCNA) in oral submucous fibrosis, oral epithelial hyperkeratosis and oral epithelial dysplasia in Taiwan. *Oral Oncology* 36(4), pp. 353–359. doi: 10.1016/S1368-8375(00)00014-2.

Chilosi, M. et al. 2003. Aberrant Wnt/β-catenin pathway activation in idiopathic pulmonary fibrosis. *American Journal of Pathology* 162(5), pp. 1495–1502. doi: 10.1016/S0002-9440(10)64282-4.

Christopoulos, A. 2014. Advances in G protein-coupled receptor allostery: from function to structure. *Molecular pharmacology* 86(5), pp. 463–478. doi: 10.1124/MOL.114.094342.

Codo, A.C. et al. 2020. Elevated Glucose Levels Favor SARS-CoV-2 Infection and Monocyte Response through a HIF-1α/Glycolysis-Dependent Axis. *Cell Metabolism* 32(3), pp. 437-446.e5. doi: 10.1016/j.cmet.2020.07.007.

Coker, R.K., Laurent, G.J., Shahzeidi, S., Lympany, P.A., Du Bois, R.M., Jeffery, P.K. and McAnulty, R.J. 1997. Transforming growth factors-beta 1, -beta 2, and -beta 3 stimulate fibroblast procollagen production in vitro but are differentially expressed during bleomycin-induced lung fibrosis. *The American Journal of Pathology* 150(3), p. 981.

Collard, H.R. et al. 2016. Acute exacerbation of idiopathic pulmonary fibrosis an international working group report. *American Journal of Respiratory and Critical Care Medicine* 194(3), pp. 265–275. doi: 10.1164/rccm.201604-0801CI.

Conigrave, A.D. and Hampson, D.R. 2010. Broad-spectrum amino acid-sensing

class C G-protein coupled receptors: Molecular mechanisms, physiological significance and options for drug development. *Pharmacology and Therapeutics* 127(3), pp. 252–260. doi: 10.1016/j.pharmthera.2010.04.007.

Conigrave, A.D. and Ward, D.T. 2013. Calcium-sensing receptor (CaSR): Pharmacological properties and signaling pathways. In: *Best Practice and Research: Clinical Endocrinology and Metabolism*. Bailliere Tindall Ltd, pp. 315–331. doi: 10.1016/j.beem.2013.05.010.

Connelly, M., Boland, D., Graf, E., Tissot, C. and Padmanaban, A. 2016. Performance of the RNA and the High Sensitivity RNA ScreenTape Assay for the Agilent 4200 TapeStation System. *Agilent Technologies* , pp. 1–8.

Conte, E., Gili, E., Fagone, E., Fruciano, M., Iemmolo, M. and Vancheri, C. 2014. Effect of pirfenidone on proliferation, TGF-ß-induced myofibroblast differentiation and fibrogenic activity of primary human lung fibroblasts. *European Journal of Pharmaceutical Sciences* 58, pp. 13–19. doi: 10.1016/J.EJPS.2014.02.014.

Costanza, B., Umelo, I., Bellier, J., Castronovo, V. and Turtoi, A. 2017. Stromal Modulators of TGF-ß in Cancer. *Journal of Clinical Medicine* 6(1), p. 7. doi: 10.3390/jcm6010007.

Couluris, M., Kinder, B.W., Xu, P., Gross-King, M., Krischer, J. and Panos, R.J. 2012. Treatment of idiopathic pulmonary fibrosis with losartan: a pilot project. *Lung* 190(5), pp. 523–527. doi: 10.1007/S00408-012-9410-Z.

Cutz, E. and Jackson, A. 1999. Neuroepithelial bodies as airway oxygen sensors. *Respiration Physiology* 115(2), pp. 201–214. doi: 10.1016/S0034-5687(99)00018-3.

Davey, A.E., Leach, K., Valant, C., Conigrave, A.D., Sexton, P.M. and Christopoulos, A. 2012. Positive and negative allosteric modulators promote biased signaling at the calcium-sensing receptor. *Endocrinology* 153(3), pp. 1232–1241. doi: 10.1210/EN.2011-1426.

Davidson, G. and Niehrs, C. 2010. Emerging links between CDK cell cycle regulators and Wnt signaling. *Trends in Cell Biology* 20(8), pp. 453–460. doi: 10.1016/j.tcb.2010.05.002.

Davies, S.L., Gibbons, C.E., Vizard, T. and Ward, D.T. 2006. Ca^{2+} -sensing receptor induces Rho kinase-mediated actin stress fiber assembly and altered cell morphology, but not in response to aromatic amino acids. *American Journal of Physiology-Cell Physiology* 290(6), pp. C1543–C1551. doi: 10.1152/ajpcell.00482.2005.

Davis, J.D. and Wypych, T.P. 2021. Cellular and functional heterogeneity of the airway epithelium. *Mucosal Immunology 2021 14:5* 14(5), pp. 978–990. doi: 10.1038/s41385-020-00370-7.

DeBerardinis, R.J., Lum, J.J., Hatzivassiliou, G. and Thompson, C.B. 2008. The Biology of Cancer: Metabolic Reprogramming Fuels Cell Growth and Proliferation. *Cell Metabolism* 7(1), pp. 11–20. doi: 10.1016/j.cmet.2007.10.002.

DeBerardinis, R.J., Mancuso, A., Daikhin, E., Nissim, I., Yudkoff, M., Wehrli, S. and Thompson, C.B. 2007. Beyond aerobic glycolysis: Transformed cells can engage in glutamine metabolism that exceeds the requirement for protein and nucleotide synthesis. *Proceedings of the National Academy of Sciences of the United States of America* 104(49), pp. 19345–19350. doi: 10.1073/pnas.0709747104.

Deberardinis, R.J. and Thompson, C.B. 2012. Cellular metabolism and disease: What do metabolic outliers teach us? *Cell* 148(6), pp. 1132–1144. doi: 10.1016/j.cell.2012.02.032.

Demopoulos, K., Arvanitis, D.A., Vassilakis, D.A., Siafakas, N.M. and Spandidos, D.A. 2002. MYCL1, FHIT, SPARC, p16(INK4) and TP53 genes associated to lung cancer in idiopathic pulmonary fibrosis. *Journal of cellular and molecular medicine* 6(2), pp. 215–222. doi: 10.1111/J.1582-4934.2002.TB00188.X.

Dieterle, F., Ross, A., Schlotterbeck, G. and Senn, H. 2006. Probabilistic Quotient Normalization as Robust Method to Account for Dilution of Complex Biological Mixtures. Application in 1H NMR Metabonomics. *Analytical Chemistry* 78(13), pp. 4281–4290. doi: 10.1021/AC051632C.

Dobin, A. et al. 2013. STAR: ultrafast universal RNA-seq aligner. *Bioinformatics (Oxford, England)* 29(1), pp. 15–21. doi: 10.1093/BIOINFORMATICS/BTS635.

Dowling, R.J.O., Pollak, M. and Sonenberg, N. 2009. Current status and challenges associated with targeting mTOR for cancer therapy. *BioDrugs* 23(2), pp. 77–91. doi: 10.2165/00063030-200923020-00002.

Duffield, J.S., Lupher, M., Thannickal, V.J. and Wynn, T.A. 2013. Host responses in tissue repair and fibrosis. *Annual Review of Pathology: Mechanisms of Disease* 8, pp. 241–276. doi: 10.1146/annurev-pathol-020712-163930.

Durante, W., Liao, L., Reyna, S. V., Peyton, K.J. and Schafer, A.I. 2001. Transforming growth factor-β1 stimulates L-arginine transport and metabolism in vascular smooth muscle cells: Role in polyamine and collagen synthesis. *Circulation* 103(8), pp. 1121–1127. doi: 10.1161/01.CIR.103.8.1121.

DY, Z. et al. 2013. Wnt/β-catenin signaling induces the aging of mesenchymal stem cells through promoting the ROS production. *Molecular and cellular biochemistry* 374(1–2), pp. 13–20. doi: 10.1007/S11010-012-1498-1.

Dysart, M.M., Galvis, B.R., Russell, A.G. and Barker, T.H. 2014. Environmental particulate (PM2.5) augments stiffness-induced alveolar epithelial cell mechanoactivation of transforming growth factor beta. *PLoS ONE* 9(9), p. 106821. doi: 10.1371/journal.pone.0106821.

Edlund, S., Lee, S.Y., Grimsby, S., Zhang, S., Aspenström, P., Heldin, C.-H. and Landström, M. 2005. Interaction between Smad7 and beta-catenin: importance for transforming growth factor beta-induced apoptosis. *Molecular and cellular biology* 25(4), pp. 1475–1488. doi: 10.1128/MCB.25.4.1475-1488.2005.

Egan, J.J., Stewart, J.P., Hasleton, P.S., Arrand, J.R., Carroll, K.B. and Woodcock, A.A. 1995. Epstein-Barr virus replication within pulmonary epithelial cells in cryptogenic fibrosing alveolitis. *Thorax* 50(12), pp. 1234–1239. doi:

10.1136/THX.50.12.1234.

Egan, J.J., Woodcock, A.A. and Stewart, J.P. 1997. Viruses and idiopathic pulmonary fibrosis. *Eur Respir J* 10, pp. 1433–1437. doi: 10.1183/09031936.97.10071433.

Elias, J.A., Jimenez, S.A. and Freundlich, B. 1987. Recombinant gamma, alpha, and beta interferon regulation of human lung fibroblast proliferation. *American Review of Respiratory Disease* 135(1), pp. 62–65. doi: 10.1164/arrd.1987.135.1.62.

Emblom-Callahan, M.C. et al. 2010. Genomic phenotype of non-cultured pulmonary fibroblasts in idiopathic pulmonary fibrosis. *Genomics* 96(3), pp. 134–145. doi: 10.1016/j.ygeno.2010.04.005.

Engelman, J.A. 2009. Targeting PI3K signalling in cancer: Opportunities, challenges and limitations. *Nature Reviews Cancer* 9(8), pp. 550–562. doi: 10.1038/nrc2664.

Fala, L. 2015. Ofev (Nintedanib): First Tyrosine Kinase Inhibitor Approved for the Treatment of Patients with Idiopathic Pulmonary Fibrosis. *American Health & Drug Benefits* 8(Spec Feature), p. 101.

Fandiño, J., Toba, L., González-Matías, L.C., Diz-Chaves, Y. and Mallo, F. 2020. GLP-1 receptor agonist ameliorates experimental lung fibrosis. *Scientific Reports* 10(1), pp. 1–15. doi: 10.1038/s41598-020-74912-1.

Farley, J.M. 1994. Airway Smooth Muscle Ion Channels. *Methods in Neurosciences* 19(C), pp. 220–239. doi: 10.1016/B978-0-12-185287-0.50018-1.

Fernandez, I.E. and Eickelberg, O. 2012. The impact of TGF-β on lung fibrosis: From targeting to biomarkers. *Proceedings of the American Thoracic Society* 9(3), pp. 111–116. doi: 10.1513/pats.201203-023AW.

Fingerlin, T.E. et al. 2013. Genome-wide association study identifies multiple susceptibility loci for pulmonary fibrosis. *Nature Genetics* 45(6), pp. 613–620. doi: 10.1038/ng.2609.

Finney, B.A. et al. 2008. Regulation of mouse lung development by the extracellular calcium-sensing receptor, CaR. *The Journal of physiology* 586(24), pp. 6007–6019. doi: 10.1113/JPHYSIOL.2008.161687.

Firpo, M.R. and Mounce, B.C. 2020. Diverse functions of polyamines in virus infection. *Biomolecules* 10(4). doi: 10.3390/biom10040628.

Fitzpatrick, L.A., Dabrowski, C.E., Cicconetti, G., Gordon, D.N., Papapoulos, S., Bone, H.G. and Bilezikian, J.P. 2011. The effects of ronacaleret, a calcium-sensing receptor antagonist, on bone mineral density and biochemical markers of bone turnover in postmenopausal women with low bone mineral density. *The Journal of clinical endocrinology and metabolism* 96(8), pp. 2441–2449. doi: 10.1210/JC.2010-2855.

Flock, T., Hauser, A.S., Lund, N., Gloriam, D.E., Balaji, S. and Babu, M.M. 2017. Selectivity determinants of GPCR-G-protein binding. *Nature* 545(7654), pp. 317–322. doi: 10.1038/NATURE22070.

Florin, L. et al. 2006. Delayed wound healing and epidermal hyperproliferation in mice lacking JunB in the skin. *Journal of Investigative Dermatology* 126(4), pp. 902–911. doi: 10.1038/sj.jid.5700123.

Flynn, A. and Hogarty, M. 2018. Myc, Oncogenic Protein Translation, and the Role of Polyamines. *Medical Sciences* 6(2), p. 41. doi: 10.3390/medsci6020041.

Frangogiannis, N.G. 2020. Transforming growth factor–β in tissue fibrosis. *Journal of Experimental Medicine* 217(3). doi: 10.1084/jem.20190103.

Fredriksson, R., Lagerström, M.C., Lundin, L.G. and Schiöth, H.B. 2003. The G-protein-coupled receptors in the human genome form five main families. Phylogenetic analysis, paralogon groups, and fingerprints. *Molecular pharmacology* 63(6), pp. 1256–1272. doi: 10.1124/MOL.63.6.1256.

Gabasa, M. et al. 2017. Epithelial contribution to the profibrotic stiff microenvironment and myofibroblast population in lung fibrosis. *Molecular Biology of the Cell* . doi: 10.1091/mbc.E17-01-0026.

Galli, J.A., Pandya, A., Vega-Olivo, M., Dass, C., Zhao, H. and Criner, G.J. 2017. Pirfenidone and nintedanib for pulmonary fibrosis in clinical practice: Tolerability and adverse drug reactions. *Respirology* 22(6), pp. 1171–1178. doi: 10.1111/resp.13024.

Gallob, F., Brcic, L., Eidenhammer, S., Rumpp, F., Nerlich, A. and Popper, H. 2021. Senescence and autophagy in usual interstitial pneumonia of different etiology. *Virchows Archiv* 478(3), pp. 497–506. doi: 10.1007/s00428-020-02917-2.

Galuppo, M., Esposito, E., Mazzon, E., Di Paola, R., Paterniti, I., Impellizzeri, D. and Cuzzocrea, S. 2011. MEK inhibition suppresses the development of lung fibrosis in the bleomycin model. *Naunyn-Schmiedeberg's Archives of Pharmacology* 384(1), pp. 21–37. doi: 10.1007/s00210-011-0637-7.

Gamble, L.D. et al. 2019. Inhibition of polyamine synthesis and uptake reduces tumor progression and prolongs survival in mouse models of neuroblastoma. *Science Translational Medicine* 11(477), p. 1099. doi: 10.1126/scitranslmed.aau1099.

Ganuza, M. et al. 2012. Genetic inactivation of Cdk7 leads to cell cycle arrest and induces premature aging due to adult stem cell exhaustion. *EMBO Journal* 31(11), pp. 2498–2510. doi: 10.1038/emboj.2012.94.

Gatica, D. and Klionsky, D.J. 2017. New insights into MTORC1 amino acid sensing and activation. *Biotarget* 1, pp. 2–2. doi: 10.21037/BIOTARGET.2017.04.01.

Ge, J. et al. 2018. Glutaminolysis promotes collagen translation and stability via a-ketoglutarate-mediated mTOR activation and proline hydroxylation. *American Journal of Respiratory Cell and Molecular Biology* 58(3), pp. 378–390. doi: 10.1165/rcmb.2017-0238OC.

Geng, Y. et al. 2019. PD-L1 on invasive fibroblasts drives fibrosis in a humanized model of idiopathic pulmonary fibrosis. *JCI Insight* 4(6). doi: 10.1172/jci.insight.125326.

Gerbino, A. and Colella, M. 2018. The Different Facets of Extracellular Calcium

Sensors: Old and New Concepts in Calcium-Sensing Receptor Signalling and Pharmacology. *International journal of molecular sciences* 19(4). doi: 10.3390/ijms19040999.

Gharaee-Kermani, M., Hu, B., Phan, S. and Gyetko, M. 2009. Recent Advances in Molecular Targets and Treatment of Idiopathic Pulmonary Fibrosis: Focus on TGFβ Signaling and the Myofibroblast. *Current Medicinal Chemistry* 16(11), pp. 1400–1417. doi: 10.2174/092986709787846497.

Gil, J. and Peters, G. 2006. Regulation of the INK4b-ARF-INK4a tumour suppressor locus: All for one or one for all. *Nature Reviews Molecular Cell Biology* 7(9), pp. 667–677. doi: 10.1038/nrm1987.

Glasser, S.W., Hagood, J.S., Wong, S., Taype, C.A., Madala, S.K. and Hardie, W.D. 2016. Mechanisms of Lung Fibrosis Resolution. *The American Journal of Pathology* 186(5), pp. 1066–1077. doi: 10.1016/J.AJPATH.2016.01.018.

Gonzalez, A.C.D.O., Andrade, Z.D.A., Costa, T.F. and Medrado, A.R.A.P. 2016. Wound healing - A literature review. *Anais Brasileiros de Dermatologia* 91(5), p. 614. doi: 10.1590/ABD1806-4841.20164741.

Gorres, K.L. and Raines, R.T. 2010. Prolyl 4-hydroxylase. *Critical Reviews in Biochemistry and Molecular Biology* 45(2), pp. 106–124. doi: 10.3109/10409231003627991.

Gowen, M. et al. 2000. Antagonizing the parathyroid calcium receptor stimulates parathyroid hormone secretion and bone formation in osteopenic rats. *The Journal of clinical investigation* 105(11), pp. 1595–1604. doi: 10.1172/JCI9038.

Grant, M.P., Stepanchick, A., Cavanaugh, A. and Breitwieser, G.E. 2011. Agonist-driven maturation and plasma membrane insertion of calcium-sensing receptors dynamically control signal amplitude. *Science signaling* 4(200). doi: 10.1126/SCISIGNAL.2002208.

Grasemann, H. et al. 2015. Arginase inhibition prevents bleomycin-induced pulmonary hypertension, vascular remodeling, and collagen deposition in neonatal rat lungs. *American Journal of Physiology-Lung Cellular and Molecular Physiology* 308(6), pp. L503–L510. doi: 10.1152/ajplung.00328.2014.

Grasemann, H., Shehnaz, D., Enomoto, M., Leadley, M., Belik, J. and Ratjen, F. 2012. L-Ornithine Derived Polyamines in Cystic Fibrosis Airways. *PLoS ONE* 7(10). doi: 10.1371/journal.pone.0046618.

Groves, A.M. et al. 2009. Idiopathic Pulmonary Fibrosis and Diffuse Parenchymal Lung Disease: Implications from Initial Experience with 18 F-FDG PET/CT. *J Nucl Med* 50, pp. 538–545. doi: 10.2967/jnumed.108.057901.

Grynkiewicz, G., Poenie, M. and Tsien, R.Y. 1985. A new generation of Ca2+ indicators with greatly improved fluorescence properties. *Journal of Biological Chemistry* 260(6), pp. 3440–3450. doi: 10.1016/s0021-9258(19)83641-4.

Guillotin, D. et al. 2020. Transcriptome analysis of IPF fibroblastic foci identifies key pathways involved in fibrogenesis. *Thorax* , p. thoraxjnl-2020-214902. doi: 10.1136/thoraxjnl-2020-214902.

Guiot, J., Moermans, C., Henket, M., Corhay, J.-L. and Louis, R. 2017. Blood Biomarkers in Idiopathic Pulmonary Fibrosis. *Lung* 195(3), pp. 273–280. doi: 10.1007/s00408-017-9993-5.

Guo, L. et al. 2019a. Kindlin-2 links mechano-environment to proline synthesis and tumor growth. *Nature Communications* 10(1), pp. 1–20. doi: 10.1038/s41467-019-08772-3.

Guo, Q., Huang, J.A., Yamamura, A., Yamamura, H., Zimnicka, A.M., Fernandez, R. and Yuan, J.X.J. 2013. Inhibition of the Ca2+-sensing receptor rescues pulmonary hypertension in rats and mice. *Hypertension Research 2014 37:2* 37(2), pp. 116–124. doi: 10.1038/hr.2013.129.

Guo, X., Rao, J.N., Liu, L., Rizvi, M., Turner, D.J. and Wang, J.-Y. 2002. Polyamines regulate β-catenin tyrosine phosphorylation via Ca^{2+} during intestinal epithelial cell migration. *American Journal of Physiology-Cell Physiology* 283(3), pp. C722–C734. doi: 10.1152/ajpcell.00054.2002.

Guo, Y., Ying, S., Zhao, X., Liu, J. and Wang, Y. 2019b. Increased expression of lung TRPV1/TRPA1 in a cough model of bleomycin-induced pulmonary fibrosis in Guinea pigs. *BMC Pulmonary Medicine* 19(1), pp. 1–11. doi: 10.1186/s12890-019-0792-z.

Haak, A.J., Ducharme, M.T., Diaz Espinosa, A.M. and Tschumperlin, D.J. 2020. Targeting GPCR Signaling for Idiopathic Pulmonary Fibrosis Therapies. *Trends in Pharmacological Sciences* 41(3), pp. 172–182. doi: 10.1016/j.tips.2019.12.008.

Habermann, A.C. et al. 2020. Single-cell RNA sequencing reveals profibrotic roles of distinct epithelial and mesenchymal lineages in pulmonary fibrosis. *Science Advances* 6(28), p. eaba1972. doi: 10.1126/sciadv.aba1972.

Hackstadt, A.J. and Hess, A.M. 2009. Filtering for increased power for microarray data analysis. *BMC Bioinformatics* 10(1), pp. 1–12. doi: 10.1186/1471-2105-10-11/FIGURES/4.

Halse, J. et al. 2014. A phase 2, randomized, placebo-controlled, dose-ranging study of the calcium-sensing receptor antagonist MK-5442 in the treatment of postmenopausal women with osteoporosis. *The Journal of clinical endocrinology and metabolism* 99(11), pp. E2207–E2215. doi: 10.1210/JC.2013-4009.

Hamanaka, R.B. et al. 2018. Inhibition of phosphoglycerate dehydrogenase attenuates bleomycin-induced pulmonary fibrosis. *American Journal of Respiratory Cell and Molecular Biology* 58(5), pp. 585–593. doi: 10.1165/rcmb.2017-0186OC.

Hamanaka, R.B. et al. 2019. Glutamine metabolism is required for collagen protein synthesis in lung fibroblasts. *American Journal of Respiratory Cell and Molecular Biology* 61(5), pp. 597–606. doi: 10.1165/rcmb.2019-0008OC.

Hamburg, E., DiNuoscio, G.J., Mullin, N.K., Lafayatis, R. and Atit, R.P. 2015. Sustained β-catenin activity in dermal fibroblasts promotes fibrosis by up-regulating expression of extracellular matrix protein-coding genes. *The Journal of pathology* 235(5), p. 686. doi: 10.1002/PATH.4481.

Hancock, L.A. et al. 2018. Muc5b overexpression causes mucociliary dysfunction

and enhances lung fibrosis in mice. *Nature Communications 2018 9:1* 9(1), pp. 1–10. doi: 10.1038/s41467-018-07768-9.

Handlogten, M.E., Shiraishi, N., Awata, H., Huang, C. and Miller, R.T. 2000. Extracellular Ca(2+)-sensing receptor is a promiscuous divalent cation sensor that responds to lead. *American journal of physiology. Renal physiology* 279(6). doi: 10.1152/AJPRENAL.2000.279.6.F1083.

Hannan, F.M., Kallay, E., Chang, W., Brandi, M.L. and Thakker, R. V. 2018a. The calcium-sensing receptor in physiology and in calcitropic and noncalcitropic diseases. *Nature Reviews Endocrinology* 15(1), pp. 33–51. doi: 10.1038/s41574-018-0115-0.

Hannan, F.M., Olesen, M.K. and Thakker, R. V. 2018b. Calcimimetic and calcilytic therapies for inherited disorders of the calcium-sensing receptor signalling pathway. *British journal of pharmacology* 175(21), pp. 4083–4094. doi: 10.1111/BPH.14086.

Hansel, C., Jendrossek, V. and Klein, D. 2020. Cellular senescence in the lung: The central role of senescent epithelial cells. *International Journal of Molecular Sciences* 21(9). doi: 10.3390/ijms21093279.

Hashimoto, S., Yamanaka, M., Yamochi, T., Iwata, H., Kawahara-Miki, R., Inoue, M. and Morimoto, Y. 2019. Mitochondrial function in immature bovine oocytes is improved by an increase of cellular cyclic AMP. *Scientific Reports* 9(1), pp. 1–14. doi: 10.1038/s41598-019-41610-6.

Hassanein, M. et al. 2015. Targeting SLC1a5-mediated glutamine dependence in non-small cell lung cancer. *International Journal of Cancer* 137(7), pp. 1587–1597. doi: 10.1002/ijc.29535.

Hauser, A.S., Chavali, S., Masuho, I., Jahn, L.J., Martemyanov, K.A., Gloriam, D.E. and Babu, M.M. 2018. Pharmacogenomics of GPCR Drug Targets. *Cell* 172(1–2), pp. 41-54.e19. doi: 10.1016/J.CELL.2017.11.033.

Hayashi, H. et al. 1997. The MAD-related protein Smad7 associates with the TGFß receptor and functions as an antagonist of TGFß signaling. *Cell* 89(7), pp. 1165–1173. doi: 10.1016/S0092-8674(00)80303-7.

Hayashi, T. et al. 1996. Immunohistochemical study of metalloproteinases and their tissue inhibitors in the lungs of patients with diffuse alveolar damage and idiopathic pulmonary fibrosis. *American Journal of Pathology* 149(4), pp. 1241–1256.

Hayes, G.M. et al. 2015. Antitumor activity of an anti-CD98 antibody. *International Journal of Cancer* 137(3), pp. 710–720. doi: 10.1002/ijc.29415.

He, Y.Y. et al. 2020. Spermine promotes pulmonary vascular remodelling and its synthase is a therapeutic target for pulmonary arterial hypertension. *European Respiratory Journal* 56(5). doi: 10.1183/13993003.00522-2020.

Henderson, W.R. et al. 2010. Inhibition of Wnt/ß-catenin/CREB binding protein (CBP) signaling reverses pulmonary fibrosis. *Proceedings of the National Academy of Sciences of the United States of America* 107(32), pp. 14309–14314. doi: 10.1073/pnas.1001520107.

Hewlett, J.C., Kropski, J.A. and Blackwell, T.S. 2018. Idiopathic Pulmonary Fibrosis: Epithelial-mesenchymal interactions and emerging therapeutic targets. *Matrix biology : journal of the International Society for Matrix Biology* 71–72, p. 112. doi: 10.1016/J.MATBIO.2018.03.021.

Hinz, B. 2010. The myofibroblast: Paradigm for a mechanically active cell. *Journal of Biomechanics* 43(1), pp. 146–155. doi: 10.1016/J.JBIOMECH.2009.09.020.

Hinz, B. et al. 2012. Recent developments in myofibroblast biology: Paradigms for connective tissue remodeling. *American Journal of Pathology* 180(4), pp. 1340–1355. doi: 10.1016/j.ajpath.2012.02.004.

Hobson, S.A., McNeil, S.E., Lee, F. and Rodland, K.D. 2000. Signal transduction mechanisms linking increased extracellular calcium to proliferation in ovarian surface epithelial cells. *Experimental Cell Research* 258(1), pp. 1–11. doi: 10.1006/excr.2000.4910.

Hodgson, U., Laitinen, T. and Tukiainen, P. 2002. Nationwide prevalence of sporadic and familial idiopathic pulmonary fibrosis: Evidence of founder effect among multiplex families in Finland. *Thorax* 57(4), pp. 338–342. doi: 10.1136/thorax.57.4.338.

Hoet, P.H.M. and Nemery, B. 2000. Polyamines in the lung: polyamine uptake and polyamine-linked pathological or toxicological conditions. *American Journal of Physiology-Lung Cellular and Molecular Physiology* 278(3), pp. L417–L433. doi: 10.1152/ajplung.2000.278.3.L417.

Hope-Gill, B.D.M., Hilldrup, S., Davies, C., Newton, R.P. and Harrison, N.K. 2003. A Study of the Cough Reflex in Idiopathic Pulmonary Fibrosis. *American Journal of Respiratory and Critical Care Medicine* 168(8), pp. 995–1002. doi: 10.1164/rccm.200304-597OC.

Horowitz, J.C. and Thannickal, V.J. 2006. Epithelial–Mesenchymal Interactions in Pulmonary Fibrosis. *Seminars in respiratory and critical care medicine* 27(6), p. 600. doi: 10.1055/S-2006-957332.

Hough, K.P., Curtiss, M.L., Blain, T.J., Liu, R.M., Trevor, J., Deshane, J.S. and Thannickal, V.J. 2020. Airway Remodeling in Asthma. *Frontiers in Medicine* 7, p. 191. doi: 10.3389/FMED.2020.00191/BIBTEX.

Hoyt, D.G. and Lazo, J.S. 1988. Alterations in pulmonary mRNA encoding procollagens, fibronectin and transforming growth factor-beta precede bleomycin-induced pulmonary fibrosis in mice. *Journal of Pharmacology and Experimental Therapeutics* 246(2)

Hu, B., Wu, Z. and Phan, S.H. 2003. Smad3 mediates transforming growth factor-beta-induced alpha-smooth muscle actin expression. *American journal of respiratory cell and molecular biology* 29(3 Pt 1), pp. 397–404. doi: 10.1165/RCMB.2003-0063OC.

Hu, J. and Spiegel, A.M. 2007. Structure and function of the human calcium-sensing receptor: insights from natural and engineered mutations and allosteric modulators. *Journal of Cellular and Molecular Medicine* 11(5), p. 908. doi:

10.1111/J.1582-4934.2007.00096.X.

Hua, W., ten Dijke, P., Kostidis, S., Giera, M. and Hornsveld, M. 2020. TGFß-induced metabolic reprogramming during epithelial-to-mesenchymal transition in cancer. *Cellular and Molecular Life Sciences* 77(11), pp. 2103–2123. doi: 10.1007/s00018-019-03398-6.

Huang, L.S. and Natarajan, V. 2015. Sphingolipids in pulmonary fibrosis. *Advances in biological regulation* 57, pp. 55–63. doi: 10.1016/J.JBIOR.2014.09.008.

Huang, S.K., Wettlaufer, S.H., Chung, J. and Peters-Golden, M. 2008. Prostaglandin E2 inhibits specific lung fibroblast functions via selective actions of PKA and Epac-1. *American Journal of Respiratory Cell and Molecular Biology* 39(4), pp. 482–489. doi: 10.1165/rcmb.2008-0080OC.

Hurta, R.A.R., Lee, J. and Voskas, D. 2001. *Transformation by H-ras Can Result in Aberrant Regulation of Ornithine Decarboxylase Gene Expression by Transforming Growth Factor-b 1*. doi: 10.1002/1097-4644.

Huter, P. et al. 2017. Structural Basis for Polyproline-Mediated Ribosome Stalling and Rescue by the Translation Elongation Factor EF-P. *Molecular Cell* 68(3), pp. 515-527.e6. doi: 10.1016/j.molcel.2017.10.014.

Inagakis, Y., Truter, S. and Ramirezo, F. 1994. Transforming Growth Factor+ Stimulates a2(I) Collagen Gene Expression through a cis-Acting Element That Contains an Spl-binding Site. *THE JOURNAL OF BIOLOGICAL CHEMISTRY* 269(20), pp. 14828–14834. doi: 10.1016/S0021-9258(17)36699-1.

de Ingeniis, J. et al. 2012. Functional Specialization in Proline Biosynthesis of Melanoma. *PLoS ONE* 7(9), p. 45190. doi: 10.1371/journal.pone.0045190.

Insel, P.A. et al. 2012. cAMP and Epac in the regulation of tissue fibrosis. *British Journal of Pharmacology* 166(2), pp. 447–456. doi: 10.1111/j.1476-5381.2012.01847.x.

Inui, N., Sakai, S. and Kitagawa, M. 2021. Molecular Pathogenesis of Pulmonary Fibrosis, with Focus on Pathways Related to TGF-ß and the Ubiquitin-Proteasome Pathway. *International Journal of Molecular Sciences* 22(11). doi: 10.3390/IJMS22116107.

Iyer, S.N., Margolin, S.B., Hyde, D.M. and Giri, S.N. 1998. Lung fibrosis is ameliorated by pirfenidone fed in diet after the second dose in a three-dose bleomycin-hamster model. *Experimental Lung Research* 24(1), pp. 119–133. doi: 10.3109/01902149809046058.

Jain, V. 2018. Role of Polyamines in Asthma Pathophysiology. *Medical Sciences* 6(1), p. 4. doi: 10.3390/medsci6010004.

Janssen, K., Rosielle, D., Wang, Q. and Kim, H.J. 2020. The impact of palliative care on quality of life, anxiety, and depression in idiopathic pulmonary fibrosis: A randomized controlled pilot study. *Respiratory Research* 21(1), pp. 1–9. doi: 10.1186/s12931-019-1266-9.

Janssen, L.J., Mukherjee, S. and Ask, K. 2015. Calcium Homeostasis and Ionic

Mechanisms in Pulmonary Fibroblasts. *American Journal of Respiratory Cell and Molecular Biology* 53(2), pp. 135–148. doi: 10.1165/rcmb.2014-0269TR.

Jenkins, R.G. et al. 2015. Longitudinal change in collagen degradation biomarkers in idiopathic pulmonary fibrosis: an analysis from the prospective, multicentre PROFILE study. *The Lancet. Respiratory medicine* 3(6), pp. 462–72. doi: 10.1016/S2213-2600(15)00048-X.

Jensen, K., Nizamutdinov, D., Guerrier, M., Afroze, S., Dostal, D. and Glaser, S. 2012. General mechanisms of nicotine-induced fibrogenesis. *FASEB Journal* 26(12), pp. 4778–4787. doi: 10.1096/fj.12-206458.

Ji, H., Tang, H., Lin, H., Mao, J., Gao, L., Liu, J. and Wu, T. 2014. Rho/Rock cross-talks with transforming growth factor-β/Smad pathway participates in lung fibroblast-myofibroblast differentiation. *Biomedical Reports* 2(6), pp. 787–792. doi: 10.3892/br.2014.323.

Jindal, S. 2016. Remodeling in asthma and COPD—recent concepts. *Lung India : Official Organ of Indian Chest Society* 33(1), p. 1. doi: 10.4103/0970-2113.173074.

Johannson, K.A. et al. 2014. Acute exacerbation of idiopathic pulmonary fibrosis associated with air pollution exposure. *The European respiratory journal* 43(4), pp. 1124–31. doi: 10.1183/09031936.00122213.

Johannson, K.A. et al. 2017. Antacid therapy in idiopathic pulmonary fibrosis: more questions than answers? *The Lancet Respiratory Medicine* 5(7), pp. 591–598. doi: 10.1016/S2213-2600(17)30219-9.

John, A.E., Joseph, C., Jenkins, G. and Tatler, A.L. 2021. COVID-19 and pulmonary fibrosis: A potential role for lung epithelial cells and fibroblasts. *Immunological reviews* 302(1), pp. 228–240. doi: 10.1111/IMR.12977.

John, M.R. et al. 2014. AXT914 a novel, orally-active parathyroid hormone-releasing drug in two early studies of healthy volunteers and postmenopausal women. *Bone* 64, pp. 204–210. doi: 10.1016/J.BONE.2014.04.015.

John MacLeod, R., Yano, S., Chattopadhyay, N. and Brown, E.. 2004. Extracellular calcium-sensing receptor transactivates the epidermal growth factor receptor by a triple-membrane-spanning signaling mechanism. *Biochemical and Biophysical Research Communications* 320(2), pp. 455–460. doi: 10.1016/j.bbrc.2004.05.198.

Jones, R.L., Noble, P.B., Elliot, J.G. and James, A.L. 2016. Airway remodelling in COPD: It's not asthma! *Respirology (Carlton, Vic.)* 21(8), pp. 1347–1356. doi: 10.1111/RESP.12841.

Justet, A. et al. 2017. [18F]FDG PET/CT predicts progression-free survival in patients with idiopathic pulmonary fibrosis. *Respiratory Research* 18(1). doi: 10.1186/s12931-017-0556-3.

Kamijo, T., Weber, J.D., Zambetti, G., Zindy, F., Roussel, M.F. and Sherr, C.J. 1998. Functional and physical interactions of the ARF tumor suppressor with p53 and Mdm2. *Proceedings of the National Academy of Sciences of the United States of America* 95(14), pp. 8292–8297. doi: 10.1073/pnas.95.14.8292.

Kang, Y.P. et al. 2016. Metabolic profiling regarding pathogenesis of idiopathic pulmonary fibrosis. *Journal of Proteome Research* 15(5), pp. 1717–1724. doi: 10.1021/acs.jproteome.6b00156.

Kenakin, T. and Christopoulos, A. 2013. Signalling bias in new drug discovery: detection, quantification and therapeutic impact. *Nature reviews. Drug discovery* 12(3), pp. 205–216. doi: 10.1038/NRD3954.

Keshav, R. and Narayanappa, U. 2015. Expression of proliferating cell nuclear antigen (PCNA) in oral submucous fibrosis: An immunohistochemical study. *Journal of Clinical and Diagnostic Research* 9(5), pp. ZC20–ZC23. doi: 10.7860/JCDR/2015/13046.5885.

Khalil, N. et al. 2001. Regulation of the effects of TGF-ß1 by activation of latentTGF-ß1 and differential expression of TGF-ß receptors (TßR-I andTßR-II) in idiopathic pulmonary fibrosis. *Thorax* 56(12), p. 907. doi: 10.1136/THORAX.56.12.907.

Khalil, N. et al. 2019. Phase 2 clinical trial of PBI-4050 in patients with idiopathic pulmonary fibrosis. *The European Respiratory Journal* 53(3). doi: 10.1183/13993003.00663-2018.

Kifor, O. et al. 2001. Regulation of MAP kinase by calcium-sensing receptor in bovine parathyroid and CaR-transfected HEK293 cells. *American Journal of Physiology - Renal Physiology* 280(2 49-2). doi: 10.1152/ajprenal.2001.280.2.f291.

Kim, H.-S., Kim, M.-R., Lee, M.S., Chung, I.P. and Jang, J.-J. 2009. P13: Roles of cyclin A, PCNA and p21 in proliferation of the hepatic stellate cells in dimethylnitrosamine-induced rat hepatic fibrosis. *Experimental and Toxicologic Pathology* 61(3), p. 287. doi: 10.1016/j.etp.2009.02.050.

Kim, K.K., Sheppard, D. and Chapman, H.A. 2018. TGF-ß1 Signaling and Tissue Fibrosis. doi: 10.1101/cshperspect.a022293.

Kim, T.H. et al. 2011. Blockade of the Wnt/ß-catenin pathway attenuates bleomycin-induced pulmonary fibrosis. *The Tohoku journal of experimental medicine* 223(1), pp. 45–54. doi: 10.1620/tjem.223.45.

King, J. et al. 2000. American Thoracic Society. Idiopathic pulmonary fibrosis: diagnosis and treatment. International consensus statement. American Thoracic Society (ATS), and the European Respiratory Society (ERS). *American journal of respiratory and critical care medicine* 161(2 Pt 1), pp. 646–664. doi: 10.1164/AJRCCM.161.2.ATS3-00.

King, T.E. et al. 2014. A Phase 3 Trial of Pirfenidone in Patients with Idiopathic Pulmonary Fibrosis. *New England Journal of Medicine* 370(22), pp. 2083–2092. doi: 10.1056/NEJMoa1402582.

King, T.E., Pardo, A. and Selman, M. 2011. Idiopathic pulmonary fibrosis. *The Lancet* 378(9807), pp. 1949–1961. doi: 10.1016/S0140-6736(11)60052-4.

Kitowska, K. et al. 2008. Functional role and species-specific contribution of arginases in pulmonary fibrosis. *American Journal of Physiology - Lung Cellular and Molecular Physiology* 294(1). doi: 10.1152/ajplung.00007.2007.

Klinkhammer, B.M., Floege, J. and Boor, P. 2018. PDGF in organ fibrosis. *Molecular Aspects of Medicine* 62, pp. 44–62. doi: 10.1016/j.mam.2017.11.008.

Kobayashi, Y. et al. 2020. Persistence of a regeneration-associated, transitional alveolar epithelial cell state in pulmonary fibrosis. *Nature cell biology* 22(8), pp. 934–946. doi: 10.1038/S41556-020-0542-8.

Koch, C.M., Chiu, S.F., Akbarpour, M., Bharat, A., Ridge, K.M., Bartom, E.T. and Winter, D.R. 2018. A beginner's guide to analysis of RNA sequencing data. *American Journal of Respiratory Cell and Molecular Biology* 59(2), pp. 145–157. doi: 10.1165/RCMB.2017-0430TR/SUPPL_FILE/DISCLOSURES.PDF.

Kohan, M., Muro, A.F., White, E.S. and Berkman, N. 2010. EDA-containing cellular fibronectin induces fibroblast differentiation through binding to $\alpha_4\beta_7$ integrin receptor and MAPK/Erk 1/2-dependent signaling. *The FASEB Journal* 24(11), pp. 4503–4512. doi: 10.1096/fj.10-154435.

Kolb, M., Bonniaud, P., Galt, T., Sime, P.J., Kelly, M.M., Margetts, P.J. and Gauldie, J. 2002. Differences in the Fibrogenic Response after Transfer of Active Transforming Growth Factor-β1 Gene to Lungs of "Fibrosis-prone" and "Fibrosis-resistant" Mouse Strains. *American Journal of Respiratory Cell and Molecular Biology* 27(2), pp. 141–150. doi: 10.1165/ajrcmb.27.2.4674.

Kolb, M. and Vašáková, M. 2019. The natural history of progressive fibrosing interstitial lung diseases. *Respiratory research* 20(1). doi: 10.1186/S12931-019-1022-1.

Komuves, L., Oda, Y., Tu, C.L., Chang, W.H., Ho-Pao, C.L., Mauro, T. and Bikle, D.D. 2002. Epidermal expression of the full-length extracellular calcium-sensing receptor is required for normal keratinocyte differentiation. *Journal of cellular physiology* 192(1), pp. 45–54. doi: 10.1002/JCP.10107.

Kopylova, E., Noé, L. and Touzet, H. 2012. SortMeRNA: fast and accurate filtering of ribosomal RNAs in metatranscriptomic data. *Bioinformatics* 28(24), pp. 3211–3217. doi: 10.1093/BIOINFORMATICS/BTS611.

Kottmann, R.M. et al. 2012. Lactic acid is elevated in idiopathic pulmonary fibrosis and induces myofibroblast differentiation via pH-dependent activation of transforming growth factor-β. *American Journal of Respiratory and Critical Care Medicine* 186(8), pp. 740–751. doi: 10.1164/rccm.201201-0084OC.

Kottmann, R.M. et al. 2015. Pharmacologic inhibition of lactate production prevents myofibroblast differentiation. *American Journal of Physiology-Lung Cellular and Molecular Physiology* 309(11), pp. L1305–L1312. doi: 10.1152/ajplung.00058.2015.

Kovacs, T. et al. 2014. Alteration in the Wnt microenvironment directly regulates molecular events leading to pulmonary senescence. *Aging Cell* 13(5), pp. 838–849. doi: 10.1111/acel.12240.

Kreuter, M. et al. 2016. Impact of Comorbidities on Mortality in Patients with Idiopathic Pulmonary Fibrosis. *PloS one* 11(3). doi: 10.1371/JOURNAL.PONE.0151425.

Kroeze, W.K., Sheffler, D.J. and Roth, B.L. 2003. G-protein-coupled receptors at

a glance. *Journal of Cell Science* 116(24), pp. 4867–4869. doi: 10.1242/JCS.00902.

Kühl, M., Sheldahl, L.C., Park, M., Miller, J.R. and Moon, R.T. 2000. The Wnt/Ca2+ pathway A new vertebrate Wnt signaling pathway takes shape. *Trends in Genetics* 16(7), pp. 279–283. doi: 10.1016/S0168-9525(00)02028-X.

Kuhn, C. and McDonald, J.A. 1991. The roles of the myofibroblast in idiopathic pulmonary fibrosis. Ultrastructural and immunohistochemical features of sites of active extracellular matrix synthesis. *The American Journal of Pathology* 138(5), p. 1257.

Kuilman, T. et al. 2008. Oncogene-Induced Senescence Relayed by an Interleukin-Dependent Inflammatory Network. *Cell* 133(6), pp. 1019–1031. doi: 10.1016/j.cell.2008.03.039.

Kular, J.K., Basu, S. and Sharma, R.I. 2014. The extracellular matrix: Structure, composition, age-related differences, tools for analysis and applications for tissue engineering. *Journal of Tissue Engineering* 5. doi: 10.1177/2041731414557112.

Kulkarni, A.B. and Karlsson, S. 1993. Transforming growth factor-beta 1 knockout mice. A mutation in one cytokine gene causes a dramatic inflammatory disease. *The American Journal of Pathology* 143(1), p. 3.

Kumar, S. et al. 2010. An orally active calcium-sensing receptor antagonist that transiently increases plasma concentrations of PTH and stimulates bone formation. *Bone* 46(2), pp. 534–542. doi: 10.1016/J.BONE.2009.09.028.

Kurundkar, A. and Thannickal, V.J. 2016. Redox mechanisms in age-related lung fibrosis. *Redox Biology* 9, pp. 67–76. doi: 10.1016/J.REDOX.2016.06.005.

Kwan, J.A. et al. 2004. Matrix metalloproteinase-2 (MMP-2) is present in the nucleus of cardiac myocytes and is capable of cleaving poly (ADP-ribose) polymerase (PARP) in vitro. *The FASEB journal : official publication of the Federation of American Societies for Experimental Biology* 18(6), pp. 690–692. doi: 10.1096/fj.02-1202fje.

Lam, A.P. and Gottardi, C.J. 2011. β-catenin signaling: A novel mediator of fibrosis and potential therapeutic target. *Current Opinion in Rheumatology* 23(6), pp. 562–567. doi: 10.1097/BOR.0b013e32834b3309.

Landau, G., Bercovich, Z., Park, M.H. and Kahana, C. 2010. The role of polyamines in supporting growth of mammalian cells is mediated through their requirement for translation initiation and elongation. *Journal of Biological Chemistry* 285(17), pp. 12474–12481. doi: 10.1074/jbc.M110.106419.

Lapiere, J.C., Chen, J.D., Iwasaki, T., Hu, L., Uitto, J. and Woodley, D.T. 1994. Type VII collagen specifically binds fibronectin via a unique subdomain within the collagenous triple helix. *Journal of Investigative Dermatology* 103(5), pp. 637–641. doi: 10.1111/1523-1747.ep12398270.

Lasbury, M.E., Merali, S., Durant, P.J., Tschang, D., Ray, C.A. and Lee, C.-H. 2007. Polyamine-mediated apoptosis of alveolar macrophages during Pneumocystis pneumonia. *The Journal of biological chemistry* 282(15), pp.

11009–20. doi: 10.1074/jbc.M611686200.

Lasky, J. et al. 1998. Connective tissue growth factor mRNA expression is upregulated in bleomycin-induced lung fibrosis. *American Journal of Physiology - Lung Cellular and Molecular Physiology* 275(2 19-2). doi: 10.1152/ajplung.1998.275.2.l365.

Della Latta, V., Cabiati, M., Rocchiccioli, S., Del Ry, S. and Morales, M.A. 2013. The role of the adenosinergic system in lung fibrosis. *Pharmacological research* 76, pp. 182–189. doi: 10.1016/J.PHRS.2013.08.004.

Lauweryns, J.M., Cokelaere, M. and Theunynck, P. 1972. Neuro-epithelial bodies in the respiratory mucosa of various mammals. *Zeitschrift f*r Zellforschung und Mikroskopische Anatomie* 135(4), pp. 569–592. doi: 10.1007/BF00583438.

Lawrence, J. and Nho, R. 2018. The Role of the Mammalian Target of Rapamycin (mTOR) in Pulmonary Fibrosis. *International journal of molecular sciences* 19(3). doi: 10.3390/IJMS19030778.

Leach, K. et al. 2016. Towards a structural understanding of allosteric drugs at the human calcium-sensing receptor. *Cell research* 26(5), pp. 574–592. doi: 10.1038/CR.2016.36.

Leach, K. et al. 2020. International Union of Basic and Clinical Pharmacology. CVIII. Calcium-Sensing Receptor Nomenclature, Pharmacology, and Function. *Pharmacological Reviews* 72(3), pp. 558–604. doi: 10.1124/PR.119.018531.

Leach, K., Sexton, P.M., Christopoulos, A. and Conigrave, A.D. 2014. Engendering biased signalling from the calcium-sensing receptor for the pharmacotherapy of diverse disorders. *British Journal of Pharmacology* . doi: 10.1111/bph.12420.

Leask, A. 2012. MEK/ERK inhibitors: Proof-of-concept studies in lung fibrosis. *Journal of Cell Communication and Signaling* 6(1), pp. 59–60. doi: 10.1007/s12079-011-0156-9.

Lederer, D.J. and Martinez, F.J. 2018. Idiopathic Pulmonary Fibrosis. Longo, D. L. ed. *The New England journal of medicine* 378(19), pp. 1811–1823. doi: 10.1056/NEJMRA1705751.

Lee, C.G. et al. 2004. Early growth response gene 1-mediated apoptosis is essential for transforming growth factor beta1-induced pulmonary fibrosis. *The Journal of experimental medicine* 200(3), pp. 377–389. doi: 10.1084/JEM.20040104.

Lee, H.J., Mun, H.-C., Lewis, N.C., Crouch, M.F., Culverston, E.L., Mason, R.S. and Conigrave, A.D. 2007. Allosteric activation of the extracellular Ca2+-sensing receptor by L-amino acids enhances ERK1/2 phosphorylation. *The Biochemical journal* 404(1), pp. 141–9. doi: 10.1042/BJ20061826.

Lee, J.S. et al. 2021. Molecular markers of telomere dysfunction and senescence are common findings in the usual interstitial pneumonia pattern of lung fibrosis. *Histopathology* 79(1), pp. 67–76. doi: 10.1111/his.14334.

Lee, J.S., Song, J.W., Wolters, P.J., Elicker, B.M., King, T.E., Kim, D.S. and

Collard, H.R. 2012. Bronchoalveolar lavage pepsin in acute exacerbation of idiopathic pulmonary fibrosis. *European Respiratory Journal* 39(2), pp. 352–358. doi: 10.1183/09031936.00050911.

Lee, J.W. et al. 2017. NPS2143 Inhibits MUC5AC and Proinflammatory Mediators in Cigarette Smoke Extract (CSE)-Stimulated Human Airway Epithelial Cells. *Inflammation* 40(1), pp. 184–194. doi: 10.1007/S10753-016-0468-2.

Lee, T.Y., Chin, G.S., Kim, W.J.H., Chau, D., Gittes, G.K. and Longaker, M.T. 1999. Expression of transforming growth factor beta 1, 2, and 3 proteins in keloids. *Annals of Plastic Surgery* 43(2), pp. 179–184. doi: 10.1097/00000637-199943020-00013.

Leigh, M.W., Kylander, J.E., Yankaskas, J.R. and Boucher, R.C. 1995. Cell proliferation in bronchial epithelium and submucosal glands of cystic fibrosis patients. *American journal of respiratory cell and molecular biology* 12(6), pp. 605–612. doi: 10.1165/ajrcmb.12.6.7766425.

Lembrechts, R. et al. 2013. Functional expression of the multimodal extracellular calcium-sensing receptor in pulmonary neuroendocrine cells. *Journal of cell science* 126(Pt 19), pp. 4490–501. doi: 10.1242/jcs.131656.

Lembrechts, R., Brouns, I., Schnorbusch, K., Pintelon, I., Timmermans, J.-P. and Adriaensen, D. 2012. Neuroepithelial Bodies as Mechanotransducers in the Intrapulmonary Airway Epithelium. *American Journal of Respiratory Cell and Molecular Biology* 47(3), pp. 315–323. doi: 10.1165/rcmb.2012-0068OC.

Letz, S. et al. 2014. Amino Alcohol- (NPS-2143) and Quinazolinone-Derived Calcilytics (ATF936 and AXT914) Differentially Mitigate Excessive Signalling of Calcium-Sensing Receptor Mutants Causing Bartter Syndrome Type 5 and Autosomal Dominant Hypocalcemia. Valenti, G. ed. *PLoS ONE* 9(12), p. e115178. doi: 10.1371/journal.pone.0115178.

Ley, B. et al. 2017a. The MUC5B promoter polymorphism and telomere length in patients with chronic hypersensitivity pneumonitis: an observational cohort-control study. *The Lancet Respiratory Medicine* 5(8), pp. 639–647. doi: 10.1016/S2213-2600(17)30216-3.

Ley, B. and Collard, H.R. 2013. Epidemiology of idiopathic pulmonary fibrosis. *Clinical Epidemiology* 5(1), pp. 483–492. doi: 10.2147/CLEP.S54815.

Ley, B., Swigris, J., Day, B. mo, Stauffer, J.L., Raimundo, K., Chou, W. and Collard, H.R. 2017b. Pirfenidone reduces respiratory-related hospitalizations in idiopathic pulmonary fibrosis. *American Journal of Respiratory and Critical Care Medicine* 196(6), pp. 756–761. doi: 10.1164/RCCM.201701-0091OC/SUPPL_FILE/DISCLOSURES.PDF.

Li, M.O., Wan, Y.Y., Sanjabi, S., Robertson, A.K.L. and Flavell, R.A. 2006. Transforming growth factor-β regulation of immune responses. *Annual Review of Immunology* 24, pp. 99–146. doi: 10.1146/annurev.immunol.24.021605.090737.

Liao, Y., Smyth, G.K. and Shi, W. 2014. featureCounts: an efficient general purpose program for assigning sequence reads to genomic features. *Bioinformatics* 30(7), pp. 923–930. doi: 10.1093/BIOINFORMATICS/BTT656.

Limb, G.A., Matter, K., Murphy, G., Cambrey, A.D., Bishop, P.N., Morris, G.E. and Khaw, P.T. 2005. Matrix metalloproteinase-1 associates with intracellular organelles and confers resistance to lamin A/C Degradation during apoptosis. *American Journal of Pathology* 166(5), pp. 1555–1563. doi: 10.1016/S0002-9440(10)62371-1.

Lin, J., Wu, Y., Yang, D. and Zhao, Y. 2013. Induction of apoptosis and antitumor effects of a small molecule inhibitor of Bcl-2 and Bcl-xl, gossypol acetate, in multiple myeloma in vitro and in vivo. *Oncology Reports* 30(2), pp. 731–738. doi: 10.3892/or.2013.2489.

Lin, Y. and Xu, Z. 2020. Fibroblast Senescence in Idiopathic Pulmonary Fibrosis. *Frontiers in Cell and Developmental Biology* 8, p. 1398. doi: 10.3389/fcell.2020.593283.

Lindahl, G.E. et al. 2013. Microarray profiling reveals suppressed interferon stimulated gene program in fibroblasts from scleroderma-associated interstitial lung disease. *Respiratory Research* 14(1), p. 80. doi: 10.1186/1465-9921-14-80.

Lindenschmidt, R.C. and Witschi, H. 1985. Attenuation of pulmonary fibrosis in mice by aminophylline. *Biochemical pharmacology* 34(24), pp. 4269–4273. doi: 10.1016/0006-2952(85)90283-7.

Linnoila, R.I. 2006. Functional facets of the pulmonary neuroendocrine system. *Laboratory Investigation* 86(5), pp. 425–444. doi: 10.1038/labinvest.3700412.

Liu, G. and Summer, R. 2019. Cellular Metabolism in Lung Health and Disease. *Annual review of physiology* 81, p. 403. doi: 10.1146/ANNUREV-PHYSIOL-020518-114640.

Liu, R., Li, P., Bi, C.W., Ma, R., Yin, Y., Bi, K. and Li, Q. 2017. Plasma N-acetylputrescine, cadaverine and 1,3-diaminopropane: Potential biomarkers of lung cancer used to evaluate the efficacy of anticancer drugs. *Oncotarget* 8(51), pp. 88575–88585. doi: 10.18632/oncotarget.19304.

López-Contreras, F. et al. 2020. Searching for Drug Synergy Against Cancer Through Polyamine Metabolism Impairment: Insight Into the Metabolic Effect of Indomethacin on Lung Cancer Cells. *Frontiers in Pharmacology* 10, p. 1670. doi: 10.3389/fphar.2019.01670.

López-Hernández, Y. et al. 2021. Targeted metabolomics identifies high performing diagnostic and prognostic biomarkers for COVID-19. *Scientific Reports* 11(1), p. 14732. doi: 10.1038/s41598-021-94171-y.

Love, M.I., Huber, W. and Anders, S. 2014. Moderated estimation of fold change and dispersion for RNA-seq data with DESeq2. *Genome Biology* 15(12), pp. 1–21. doi: 10.1186/S13059-014-0550-8/FIGURES/9.

Lu, M., Leng, B., He, X., Zhang, Z., Wang, H. and Tang, F. 2018. Calcium Sensing Receptor-Related Pathway Contributes to Cardiac Injury and the Mechanism of Astragaloside IV on Cardioprotection. *Frontiers in Pharmacology* 9, p. 1163. doi: 10.3389/FPHAR.2018.01163/BIBTEX.

Luengo, A., Gui, D.Y. and Heiden, M.G. Vander 2017. Targeting Metabolism for Cancer Therapy. *Cell chemical biology* 24(9), p. 1161. doi:

10.1016/J.CHEMBIOL.2017.08.028.

Lujambio, A. 2016. To clear, or not to clear (senescent cells)? That is the question. *Inside the Cell* 1(2), pp. 87–95. doi: 10.1002/icl3.1046.

Lung, M.L., So, S.Y., Chan, K.H., Lam, W.K., Lam, W.P. and Ng, M.H. 1985. Evidence that respiratory tract is major reservoir for Epstein-Barr virus. *Lancet (London, England)* 1(8434), pp. 889–892. doi: 10.1016/S0140-6736(85)91671-X.

Luppi, F., Kalluri, M., Faverio, P., Kreuter, M. and Ferrara, G. 2021. Idiopathic pulmonary fibrosis beyond the lung: understanding disease mechanisms to improve diagnosis and management. *Respiratory Research 2021 22:1* 22(1), pp. 1–16. doi: 10.1186/S12931-021-01711-1.

Luttrell, L.M. 2003. 'Location, location, location': activation and targeting of MAP kinases by G protein-coupled receptors. *Journal of Molecular Endocrinology* 30(2), pp. 117–126. doi: 10.1677/JME.0.0300117.

Luttrell, L.M. 2014. Minireview: More than just a hammer: ligand 'bias' and pharmaceutical discovery. *Molecular endocrinology (Baltimore, Md.)* 28(3), pp. 281–294. doi: 10.1210/ME.2013-1314.

Luzina, I.G., Todd, N.W., Sundararajan, S. and Atamas, S.P. 2015a. The cytokines of pulmonary fibrosis: Much learned, much more to learn. *Cytokine* 74(1), pp. 88–100. doi: 10.1016/j.cyto.2014.11.008.

Luzina, I.G., Todd, N.W., Sundararajan, S. and Atamas, S.P. 2015b. The cytokines of pulmonary fibrosis: Much learned, much more to learn. *Cytokine* 74(1), pp. 88–100. doi: 10.1016/j.cyto.2014.11.008.

Lv, Q., Zhang, J., Yi, Y., Huang, Y., Wang, Y., Wang, Y. and Zhang, W. 2015. Proliferating Cell Nuclear Antigen Has an Association with Prognosis and Risks Factors of Cancer Patients: a Systematic Review. *Molecular Neurobiology 2015 53:9* 53(9), pp. 6209–6217. doi: 10.1007/S12035-015-9525-3.

Lv, X.T. et al. 2020. High serum lactate dehydrogenase and dyspnea: Positive predictors of adverse outcome in critical COVID-19 patients in Yichang. *World Journal of Clinical Cases* 8(22), pp. 5535–5546. doi: 10.12998/WJCC.V8.I22.5535.

Maarsingh, H. et al. 2011. Increased arginase activity contributes to airway remodelling in chronic allergic asthma. *The European respiratory journal* 38(2), pp. 318–28. doi: 10.1183/09031936.00057710.

Maarsingh, H., Pera, T. and Meurs, H. 2008a. Arginase and pulmonary diseases. *Naunyn-Schmiedeberg's archives of pharmacology* 378(2), pp. 171–84. doi: 10.1007/s00210-008-0286-7.

Maarsingh, H., Zaagsma, J. and Meurs, H. 2008b. Arginine homeostasis in allergic asthma. *European Journal of Pharmacology* 585(2–3), pp. 375–384. doi: 10.1016/J.EJPHAR.2008.02.096.

MacLeod, R., Yano, S., Chattopadhyay, N. and Brown, E.M. 2004. Extracellular calcium-sensing receptor transactivates the epidermal growth factor receptor by a triple-membrane-spanning signaling mechanism. *Biochemical and Biophysical Research Communications* 320(2), pp. 455–460. doi: 10.1016/j.bbrc.2004.05.198.

Maekawa, M. et al. 1999. Signaling from Rho to the actin cytoskeleton through protein kinases ROCK and LIM-kinase. *Science (New York, N.Y.)* 285(5429), pp. 895–898. doi: 10.1126/SCIENCE.285.5429.895.

Maher, T.M. 2021. Small airways in idiopathic pulmonary fibrosis: Quiet but not forgotten. *American Journal of Respiratory and Critical Care Medicine* 204(9), pp. 1010–1011. doi: 10.1164/RCCM.202108-2007ED/SUPPL_FILE/DISCLOSURES.PDF.

Maher, T.M. and Strek, M.E. 2019. Antifibrotic therapy for idiopathic pulmonary fibrosis: Time to treat. *Respiratory Research* 20(1), p. 205. doi: 10.1186/s12931-019-1161-4.

Malathi, N., Mythili, S. and Vasanthi, H.R. 2014. Salivary diagnostics: a brief review. *ISRN dentistry* 2014, p. 158786. doi: 10.1155/2014/158786.

Malizia, A.P., Keating, D.T., Smith, S.M., Walls, D., Doran, P.P. and Egan, J.J. 2008. Alveolar epithelial cell injury with Epstein-Barr virus upregulates TGFß1 expression. *American Journal of Physiology - Lung Cellular and Molecular Physiology* 295(3), pp. 451–460. doi: 10.1152/ajplung.00376.2007.

Mamillapalli, R., VanHouten, J., Zawalich, W. and Wysolmerski, J. 2008. Switching of G-protein usage by the calcium-sensing receptor reverses its effect on parathyroid hormone-related protein secretion in normal versus malignant breast cells. *The Journal of biological chemistry* 283(36), pp. 24435–24447. doi: 10.1074/JBC.M801738200.

Mamillapalli, R. and Wysolmerski, J. 2010. The calcium-sensing receptor couples to Galpha(s) and regulates PTHrP and ACTH secretion in pituitary cells. *The Journal of endocrinology* 204(3), pp. 287–297. doi: 10.1677/JOE-09-0183.

Van Manen, M.J.G., Geelhoed, J.J.M., Tak, N.C. and Wijsenbeek, M.S. 2017. Optimizing quality of life in patients with idiopathic pulmonary fibrosis. *Therapeutic advances in respiratory disease* 11(3), pp. 157–169. doi: 10.1177/1753465816686743.

Manicone, A.M. and McGuire, J.K. 2008. Matrix metalloproteinases as modulators of inflammation. *Seminars in Cell and Developmental Biology* 19(1), pp. 34–41. doi: 10.1016/j.semcdb.2007.07.003.

Mansfield, B. et al. 2019. Calcium-sensing receptor (CaSR) antagonists (calcilytics) prevent urban particulate matter (UPM)-induced dendritic cell activation. *European Respiratory Journal* 54(suppl 63), p. PA2401. doi: 10.1183/13993003.CONGRESS-2019.PA2401.

Marshall, D.C., Salciccioli, J.D., Shea, B.S. and Akuthota, P. 2018. Trends in mortality from idiopathic pulmonary fibrosis in the European Union: an observational study of the WHO mortality database from 2001-2013. *The European respiratory journal* 51(1), p. 1701603. doi: 10.1183/13993003.01603-2017.

Marshall, R.P., McAnulty, R.J. and Laurent, G.J. 1997. The pathogenesis of pulmonary fibrosis: Is there a fibrosis gene? *International Journal of Biochemistry and Cell Biology* 29(1), pp. 107–120. doi: 10.1016/S1357-

2725(96)00141-0.

Martin-Medina, A. et al. 2018. Increased Extracellular Vesicles Mediate WNT5A Signaling in Idiopathic Pulmonary Fibrosis. *American journal of respiratory and critical care medicine* 198(12), pp. 1527–1538. doi: 10.1164/RCCM.201708-1580OC.

Massagué, J. 2003. TGF-β SIGNAL TRANSDUCTION. *https://doi.org/10.1146/annurev.biochem.67.1.753* 67, pp. 753–791. doi: 10.1146/ANNUREV.BIOCHEM.67.1.753.

McDonough, J.E. et al. 2019a. Transcriptional regulatory model of fibrosis progression in the human lung. *JCI Insight* 4(22), p. 131597. doi: 10.1172/jci.insight.131597.

McDonough, J.E., Kaminski, N., Thienpont, B., Hogg, J.C., Vanaudenaerde, B.M. and Wuyts, W.A. 2019b. Gene correlation network analysis to identify regulatory factors in idiopathic pulmonary fibrosis. *Thorax* 74(2), pp. 132–140. doi: 10.1136/thoraxjnl-2018-211929.

McLarnon, S.J., Holden, D., Ward, D.T., Jones, M.N., Elliott, A.C. and Riccardi, D. 2002. Aminoglycoside antibiotics induce pH-sensitive activation of the calcium-sensing receptor. *Biochemical and Biophysical Research Communications* 297(1), pp. 71–77. doi: 10.1016/S0006-291X(02)02133-2.

McNeil, S.E., Hobson, S.A., Nipper, V. and Rodland, K.D. 1998. Functional calcium-sensing receptors in rat fibroblasts are required for activation of SRC kinase and mitogen-activated protein kinase in response to extracellular calcium. *The Journal of biological chemistry* 273(2), pp. 1114–20. doi: 10.1074/JBC.273.2.1114.

Meiners, S., Eickelberg, O. and Königshoff, M. 2015. Hallmarks of the ageing lung. *European Respiratory Journal* 45(3), pp. 807–827. doi: 10.1183/09031936.00186914.

Meng, D., Frank, A.R. and Jewell, J.L. 2018. mTOR signaling in stem and progenitor cells. *Development (Cambridge)* 145(1). doi: 10.1242/dev.152595.

Mercer, P.F. et al. 2016. Exploration of a potent PI3 kinase/mTOR inhibitor as a novel anti-fibrotic agent in IPF. *Thorax* 71(8), pp. 701–11. doi: 10.1136/thoraxjnl-2015-207429.

Michael, A.J. 2016. Biosynthesis of polyamines and polyamine-containing molecules. *Biochemical Journal* 473(15), pp. 2315–2329. doi: 10.1042/BCJ20160185.

Mikolasch, T.A., Garthwaite, H.S. and Porter, J.C. 2017. Update in diagnosis and management of interstitial lung disease. *Clinical medicine (London, England)* 17(2), pp. 146–153. doi: 10.7861/CLINMEDICINE.17-2-146.

Min, P.I., Spurney, R.F., Qisheng, T.U., Hinson, T. and Darryl Quarles, L. 2002. Calcium-sensing receptor activation of rho involves filamin and rho-guanine nucleotide exchange factor. *Endocrinology* 143(10), pp. 3830–3838. doi: 10.1210/EN.2002-220240.

Minois, N. 2014. Molecular basis of the 'anti-aging' effect of spermidine and other natural polyamines - A mini-review. *Gerontology* 60(4), pp. 319–326. doi: 10.1159/000356748.

Minois, N., Carmona-Gutierrez, D. and Madeo, F. 2011. Polyamines in aging and disease. *Aging* 3(8), pp. 716–32. doi: 10.18632/aging.100361.

Molostvov, G., Fletcher, S., Bland, R. and Zehnder, D. 2008. Extracellular Calcium-Sensing Receptor Mediated Signalling is Involved in Human Vascular Smooth Muscle Cell Proliferation and Apoptosis. *Cellular Physiology and Biochemistry* 22(5–6), pp. 413–422. doi: 10.1159/000185484.

Montesi, S.B., Fisher, J.H., Martinez, F.J., Selman, M., Pardo, A. and Johannson, K.A. 2020. Update in Interstitial Lung Disease 2019. *American journal of respiratory and critical care medicine* 202(4), pp. 500–507. doi: 10.1164/RCCM.202002-0360UP.

Mookherjee, N., Piyadasa, H., Ryu, M.H., Rider, C.F., Ezzati, P., Spicer, V. and Carlsten, C. 2018. Inhaled diesel exhaust alters the allergen-induced bronchial secretome in humans. *European Respiratory Journal* 51(1). doi: 10.1183/13993003.01385-2017.

Moore, B.B., Lawson, W.E., Oury, T.D., Sisson, T.H., Raghavendran, K. and Hogaboam, C.M. 2013. Animal models of fibrotic lung disease. *American Journal of Respiratory Cell and Molecular Biology* 49(2), pp. 167–179. doi: 10.1165/rcmb.2013-0094TR.

Moore, C. et al. 2019. Resequencing study confirms that host defense and cell senescence gene variants contribute to the risk of idiopathic pulmonary fibrosis. *American Journal of Respiratory and Critical Care Medicine* 200(2), pp. 199–208. doi: 10.1164/rccm.201810-1891OC.

Morris, S.M. 2007. Arginine Metabolism: Boundaries of Our Knowledge. *The Journal of Nutrition* 137(6), pp. 1602S-1609S. doi: 10.1093/jn/137.6.1602S.

Morse, C. et al. 2019. Proliferating SPP1/MERTK-expressing macrophages in idiopathic pulmonary fibrosis. *European Respiratory Journal* 54(2). doi: 10.1183/13993003.02441-2018.

Moshier, J.A., Dosescu, J., Skunca, M. and Luk, G.D. 1993. Transformation of NIH/3T3 Cells by Ornithine Decarboxylase Overexpression. *Cancer Research* 53(11)

Mostafaei, S. et al. 2021. The role of viral and bacterial infections in the pathogenesis of IPF: a systematic review and meta-analysis. *Respiratory Research* 22(1), pp. 1–14. doi: 10.1186/s12931-021-01650-x.

Moussad, E.E.D.A. and Brigstock, D.R. 2000. Connective tissue growth factor: What's in a name? *Molecular Genetics and Metabolism* 71(1–2), pp. 276–292. doi: 10.1006/mgme.2000.3059.

Moustakas, A. and Heldin, C.H. 2005. Non-Smad TGF-ß signals. *Journal of Cell Science* 118(16), pp. 3573–3584. doi: 10.1242/jcs.02554.

Mrgan, M., Nielsen, S. and Brixen, K. 2014. Familial Hypocalciuric Hypercalcemia

and Calcium Sensing Receptor. *Acta clinica Croatica* 53.(2.), pp. 220–224.

Mu, Y., Gudey, S.K. and Landström, M. 2012. Non-Smad signaling pathways. *Cell and Tissue Research* 347(1), pp. 11–20. doi: 10.1007/S00441-011-1201-Y/FIGURES/2.

Muhammad, N., Lee, H.M. and Kim, J. 2020. Oncology Therapeutics Targeting the Metabolism of Amino Acids. *Cells* 9(8). doi: 10.3390/cells9081904.

Mukherjee, S., A. Ayaub, E., Murphy, J., Lu, C., Kolb, M., Ask, K. and J. Janssen, L. 2015. Disruption of Calcium Signaling in Fibroblasts and Attenuation of Bleomycin-Induced Fibrosis by Nifedipine. *American Journal of Respiratory Cell and Molecular Biology* 53(4), pp. 450–458. doi: 10.1165/rcmb.2015-0009OC.

Muñoz-Espín, D. and Serrano, M. 2014. Cellular senescence: from physiology to pathology. *Nature reviews. Molecular cell biology* 15(7), pp. 482–496. doi: 10.1038/NRM3823.

Muramatsu, T. et al. 2016. The hypusine cascade promotes cancer progression and metastasis through the regulation of RhoA in squamous cell carcinoma. *Oncogene* 35(40), pp. 5304–5316. doi: 10.1038/onc.2016.71.

Murray, L.A. et al. 2008. Hyper-responsiveness of IPF/UIP fibroblasts: Interplay between TGFβ1, IL-13 and CCL2. *The International Journal of Biochemistry & Cell Biology* 40(10), pp. 2174–2182. doi: 10.1016/j.biocel.2008.02.016.

Murtha, L.A. et al. 2017. The processes and mechanisms of cardiac and pulmonary fibrosis. *Frontiers in Physiology* 8(OCT), p. 777. doi: 10.3389/FPHYS.2017.00777/BIBTEX.

Myllyharju, J. 2008. Prolyl 4-hydroxylases, key enzymes in the synthesis of collagens and regulation of the response to hypoxia, and their roles as treatment targets. *Annals of Medicine* 40(6), pp. 402–417. doi: 10.1080/07853890801986594.

Nachef, M., Ali, A.K., Almutairi, S.M. and Lee, S.H. 2021. Targeting SLC1A5 and SLC3A2/SLC7A5 as a Potential Strategy to Strengthen Anti-Tumor Immunity in the Tumor Microenvironment. *Frontiers in Immunology* 12, p. 1311. doi: 10.3389/fimmu.2021.624324.

Nakanishi, S. and Cleveland, J.L. 2016. Targeting the polyamine-hypusine circuit for the prevention and treatment of cancer. *Amino Acids* 48(10), pp. 2353–2362. doi: 10.1007/s00726-016-2275-3.

Nakazato, H., Oku, H., Yamane, S., Tsuruta, Y. and Suzuki, R. 2002. A novel anti-fibrotic agent pirfenidone suppresses tumor necrosis factor-α at the translational level. *European Journal of Pharmacology* 446(1–3), pp. 177–185. doi: 10.1016/S0014-2999(02)01758-2.

Napolitano, L. et al. 2017. Potent inhibitors of human LAT1 (SLC7A5) transporter based on dithiazole and dithiazine compounds for development of anticancer drugs. *Biochemical Pharmacology* 143, pp. 39–52. doi: 10.1016/j.bcp.2017.07.006.

Navaratnam, V., Fleming, K.M., West, J., Smith, C.J.P., Jenkins, R.G., Fogarty,

A. and Hubbard, R.B. 2011. The rising incidence of idiopathic pulmonary fibrosis in the UK. *Thorax* 66(6), pp. 462–467. doi: 10.1136/thx.2010.148031.

Nemeth, E.F. 2002. The search for calcium receptor antagonists (calcilytics). *Journal of molecular endocrinology* 29(1), pp. 15–21. doi: 10.1677/JME.0.0290015.

Nemeth, E.F. and Fox, J. 1999. Calcimimetic Compounds: a Direct Approach to Controlling Plasma Levels of Parathyroid Hormone in Hyperparathyroidism. *Trends in endocrinology and metabolism: TEM* 10(2), pp. 66–71. doi: 10.1016/S1043-2760(98)00119-2.

Nemeth, E.F. and Goodman, W.G. 2016. Calcimimetic and Calcilytic Drugs: Feats, Flops, and Futures. *Calcified Tissue International* 98(4), pp. 341–358. doi: 10.1007/s00223-015-0052-z.

Nemeth, E.F. and Shoback, D. 2013. Calcimimetic and calcilytic drugs for treating bone and mineral-related disorders. *Best Practice & Research Clinical Endocrinology & Metabolism* 27(3), pp. 373–384. doi: 10.1016/j.beem.2013.02.008.

Nemeth, E.F., Steffey, M.E., Hammerland, L.G., Hung, B.C.P., Van Wagenen, B.C., DelMar, E.G. and Balandrin, M.F. 1998. Calcimimetics with potent and selective activity on the parathyroid calcium receptor. *Proceedings of the National Academy of Sciences of the United States of America* 95(7), pp. 4040–4045. doi: 10.1073/PNAS.95.7.4040.

Nesbit, M.A. et al. 2013. Mutations affecting G-protein subunit α11 in hypercalcemia and hypocalcemia. *The New England journal of medicine* 368(26), pp. 2476–2486. doi: 10.1056/NEJMOA1300253.

Newman, D.R., Sills, W.S., Hanrahan, K., Ziegler, A., Tidd, K.M.G., Cook, E. and Sannes, P.L. 2016. Expression of WNT5A in Idiopathic Pulmonary Fibrosis and Its Control by TGF-β and WNT7B in Human Lung Fibroblasts. *Journal of Histochemistry and Cytochemistry* 64(2), pp. 99–111. doi: 10.1369/0022155415617988.

Ng, B., Cook, S.A. and Schafer, S. 2020. Interleukin-11 signaling underlies fibrosis, parenchymal dysfunction, and chronic inflammation of the airway. *Experimental & Molecular Medicine 2020 52:12* 52(12), pp. 1871–1878. doi: 10.1038/s12276-020-00531-5.

NICE 2013. Idiopathic pulmonary fibrosis in adults: diagnosis and management. Available at: https://www.nice.org.uk/guidance/CG163/evidence [Accessed: 14 March 2022].

Nicholson, A.G., Fulford, L.G., Colby, T. V., Du Bois, R.M., Hansell, D.M. and Wells, A.U. 2002. The relationship between individual histologic features and disease progression in idiopathic pulmonary fibrosis. *American journal of respiratory and critical care medicine* 166(2), pp. 173–177. doi: 10.1164/RCCM.2109039.

Nie, Y., Yang, Y., Zhang, J., Cai, G., Chang, Y., Chai, G. and Guo, C. 2017. Shikonin suppresses pulmonary fibroblasts proliferation and activation by

regulating Akt and p38 MAPK signaling pathways. *Biomedicine and Pharmacotherapy* 95, pp. 1119–1128. doi: 10.1016/j.biopha.2017.09.023.

Nigdelioglu, R. et al. 2016. De novo serine synthesis and collagen 1 TGF-ß promotes de novo serine synthesis for collagen production. doi: 10.1074/jbc.M116.756247.

Noguchi, M., Furukawa, K.T. and Morimoto, M. 2021. Pulmonary neuroendocrine cells: Physiology, tissue homeostasis and disease. *DMM Disease Models and Mechanisms* 13(12). doi: 10.1242/DMM.046920.

Noor, S., Nawaz, S. and Chaudhuri, N. 2021. Real-World Study Analysing Progression and Survival of Patients with Idiopathic Pulmonary Fibrosis with Preserved Lung Function on Antifibrotic Treatment. *Advances in Therapy* 38(1), pp. 268–277. doi: 10.1007/S12325-020-01523-7/FIGURES/2.

Nyström, A., Velati, D., Mittapalli, V.R., Fritsch, A., Kern, J.S. and Bruckner-Tuderman, L. 2013. Collagen VII plays a dual role in wound healing. *Journal of Clinical Investigation* 123(8), pp. 3498–3509. doi: 10.1172/JCI68127.

O'Dwyer, D.N. et al. 2013. The toll-like receptor 3 L412F polymorphism and disease progression in idiopathic pulmonary fibrosis. *American Journal of Respiratory and Critical Care Medicine* 188(12), pp. 1442–1450. doi: 10.1164/rccm.201304-0760OC.

O'Dwyer, D.N. et al. 2017. The peripheral blood proteome signature of idiopathic pulmonary fibrosis is distinct from normal and is associated with novel immunological processes. *Scientific reports* 7, p. 46560. doi: 10.1038/srep46560.

O'Dwyer, D.N., Gurczynski, S.J. and Moore, B.B. 2018. Pulmonary immunity and extracellular matrix interactions. *Matrix Biology* 73, pp. 122–134. doi: 10.1016/j.matbio.2018.04.003.

OECD/European Union 2020. *Health at a Glance: Europe 2020*. OECD. doi: 10.1787/82129230-en.

Oku, H. et al. 2008. Antifibrotic action of pirfenidone and prednisolone: Different effects on pulmonary cytokines and growth factors in bleomycin-induced murine pulmonary fibrosis. *European Journal of Pharmacology* 590(1–3), pp. 400–408. doi: 10.1016/j.ejphar.2008.06.046.

Olson, J.W., Atkinson, J.E., Hacker, A.D., Altiere, R.J. and Gillespie, M.N. 1985. Suppression of polyamine biosynthesis prevents monocrotaline-induced pulmonary edema and arterial medial thickening. *Toxicology and Applied Pharmacology* 81(1), pp. 91–99. doi: 10.1016/0041-008X(85)90124-3.

Overed-Sayer, C., Rapley, L., Mustelin, T. and Clarke, D.L. 2014. Are mast cells instrumental for fibrotic diseases? *Frontiers in Pharmacology* 4 JAN, p. 174. doi: 10.3389/FPHAR.2013.00174/BIBTEX.

Pablos, J.L., Carreira, P.E., Serrano, L., Del Castillo, P. and Gomez-Reino, J.J. 1997. Apoptosis and proliferation of fibroblasts during postnatal skin development and scleroderma in the tight-skin mouse. *Journal of Histochemistry and Cytochemistry* 45(5), pp. 711–719. doi:

10.1177/002215549704500509.

Palmer, A.J. and Wallace, H.M. 2010. The polyamine transport system as a target for anticancer drug development. *Amino Acids* 38(2), pp. 415–422. doi: 10.1007/S00726-009-0400-2.

Palmer, S.M. et al. 2018. Randomized, Double-Blind, Placebo-Controlled, Phase 2 Trial of BMS-986020, a Lysophosphatidic Acid Receptor Antagonist for the Treatment of Idiopathic Pulmonary Fibrosis. *Chest* 154(5), pp. 1061–1069. doi: 10.1016/J.CHEST.2018.08.1058.

Pan, L.H., Yamauchi, K., Uzuki, M., Nakanishi, T., Takigawa, M., Inoue, H. and Sawai, T. 2001. Type II alveolar epithelial cells and interstitial fibroblasts express connective tissue growth factor in IPF. *European Respiratory Journal* 17(6), pp. 1220–1227. doi: 10.1183/09031936.01.00074101.

Pandur, P., Maurus, D. and Kühl, M. 2002. Increasingly complex: New players enter the Wnt signaling network. *BioEssays* 24(10), pp. 881–884. doi: 10.1002/bies.10164.

Papiris, S.A. et al. 2018. High levels of IL-6 and IL-8 characterize early-on idiopathic pulmonary fibrosis acute exacerbations. *Cytokine* 102, pp. 168–172. doi: 10.1016/J.CYTO.2017.08.019.

Para, R., Romero, F., George, G. and Summer, R. 2019. Metabolic Reprogramming as a Driver of Fibroblast Activation in PulmonaryFibrosis. *American Journal of the Medical Sciences* 357(5), pp. 394–398. doi: 10.1016/j.amjms.2019.02.003.

Pardo, A. et al. 2005. Up-regulation and profibrotic role of osteopontin in human idiopathic pulmonary fibrosis. *PLoS Medicine* 2(9), pp. 0891–0903. doi: 10.1371/journal.pmed.0020251.

Pardo, A. and Selman, M. 2006. Matrix metalloproteases in aberrant fibrotic tissue remodeling. *Proceedings of the American Thoracic Society* 3(4), pp. 383–388. doi: 10.1513/pats.200601-012TK.

Pardo, A. and Selman, M. 2021. The interplay of the genetic architecture, aging, and environmental factors in the pathogenesis of idiopathic pulmonary fibrosis. *American Journal of Respiratory Cell and Molecular Biology* 64(2), pp. 163–172. doi: 10.1165/RCMB.2020-0373PS.

Pardo, A., Selman, M. and Kaminski, N. 2008. Approaching the degradome in idiopathic pulmonary fibrosis. *International Journal of Biochemistry and Cell Biology* 40(6–7), pp. 1141–1155. doi: 10.1016/j.biocel.2007.11.020.

Park, Y., Reyna-Neyra, A., Philippe, L. and Thoreen, C.C. 2017. mTORC1 Balances Cellular Amino Acid Supply with Demand for Protein Synthesis through Post-transcriptional Control of ATF4. *Cell Reports* 19(6), pp. 1083–1090. doi: 10.1016/j.celrep.2017.04.042.

Parra, E.R., Kairalla, R.A., Ribeiro De Carvalho, C.R., Eher, E. and Capelozzi, V.L. 2007. Inflammatory cell phenotyping of the pulmonary interstitium in idiopathic interstitial pneumonia. *Respiration* 74(2), pp. 159–169. doi: 10.1159/000097133.

Paxson, J.A., Gruntman, A.M., Davis, A.M., Parkin, C.M., Ingenito, E.P. and Hoffman, A.M. 2013. Age Dependence of Lung Mesenchymal Stromal Cell Dynamics Following Pneumonectomy. *Stem Cells and Development* 22(24), p. 3214. doi: 10.1089/SCD.2012.0477.

Pegg, A.E. 2006. Regulation of ornithine decarboxylase. *Journal of Biological Chemistry* 281(21), pp. 14529–14532. doi: 10.1074/jbc.R500031200.

Pegg, A.E. 2013. Toxicity of polyamines and their metabolic products. *Chemical Research in Toxicology* 26(12), pp. 1782–1800. doi: 10.1021/tx400316s.

Pegg, A.E. and Casero, R.A. 2011. Current status of the polyamine research field. *Methods in molecular biology (Clifton, N.J.)* 720, pp. 3–35. doi: 10.1007/978-1-61779-034-8_1.

Pérez-Gómez, C. et al. 2005. Co-expression of glutaminase K and L isoenzymes in human tumour cells. *Biochemical Journal* 386(3), pp. 535–542. doi: 10.1042/BJ20040996.

Peyser, R. et al. 2019. Defining the activated fibroblast population in lung fibrosis using single-cell sequencing. *American Journal of Respiratory Cell and Molecular Biology* 61(1), pp. 74–85. doi: 10.1165/rcmb.2018-0313OC.

Phan, S.H. 2012. Genesis of the myofibroblast in lung injury and fibrosis. *Proceedings of the American Thoracic Society* 9(3), pp. 148–152. doi: 10.1513/pats.201201-011AW.

Phang, J.M., Liu, W., Hancock, C.N. and Fischer, J.W. 2015. Proline metabolism and cancer: Emerging links to glutamine and collagen. *Current Opinion in Clinical Nutrition and Metabolic Care* 18(1), pp. 71–77. doi: 10.1097/MCO.0000000000000121.

Plantier, L., Crestani, B., Wert, S.E., Dehoux, M., Zweytick, B., Guenther, A. and Whitsett, J.A. 2011. Ectopic respiratory epithelial cell differentiation in bronchiolised distal airspaces in idiopathic pulmonary fibrosis. *Thorax* 66(8), pp. 651–657. doi: 10.1136/thx.2010.151555.

Plantier, L., Renaud, H., Respaud, R., Marchand-Adam, S. and Crestani, B. 2016. Transcriptome of cultured lung fibroblasts in idiopathic pulmonary fibrosis: Meta-analysis of publically available microarray datasets reveals repression of inflammation and immunity pathways. *International Journal of Molecular Sciences* 17(12). doi: 10.3390/ijms17122091.

Plataki, M., Koutsopoulos, A. V., Darivianaki, K., Delides, G., Siafakas, N.M. and Bouros, D. 2005. Expression of apoptotic and antiapoptotic markers in epithelial cells in idiopathic pulmonary fibrosis. *Chest* 127(1), pp. 266–274. doi: 10.1378/CHEST.127.1.266.

Platé, M., Guillotin, D. and Chambers, R.C. 2020. The promise of mTOR as a therapeutic target pathway in idiopathic pulmonary fibrosis. *European respiratory review : an official journal of the European Respiratory Society* 29(157). doi: 10.1183/16000617.0269-2020.

Podolanczuk, A.J., Wong, A.W., Saito, S., Lasky, J.A., Ryerson, C.J. and Eickelberg, O. 2021. Update in Interstitial Lung Disease 2020. *American journal*

of respiratory and critical care medicine 203(11), pp. 1343–1352. doi: 10.1164/RCCM.202103-0559UP.

Pomaznoy, M., Ha, B. and Peters, B. 2018. GOnet: A tool for interactive Gene Ontology analysis. *BMC Bioinformatics* 19(1), pp. 1–8. doi: 10.1186/S12859-018-2533-3/FIGURES/2.

Pongracz, J.E. and Stockley, R.A. 2006. Wnt signalling in lung development and diseases. *Respiratory Research* 7(1). doi: 10.1186/1465-9921-7-15.

Posey, K.L., Coustry, F. and Hecht, J.T. 2018. Cartilage oligomeric matrix protein: COMPopathies and beyond. *Matrix Biology* 71–72, pp. 161–173. doi: 10.1016/j.matbio.2018.02.023.

Possemato, R. et al. 2011. Functional genomics reveal that the serine synthesis pathway is essential in breast cancer. *Nature* 476(7360), pp. 346–350. doi: 10.1038/nature10350.

Prasse, A. et al. 2019. BAL Cell Gene Expression Is Indicative of Outcome and Airway Basal Cell Involvement in Idiopathic Pulmonary Fibrosis. *American Journal of Respiratory and Critical Care Medicine* 199(5), pp. 622–630. doi: 10.1164/rccm.201712-2551OC.

Prud'homme, G.J. 2007. Pathobiology of transforming growth factor ß in cancer, fibrosis and immunologic disease, and therapeutic considerations. *Laboratory Investigation* 87(11), pp. 1077–1091. doi: 10.1038/labinvest.3700669.

Puleston, D.J., Buck, M.D., Klein, R.I., Pearce, E.J., Balabanov, S. and Pearce, E.L. 2019. Polyamines and eIF5A Hypusination Modulate Mitochondrial Respiration and Macrophage Activation Graphical Abstract Highlights d The polyamine synthesis pathway and hypusinated eIF5A modulate mitochondrial OXPHOS d Hypusinated eIF5A maintains TCA cycle and ETC integrity in macrophages d Some mitochondrial enzymes depend on eIF5A H for efficient expression d Inhibition of hypusinated eIF5A blunts macrophage alternative activation. *Cell Metabolism* 30, pp. 352–363. doi: 10.1016/j.cmet.2019.05.003.

Pulkkinen, V. et al. 2012. A novel screening method detects herpesviral DNA in the idiopathic pulmonary fibrosis lung. *Annals of Medicine* 44(2), pp. 178–186. doi: 10.3109/07853890.2010.532151.

Quinn, C., Wisse, A. and Manns, S.T. 2019. Clinical course and management of idiopathic pulmonary fibrosis. *Multidisciplinary respiratory medicine* 14(1). doi: 10.1186/S40248-019-0197-0.

Quinn, S.J., Ye, C.-P., Diaz, R., Kifor, O., Bai, M., Vassilev, P. and Brown, E. 1997. The Ca^{2+} -sensing receptor: a target for polyamines. *American Journal of Physiology-Cell Physiology* 273(4), pp. C1315–C1323. doi: 10.1152/ajpcell.1997.273.4.C1315.

R Core Team 2018. R: A language and environment for statistical computing. . Available at: https://www.r-project.org/ [Accessed: 22 November 2021].

Radeff-Huang, J., Seasholtz, T.M., Matteo, R.G. and Brown, J.H. 2004. G protein mediated signaling pathways in lysophospholipid induced cell proliferation and survival. *Journal of cellular biochemistry* 92(5), pp. 949–966. doi:

10.1002/JCB.20094.

Radisky, D.C., Kenny, P.A. and Bissell, M.J. 2007. Fibrosis and Cancer: Do Myofibroblasts Come Also From Epithelial Cells Via EMT? *Journal of cellular biochemistry* 101(4), p. 830. doi: 10.1002/JCB.21186.

Raghu, G. et al. 1991. Azathioprine combined with prednisone in the treatment of idiopathic pulmonary fibrosis: A prospective double-blind, randomized, placebo-controlled clinical trial. *American Review of Respiratory Disease* 144(2), pp. 291–296. doi: 10.1164/ajrccm/144.2.291.

Raghu, G. et al. 2011. An Official ATS/ERS/JRS/ALAT Statement: Idiopathic pulmonary fibrosis: Evidence-based guidelines for diagnosis and management. *American Journal of Respiratory and Critical Care Medicine* 183(6), pp. 788–824. doi: 10.1164/rccm.2009-040GL.

Raghu, G. et al. 2013. Treatment of idiopathic pulmonary fibrosis with ambrisentan: a parallel, randomized trial. *Annals of internal medicine* 158(9), pp. 641–649. doi: 10.7326/0003-4819-158-9-201305070-00003.

Raghu, G. et al. 2015a. An Official ATS/ERS/JRS/ALAT Clinical Practice Guideline: Treatment of Idiopathic Pulmonary Fibrosis. An Update of the 2011 Clinical Practice Guideline. *American Journal of Respiratory and Critical Care Medicine* 192(2), pp. e3–e19. doi: 10.1164/rccm.201506-1063ST.

Raghu, G., Amatto, V.C., Behr, J. and Stowasser, S. 2015b. Comorbidities in idiopathic pulmonary fibrosis patients: a systematic literature review. *The European respiratory journal* 46(4), pp. 1113–1130. doi: 10.1183/13993003.02316-2014.

Raghu, G., Anstrom, K.J., King, T.E., Lasky, J.A. and Martinez, F.J. 2012. Prednisone, Azathioprine, and N -Acetylcysteine for Pulmonary Fibrosis. *New England Journal of Medicine* 366(21), pp. 1968–1977. doi: 10.1056/nejmoa1113354.

Rangarajan, S. et al. 2018. Metformin reverses established lung fibrosis in a bleomycin model. *Nature Medicine* 24(8), pp. 1121–1131. doi: 10.1038/s41591-018-0087-6.

Rayego-Mateos, S. et al. 2013. Connective tissue growth factor is a new ligand of epidermal growth factor receptor. *Journal of Molecular Cell Biology* 5(5), pp. 323–335. doi: 10.1093/jmcb/mjt030.

Rayego-Mateos, S. et al. 2018a. Connective tissue growth factor induces renal fibrosis via epidermal growth factor receptor activation. *Journal of Pathology* 244(2), pp. 227–241. doi: 10.1002/path.5007.

Rayego-Mateos, S., Rodrigues-Diez, R., Morgado-Pascual, J.L., Valentijn, F., Valdivielso, J.M., Goldschmeding, R. and Ruiz-Ortega, M. 2018b. Role of epidermal growth factor receptor (EGFR) and its ligands in kidney inflammation and damage. *Mediators of Inflammation* 2018. doi: 10.1155/2018/8739473.

Ren, Z. et al. 2020. Calcium-Sensing Receptor on Neutrophil Promotes Myocardial Apoptosis and Fibrosis After Acute Myocardial Infarction via NLRP3 Inflammasome Activation. *Canadian Journal of Cardiology* 36(6), pp. 893–905.

doi: 10.1016/j.cjca.2019.09.026.

Renzoni, E.A., Poletti, V. and Mackintosh, J.A. 2021. Disease pathology in fibrotic interstitial lung disease: is it all about usual interstitial pneumonia? *The Lancet* 398(10309), pp. 1437–1449. doi: 10.1016/S0140-6736(21)01961-9.

Rey, O., Young, S.H., Yuan, J., Slice, L. and Rozengurt, E. 2005. Amino acid-stimulated Ca2+ oscillations produced by the Ca 2+-sensing receptor are mediated by a phospholipase C/inositol 1,4,5-trisphosphate-independent pathway that requires G12, Rho, filamin-A, and the actin cytoskeleton. *Journal of Biological Chemistry* 280(24), pp. 22875–22882. doi: 10.1074/jbc.M503455200.

Reyfman, P.A. et al. 2019. Single-cell transcriptomic analysis of human lung provides insights into the pathobiology of pulmonary fibrosis. *American Journal of Respiratory and Critical Care Medicine* 199(12), pp. 1517–1536. doi: 10.1164/rccm.201712-2410OC.

Riario Sforza, G.G. and Marinou, A. 2017. Hypersensitivity pneumonitis: A complex lung disease. *Clinical and Molecular Allergy* 15(1), pp. 1–8. doi: 10.1186/S12948-017-0062-7/TABLES/2.

Ricard-Blum, S. 2011. The Collagen Family. *Cold Spring Harbor Perspectives in Biology* 3(1), pp. 1–19. doi: 10.1101/cshperspect.a004978.

Riccardi, D., Brennan, S.C. and Chang, W. 2013. The extracellular calcium-sensing receptor, CaSR, in fetal development. *Best Practice & Research Clinical Endocrinology & Metabolism* 27(3), pp. 443–453. doi: 10.1016/J.BEEM.2013.02.010.

Riccardi, D. and Brown, E.M. 2010. Physiology and pathophysiology of the calcium-sensing receptor in the kidney. *American journal of physiology. Renal physiology* 298(3), pp. F485-99. doi: 10.1152/ajprenal.00608.2009.

Riccardi, D. and Kemp, P.J. 2012. The Calcium-Sensing Receptor Beyond Extracellular Calcium Homeostasis: Conception, Development, Adult Physiology, and Disease. *Annual Review of Physiology* 74(1), pp. 271–297. doi: 10.1146/annurev-physiol-020911-153318.

Richeldi, L. et al. 2011. Efficacy of a tyrosine kinase inhibitor in idiopathic pulmonary fibrosis. *The New England journal of medicine* 365(12), pp. 1079–1087. doi: 10.1056/NEJMOA1103690.

Richeldi, L. et al. 2014. Efficacy and Safety of Nintedanib in Idiopathic Pulmonary Fibrosis. *New England Journal of Medicine* 370(22), pp. 2071–2082. doi: 10.1056/NEJMoa1402584.

Richeldi, L. et al. 2020. Pamrevlumab, an anti-connective tissue growth factor therapy, for idiopathic pulmonary fibrosis (PRAISE): a phase 2, randomised, double-blind, placebo-controlled trial. *The Lancet Respiratory Medicine* 8(1), pp. 25–33. doi: 10.1016/S2213-2600(19)30262-0.

Rock, J.R. et al. 2011. Multiple stromal populations contribute to pulmonary fibrosis without evidence for epithelial to mesenchymal transition. *Proceedings of the National Academy of Sciences of the United States of America* 108(52), p.

E1475. doi: 10.1073/pnas.1117988108.

Rockey, D.C., Bell, P.D. and Hill, J.A. 2015. Fibrosis — A Common Pathway to Organ Injury and Failure. Longo, D. L. ed. *New England Journal of Medicine* 372(12), pp. 1138–1149. doi: 10.1056/NEJMra1300575.

Rodriguez, L.R. et al. 2018. Global Gene Expression Analysis in an in vitro Fibroblast Model of Idiopathic Pulmonary Fibrosis Reveals Potential Role for CXCL14/CXCR4. *Scientific Reports* 8(1), p. 3983. doi: 10.1038/s41598-018-21889-7.

Rubtsov, Y.P. and Rudensky, A.Y. 2007. TGFβ signalling in control of T-cell-mediated self-reactivity. *Nature Reviews Immunology* 7(6), pp. 443–453. doi: 10.1038/nri2095.

Ruffenach, G., Hong, J., Vaillancourt, M., Medzikovic, L. and Eghbali, M. 2020. Pulmonary hypertension secondary to pulmonary fibrosis: clinical data, histopathology and molecular insights. *Respiratory Research 2020 21:1* 21(1), pp. 1–14. doi: 10.1186/S12931-020-01570-2.

Ruiying, C., Zeyun, L., Yongliang, Y., Zijia, Z., Ji, Z., Xin, T. and Xiaojian, Z. 2020. A comprehensive analysis of metabolomics and transcriptomics in non-small cell lung cancer. *PLoS ONE* 15(5). doi: 10.1371/journal.pone.0232272.

Rybchyn, M.S. et al. 2019. Homer1 mediates CaSR-dependent activation of mTOR complex 2 and initiates a novel pathway for AKT-dependent β-catenin stabilization in osteoblasts. *Journal of Biological Chemistry* 294(44), pp. 16337–16350. doi: 10.1074/jbc.RA118.006587.

Rybczyńska, A., Marchwińska, A., Dyś, A., Boblewski, K., Lehmann, A. and Lewko, B. 2017. Activity of the calcium-sensing receptor influences blood glucose and insulin levels in rats. *Pharmacological reports : PR* 69(4), pp. 709–713. doi: 10.1016/J.PHAREP.2017.01.034.

Rydell-Törmänen, K., Zhou, X.H., Hallgren, O., Einarsson, J., Eriksson, L., Andersson-Sjöland, A. and Westergren-Thorsson, G. 2016. Aberrant nonfibrotic parenchyma in idiopathic pulmonary fibrosis is correlated with decreased β-catenin inhibition and increased Wnt5a/b interaction. *Physiological Reports* 4(5). doi: 10.14814/phy2.12727.

Ryu, J.H., Daniels, C.E., Hartman, T.E. and Yi, E.S. 2007. Diagnosis of Interstitial Lung Diseases. *Mayo Clinic Proceedings* 82(8), pp. 976–986. doi: 10.4065/82.8.976.

Sack, C. and Raghu, G. 2019. Idiopathic pulmonary fibrosis: Unmasking cryptogenic environmental factors. *European Respiratory Journal* 53(2). doi: 10.1183/13993003.01699-2018.

Saini, P., Eyler, D.E., Green, R. and Dever, T.E. 2009. Hypusine-containing protein eIF5A promotes translation elongation. *Nature* 459(7243), pp. 118–121. doi: 10.1038/nature08034.

Salez, F., Gosset, P., Copin, M.C., Lamblin Degros, C., Tonnel, A.B. and Wallaert, B. 1998. Transforming growth factor-beta1 in sarcoidosis. *The European respiratory journal* 12(4), pp. 913–919. doi:

10.1183/09031936.98.12040913.

Samarakoon, R. et al. 2013. Induction of renal fibrotic genes by TGF-ß1 requires EGFR activation, p53 and reactive oxygen species. *Cellular Signalling* 25(11), pp. 2198–2209. doi: 10.1016/j.cellsig.2013.07.007.

Schaefer, C.J., Ruhrmund, D.W., Pan, L., Seiwert, S.D. and Kossen, K. 2011. Antifibrotic activities of pirfenidone in animal models. *European Respiratory Review* 20(120), pp. 85–97. doi: 10.1183/09059180.00001111.

Schafer, S. et al. 2017. IL-11 is a crucial determinant of cardiovascular fibrosis. *Nature* 552(7683), pp. 110–115. doi: 10.1038/nature24676.

Schepelmann, M. et al. 2016. The vascular Ca2+-sensing receptor regulates blood vessel tone and blood pressure. *American journal of physiology. Cell physiology* 310(3), pp. C193-204. doi: 10.1152/ajpcell.00248.2015.

Schreckenberg, R. and Schlüter, K.-D. 2018. Calcium sensing receptor expression and signalling in cardiovascular physiology and disease. *Vascular Pharmacology* 107, pp. 35–42. doi: 10.1016/J.VPH.2018.02.007.

Schuller, A.P., Wu, C.C.C., Dever, T.E., Buskirk, A.R. and Green, R. 2017. eIF5A Functions Globally in Translation Elongation and Termination. *Molecular Cell* 66(2), pp. 194-205.e5. doi: 10.1016/j.molcel.2017.03.003.

Schulze, A. and Harris, A.L. 2012. How cancer metabolism is tuned for proliferation and vulnerable to disruption. *Nature* 491(7424), pp. 364–373. doi: 10.1038/nature11706.

Schwartz, D.A. 2018. Idiopathic pulmonary fibrosis is a genetic disease involving mucus and the peripheral airways. In: *Annals of the American Thoracic Society*. American Thoracic Society, pp. S192–S197. doi: 10.1513/AnnalsATS.201802-144AW.

Schwörer, S. et al. 2020. Proline biosynthesis is a vent for TGFß-induced mitochondrial redox stress. *The EMBO Journal* 39(8). doi: 10.15252/embj.2019103334.

Scruggs, A.M., Grabauskas, G. and Huang, S.K. 2020. The role of KCNMB1 and BK channels in myofibroblast differentiation and pulmonary fibrosis. *American Journal of Respiratory Cell and Molecular Biology* 62(2), pp. 191–203. doi: 10.1165/rcmb.2019-0163OC.

Scruggs, A.M., Koh, H.B., Tripathi, P., Leeper, N.J., White, E.S. and Huang, S.K. 2018. Loss of CDKN2B Promotes Fibrosis via Increased Fibroblast Differentiation Rather Than Proliferation. doi: 10.1165/rcmb.2017-0298OC.

Seibold, M.A. et al. 2011. A Common MUC5B Promoter Polymorphism and Pulmonary Fibrosis. *New England Journal of Medicine* 364(16), pp. 1503–1512. doi: 10.1056/nejmoa1013660.

Seibold, M.A. et al. 2013. The Idiopathic Pulmonary Fibrosis Honeycomb Cyst Contains A Mucocilary Pseudostratified Epithelium. *PLOS ONE* 8(3), p. e58658. doi: 10.1371/JOURNAL.PONE.0058658.

Selman, M., López-Otín, C. and Pardo, A. 2016. Age-driven developmental drift

in the pathogenesis of idiopathic pulmonary fibrosis. *The European respiratory journal* 48(2), pp. 538–52. doi: 10.1183/13993003.00398-2016.

Selman, M. and Pardo, A. 2021. When things go wrong: Exploring possible mechanisms driving the progressive fibrosis phenotype in interstitial lung diseases. *European Respiratory Journal* 58(3). doi: 10.1183/13993003.04507-2020.

Selman, M., Ruiz, V., Cabrera, S., Segura, L., Ramírez, R., Barrios, R. and Pardo, A. 2000. TIMP-1, -2, -3, and -4 in idiopathic pulmonary fibrosis. A prevailing nondegradative lung microenvironment? *American Journal of Physiology - Lung Cellular and Molecular Physiology* 279(3 23-3). doi: 10.1152/ajplung.2000.279.3.l562.

Selman, M., Thannickal, V.J., Pardo, A., Zisman, D.A., Martinez, F.J. and Lynch, J.P. 2004. Idiopathic pulmonary fibrosis: pathogenesis and therapeutic approaches. *Drugs* 64(4), pp. 405–430. doi: 10.2165/00003495-200464040-00005.

Selvarajah, B. et al. 2019. MTORC1 amplifies the ATF4-dependent de novo serine-glycine pathway to supply glycine during TGF-1-induced collagen biosynthesis. *Science Signaling* 12(582). doi: 10.1126/scisignal.aav3048.

Serrano, M., Lin, A.W., McCurrach, M.E., Beach, D. and Lowe, S.W. 1997. Oncogenic ras provokes premature cell senescence associated with accumulation of p53 and p16(INK4a). *Cell* 88(5), pp. 593–602. doi: 10.1016/S0092-8674(00)81902-9.

Sesé, L., Annesi-Maesano, I. and Nunes, H. 2018. Impact of Particulate Matter on the Natural History of IPF: A Matter of Concentrations? *Chest* 154(3), pp. 726–727. doi: 10.1016/j.chest.2018.05.043.

Shah, M., Foreman, D.M. and Ferguson, M.W. 1995. Neutralisation of TGF-beta 1 and TGF-beta 2 or exogenous addition of TGF-beta 3 to cutaneous rat wounds reduces scarring. *Journal of Cell Science* 108(3), pp. 985 LP – 1002.

Shantz, L.M. 2004. Transcriptional and translational control of ornithine decarboxylase during Ras transformation. *Biochemical Journal* 377(1), pp. 257–264. doi: 10.1042/BJ20030778.

Shenderov, K., Collins, S.L., Powell, J.D. and Horton, M.R. 2021. Immune dysregulation as a driver of idiopathic pulmonary fibrosis. *The Journal of Clinical Investigation* 131(2). doi: 10.1172/JCI143226.

Sheng, G. et al. 2020. Viral Infection Increases the Risk of Idiopathic Pulmonary Fibrosis: A Meta-Analysis. *Chest* 157(5), pp. 1175–1187. doi: 10.1016/j.chest.2019.10.032.

Shinde, A. V. and Frangogiannis, N.G. 2014. Fibroblasts in myocardial infarction: a role in inflammation and repair. *Journal of molecular and cellular cardiology* 70, pp. 74–82. doi: 10.1016/J.YJMCC.2013.11.015.

Shivkumar, M., Lawler, C., Milho, R. and Stevenson, P.G. 2016. Herpes Simplex Virus 1 Interaction with Myeloid Cells In Vivo. *Journal of Virology* 90(19), pp. 8661–8672. doi: 10.1128/jvi.00881-16.

Shu, D.Y., Hutcheon, A.E.K., Zieske, J.D. and Guo, X. 2019. Epidermal Growth Factor Stimulates Transforming Growth Factor-Beta Receptor Type II Expression In Corneal Epithelial Cells. *Scientific Reports* 9(1), pp. 1–11. doi: 10.1038/s41598-019-42969-2.

Sides, M.D. et al. 2012. The Epstein-Barr Virus Latent Membrane Protein 1 and Transforming Growth Factor–β1 Synergistically Induce Epithelial–Mesenchymal Transition in Lung Epithelial Cells. *https://doi.org/10.1165/rcmb.2009-0232OC* 44(6), pp. 852–862. doi: 10.1165/RCMB.2009-0232OC.

Sievert, H. et al. 2014. A novel mouse model for inhibition of DOHH-mediated hypusine modification reveals a crucial function in embryonic development, proliferation and oncogenic transformation. *DMM Disease Models and Mechanisms* 7(8), pp. 963–976. doi: 10.1242/dmm.014449.

Sime, P.J., Xing, Z., Graham, F.L., Csaky, K.G. and Gauldie, J. 1997. Adenovector-mediated gene transfer of active transforming growth factor-beta1 induces prolonged severe fibrosis in rat lung. *The Journal of clinical investigation* 100(4), pp. 768–776. doi: 10.1172/JCI119590.

Smith, J.S., Lefkowitz, R.J. and Rajagopal, S. 2018. Biased Signalling: From Simple Switches to Allosteric Microprocessors. *Nature reviews. Drug discovery* 17(4), p. 243. doi: 10.1038/NRD.2017.229.

Smith, K.A., Ayon, R.J., Tang, H., Makino, A. and Yuan, J.X.-J. 2016. Calcium-Sensing Receptor Regulates Cytosolic [Ca2+] and Plays a Major Role in the Development of Pulmonary Hypertension. *Frontiers in Physiology* 7, p. 517. doi: 10.3389/fphys.2016.00517.

Soares-Silva, M., Diniz, F.F., Gomes, G.N. and Bahia, D. 2016. The mitogen-activated protein kinase (MAPK) pathway: Role in immune evasion by trypanosomatids. *Frontiers in Microbiology* 7(FEB), p. 183. doi: 10.3389/FMICB.2016.00183/BIBTEX.

Sorokin, S.P., Hoyt, R.F. and Shaffer, M.J. 1997. Ontogeny of neuroepithelial bodies: Correlations with mitogenesis and innervation. *Microscopy Research and Technique* 37(1), pp. 43–61. doi: 10.1002/(SICI)1097-0029(19970401)37:1<43::AID-JEMT5>3.0.CO;2-X.

Soulet, D., Gagnon, B., Rivest, S., Audette, M. and Poulin, R. 2004. A fluorescent probe of polyamine transport accumulates into intracellular acidic vesicles via a two-step mechanism. *Journal of Biological Chemistry* 279(47), pp. 49355–49366. doi: 10.1074/jbc.M401287200.

Spanjer, A.I.R. et al. 2016. TGF-β-induced profibrotic signaling is regulated in part by the WNT receptor Frizzled-8. *The FASEB Journal* 30(5), pp. 1823–1835. doi: 10.1096/fj.201500129.

Sriram, K. and Insel, P.A. 2018. G Protein-Coupled Receptors as Targets for Approved Drugs: How Many Targets and How Many Drugs? *Molecular pharmacology* 93(4), pp. 251–258. doi: 10.1124/MOL.117.111062.

Stewart, C.A. and Dell'orco, R.T. 1992. Age related decline in the expression of proliferating cell nuclear antigen in human diploid fibroblasts. *Mechanisms of*

Ageing and Development 66(1), pp. 71–80. doi: 10.1016/0047-6374(92)90074-N.

Stoimenov, I. and Helleday, T. 2009. PCNA on the crossroad of cancer. In: *Biochemical Society Transactions*. Portland Press, pp. 605–613. doi: 10.1042/BST0370605.

Stum, M.G. et al. 2021. Genetic analysis of Pycr1 and Pycr2 in mice . *Genetics* . doi: 10.1093/genetics/iyab048.

Subramaniam, M. et al. 2003. Bombesin-like peptides and mast cell responses: relevance to bronchopulmonary dysplasia? *American journal of respiratory and critical care medicine* 168(5), pp. 601–611. doi: 10.1164/RCCM.200212-1434OC.

Sun, J., Li, Z.M., Hu, Z.Y., Zeng, Z.L., Yang, D.J. and Jiang, W.Q. 2009. Apogossypolone inhibits cell growth by inducing cell cycle arrest in U937 cells. *Oncology Reports* 22(1), pp. 193–198. doi: 10.3892/or_00000424.

Sun, K.H., Chang, Y., Reed, N.I. and Sheppard, D. 2016. α-smooth muscle actin is an inconsistent marker of fibroblasts responsible for force-dependent TGFβ activation or collagen production across multiple models of organ fibrosis. *American Journal of Physiology - Lung Cellular and Molecular Physiology* 310(9), pp. L824–L836. doi: 10.1152/ajplung.00350.2015.

Sun, T. et al. 2021. TGFβ2 and TGFβ3 isoforms drive fibrotic disease pathogenesis. *Science Translational Medicine* 13(605), p. eabe0407. doi: 10.1126/scitranslmed.abe0407.

Sundararaman, S.S. and van der Vorst, E.P.C. 2021. Calcium-sensing receptor (Casr), its impact on inflammation and the consequences on cardiovascular health. *International Journal of Molecular Sciences* 22(5), pp. 1–16. doi: 10.3390/ijms22052478.

Sunday, M.E. 2014. Oxygen, Gastrin-Releasing Peptide, and Pediatric Lung Disease: Life in the Balance. *Frontiers in Pediatrics* 2, p. 72. doi: 10.3389/fped.2014.00072.

Tager, A.M. et al. 2008. The lysophosphatidic acid receptor LPA1 links pulmonary fibrosis to lung injury by mediating fibroblast recruitment and vascular leak. *Nature medicine* 14(1), pp. 45–54. doi: 10.1038/NM1685.

Tan, J. et al. 2016. Expression of RXFP1 Is Decreased in Idiopathic Pulmonary Fibrosis. Implications for Relaxin-based Therapies. *American journal of respiratory and critical care medicine* 194(11), pp. 1392–1402. doi: 10.1164/RCCM.201509-1865OC.

Tan, R. et al. 2020. Phenylalanine induces pulmonary hypertension through calcium-sensing receptor activation. *American Journal of Physiology - Lung Cellular and Molecular Physiology* 319(6), pp. L1010–L1020. doi: 10.1152/AJPLUNG.00215.2020/ASSET/IMAGES/LARGE/AJ-ALUN200025F005.JPEG.

Tan, W.S.D., Liao, W., Zhou, S., Mei, D. and Wong, W.S.F. 2018. Targeting the renin-angiotensin system as novel therapeutic strategy for pulmonary diseases. *Current opinion in pharmacology* 40, pp. 9–17. doi: 10.1016/J.COPH.2017.12.002.

Tang, B. et al. 1998. Transforming growth factor-beta1 is a new form of tumor suppressor with true haploid insufficiency. *Nature medicine* 4(7), pp. 802–807. doi: 10.1038/NM0798-802.

Tang, H. et al. 2016. Pathogenic role of calcium-sensing receptors in the development and progression of pulmonary hypertension. *American Journal of Physiology - Lung Cellular and Molecular Physiology* 310(9), pp. L846–L859. doi: 10.1152/ajplung.00050.2016.

Tarride, J.-E. et al. 2018. Clinical and economic burden of idiopathic pulmonary fibrosis in Quebec, Canada. *ClinicoEconomics and outcomes research : CEOR* 10, pp. 127–137. doi: 10.2147/CEOR.S154323.

Taskar, V. and Coultas, D. 2008. Exposures and idiopathic lung disease. *Seminars in Respiratory and Critical Care Medicine* 29(6), pp. 670–679. doi: 10.1055/s-0028-1101277.

Taskar, V.S. and Coultas, D.B. 2006. Is idiopathic pulmonary fibrosis an environmental disease? *Proceedings of the American Thoracic Society* 3(4), pp. 293–298. doi: 10.1513/pats.200512-131TK.

Tcherakian, C. et al. 2011. Progression of idiopathic pulmonary fibrosis: lessons from asymmetrical disease. *Thorax* 66(3), pp. 226–231. doi: 10.1136/THX.2010.137190.

Tfelt-Hansen, J. et al. 2003. Calcium-sensing receptor stimulates PTHrP release by pathways dependent on PKC, p38 MAPK, JNK, and ERK1/2 in H-500 cells. *American Journal of Physiology - Endocrinology and Metabolism* 285(2 48-2). doi: 10.1152/AJPENDO.00489.2002/ASSET/IMAGES/LARGE/H10731371005.JPEG.

Thai, M. et al. 2015. MYC-induced reprogramming of glutamine catabolism supports optimal virus replication. *Nature Communications* 6. doi: 10.1038/ncomms9873.

Thakker, R. V. 2004. Diseases associated with the extracellular calcium-sensing receptor. *Cell Calcium* 35(3), pp. 275–282. doi: 10.1016/J.CECA.2003.10.010.

Thannickal, V.J. et al. 2015. Blue Journal Conference. Aging and Susceptibility to Lung Disease. *https://doi.org/10.1164/rccm.201410-1876PP* 191(3), pp. 261–269. doi: 10.1164/RCCM.201410-1876PP.

Thermo Fisher Scientific [no date]. Fura-2 Calcium Indicator | Thermo Fisher Scientific - UK. Available at: https://www.thermofisher.com/uk/en/home/industrial/pharma-biopharma/drug-discovery-development/target-and-lead-identification-and-validation/g-protein-coupled/cell-based-second-messenger-assays/fura-2-calcium-indicator.html [Accessed: 25 November 2021].

Thomas, B. and Beal, M.F. 2010. Mitochondrial therapies for Parkinson's disease. *Movement Disorders* 25(SUPPL. 1). doi: 10.1002/mds.22781.

Thomsen, A.R.B., Hvidtfeldt, M. and Bräuner-Osborne, H. 2012. Biased agonism of the calcium-sensing receptor. *Cell calcium* 51(2), pp. 107–116. doi: 10.1016/J.CECA.2011.11.009.

Tighe, R.M. et al. 2019. Immediate Release of Gastrin-Releasing Peptide Mediates Delayed Radiation-Induced Pulmonary Fibrosis. *The American journal of pathology* 189(5), pp. 1029–1040. doi: 10.1016/j.ajpath.2019.01.017.

Tomlins, S.A., Bolllinger, N., Creim, J. and Rodland, K.D. 2005. Cross-talk between the calcium-sensing receptor and the epidermal growth factor receptor in Rat-1 fibroblasts. *Experimental Cell Research* 308(2), pp. 439–445. doi: 10.1016/j.yexcr.2005.04.032.

Torres, M.A., Yang-Snyder, J.A., Purcell, S.M., DeMarais, A.A., McGrew, L.L. and Moon, R.T. 1996. Activities of the Wnt-1 class of secreted signaling factors are antagonized by the Wnt-5A class and by a dominant negative cadherin in early Xenopus development. *Journal of Cell Biology* 133(5), pp. 1123–1137. doi: 10.1083/jcb.133.5.1123.

Tsuchiya, K. et al. 2007. Elemental analysis of inorganic dusts in lung tissues of interstitial pneumonias. *Journal of Medical and Dental Sciences* 54(1), pp. 9–16.

Tsukamoto, K., Hayakawa, H., Sato, A., Chida, K., Nakamura, H. and Miura, K. 2000. Involvement of Epstein-Barr virus latent membrane protein 1 in disease progression in patients with idiopathic pulmonary fibrosis. *Thorax* 55(11), pp. 958–961. doi: 10.1136/THORAX.55.11.958.

Tsukui, T. et al. 2020. Collagen-producing lung cell atlas identifies multiple subsets with distinct localization and relevance to fibrosis. *Nature Communications* 11(1), pp. 1–16. doi: 10.1038/s41467-020-15647-5.

Tzouvelekis, A. et al. 2020. Impact of Depression on Patients With Idiopathic Pulmonary Fibrosis. *Frontiers in Medicine* 7, p. 29. doi: 10.3389/fmed.2020.00029.

Uemura, T. et al. 2008. Identification and Characterization of a Diamine Exporter in Colon Epithelial Cells. *The Journal of Biological Chemistry* 283(39), p. 26428. doi: 10.1074/JBC.M804714200.

Uemura, T., Stringer, D.E., Blohm-Mangone, K.A. and Gerner, E.W. 2010. Polyamine transport is mediated by both endocytic and solute carrier transport mechanisms in the gastrointestinal tract. *American Journal of Physiology-Gastrointestinal and Liver Physiology* 299(2), pp. G517–G522. doi: 10.1152/ajpgi.00169.2010.

Uguccioni, M. et al. 1995. Endothelin-1 in idiopathic pulmonary fibrosis. *Journal of clinical pathology* 48(4), pp. 330–334. doi: 10.1136/JCP.48.4.330.

Uhlén, M. et al. 2015. Tissue-based map of the human proteome. *Science* 347(6220). doi: 10.1126/science.1260419.

Upagupta, C., Shimbori, C., Alsilmi, R. and Kolb, M. 2018. Matrix abnormalities in pulmonary fibrosis. *European respiratory review : an official journal of the European Respiratory Society* 27(148), p. 180033. doi: 10.1183/16000617.0033-2018.

Ushakumary, M.G., Riccetti, M. and Perl, A.K.T. 2021. Resident interstitial lung fibroblasts and their role in alveolar stem cell niche development, homeostasis, injury, and regeneration. *STEM CELLS Translational Medicine* 10(7), pp. 1021–

1032. doi: 10.1002/SCTM.20-0526.

Vancheri, C. 2013. Common pathways in idiopathic pulmonary fibrosis and cancer. *European respiratory review : an official journal of the European Respiratory Society* 22(129), pp. 265–72. doi: 10.1183/09059180.00003613.

Vancheri, C., Failla, M., Crimi, N. and Raghu, G. 2010. Idiopathic pulmonary fibrosis: a disease with similarities and links to cancer biology. *The European respiratory journal* 35(3), pp. 496–504. doi: 10.1183/09031936.00077309.

Varet, H., Brillet-Guéguen, L., Coppée, J.Y. and Dillies, M.A. 2016. SARTools: A DESeq2- and EdgeR-Based R Pipeline for Comprehensive Differential Analysis of RNA-Seq Data. *PLOS ONE* 11(6), p. e0157022. doi: 10.1371/JOURNAL.PONE.0157022.

Verckist, L., Lembrechts, R., Thys, S., Pintelon, I., Timmermans, J.-P., Brouns, I. and Adriaensen, D. 2017. Selective gene expression analysis of the neuroepithelial body microenvironment in postnatal lungs with special interest for potential stem cell characteristics. *Respiratory Research* 18(1), p. 87. doi: 10.1186/s12931-017-0571-4.

Verckist, L., Pintelon, I., Timmermans, J.-P., Brouns, I. and Adriaensen, D. 2018. Selective activation and proliferation of a quiescent stem cell population in the neuroepithelial body microenvironment. *Respiratory Research* 19(1), p. 207. doi: 10.1186/s12931-018-0915-8.

Vu, T.N., Chen, X., Foda, H.D., Smaldone, G.C. and Hasaneen, N.A. 2019. Interferon-γenhances the antifibrotic effects of pirfenidone by attenuating IPF lung fibroblast activation and differentiation. *Respiratory Research* 20(1), p. 206. doi: 10.1186/s12931-019-1171-2.

Vuga, L.J., Ben-Yehudah, A., Kovkarova-Naumovski, E., Oriss, T., Gibson, K.F., Feghali-Bostwick, C. and Kaminski, N. 2009. WNT5A is a regulator of fibroblast proliferation and resistance to apoptosis. *American Journal of Respiratory Cell and Molecular Biology* 41(5), pp. 583–589. doi: 10.1165/rcmb.2008-0201OC.

Wallis, A. and Spinks, K. 2015. The diagnosis and management of interstitial lung diseases. *BMJ (Clinical research ed.)* 350. doi: 10.1136/BMJ.H2072.

Wang, H., Wu, C., Wan, S., Zhang, H., Zhou, S. and Liu, G. 2013. Shikonin attenuates lung cancer cell adhesion to extracellular matrix and metastasis by inhibiting integrin ß1 expression and the ERK1/2 signaling pathway. *Toxicology* 308, pp. 104–112. doi: 10.1016/j.tox.2013.03.015.

Wang, J.Y., Viar, M.J., Li, J.I., Shi, H.J., Mccormack, S.A. and Johnson, L.R. 1997. Polyamines are necessary for normal expression of the transforming growth factor-ß gene during cell migration. *American Journal of Physiology - Gastrointestinal and Liver Physiology* 272(4 35-4). doi: 10.1152/ajpgi.1997.272.4.g713.

Wang, K. et al. 2020. CD147-spike protein is a novel route for SARS-CoV-2 infection to host cells. *Signal Transduction and Targeted Therapy* 5(1). doi: 10.1038/s41392-020-00426-x.

Wang, L., Kong, W., Liu, B. and Zhang, X. 2018. Proliferating cell nuclear

antigen promotes cell proliferation and tumorigenesis by up-regulating STAT3 in non-small cell lung cancer. *Biomedicine and Pharmacotherapy* 104, pp. 595–602. doi: 10.1016/j.biopha.2018.05.071.

Wang, W., Schulze, C.J., Suarez-Pinzon, W.L., Dyck, J.R.B., Sawicki, G. and Schulz, R. 2002. Intracellular action of matrix metalloproteinase-2 accounts for acute myocardial ischemia and reperfusion injury. *Circulation* 106(12), pp. 1543–1549. doi: 10.1161/01.CIR.0000028818.33488.7B.

Ward, D.T., McLarnon, S.J. and Riccardi, D. 2002. Aminoglycosides increase intracellular calcium levels and ERK activity in proximal tubular OK cells expressing the extracellular calcium-sensing receptor. *Journal of the American Society of Nephrology : JASN* 13(6), pp. 1481–1489. doi: 10.1097/01.ASN.0000015623.73739.B8.

Warheit-Niemi, H.I., Hult, E.M. and Moore, B.B. 2019. A pathologic two-way street: how innate immunity impacts lung fibrosis and fibrosis impacts lung immunity. *Clinical and Translational Immunology* 8(6). doi: 10.1002/cti2.1065.

Warshamana, G.S., Pociask, D.A., Fisher, K.J., Liu, J.Y., Sime, P.J. and Brody, A.R. 2002. Titration of non-replicating adenovirus as a vector for transducing active TGF-beta1 gene expression causing inflammation and fibrogenesis in the lungs of C57BL/6 mice. *International journal of experimental pathology* 83(4), pp. 183–202. doi: 10.1046/J.1365-2613.2002.00229.X.

Watts, K.L., Cottrell, E., Hoban, P.R. and Spiteri, M.A. 2006. RhoA signaling modulates cyclin D1 expression in human lung fibroblasts; implications for idiopathic pulmonary fibrosis. *Respiratory Research* 7(1). doi: 10.1186/1465-9921-7-88.

Wei, J., Marangoni, R.G., Fang, F., Wang, W., Huang, J., Distler, J.H.W. and Varga, J. 2018. The non-neuronal cyclin-dependent kinase 5 is a fibrotic mediator potentially implicated in systemic sclerosis and a novel therapeutic target. *Oncotarget* 9(12), pp. 10294–10306. doi: 10.18632/oncotarget.23516.

Wei, Y. et al. 2017. Fibroblast-specific inhibition of TGF-β1 signaling attenuates lung and tumor fibrosis. *The Journal of clinical investigation* 127(10), pp. 3675–3688. doi: 10.1172/JCI94624.

White, E.S. 2015. Lung extracellular matrix and fibroblast function. *Annals of the American Thoracic Society* 12(Suppl 1), pp. S30–S33. doi: 10.1513/ANNALSATS.201406-240MG/SUPPL_FILE/DISCLOSURES.PDF.

WHO 2018. Ageing and health. Available at: https://www.who.int/news-room/fact-sheets/detail/ageing-and-health [Accessed: 30 September 2021].

Wicher, S.A., Roos, B.B., Teske, J.J., Fang, Y.H., Pabelick, C. and Prakash, Y.S. 2021. Aging increases senescence, calcium signaling, and extracellular matrix deposition in human airway smooth muscle. *PLOS ONE* 16(7), p. e0254710. doi: 10.1371/JOURNAL.PONE.0254710.

Willis, B.C. and Borok, Z. 2007. TGF-β-induced EMT: Mechanisms and implications for fibrotic lung disease. *American Journal of Physiology - Lung Cellular and Molecular Physiology* 293(3). doi: 10.1152/ajplung.00163.2007.

Wilson, M.S. and Wynn, T.A. 2009. Pulmonary fibrosis: pathogenesis, etiology and regulation. *Mucosal immunology* 2(2), pp. 103–21. doi: 10.1038/mi.2008.85.

Win, T. et al. 2018. Pulmonary 18F-FDG uptake helps refine current risk stratification in idiopathic pulmonary fibrosis (IPF). *European Journal of Nuclear Medicine and Molecular Imaging* 45(5), pp. 806–815. doi: 10.1007/s00259-017-3917-8.

Winterbottom, C.J. et al. 2018. Exposure to Ambient Particulate Matter Is Associated With Accelerated Functional Decline in Idiopathic Pulmonary Fibrosis. *Chest* 153(5), pp. 1221–1228. doi: 10.1016/J.CHEST.2017.07.034.

Winters, N.I., Burman, A., Kropski, J.A. and Blackwell, T.S. 2019. Epithelial Injury and Dysfunction in the Pathogenesis of Idiopathic PulmonaryFibrosis. *The American journal of the medical sciences* 357(5), pp. 374–378. doi: 10.1016/J.AMJMS.2019.01.010.

WMA 2013. World Medical Association Declaration of Helsinki: ethical principles for medical research involving human subjects. *JAMA* 310(20), pp. 2191–2194. doi: 10.1001/JAMA.2013.281053.

Wolff, E.C., Young Bok Lee, Soo Il Chung, Folk, J.E. and Myung Hee Park 1995. Deoxyhypusine synthase from rat testis: Purification and characterization. *Journal of Biological Chemistry* 270(15), pp. 8660–8666. doi: 10.1074/jbc.270.15.8660.

Wollin, L., Wex, E., Pautsch, A., Schnapp, G., Hostettler, K.E., Stowasser, S. and Kolb, M. 2015. Mode of action of nintedanib in the treatment of idiopathic pulmonary fibrosis. *The European respiratory journal* 45(5), pp. 1434–45. doi: 10.1183/09031936.00174914.

Wolters, P.J., Collard, H.R. and Jones, K.D. 2014. Pathogenesis of idiopathic pulmonary fibrosis. *Annual Review of Pathology: Mechanisms of Disease* 9, pp. 157–179. doi: 10.1146/annurev-pathol-012513-104706.

Woodcock, H. V. et al. 2019. The mTORC1/4E-BP1 axis represents a critical signaling node during fibrogenesis. *Nature Communications* 10(1). doi: 10.1038/s41467-018-07858-8.

Wright, C.E., Fraser, S.D., Brindle, K., Morice, A.H., Hart, S.P. and Crooks, M.G. 2017. Inhaled beclomethasone/formoterol in idiopathic pulmonary fibrosis: a randomised controlled exploratory study. *ERJ open research* 3(4). doi: 10.1183/23120541.00100-2017.

Wu, B., Crampton, S.P. and Hughes, C.C.W. 2007. Wnt Signaling Induces Matrix Metalloproteinase Expression and Regulates T Cell Transmigration. *Immunity* 26(2), pp. 227–239. doi: 10.1016/j.immuni.2006.12.007.

Wu, C.H., Tang, S.C., Wang, P.H., Lee, H. and Ko, J.L. 2012. Nickel-induced epithelial-mesenchymal transition by reactive oxygen species generation and E-cadherin promoter hypermethylation. *Journal of Biological Chemistry* 287(30), pp. 25292–25302. doi: 10.1074/jbc.M111.291195.

Wu, H. et al. 2016. Resveratrol ameliorates myocardial fibrosis by inhibiting ROS/ERK/TGF-ß/periostin pathway in STZ-induced diabetic mice. *BMC*

Cardiovascular Disorders 16(1), p. 5. doi: 10.1186/s12872-015-0169-z.

Wu, H. et al. 2020a. Progressive Pulmonary Fibrosis Is Caused by Elevated Mechanical Tension on Alveolar Stem Cells. *Cell* 180(1), pp. 107-121.e17. doi: 10.1016/J.CELL.2019.11.027.

Wu, H., Zhao, H. and Chen, L. 2020b. Deoxyshikonin Inhibits Viability and Glycolysis by Suppressing the Akt/mTOR Pathway in Acute Myeloid Leukemia Cells. *Frontiers in Oncology* 0, p. 1253. doi: 10.3389/FONC.2020.01253.

Wu, S., Platteau, A., Chen, S., McNamara, G., Whitsett, J. and Bancalari, E. 2010. Conditional Overexpression of Connective Tissue Growth Factor Disrupts Postnatal Lung Development. *American Journal of Respiratory Cell and Molecular Biology* 42(5), p. 552. doi: 10.1165/RCMB.2009-0068OC.

Wu, Y. et al. 2021. Serum lactate dehydrogenase activities as systems biomarkers for 48 types of human diseases. *Scientific Reports 2021 11:1* 11(1), pp. 1–8. doi: 10.1038/s41598-021-92430-6.

Wuyts, W.A. et al. 2013. The pathogenesis of pulmonary fibrosis: a moving target. *The European respiratory journal* 41(5), pp. 1207–1218. doi: 10.1183/09031936.00073012.

Wygrecka, M., Zakrzewicz, D., Taborski, B., Didiasova, M., Kwapiszewska, G., Preissner, K.T. and Markart, P. 2012. TGF-β1 induces tissue factor expression in human lung fibroblasts in a PI3K/JNK/Akt-dependent and AP-1-dependent manner. *American Journal of Respiratory Cell and Molecular Biology* 47(5), pp. 614–627. doi: 10.1165/rcmb.2012-0097OC.

Wynn, T.A. 2007. Common and unique mechanisms regulate fibrosis in various fibroproliferative diseases. *Journal of Clinical Investigation* 117(3), pp. 524–529. doi: 10.1172/JCI31487.

Wynn, T.A. 2011. Integrating mechanisms of pulmonary fibrosis. *The Journal of experimental medicine* 208(7), pp. 1339–50. doi: 10.1084/jem.20110551.

Xia, J., Psychogios, N., Young, N. and Wishart, D.S. 2009. MetaboAnalyst: a web server for metabolomic data analysis and interpretation. *Nucleic acids research* 37(Web Server issue). doi: 10.1093/NAR/GKP356.

Xie, N. et al. 2015. Glycolytic Reprogramming in Myofibroblast Differentiation and Lung Fibrosis. *American Journal of Respiratory and Critical Care Medicine* 192(12), pp. 1462–1474. doi: 10.1164/rccm.201504-0780OC.

Xie, N. et al. 2020. NAD+ metabolism: pathophysiologic mechanisms and therapeutic potential. *Signal Transduction and Targeted Therapy 2020 5:1* 5(1), pp. 1–37. doi: 10.1038/s41392-020-00311-7.

Xie, T. et al. 2016. Transcription factor TBX4 regulates myofibroblast accumulation and lung fibrosis. *Journal of Clinical Investigation* 126(8), pp. 3063–3079. doi: 10.1172/JCI85328.

Xie, T. et al. 2018. Single-Cell Deconvolution of Fibroblast Heterogeneity in Mouse Pulmonary Fibrosis. *Cell Reports* 22(13), pp. 3625–3640. doi: 10.1016/j.celrep.2018.03.010.

Xu, D. and Hemler, M.E. 2005. Metabolic activation-related CD147-CD98 complex. *Molecular and Cellular Proteomics* 4(8), pp. 1061–1071. doi: 10.1074/mcp.M400207-MCP200.

Xu, S. et al. 2014. Proteomic analysis of the human cyclindependent kinase family reveals a novel CDK5 complex involved in cell growth and migration. *Molecular and Cellular Proteomics* 13(11), pp. 2986–3000. doi: 10.1074/mcp.M113.036699.

Xu, Y. et al. 2016. Single-cell RNA sequencing identifies diverse roles of epithelial cells in idiopathic pulmonary fibrosis. *JCI Insight* 1(20). doi: 10.1172/jci.insight.90558.

Yamaguchi, M. et al. 2016. Fibroblastic foci, covered with alveolar epithelia exhibiting epithelial–mesenchymal transition, destroy alveolar septa by disrupting blood flow in idiopathic pulmonary fibrosis. *Laboratory Investigation 2017 97:3* 97(3), pp. 232–242. doi: 10.1038/labinvest.2016.135.

Yamamura, A. et al. 2012. Enhanced Ca(2+)-sensing receptor function in idiopathic pulmonary arterial hypertension. *Circulation research* 111(4), pp. 469–81. doi: 10.1161/CIRCRESAHA.112.266361.

Yang, C. et al. 2014. Glutamine oxidation maintains the TCA cycle and cell survival during impaired mitochondrial pyruvate transport. *Molecular Cell* 56(3), pp. 414–424. doi: 10.1016/j.molcel.2014.09.025.

Yang, X.H. et al. 2020. Integrated Non-targeted and Targeted Metabolomics Uncovers Amino Acid Markers of Oral Squamous Cell Carcinoma. *Frontiers in Oncology* 10, p. 426. doi: 10.3389/fonc.2020.00426.

Yano, S., Macleod, R.J., Chattopadhyay, N., Tfelt-Hansen, J., Kifor, O., Butters, R.R. and Brown, E.M. 2004. Calcium-sensing receptor activation stimulates parathyroid hormone-related protein secretion in prostate cancer cells: Role of epidermal growth factor receptor transactivation. *Bone* 35(3), pp. 664–672. doi: 10.1016/j.bone.2004.04.014.

Yarova, P. et al. 2016. Inhaled calcilytics: effects on airway inflammation and remodeling. *Respiratory Drug Delivery* 1, pp. 1–12.

Yarova, P.L. et al. 2015. Calcium-sensing receptor antagonists abrogate airway hyperresponsiveness and inflammation in allergic asthma. *Science translational medicine* 7(284), p. 284ra60. doi: 10.1126/scitranslmed.aaa0282.

Yarova, P.L. et al. 2020. Characterisation of negative allosteric modulators of the calcium-sensing receptor, CaSR, for repurposing as a treatment for asthma. *Journal of Pharmacology and Experimental Therapeutics* 376(1), pp. 51–63. doi: 10.1124/JPET.120.000281.

Yates, A.D. et al. 2020. Ensembl 2020. *Nucleic acids research* 48(D1), pp. D682–D688. doi: 10.1093/NAR/GKZ966.

Yi, E.S. et al. 1996. Radiation-induced lung injury in vivo: expression of transforming growth factor-beta precedes fibrosis. *Inflammation* 20(4), pp. 339–352. doi: 10.1007/BF01486737.

Yoshihara, T. et al. 2020. Periostin plays a critical role in the cell cycle in lung fibroblasts. *Respiratory Research* 21(1), p. 38. doi: 10.1186/s12931-020-1299-0.

Yu, M. et al. 2019. Increased circulating Wnt5a protein in patients with rheumatoid arthritis-associated interstitial pneumonia (RA-ILD). *Immunobiology* 224(4), pp. 551–559. doi: 10.1016/J.IMBIO.2019.04.006.

Yuan, H. et al. 2019. Calcium-sensing receptor promotes high glucose-induced myocardial fibrosis via upregulation of the TGF-β1/Smads pathway in cardiac fibroblasts. *Molecular Medicine Reports* . doi: 10.3892/mmr.2019.10330.

Yuan, H. et al. 2020. Activation of calcium-sensing receptor-mediated autophagy in high glucose-induced cardiac fibrosis in vitro. *Molecular Medicine Reports* 22(3), p. 2021. doi: 10.3892/MMR.2020.11277.

Yue, X., Shan, B. and A. Lasky, J. 2010. TGF-β : Titan of Lung Fibrogenesis. *Current Enzyme Inhibition* 6(2), pp. 67–77. doi: 10.2174/157340810791233033.

Zanin, S., Lidron, E., Rizzuto, R. and Pallafacchina, G. 2019. Methods to Measure Intracellular Ca<Superscript>2+</Superscript> Concentration Using Ca<Superscript>2+</Superscript>-Sensitive Dyes. *Methods in Molecular Biology* 1925, pp. 43–58. doi: 10.1007/978-1-4939-9018-4_4.

Zank, D.C., Bueno, M., Mora, A.L. and Rojas, M. 2018. Idiopathic Pulmonary Fibrosis: Aging, Mitochondrial Dysfunction, and Cellular Bioenergetics. *Frontiers in Medicine* 5, p. 10. doi: 10.3389/fmed.2018.00010.

Zhan, T., Rindtorff, N. and Boutros, M. 2017. Wnt signaling in cancer. *Oncogene* 36(11), pp. 1461–1473. doi: 10.1038/onc.2016.304.

Zhang, H.Y., Gharaee-Kermani, M., Zhang, K., Karmiol, S. and Phan, S.H. 1996. Lung fibroblast alpha-smooth muscle actin expression and contractile phenotype in bleomycin-induced pulmonary fibrosis. *The American Journal of Pathology* 148(2), p. 527.

Zhang, J., Cicero, S.A., Wang, L., Romito-DiGiacomo, R.R., Yang, Y. and Herrup, K. 2008. Nuclear localization of Cdk5 is a key determinant in the postmitotic state of neurons. *Proceedings of the National Academy of Sciences of the United States of America* 105(25), pp. 8772–8777. doi: 10.1073/pnas.0711355105.

Zhang, M., Wang, H. and Tracey, K.J. 2000. Regulation of macrophage activation and inflammation by spermine: A new chapter in an old story. *Critical Care Medicine* 28(4 SUPPL.). doi: 10.1097/00003246-200004001-00007.

Zhang, Q. et al. 2018. The transient receptor potential vanilloid-3 regulates hypoxia-mediated pulmonary artery smooth muscle cells proliferation via PI3K/AKT signaling pathway. *Cell Proliferation* 51(3). doi: 10.1111/cpr.12436.

Zhang, X. et al. 2014. Calcium sensing receptor promotes cardiac fibroblast proliferation and extracellular matrix secretion. *Cellular physiology and biochemistry : international journal of experimental cellular physiology, biochemistry, and pharmacology* 33(3), pp. 557–68. doi: 10.1159/000358634.

Zhang, Y., Xiong, Y. and Yarbrough, W.G. 1998. ARF promotes MDM2 degradation and stabilizes p53: ARF-INK4a locus deletion impairs both the Rb and p53 tumor

suppression pathways. *Cell* 92(6), pp. 725–734. doi: 10.1016/S0092-8674(00)81401-4.

Zhao, H. et al. 2004. Differential Inhibition of Membrane Type 3 (MT3)-Matrix Metalloproteinase (MMP) and MT1-MMP by Tissue Inhibitor of Metalloproteinase (TIMP)-2 and TIMP-3 Regulates Pro-MMP-2 Activation. *Journal of Biological Chemistry* 279(10), pp. 8592–8601. doi: 10.1074/jbc.M308708200.

Zhao, H. et al. 2020. Baicalin alleviates bleomycin-induced pulmonary fibrosis and fibroblast proliferation in rats via the PI3K/AKT signaling pathway. *Molecular Medicine Reports* 21(6), pp. 2321–2334. doi: 10.3892/MMR.2020.11046.

Zhao, H., Dennery, P.A. and Yao, H. 2018. Metabolic reprogramming in the pathogenesis of chronic lung diseases, including BPD, COPD, and pulmonary fibrosis. *American Journal of Physiology - Lung Cellular and Molecular Physiology* 314(4), pp. L544–L554. doi: 10.1152/ajplung.00521.2017.

Zhao, J. et al. 2002. Smad3 deficiency attenuates bleomycin-induced pulmonary fibrosis in mice. *American journal of physiology. Lung cellular and molecular physiology* 282(3). doi: 10.1152/AJPLUNG.00151.2001.

Zhao, Y.D. et al. 2017. Metabolic heterogeneity of idiopathic pulmonary fibrosis: a metabolomic study. *BMJ Open Respiratory Research* 4(1), p. e000183. doi: 10.1136/bmjresp-2017-000183.

Zhu, L. et al. 2019. Spermine on endothelial extracellular vesicles mediates smoking-induced pulmonary hypertension partially through calcium-sensing receptor. *Arteriosclerosis, Thrombosis, and Vascular Biology* 39(3), pp. 482–495. doi: 10.1161/ATVBAHA.118.312280.

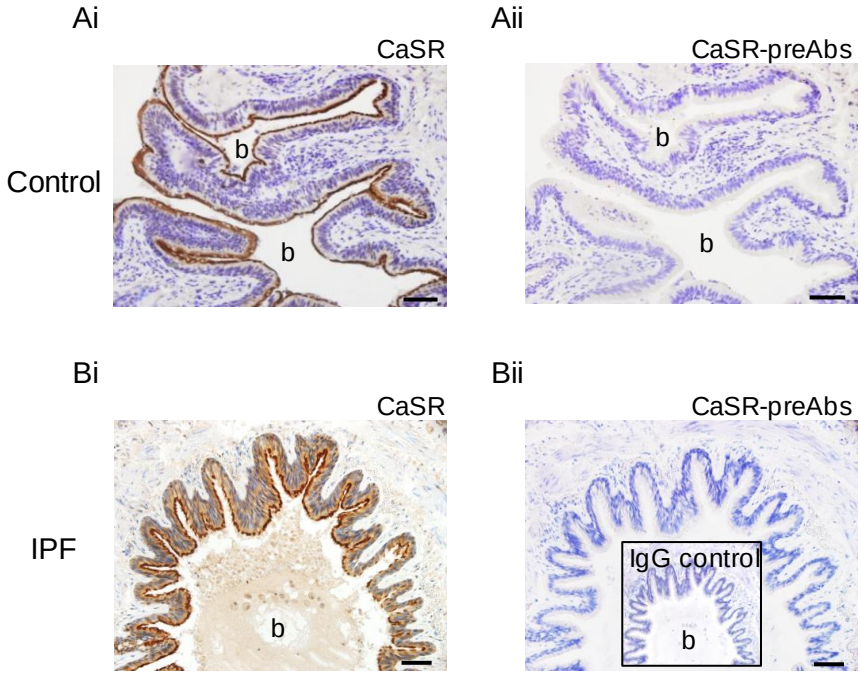

Figure S1 CaSR is expressed in the epithelium of peripheral bronchioles in control and IPF lungs. Consecutive paraffin sections of control (**Ai, ii**) and IPF lungs (**Bi, ii**) used for CaSR immunostaining controls. CaSR is expressed in the epithelium of peripheral bronchioles; especially on the apical membrane of ciliated cells in both control and IPF lungs (**Ai, Bi**). CaSR immunostaining in the airway epithelium is fully abolished after preabsorption of the CaSR antibodies with CaSR antigenic peptide (**Aii, Bii**). No staining can be seen in the epithelium when the primary CaSR antibody is replaced by a non-immune isotype IgG control (**Bii inset**). *N* = 5 control donors; 7 IPF donors. b: lumen of bronchiole in figures. Scale bars: 100 μm.

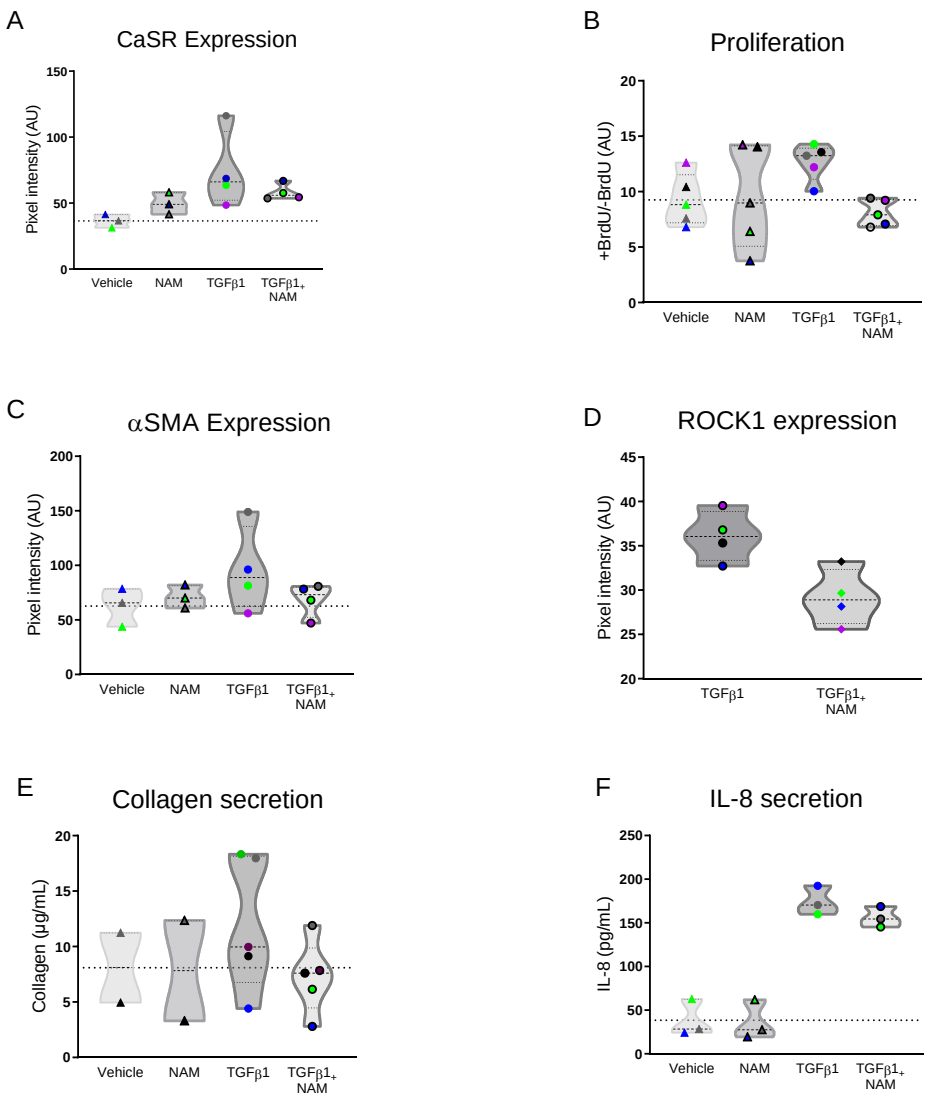

Figure S2 Raw data showing that the negative allosteric modulator of the calcium-sensing receptor (NAM), NPS2143 (1 µM) selectively reduces pro-fibrotic changes induced by TGFß1 in normal human lung fibroblasts (NHLF). Treatment with TGFß1 induces NHLF CaSR expression (**A**), proliferation (**B**), αSMA expression (**C**), ROCK1 expression (**D**), collagen secretion (**E**), and IL-8 secretion (**F**) while NAM reduces these effects. *N* = 2-4 donors; n = 2-5 independent experiments. Quantification of CaSR and αSMA immunofluorescent expression was done using StrataQuest, proliferation was assessed using a BrdU assay, collagen and IL-8 secretion were assessed using Sircol total collagen assay and IL-8 ELISA, respectively.